

Analysing Apc Function in the Mammary Gland

Catherine Naughton

Submitted for Degree of Doctor of Philosophy

University of Edinburgh

December 2002



Declaration

I declare that the work presented in this thesis is my own, except where otherwise stated. All experiments were designed by myself, or in collaboration with my supervisors Dr. John Mason and Dr. Michael Clinton.

Catherine Naughton, December 2002

Acknowledgements

Firstly I would like to thank my supervisors Dr. John O. Mason and Dr. Mike Clinton for their patience, advice, support and encouragement during the course of this project.

Thanks also to all the members of the Mason, Price, Kind and Spears laboratories for the help, advice and friendship, which has made the past three years all the more enjoyable. In particular I would like to thank Ronnie and Ian for all the help and advice, and also Tom, Dave M, Dave T, Celestial, Jeni, Ben and Paulette for their much valued friendship. I would also like to thank Duncan, Andrew and Elise for all their assistance with the animal work.

To all the Roslin gang, especially Derek, Gino and Elaine, my grateful thanks for helping me to get out of there as soon as possible.

To the girls, Gill, Hazel and Alyson, for the laughs, tears, lunches, beers, but most especially their friendship, thank you.

To my parents, Kathleen and Billy for their love, support and money when I had none.

Finally, to Chris, thank you for everything, love, patience, help, advice, money, holidays and most importantly chocolate.

Table of Contents

Title page.....	1
Declaration.....	2
Acknowledgements.....	3
Table of Contents.....	4
Abbreviations.....	10
Abstract.....	13
1. INTRODUCTION.....	15
1.1 Biology of the mammary gland.....	15
1.1.1 Growth and development of the mammary gland.....	15
1.1.2 Mammary gland branching morphogenesis.....	19
1.1.3. Mouse mammary tumour virus (MMTV).....	22
1.2 <i>Wnt</i> Genes in the mammary gland.....	23
1.3 The WNT/Wingless Signalling Pathway.....	24
1.3.1 Wnts.....	24
1.3.2 Wnt Receptors.....	27
1.3.2.1 Frizzled.....	27
1.3.2.2 Low-density lipoprotein (LDL)-receptor related protein (LRP).....	28
1.3. 2.3 Heparan Sulphate Proteoglycans (HSPGs).....	28
1.3.3 Wnt Antagonists.....	29
1.3.4 Wnt Signalling Pathways.....	30
1.3.4.1 The Canonical Wnt Pathway.....	31
1.3.4.2 β -catenin.....	34
1.4 Adenomatous Polyposis Coli (APC).....	37
1.4.1 <i>APC</i>	37
1.4.1.1 Genomic organisation in human and mouse.....	37
1.4.1.2 Mutations of the <i>APC</i> gene.....	39
1.4.1.2.1 Familial Adenomatous Polyposis ...	40
1.4.2. The APC tumour suppressor protein.....	40
1.4.2.1 Structure and protein interactions.....	40
1.4.2.2 Subcellular localisation.....	44
1.4.3 Functions of APC.....	44
1.4.3.1 APC in the Wnt signalling pathway.....	45
1.4.3.2 APC and the cytoskeleton.....	46
1.5 The APC Tumour Suppressor Protein in Cancer.....	48
1.5.1 The APC tumour suppressor protein and breast cancer.....	50
1.5.1.1 The <i>Min</i> (Multiple intestinal neoplasia) mouse.....	50
1.5.1.2 APC and human breast cancer.....	52
1.5.1.3 Wnt signalling and mouse mammary carcinomas...	53

1.5.1.3.1 β -catenin overexpression.....	53
1.5.1.3.2 Cyclin D1 overexpression.....	54
1.6 Conditional gene targeting in the mouse mammary gland.....	54
1.6.1 Cre- <i>loxP</i> recombination system.....	55
1.6.2 Conditional β -catenin overexpression.....	55
1.6.3 Conditional inactivation of <i>APC</i>	59
1.7 AIMS.....	66
2. MATERIALS AND METHODS.....	67
2.1 Basic Cloning Methodology.....	67
2.1.1 Agarose gel electrophoresis of DNA.....	67
2.1.2 Restriction endonuclease digestion of DNA.....	67
2.1.3 Phenol: chloroform extraction and ethanol precipitation of DNA.....	68
2.1.4 Extraction of DNA fragments from agarose gels.....	68
2.1.5 DNA ligation reactions.....	69
2.1.5.1 Dephosphorylation of vector DNA.....	69
2.1.5.2 Ligation reaction.....	69
2.1.6 Transformation of competent bacteria.....	70
2.1.7 Preparation of plasmid DNA.....	70
2.1.8 Preparation of bacterial glycerol stocks.....	72
2.1.9 ExSite™ PCR-based site-directed mutagenesis.....	72
2.2 Differential Display RT-PCR.....	73
2.2.1 Isolation of total RNA from murine mammary glands.....	73
2.2.2 Synthesis of first-strand cDNA.....	74
2.2.3 Differential Display PCR.....	74
2.2.4 Recovery of cDNA from dried polyacrylamide gels.....	75
2.2.5 Modified single-strand conformation polymorphism (mSSCP).....	75
2.2.6 PCR re-amplification of mSSCP-purified candidate cDNAs.....	76
2.2.7 ‘Cold’ Southern blotting.....	77
2.3 Polyacrylamide Gel Electrophoresis.....	77
2.3.1 Preparation and pouring of polyacrylamide gels.....	77
2.3.1.1 Non-denaturing polyacrylamide gels.....	78
2.3.1.2 Denaturing polyacrylamide gels.....	78
2.3.2 Drying of polyacrylamide gels.....	79
2.4 DNA sequencing.....	79
2.4.1 Fluorescent cycle sequencing of DNA (Automated Sequencing).....	79
2.4.2 <i>Fmol</i> cycle sequencing (manual sequencing).....	80
2.5 Northern blotting.....	81
2.5.1 RNA formaldehyde gel electrophoresis.....	81
2.5.2 Northern blotting of RNA.....	82

2.6 Southern blotting	82
2.6.1 Preparation of genomic DNA.....	82
2.7 Screening a phage cDNA library	84
2.7.1 Titration of genomic phage library.....	84
2.7.2 Plating of genomic phage library.....	85
2.7.3 Phage DNA lifts.....	85
2.7.4 Primary screen of cDNA library.....	86
2.7.4.1 Prehybridisation.....	86
2.7.4.2 Generation of radiolabelled probes.....	86
2.7.4.3 Hybridisation.....	86
2.7.5 Secondary screen of phage clones.....	87
2.7.5.1 Preparation of phage DNA.....	87
2.8 <i>In vitro</i> synthesis of capped mRNA	88
2.9 <i>Xenopus</i> embryo injections	88
2.10 Histological analysis	89
2.10.1 Immunohistochemistry.....	89
2.11 General tissue culture	90
2.11.1 Human embryonic kidney (HEK 293) cells.....	90
2.11.2 Trypsinisation of cells (T75 flask)	90
2.11.3 Lipid based transfection with FuGene™6 transfection reagent.....	91
2.11.4 Isolation of stably transfected clones.....	92
2.11.5 Tunicamycin treatment.....	92
2.11.6 C57MG mouse mammary epithelial cells.....	92
2.11.7 Harvesting cells for protein (T75).....	93
2.12 Protein quantification	93
2.13 Endoglycosidase treatment	94
2.14 Western Blotting	94
2.14.1 Protein electrophoresis.....	94
2.14.2 Protein transfer.....	94
2.14.3 Antibody incubation.....	95
2.14.4 Signal detection.....	95
2.15 Animal work	96
2.15.1 Isolation of genomic DNA from murine tissues.....	96
2.16 Gene specific PCR.....	96
3 CHARACTERISATION OF CRE⁺ APC^{580S/580S} MICE	101
3.1 Introduction	101

3.2 Results	101
3.2.1 <i>Apc</i> excision and expression levels in cre ⁺ <i>Apc</i> ^{580S/580S} mouse mammary glands.....	102
3.2.2 Characterisation of metaplastic lesions from cre ⁺ <i>Apc</i> ^{580S/580S} mouse mammary glands.....	104
3.2.2.1 <i>Apc</i>	104
3.2.2.2 β -catenin.....	107
3.2.2.3 Cyclin D1.....	107
3.2.2.4 Proliferation analysis.....	107
3.3 Discussion	110
3.3.1 <i>Apc</i> inactivation dysregulates Wnt signalling in mouse mammary gland metaplastic lesions.....	110
3.3.2 <i>Apc</i> deletion and mouse mammary gland tumourigenesis.....	112
4 DIFFERENTIAL DISPLAY RT-PCR ANALYSIS OF GENE EXPRESSION IN THE CRE⁺ APC^{580S/580S} MOUSE MAMMARY GLAND	116
4.1 Introduction	116
4.1.1 Differential analysis of gene expression in the mammary gland of cre ⁺ <i>Apc</i> ^{580S/580S} mice.....	116
4.1.1.1 Differential Screening.....	116
4.1.1.2 Subtractive Hybridisation.....	117
4.1.1.3 Differential Display RT-PCR.....	118
4.1.1.3.1 Modified Single-Strand Conformation Polymorphism (mSSCP).....	119
4.1.1.3.2 'Cold' Southern Blotting.....	120
4.1.2 DDRT-PCR analysis of gene expression in the mammary gland of cre ⁺ <i>Apc</i> ^{580S/580S} mice.....	120
4.2 Results	122
4.2.1 DDRT-PCR experimental design.....	122
4.2.2 Gene expression in control (cre ⁺ <i>Apc</i> ^{+/580S} and cre ⁻ <i>Apc</i> ^{580S/580S}) and <i>Apc</i> deleted (cre ⁺ <i>Apc</i> ^{580S/580S}) mouse mammary glands.....	123
4.2.3 Transcripts identified as being differentially expressed between control (cre ⁺ <i>Apc</i> ^{+/580S} and cre ⁻ <i>Apc</i> ^{580S/580S}) and mutant (cre ⁺ <i>Apc</i> ^{580S/580S}) mammary glands.....	126
4.2.3.1 Candidate 1 (Clone 3.4).....	126
4.2.3.2 Candidate 2 (Clone 7.4).....	131
4.2.3.3 Candidate 3 (Clone 9.1).....	135
4.2.3.4 Candidate 4 (Clone 11.2).....	140
4.2.3.5 Candidate 5 (Clone 12.3).....	144
4.2.3.6 Candidate 6 (Clone 13.4).....	148
4.3 Discussion	151
4.3.1 Candidate 1/ <i>Casein delta</i>	151
4.3.2 Candidate 2 / <i>Mus musculus alpha-1 type IV collagen</i>	153

4.3.3 Candidate 3 / <i>Mus musculus</i> GM2 ganglioside activator protein mRNA.....	154
4.3.4 Candidate 4 / <i>Novel 1</i>	155
4.3.5 Candidate 5 / <i>Novel 2</i>	156
4.3.6 Candidate 6 / <i>Novel 3</i>	156
5 FURTHER ANALYSIS OF DIFFERENTIALLY EXPRESSED TRANSCRIPTS IN CRE⁺ APC^{580S/580S} MOUSE MAMMARY GLANDS.....	158
5.1 Introduction.....	158
5.2 <i>alpha-1</i> type IV collagen.....	159
5.2.1 Introduction.....	159
5.2.2 Results.....	160
5.2.3 Discussion.....	162
5.3 <i>Novel</i> genes.....	163
5.3.1 Introduction.....	163
5.3.2 Results.....	163
5.3.2.1 Characterisation of transcript ' <i>Novel 1</i> '.....	164
5.3.2.2 <i>Novel 1</i> Discussion.....	176
5.3.2.3 Characterisation of transcript ' <i>Novel 2</i> '.....	179
5.3.2.4 <i>Novel 2</i> Discussion.....	183
5.3.2.5 Characterisation of transcript ' <i>Novel 3</i> '.....	186
5.3.2.6 <i>Novel 3</i> Discussion.....	188
5.4 Summary.....	189
6 A PRELIMINARY CHARACTERISATION OF TWO <i>WNT</i> GENES (<i>WNT8B</i> & <i>WNT10A</i>) IDENTIFIED FROM MOUSE MAMMARY GLAND CDNA.....	190
6.1 Introduction.....	190
6.2 Results.....	194
6.2.1 Biochemical analysis of Wnt8b and Wnt10a.....	194
6.2.2 Functional analysis of Wnt8b and Wnt10a.....	198
6.2.2.1 Functional assay 1: C57 mammary epithelial cells.....	200
6.2.2.2 Functional assay 2: <i>Xenopus</i> embryos.....	204
6.3 Discussion.....	208
6.3.1 Biochemical analysis of Wnt8b and Wnt10a proteins.....	208
6.3.2 Functional analysis of <i>Wnt8b</i> and <i>Wnt10a</i>	211
6.3.2.1 Morphological transformation of C57MG cells.....	211
6.3.2.2 Axis duplication in <i>Xenopus</i> embryos.....	213

7 FINAL DISCUSSION.....	215
7.1 Conditional inactivation of <i>Apc</i> in the mouse mammary secretory epithelium.....	215
7.2 Technical limitations of differential display.....	216
7.3 Future Work.....	217
8 REFERENCES.....	219
Appendix A.....	242
Appendix B.....	250
Appendix C.....	253
Appendix D.....	254
Appendix E.....	271

Abbreviations

APC	Adenomatous Polyposis Coli
Asef	APC-stimulated guanine nucleotide exchange factor
BLG	beta-lactoglobulin
BM	basement membrane
BrdU	5-bromo-2'deoxyuridine
CamKII	calcium/calmodulin-regulated kinase II
CBP	Creb-binding protein
DDR-1	discoidin domain receptor-1
DDRT	differential display reverse transcription
Dkk	Dickkopf
dlg	Drosophila discs large
dNTP	deoxynucleoside triphosphate
Dsh	Dishevelled
EB1	End-binding protein 1
ECM	extracellular matrix
EDTA	disodium ethylenediamine tetraacetate
EGF	Epidermal growth factor
EHS	Engelbreth-Holm-Swarm
Endo H	Endoglycosidase H
ENU	ethylnitrosourea
FAP	Familial Adenomatous Polyposis
FGF7	fibroblast growth factor 7
Fzd	Frizzled
GBP	GSK3 β binding protein
Gm2a	ganglioside activator protein
GSK3 β	glycogen synthase kinase 3 β
HA	haemagglutinin
hdlg	human discs large
HEK	human embryonic kidney

HMG	High Mobility Group
HSGAG	Heparan sulphate glycosaminoglycan
IGF-1	Insulin-like growth factor-1
IGFBP-5	Insulin-like growth factor binding protein-5
KIF	kinesin superfamily
LB	Luria broth
LDL	Low-density lipoprotein
LOH	loss of heterozygosity
LoxP	locus of crossover P1
LRP	Low-density lipoprotein-receptor related protein
LTR	long terminal repeat
MECs	mammary epithelial cells
MEN1	multiple endocrine neoplasia type I
Min	multiple intestinal neoplasia
MMP-3	matrix metalloproteinase-3
MMTV	mouse mammary tumour virus
mSSCP	modified single-strand conformation polymorphism
NES	nuclear-export signal
NLS	nuclear-localisation signal
PCR	polymerase chain reaction
PG	progesterone
PKC	Protein Kinase C
Plg	plasminogen
PRL	prolactin
PTHrP	parathyroid hormone related peptide
Sdc1	Syndecan-1
SDS	sodium dodecyl sulphate
SSC	standard saline citrate
SSCP	single-strand conformation polymorphism
STATs	Signal Transducers and Activators of Transcription
TBE	tris borate EDTA
TCF/LEF	T cell factor/ Lymphoid enhancer factor

TE	tris EDTA
TEBs	terminal end buds
TEMED	N,N,N'N'-Tetramethylethylenediamine
TGF- β	transforming growth factor- β
Timps	tissue inhibitors of metalloproteinases
tPA	tissue-type plasminogen activator
TUNEL	TdT-mediated dUTP nick end labelling
uPA	urokinase-type plasminogen activator
UTR	untranslated region
WAP	whey acidic protein
WIF-1	Wnt-inhibitory factor-1

Abstract

Adenomatous Polyposis Coli (*APC*) encodes a tumour suppressor gene that is mutated in the majority of colorectal cancers, both inherited and spontaneous. Germline *APC* mutations are responsible for the human condition Familial Adenomatous Polyposis (FAP). Patients with FAP develop colorectal adenomas some of which eventually progress to malignant carcinomas. In the last few years, strong evidence of a link between *APC* mutation and human breast cancer has begun to accumulate. For example, somatic mutations of the *APC* gene were detected in up to 18% of primary breast cancers and it has also been shown that the *APC* promoter is frequently hypermethylated in human breast cancers.

The main function of *APC* as a tumour suppressor involves regulating β -catenin levels in the canonical Wnt signalling pathway and is mediated through at least three important functional domains. However, most tumourigenic truncation mutations of *APC* eliminate some or all of these motifs, resulting in the oncogenic activation of β -catenin. Wnts have been shown to be involved in both the normal postnatal development of the mammary gland and mammary tumourigenesis in mice. Additionally, aberrant Wnt signalling through ectopic expression of mutant stabilized forms of β -catenin or Cyclin D1 (a downstream target of the Wnt signalling pathway) promote mouse mammary tumourigenesis.

In order to analyse the role of *Apc* both in the development of the mammary gland and in mammary tumourigenesis a *cre-loxP* based strategy was used to conditionally inactivate *Apc* in mouse mammary secretory epithelium. Virgin mice harbouring mammary-specific mutations in *Apc* showed markedly delayed development of the mammary ductal network. During lactation, mice developed multiple extensive metaplastic nodules, which surprisingly never progressed to neoplasia. Immunohistochemical analysis confirmed that these metaplastic areas had lost *Apc* expression. In addition, immunohistochemistry established that *Apc* mutation causes β -catenin dysregulation and subsequent activation of Wnt target genes, including *Cyclin D1*. A differential display reverse transcription polymerase chain reaction

approach was used to identify transcriptional changes in response to loss of *Apc* in the mouse mammary gland, with the aim of providing insight into this unexpected phenotype. Genes identified through this screen included *casein*, $\alpha 1$ type IV collagen and the GM2 ganglioside activator protein, *Gm2a*. Decreased casein expression in *Apc* deleted lactating mammary glands correlated with the observation that offspring from mutant mothers did not thrive. Additionally, expression levels of $\alpha 1$ type IV collagen, which is a component of the mammary gland basement membrane, were no longer downregulated in lactating mammary glands following conditional inactivation of *Apc*. Several novel clones found to be differentially expressed following *Apc* deletion were subjected to cDNA library screening in an effort to characterise them further. Despite these efforts, the relationship between mammary gland metaplasia and *Apc* deficiency remains unclear. These observations highlight the complexity of *Apc* function in mouse mammary gland secretory epithelium. Finally, as a complementary analysis, two *Wnt* genes (*Wnt8b* and *Wnt10a*) identified in a screen of mammary gland cDNA were subcloned and their functions tested in a range of biochemical and functional assays.

1 Introduction

1.1 Biology of the mammary gland

1.1.1 Growth and development of the mammary gland

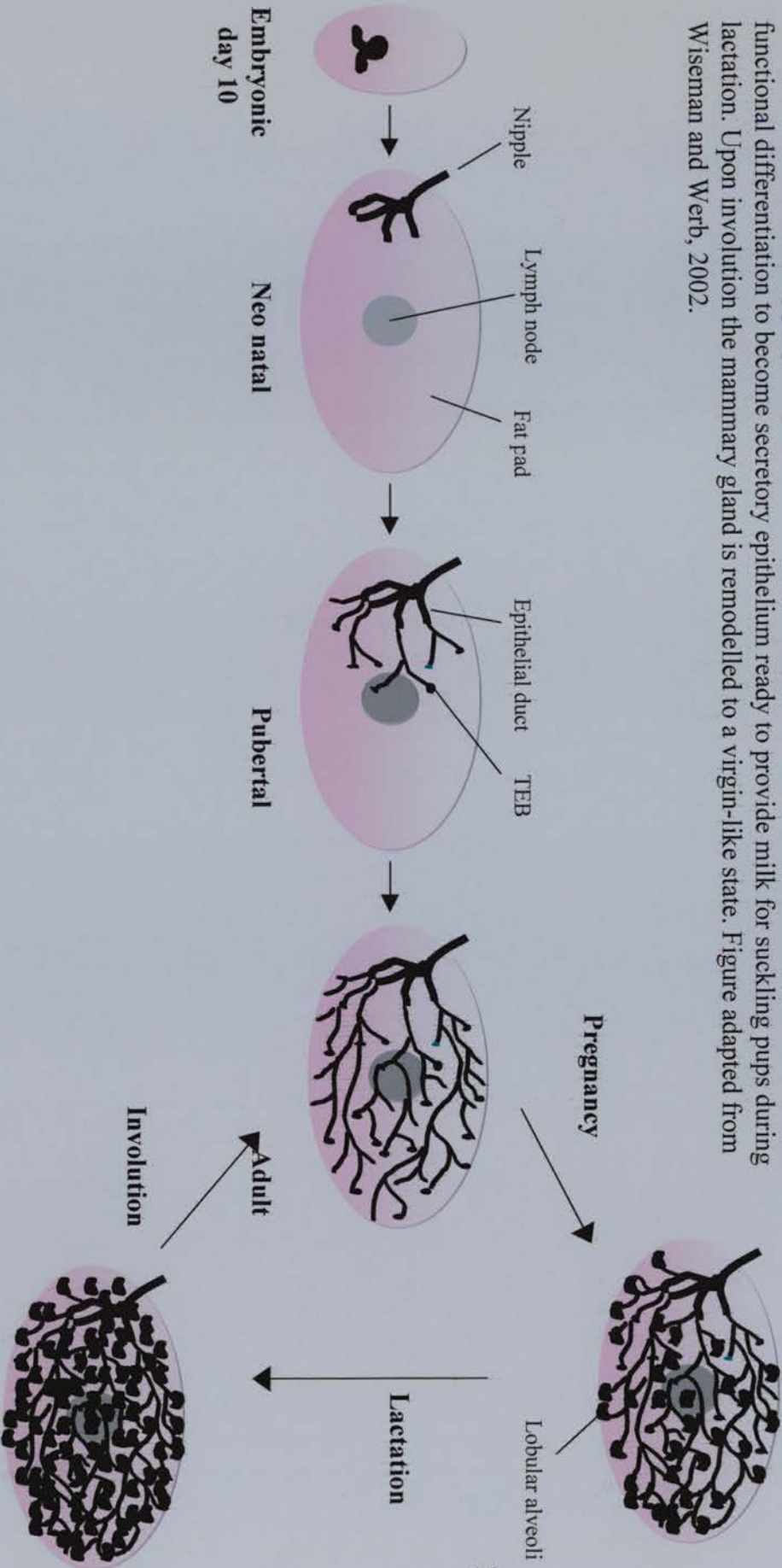
Whilst most mammalian organs are patterned during embryogenesis and maintain their basic structure through to adult life breast tissue is distinct in that it continually changes in form throughout the lifetime of the reproductively active female. Once the mammary gland is established, cycles of proliferation, functional differentiation, and death of alveolar epithelium occur repeatedly with each pregnancy (reviewed by Hennighausen *et al.*, 1998; Hennighausen *et al.*, 2001) (Fig. 1.1).

Two cellular compartments contribute to the gland, the epithelium and the surrounding stroma, which are separated by a basement membrane (BM) composed of extracellular matrix (ECM) proteins (including collagens I and IV, laminin, fibronectin and tenascin). The mammary stroma consists of multiple components including adipocytes, pre-adipocytes, fibroblasts, blood vessels, inflammatory cells and ECM proteins. Development of the mammary gland occurs in defined stages that are connected to sexual development and reproduction. These are embryonic, prepubertal, pubertal, pregnancy, lactation and involution. Epithelial-stromal interactions begin during embryonic development of the mammary gland and in combination with steroid and peptide hormones are necessary for proper ductal morphogenesis throughout all stages (Hennighausen *et al.*, 2001).

Initial stages of mammary development are dependent on reciprocal signalling between the epithelium and the mesenchyme (embryonic stroma). In the mouse this crosstalk specifies the mammary gland at embryonic day 10 (Hennighausen *et al.*, 2001) when five pairs of ectodermal placodes appear as distinct spots in the mouse embryo. These placodes form epithelial buds that are surrounded by a layer of mesenchymal cells (primary mammary mesenchyme), which express receptors for

Figure. 1.1. Stages of mouse mammary gland development

The mouse mammary gland is specified at embryonic day 10 and at birth consists of a rudimentary duct in the vicinity of the nipple. Ductal elongation and branching coincide with the onset of puberty and the release of ovarian hormones. During pregnancy lobular alveolar structures form at the ends of the ducts and undergo functional differentiation to become secretory epithelium ready to provide milk for suckling pups during lactation. Upon involution the mammary gland is remodelled to a virgin-like state. Figure adapted from Wiseman and Werb, 2002.



estrogen, some growth factors, BMP4 and FGF7 (fibroblast growth factor 7), and the transcription factors Lef-1, Msx-1 and Msx-2. Inactivation of the genes encoding these transcription factors arrests mammary gland development at the bud stage (van Genderen *et al.*, 1994; Satokata *et al.*, 2000). Embryonic mammary epithelial cells produce parathyroid hormone related peptide (PTHrP) that signals through receptors in the surrounding mesenchyme to promote elongation of the bud. This primary sprout invades from the nipple into a pad of fatty tissue called the mammary fat pad and forms a small, branched ductal network in the proximal corner of the fat pad. Interruption of PTHrP signalling arrests development resulting in a lack of primary sprout growth from the bud (Wysolmerski *et al.*, 1998; Hennighausen *et al.*, 2001).

Following the embryonic and prepubertal stages, further development of the mammary gland becomes hormone dependent and continues with the onset of puberty (around three weeks of age). Ovarian steroid hormones control ductal outgrowth and studies in mice have shown that deletion of the estrogen receptor α gene blocks this growth (Korach *et al.*, 1996). Other factors shown to be involved in ductal outgrowth include Insulin-like growth factor-1 (IGF-1) and Epidermal growth factor (EGF). IGF-1 is a potent mitogen for epithelial cells and has been shown to be a survival factor *in vitro* (O'Connor, 1998). Overexpression of IGF-1 in the mouse mammary gland delays involution and suggests that IGF-1 acts as a survival factor in mammary epithelial cells (Hadsell *et al.*, 1996; Neuenschwander *et al.*, 1996). EGF has been shown to control early ductal outgrowth through an action on stromal cells and can substitute for estrogen in ovariectomized mice (Silberstein, 2001; Coleman *et al.*, 1988). The distal ends of the mammary ducts swell into bulbous structures composed of multiple layers of cuboidal epithelial cells, called terminal end buds (TEBs). The TEBs are the invading fronts of the ducts that proliferate, extend into the fat pad and branch by bifurcation until the ducts eventually fill the fat pad by about 10 weeks of age.

In the first stage of pregnancy, ducts branch laterally and form side branches with concomitant epithelial proliferation. Alveolar structures then form on the expanded ductal tree and differentiate into lobular alveoli. Finally, the lobular alveoli

terminally differentiate and the epithelium becomes secretory, ready to provide milk for suckling pups upon parturition. At this stage, the epithelium has expanded to almost fill the mammary gland and the large fat cells have dedifferentiated into small pre-adipocytes. The hormones of pregnancy, progesterone (PG) and prolactin (PRL) are required for this continued ductal growth and branching and alveolar proliferation and differentiation. PRL gene and receptor knockout studies in mice show reduced ductal branching and impaired alveolar development of the mammary gland (Horseman, 1999; Brisken *et al.*, 1999), while targeted mutation of the PG receptor affects lobuloalveolar development (Brisken *et al.*, 1998). Finally, activins and inhibins, members of the TGF- β superfamily, have been implicated in lobuloalveolar and ductal growth regulation, as both are impaired in inhibin β gene knockout mice (Robinson and Hennighausen, 1997).

Mammary function during lactation is controlled by prolactin, secretion of which is tightly regulated and stimulated by suckling (Travers *et al.*, 1996). Prolactin activates Signal Transducers and Activators of Transcription (STATs) 5a and 5b, which are members of a family of cytoplasmic proteins with roles as signal messengers and transcription factors that participate in normal cellular responses to cytokines and growth factors (Ihle, 1996). *Stat5a* deficient mice are unable to lactate because of a failure of the gland to develop fully and undergo functional differentiation during pregnancy (Liu *et al.*, 1997). Also Oxytocin and the macrophage growth factor colony-stimulating factor-1 (CSF-1) are both required for milk ejection during lactation (Young *et al.*, 1996; Pollard and Hennighausen, 1994)

Upon involution, the secretory epithelium of the mammary gland dies by apoptosis, the fat cells redifferentiate, and the gland is remodelled back to a virgin-like state. These three processes are controlled by several factors including Stat3, which induces apoptosis, possibly through upregulation of Insulin-like growth factor binding protein-5 (IGFBP-5) a known promoter of apoptosis. IGFBP-5 has been proposed to induce apoptosis by sequestering IGF-1 to casein micelles, thus preventing it from binding to its receptor (Tonner *et al.*, 1997). Experiments in mice with conditional knockout of *Stat3* from mammary tissue show decreased apoptosis

and a dramatic delay in involution following weaning. These mice also show decreased IGFBP-5 expression (Chapman *et al.*, 1999). Proteinases such as plasmin (an extracellular serine proteinase) and matrix metalloproteinase-3 (MMP-3) are also involved in involution and studies in mice have shown that deficiencies in either affects involution (Alexander *et al.*, 2001; Lund *et al.*, 2000). Matrix metalloproteinases (MMPs) have been shown to be induced during physiological remodelling reactions and to cleave structural proteins important to maintaining the basement membrane integrity (Sternlicht and Werb, 1999). One such MMP, MMP-3/stromelysin-1, is highly expressed during mammary gland involution and cleaves basement membrane proteins (Mayer *et al.*, 1993; Werb, 1997). Stromelysin-1 has been shown to induce unscheduled apoptosis when expressed ectopically in mouse mammary glands during late pregnancy due to an acceleration of adipocyte differentiation (Alexander *et al.*, 2001). Plasmin produced from plasminogen (Plg) by urokinase-type plasminogen activator (uPA) and tissue-type plasminogen activator (tPA) also plays a role in mammary gland involution through activation of latent pro-MMPs and direct degradation of ECM substrates (Sternlicht and Werb, 1999). Plg deficient mice have defects in lactation and one-quarter of the mice studied failed to lactate. In the absence of Plg involution was perturbed with a reduction in overall mammary gland size after five days of involution being less than one-third the reduction seen in wt mice (Lund *et al.*, 2000).

1.1.2 Mammary gland branching morphogenesis

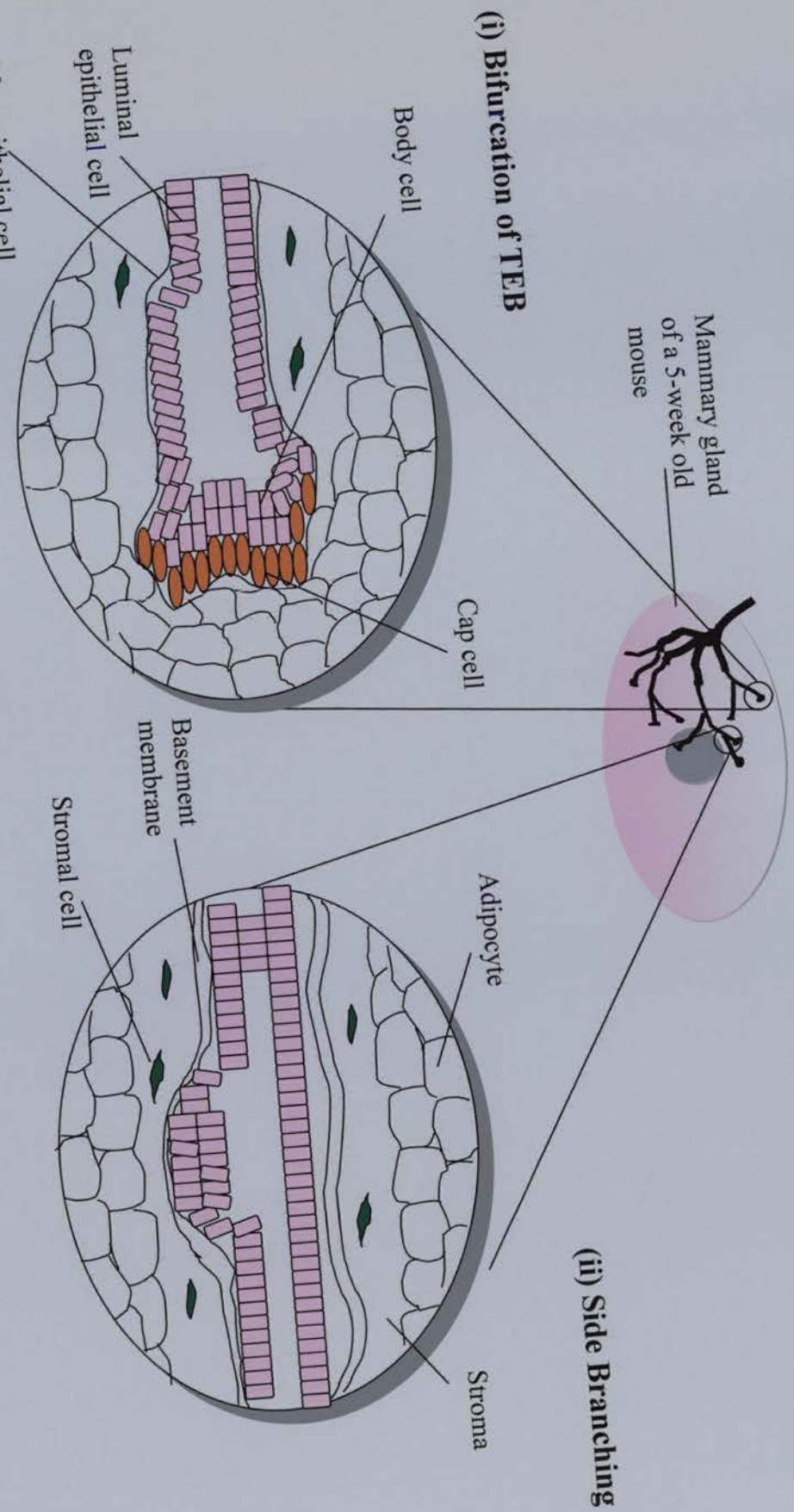
During its developmental cycle, the mammary gland displays many of the properties associated with tumour progression, such as invasion, reinitiation of cell proliferation, resistance to apoptosis, and angiogenesis. For example, terminal end buds (TEBs) are bulbous structures located at the migrating ductal forefront containing stem cells that proliferate and differentiate in response to hormones, and invade into stromal tissue. However this end bud extension is inhibited both at the fat pad boundaries and when it is in proximity to other ducts (Silberstein *et al.*, 2001). Many of the stromal factors necessary for mammary development promote or protect

against breast cancer by contributing both instructive and permissive signals, therefore crosstalk between the mammary epithelium and stroma is crucial for proper patterning and function of the mammary gland (reviewed in Wiseman and Werb, 2002). This is most evident during mammary gland branching morphogenesis. It has been shown that when some of the factors involved are mis-expressed it results in excessive side branching and eventual tumourigenesis (see below) (Sternlicht *et al.*, 1999, Ha *et al.*, 2001).

The mammary gland branches by two mechanistically distinct processes (1) TEB bifurcation and (2) sprouting of side branches (Fig. 1.2). Bifurcation of TEBs to form primary and secondary branches occurs only from immature ducts with formation of the branch point through stromal deposition at the cleft site. Throughout this process the distal epithelial cells (cap cells) are separated from the adjacent fat cells by a thin basement membrane and the ducts extend directly into the adipose tissue (Fig. 1.2.i.). The ECM creates a physical barrier that must be penetrated to allow TEB migration and branching. This is mediated through epithelial–stromal interactions and factors that regulate the ECM. These include discoidin domain receptor-1 (DDR-1) and β 1 integrin, which both act as receptors for ECM proteins. DDR-1 is a collagen receptor (collagens type I to type IV) and when knocked out in mice results in defective ductal morphogenesis, enlarged TEBs due to aberrant growth and increased ECM deposition (Vogel *et al.*, 2001). β 1 integrin recognises many ECM proteins and when inhibited resulted in reduction of both TEB number and the extent of the mammary ductal network. The result was similar when the ECM protein laminin-1, a β 1-integrin receptor ligand, was inhibited (Klinowska *et al.*, 1999). In addition several MMPs, including Stromelysin-1, and their inhibitors, tissue inhibitors of metalloproteinases (Timp) are necessary for invasion of the ducts. By virtue of regulating MMP activity, Timp may control the rapid physical expansion of mammary ducts through the ECM by limiting or focusing matrix deposition (Fata *et al.*, 1999). Stromelysin-1 can degrade numerous ECM substrates, including collagens III, IV, V, IX, X and XI, laminins and fibronectin and promotes proliferation and branching in ductal cells (in contrast to its role in differentiated secretory alveolar cells where it promotes apoptosis). Transgenic overexpression of Stromelysin-1 in

Figure 1.2. Mechanisms of branching morphogenesis in the pubertal mouse mammary gland

(i) Bifurcation of TEB: the branch point is formed through deposition of stroma at the cleft site, and the ducts extend directly into adipose tissue, without myoepithelial cells or stroma and with only a minimal basement membrane at their invasive front. (ii) Side branching: First the region where the bud is formed must be defined, then the emerging bud extrudes through and remodels a region containing layers of myoepithelial cells, basement membrane and stroma. Figure adapted from Wiseman and Werb, 2002.



mouse mammary epithelial cells promotes mammary carcinogenesis (Sternlicht *et al.*, 1999) and overexpression of membrane-type MMP-1 (MT1-MMP) in mouse mammary glands resulted in adenocarcinoma (Ha *et al.*, 2001). *Timps* are predominantly expressed in mammary epithelial cells and are found in advancing TEBs, however down-regulation of epithelial-derived *Timp-1* in transgenic mice by MMTV promoter-directed antisense RNA expression promotes ductal expansion and increases the number of ducts (Fata *et al.*, 1999).

In contrast, side branching results in the formation of a new branch from a mature duct. The region where the bud forms is defined by a specific downregulation of the growth factor, transforming growth factor- β (TGF- β). TGF- β is localised to the periductal ECM in mice and acts to inhibit inappropriate side branching. Inhibition of TGF- β signalling in mammary stroma resulted in excessive side branching (Silberstein *et al.*, 2001). The emerging bud then extends through and remodels this region consisting of myoepithelial cells, stroma and ECM to form a side branch (Fig. 1.2.ii.). Again, factors that regulate the ECM are required but also the progesterone receptor and Wnts. Experiments have shown that the progesterone receptor (PR) induces *Wnt4* in mammary epithelial cells, which then regulates the branching of neighbouring cells. This is confirmed by the findings that ductal side branching fails to occur in the absence of the PR from mammary epithelium, progesterone induces *Wnt4* expression and *Wnt4* null mammary glands show substantial reduction in ductal branching (Briskin *et al.*, 1998; Briskin *et al.*, 2000).

1.1.3. Mouse mammary tumour virus (MMTV)

Mouse mammary tumour virus (MMTV) infection can promote mouse mammary tumorigenesis and MMTV integrations have helped to identify a wide variety of interesting genes that play a role in mammary development and tumorigenesis. MMTV is a nonacute transforming retrovirus that infects mammary epithelial cells and randomly inserts its proviral DNA into the host somatic cell DNA during its replicative cycle (Ringold *et al.*, 1979; Withers-Ward *et al.*, 1994). Thus MMTV

induces mammary tumours by acting as an insertional mutagen and activating transcription of nearby genes (Tekmal *et al.*, 1997). These include members of the *Wnt* (Nusse and Varmus, 1982; Lee *et al.*, 1995; Roelink *et al.*, 1990) and fibroblast growth factor (*Fgf*) (Dickson *et al.*, 1984; MacArthur *et al.*, 1995; Peters *et al.*, 1989) gene families. Both Wnts and Fgfs play crucial roles in development by acting as short-range intercellular signalling molecules and become activated by MMTV due to the effect of enhancer sequences within the long terminal repeat (LTR) of the integrated MMTV proviral genome on the transcriptional promoter of the adjacent affected gene (Callahan and Smith, 2000).

Wnt1, originally termed *Int-1* (for MMTV integration site 1), was the first protooncogene to be identified in this way (Nusse and Varmus, 1982) and was the first mammalian *Wnt* gene to be discovered. The consequences of ectopic activation of *Wnt1* in the mammary gland were subsequently recapitulated experimentally in transgenic mice and resulted in premature ductal branching and lobuloalveolar hyperplasia, similar to that normally observed in pregnancy, with progression to mammary adenocarcinoma (Tsukamoto *et al.*, 1988). Roelink *et al.*, 1990 showed that *Wnt3* was also activated by proviral insertion in mouse mammary tumours and ectopic expression of *Wnt10b* also results in premature ductal branching and alveolar development and predisposition to mammary carcinoma (Lane and Leder, 1997).

1.2 *Wnt* Genes in the mammary gland

The observation that *Wnt1* and *Wnt3* were activated by a MMTV provirus in virus – induced mammary carcinomas suggested that Wnt signalling could control the growth and differentiation of mammary epithelial cells (MECs). Although neither of these genes turned out to be expressed in the normal mammary tissue, other *Wnt* genes are expressed and differentially regulated during mouse mammary gland development (Gavin and McMahon, 1992; Buhler *et al.*, 1993; Huguet *et al.*, 1994; Olson and Papkoff, 1994; Weber-Hall *et al.*, 1994; Lane and Leder, 1997).

Wnt10b expression occurs beginning at very early stages in the mammary rudiment and continues into puberty (Lane and Leder, 1997). *Wnt2*, *Wnt5a* and *Wnt6* are detected in the stroma at a stage preceding ductal outgrowth. During ductal development expression of these remains strong but *Wnt7b* is now also detected. *Wnt4*, *Wnt5b* and *Wnt6* are induced during pregnancy and decrease after lactation has commenced. Some *Wnt* genes (*Wnt2*, *Wnt5a*, *Wnt5b* and *Wnt7b*) are re-expressed during involution (Weber-Hall *et al.*, 1994). Although knockout mice have been generated for most of the *Wnt* genes the only one so far to produce a mammary gland phenotype was *Wnt4*, which has an essential role in side-branching early in pregnancy (Brisken *et al.*, 2000).

1.3 The WNT/Wingless Signalling Pathway

1.3.1 Wnts

Wnt genes constitute one of the major families of developmentally significant signalling molecules with a number of actions in a wide variety of organisms. The *Wnt* gene family was first identified in the mouse, when *Wnt1* was discovered to behave as an oncogene (Nusse and Varmus, 1982). This correlation with tumour development led to a great deal of study, *Wnt1* homologs were quickly identified in a wide range of species including human, *Caenorhabditis elegans* (*C. elegans*) and *Drosophila*; in the latter the conserved protein was known as *wingless* (*wg*) (Cabrera *et al.*, 1987). The discovery that *wg* was a *Wnt* family member suggested that *Wnts* may be important in embryonic development and importantly has enabled the powerful genetics of *Drosophila* to be applied to understanding *Wnt* gene function. *Wnt* genes are highly conserved between vertebrate species sharing overall sequence identity and gene structure, and are slightly less conserved between vertebrates and invertebrates. To date, in vertebrates, 16 *Wnt* genes have been identified in *Xenopus*, 11 in chick, and 12 in zebrafish. Humans have 19 *Wnt* genes and there are 18 in the mouse. In invertebrates, *Drosophila* has seven *Wnt* genes, *C. elegans* has five and Hydra at least one. A useful catalogue of *Wnt* genes can be

found at the *Wnt* gene homepage <http://www.stanford.edu/~rnusse/wntwindow.html>, maintained by Roel Nusse.

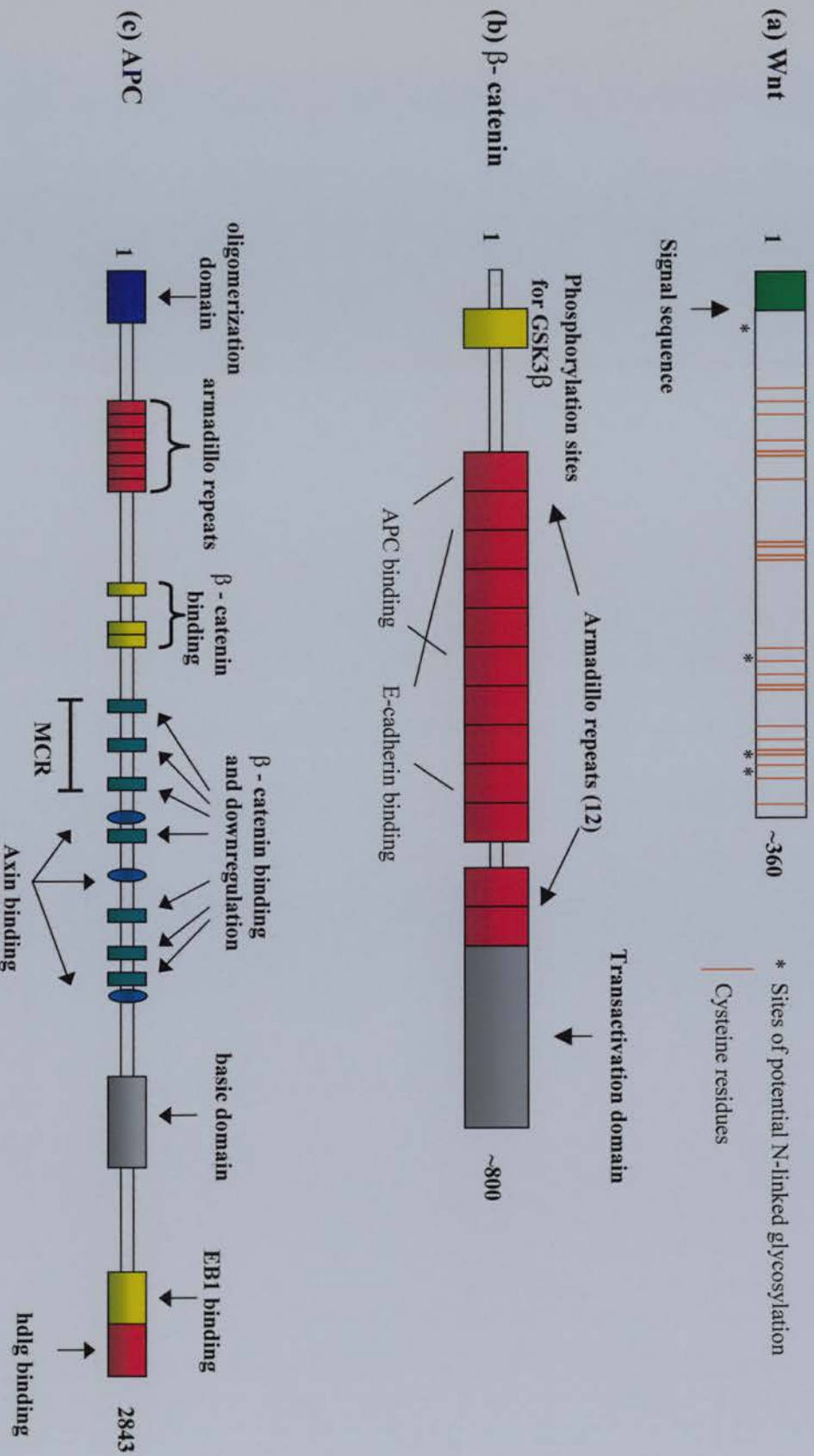
Wnt genes have been subdivided into two distinct classes, the *Wnt1* class, including: *Wnt1/3/3a/8*, and the *Wnt5a* class, including *Wnt4/5a* and *Wnt6*. This classification is based on assays carried out using mammary cell lines and *Xenopus* embryos. Over-expression of the *Wnt1* class was found to induce morphological transformations in C57 and RAC311C mammary epithelial cells and axis duplication in *Xenopus* embryos, whilst the *Wnt5a* class was found to alter morphogenetic movement during gastrulation resulting in a severe shortening of the axis, when ectopically expressed in *Xenopus* embryos (Rijsewijk *et al.*, 1987; Wong *et al.*, 1994; Du *et al.*, 1995).

Wnt proteins are secreted growth factors and have the following characteristic structural features: an amino terminal signal sequence, potential sites for N-linked glycosylation and all have 23 or 24 cysteine residues, the spacing of which is highly conserved suggesting that the folding of Wnt proteins depends on the formation of multiple intramolecular disulphide bonds (Du *et al.*, 1995) (Fig. 1.3). Once secreted, Wnt proteins associate with glycosaminoglycans in the extracellular matrix (ECM) and are bound tightly to the cell surface (Bradley *et al.*, 1990 and Reichsman *et al.*, 1996).

The *Wnt/wingless* family of genes play important developmental roles; defining segment polarity in *Drosophila*, controlling early lineage and gut development in *C. elegans* and have been implicated in determining axis formation in *Xenopus* (however there are no data concerning an endogenous *Wnt* in induction of the primary axis as no known *Wnt* is expressed in the right place at the right time) (Nusslein-Volhard and Roth, 1989; McMahon and Moon, 1989; McMahon and Moon, 1989; Nusslein-Volhard, 1991; Han, 1997). This importance in development became obvious through studies of mutations in *Wnt* genes, for example knocking out of *Wnt1* resulted in a dramatic loss of a portion of the midbrain and deletion of the rostral cerebellum (McMahon and Bradley, 1990; Thomas *et al.*, 1991).

Figure 1.3. Schematic representation of several proteins involved in Wnt signalling

(a) Structural features of the Wnt protein. The N-terminus contains a signal sequence and all Wnts contain 23/24 conserved cysteine residues. Figure adapted from Miller, 2001. (b) The structure of the β -catenin protein including the armadillo repeat region, binding sites for APC and Axin and the transactivation domain. (c) Linear representation of the APC tumour suppressor protein. Functional domains include an oligomerization domain, 2 β -catenin interacting regions and binding sites for Axin, hdlg and EB.



Wnt2 mutants die perinatally owing to placental defects (Monkley, 1996). *Wnt4* mutant mice fail to form kidneys (Stark *et al.*, 1994), have defects in mammary gland morphogenesis during pregnancy (Brisken *et al.*, 2000), and females fail to form a Mullerian duct implicating *Wnt4* in mammalian sexual dimorphism (Vainio *et al.*, 1999).

1.3.2 Wnt Receptors

1.3.2.1 Frizzled

For many years the identity of Wnt receptors remained elusive, greatly hampering understanding of Wnt signalling. However Bhanot *et al.*, (1996), found that members of the *Frizzled* (*Fzd*) gene family can function as Wnt receptors. The *frizzled* loci of a wide range of species encode seven pass transmembrane proteins; the cysteine-rich N-terminal portion being exterior with the C-terminal portion extending into the cytoplasm (Vinson *et al.*, 1996 and Bhanot *et al.*, 1996). This exterior N-terminal region, containing 10 highly conserved cysteine residues is believed to interact with the circulating Wnt proteins and thereby transfer growth signals (Bhanot *et al.*, 1996). *Fzd* receptors have been identified in vertebrates and invertebrates; there are ten known members in humans and mice, four in *Drosophila* and three in *C. elegans*. Most Wnt proteins can bind to multiple *Fzd*'s and vice versa, suggesting that receptor-ligand interactions are promiscuous. This is observed in *Drosophila* embryos where *wg* like phenotypes are only seen when both *fz* and *Dfz2* (two *Drosophila Fzd* genes) are removed (Chen and Struhl, 1999; Bhanot *et al.*, 1999).

It is not completely clear how the interactions of some Wnt and Frizzled pairings can lead to downstream modulation of the rest of the Wnt pathway. The C-terminal region of many of the Frizzled molecules contain a S/TXV motif, a candidate for binding with the PDZ domain (Songyang *et al.*, 1997). Dishevelled, a cytoplasmic scaffold protein that functions as part of the Wnt pathway, contains one of these domains at its C-terminus but evidence to date suggests that it does not interact

directly with Frizzled (Cadigan and Nusse, 1997, Nusse 1997; Nusse *et al.*, 1997). There is some suggestion that G-protein signalling may be involved. Some Wnt/Frizzled effects, such as regulation of Protein Kinase C in *Xenopus*, can be blocked through the application of G-protein inhibitors while two of the target proteins in the Wnt/wingless cascade, Axin and Dishevelled, contain motifs found in other molecules known to be involved in G-Protein signalling (Slusarski *et al.*, 1999; Fagotto *et al.*, 1999; Sheldahl *et al.*, 1999).

1.3.2.2 Low-density lipoprotein (LDL)-receptor related protein (LRP)

Members of the LDL-receptor related protein (LRP) family have been shown to act as co-receptors for Wnt proteins. Two members of the vertebrate LRP family, LRP-5 and LRP-6, can bind Wnts and may form a ternary complex with a Wnt and a Fzd (Tamai *et al.*, 2000). Mutations in LRP-6 in mice result in developmental defects similar to those seen in mice due to mutations in individual *Wnt* genes. These defects included a truncation of the axial skeleton similar to *Wnt3a* mutant mice, mid/hindbrain defects of the less severe type observed in *Wnt1* mutant mice and limb defects reminiscent of those observed in *Wnt7a* mutant mice (Pinson *et al.*, 2000). Overexpression of LRP-6 in *Xenopus* can activate the Wnt pathway and resulted in axis duplication and overexpression of *Wnt*-responsive genes (Tamai *et al.*, 2000). In *Drosophila*, *arrow* the orthologue of LRP-5 and LRP-6 is, required for optimal Wg signalling (Wehrli *et al.*, 2000).

1.3.2.3 Heparan Sulphate Proteoglycans (HSPGs)

Heparan sulphate glycosaminoglycans (HSGAGs) are members of the glycosaminoglycan family, which are complex polysaccharides that are characterised by a repeat disaccharide unit of uronic acid (either iduronic or glucuronic acid) linked to a glucosamine. *In vivo*, HSGAGs are usually found covalently attached to various core proteins; these HSGAG-protein conjugates are termed heparan sulphate

proteoglycans (HSPGs). The syndecans and the glypicans are the two main groups of cell surface HSPGs and are involved in cell signalling at the ECM interface, while the third group the perlecanans are mainly secreted (reviewed in Sasisekharan *et al.*, 2002).

Studies in *Drosophila* have shown that responses to Wg require heparan sulphate proteoglycans, which act as co-receptors during signalling (Lin *et al.*, 1999). Wg signalling is defective in both *sulfateless* (*sfl*) and *sugarless* (*sgl*) mutants (two genes in *Drosophila* encoding enzymes necessary for the formation of heparan sulphate) (Cumberledge *et al.*, 1997; Lin *et al.*, 1999). The *Drosophila* gene *dally*, encodes a glypican-type heparan sulphate proteoglycan, which when mutated disrupts wg signalling and has been shown to cooperate with frizzled as a co-receptor for Wg (Lin *et al.*, 1999). HSPGs are also required for Wnt signalling in vertebrates. Qsulf1, an avian protein related to heparan-specific N-acetyl glucosamine sulphatases, has been shown to regulate heparan-dependent Wnt signalling in cultured cells (C2C12 myogenic progenitor cells) suggesting that it can modulate Wnt signals by desulphation of cell-surface proteoglycans (Dhoot *et al.*, 2001). Syndecan-1 (*Sdc1*) is a cell-surface HSPG predominantly expressed by epithelial cells and *Sdc1* deficient mice appear normal and fertile with no defects in the mammary gland. However when crossed to transgenic mice expressing *Wnt1* in the mammary gland, a 70% reduction of *Wnt1* induced hyperplasia is observed, indicating that the Wnt1 pathway was inhibited. Thus Syndecan-1 is critical for Wnt1 induced tumourigenesis of the mouse mammary gland (Alexander *et al.*, 2000).

1.3.3 Wnt Antagonists

Several extracellular proteins have been shown to modulate Wnt signalling. These include members of the Frizzled-related protein (FRP) family (Moon *et al.*, 1997), Wnt-inhibitory factor-1 (WIF-1) (Hsieh *et al.*, 1999), Cerberus (Piccolo *et al.*, 1999) and Dickkopf (Dkk) (Nusse *et al.*, 2001). FRP's, WIF-1, and Cerberus can directly bind Wnt proteins and antagonise Wnt function by preventing their interaction with

Fzd receptors. FRP can also interact with Fzd, suggesting that FRP's may antagonise Wnt signalling through the formation of a non-functional complex with Fzd receptors (Bafico *et al.*, 1999). Dkk does not bind Wnts but instead interacts with the extracellular domain of LRP5 and LRP-6; this interaction may alter the conformation of the LRPs so that they can no longer interact with Wnt and Fzd, thereby blocking Wnt signalling (Mao *et al.*, 2001).

1.3.4 Wnt Signalling Pathways

Wnt signals are transduced through at least three distinct intracellular signalling pathways including the canonical 'Wnt/ β -catenin' pathway, the 'Wnt/ Ca^{2+} ' pathway and the 'Wnt/polarity' pathway (Adler *et al.*, 2001; Kuhl *et al.*, 2001; Miller *et al.*, 1999). Distinct sets of Wnt and Fzd ligand – receptor pairs can activate each of these pathways and lead to unique cellular responses.

The biological function of the 'Wnt/ Ca^{2+} ' pathway is unclear, however this pathway involves an increase in intracellular Ca^{2+} and activation of both Protein Kinase C (PKC) and calcium/calmodulin-regulated kinase II (CamKII) (Sheldahl *et al.*, 1999, Kuhl *et al.*, 2000)

The major function of the Wnt/polarity pathway is regulation of cytoskeletal organisation. In vertebrates this involves controlling polarized cell movements during gastrulation and neurulation (Tada *et al.*, 2000; Wallingford *et al.*, 2000; Wallingford *et al.*, 2001). In *Drosophila*, Wnt signalling has multiple developmental roles including, controlling the appropriate orientation of trichomes (hairs) of the adult wing, determining the appropriate chirality of ommatidia in the eye, and regulating asymmetric cell divisions in neuroblast populations (Adler *et al.*, 2001a, b).

1.3.4.1 The Canonical Wnt Pathway

The first Wnt pathway to be discovered and the best understood is the canonical Wnt pathway. Acting through a core set of proteins that are highly conserved in evolution, this pathway regulates the ability of β -catenin to activate transcription of specific target genes. This regulation, in turn, results in changes in expression of genes that modulate cell fate, proliferation, and apoptosis (Cadigan and Nusse, 1997; Miller *et al.*, 1999; Wordaz *et al.*, 1998).

Combined work in *Drosophila*, *C. elegans*, *Xenopus* and mice produced the main outline of the canonical Wnt/ β -catenin pathway as is currently understood. A detailed diagram of this pathway can be found at the *Wnt* gene homepage (see above) however Fig. 1.4 shows a stripped down version including only the central components. At the centre of this pathway is β -catenin, a multifunctional protein with independent roles in cadherin-mediated cell adhesion and Wnt signal transduction (Ben-Ze'ev *et al* 1998). The ultimate result of Wnt/ β -catenin pathway activation is the formation of a free, signalling pool of β -catenin in the cell that enters the nucleus where it interacts with members of the TCF/LEF (T cell factor/ Lymphoid enhancer factor) family of HMG (High Mobility Group)-domain transcription factors to stimulate expression of target genes (Behrens *et al.*, 1996; Molenaar *et al.*, 1996; Hsu *et al.*, 1998).

In the absence of a Wnt signal, free cytoplasmic β -catenin is destabilized by a multi-protein destruction complex containing Axin, glycogen synthase kinase 3 β (GSK3 β) and the Adenomatous Polyposis Coli (APC) protein (Zeng *et al.*, 1997; Behrens *et al.*, 1998; Hart *et al.*, 1998; Fagotto *et al.*, 1999; Kishida *et al.*, 1999). This destruction complex facilitates the phosphorylation of β -catenin by GSK3 β . Axin binds APC and both are key negative regulators of Wnt signalling by acting as scaffolds and subsequently binding both β -catenin and GSK3 β . This is important for two reasons; firstly GSK3 β requires both APC and Axin for β -catenin binding and secondly GSK3 β also phosphorylates APC and Axin, which leads to enhanced binding of β -catenin (Ikeda *et al.*, 1998). GSK3 β phosphorylates three conserved

Figure 1.4. The Canonical Wnt Pathway

(a) In the absence of a Wnt signal β -catenin is targeted to the proteasome for degradation. (b) Wnt signalling stabilises β -catenin which translocates to the nucleus, interacts with LEF/TCF family members and results in transcription of target genes. Figure adapted from the Wnt homepage maintained by Roel Nusse.



residues in the amino-terminal region of β -catenin, Ser33, Ser 37 and Thr41. Recent evidence however has shown that efficient phosphorylation of β -catenin by GSK3 β requires casein kinase 1(CK1) phosphorylation at Ser45. This phospho-Ser45 then serves as a priming site for subsequent phosphorylations by GSK3 β (Amit *et al.*, 2002; Liu *et al.*, 2002; Yanagawa *et al.*, 2002). This explains why mutations at Thr41 and Ser45 interfere with β -catenin turnover and are frequently found in human tumours (Polakis, 2000). Phosphorylated β -catenin is bound by the F-box protein β -TrCP, a component of the E3 ubiquitin ligase complex, and is ubiquitinated; the ubiquitin tag marks β -catenin for destruction by the proteasome (Aberle *et al.*, 1997)

Wnt activation of Fzd and LRP leads to the phosphorylation of Dishevelled (Dsh) (Axelrod *et al.*, 1998), a cytoplasmic scaffold protein perhaps through stimulation of casein kinase 1 ϵ (CK1 ϵ)(Sakanaka *et al.*, 1999; Peters *et al.*, 1999) and/or casein kinase 11 (CK11)(Willert *et al.*, 1997). Dsh then functions through its interaction with Axin to antagonize GSK3 β , preventing the phosphorylation and ubiquitination of β -catenin (Kishida *et al.*, 1999; Li *et al.*, 1999; Smalley *et al.*, 1999). In vertebrates, inhibition of GSK3 β may involve GSK3 β binding protein (GBP in *Xenopus* or its mammalian orthologue Frat 1). GBP/Frat binds to both Dsh and GSK3 β and promotes dissociation of GSK3 β from the destruction complex (Li *et al.*, 1999). Thus, unphosphorylated β -catenin escapes degradation, accumulates in the cell, and enters the nucleus where it interacts with members of the TCF/LEF family of HMG –domain transcription factors to stimulate expression of target genes (Behrens *et al.*, 1996; Molenaar *et al.*, 1996; Hsu *et al.*, 1998). These include developmental regulatory genes such as *siamois*, *twin*, and *Xnr-3* in *Xenopus* (Brannon *et al.*, 1997; Fan *et al.*, 1998; Laurent *et al.*, 1997; McKendry *et al.*, 1997) and *ultrabiothorax* in *Drosophila* (Riese *et al.*, 1997). Additional target genes in mammals include *c-myc* and *cyclin D1* genes, which are direct regulators of cell growth and proliferation and have been implicated in cancer consistent with a role for the Wnt pathway in cancer (He *et al.*, 1998; Tetsu *et al.*, 1999). It is noteworthy however that *c-myc* can also activate apoptosis (Prendergast, 1999).

The activity of TCFs is tightly controlled. In the absence of Wnt signalling, negative regulators that bind to TCF actively repress TCF target gene transcription. The transcriptional repressor Groucho (called TLE in vertebrates) can associate with the TCF/ β -catenin complex to downregulate its transcriptional activity (Parkhurst *et al.*, 1998). Another repressor CBP (Creb-binding protein) competes with β -catenin for TCF binding and acetylates a lysine residue in the N-terminus of TCF thereby abolishing its ability to interact with β -catenin and activate transcription. It has been suggested that CBP raises the threshold for β -catenin binding to TCF, keeping TCF from activating transcription until the concentration of β -catenin is high (Waltzer *et al.*, 1998). This tight regulation of TCF thus signifies the importance of incorrect activation of transcription.

Intriguingly, interactions among Wnt pathway components may vary in different developmental processes. The *C. elegans* Wnt pathway that induces endoderm (intestinal cells) differs at most steps from the pathways described above. For example, *apr-1/APC* and *sgg-1/GSK-3 β* are required positively for endoderm induction, whereas the *Drosophila* and mammalian counterparts act negatively, promoting the degradation of β -catenin in the absence of Wnt signals (Han *et al.*, 1997). A positive role for *APC* in Wnt signalling has also been suggested in *Xenopus* by the observation that *XAPC* induces a duplication of the body axis similar to that induced by Wnt (Vleminckx *et al.*, 1997).

1.3.4.2 β -catenin

β -catenin is a multifunctional protein which plays at least two important roles in the cell, firstly mediating cellular adhesion through its interactions with E-cadherin and indirectly, the cytoskeleton, and secondly functioning as a key regulator in the control of expression through the Wnt/Wingless pathway (Gumbiner *et al.*, 1995; Aberle *et al.*, 1996). β -catenin shows a great degree of cross-species conservation both in its structure and its function. Human β -catenin consists of 781 amino acids arranged broadly into 3 important domains (Hulsken *et al.*, 1994); an amino-terminal domain (130 amino acids) which contains multiple GSK-3 β phosphorylation sites

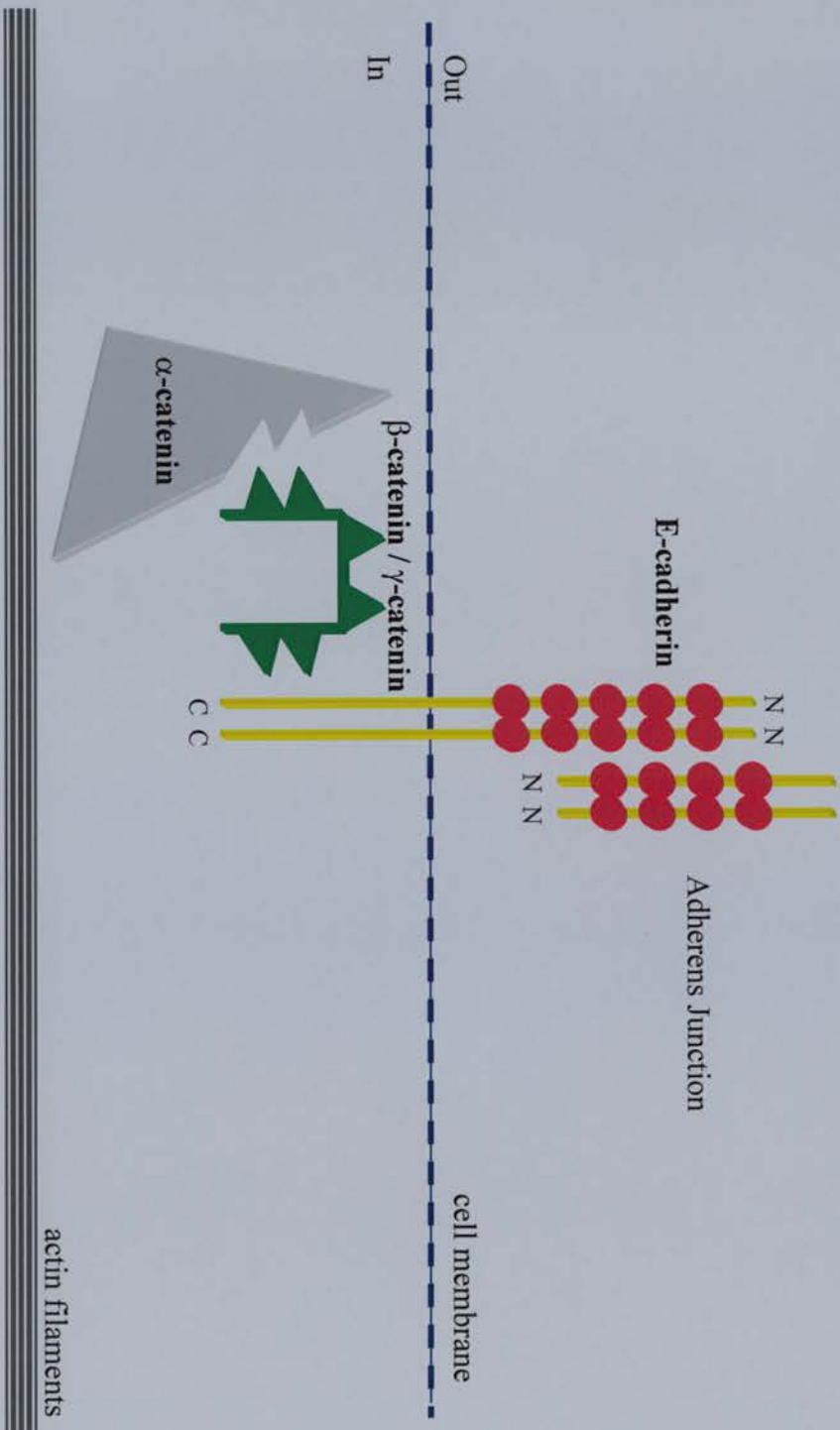
needed for its degradation (Yost *et al.*, 1996), a central domain containing twelve 42 amino acid armadillo repeats and forms an important protein interaction domain while the carboxy terminal (100 amino acids) forms a region of interaction with nuclear transcription factors (Figure 1.3.b)(van de Wetering *et al.*, 1997; Vleminckx *et al.*, 1999; Behrens *et al.*, 1996).

The armadillo repeats together form a tightly packed series of short α -helices with a positively charged central groove, a structure associated with protein-protein interactions (Huber *et al.*, 1997). Indeed, this central region does appear to be involved in the interaction of β -catenin with a number of other proteins, including, E-cadherin (Hulsken *et al.*, 1994), Axin (Nakamura *et al.*, 1998), TCF (Behrens *et al.*, 1996) and APC (Hulsken *et al.*, 1994; Rubinfeld *et al.*, 1995; Yu *et al.*, 1999; Hamada *et al.*, 1999). The interactions of the β -catenin armadillo repeat domain with E-cadherin and with α -catenin play a critical role in cellular adhesion. The cytoplasmic domains of E-cadherin, a calcium ion dependent cell adhesion molecule, bind either β -catenin or γ -catenin (plakoglobin) (Hinck *et al.*, 1994). Subsequently, either catenin molecule (γ or β) is then complexed with α -catenin, which in turn acts as a bridge to bind to actin molecules making up the cytoskeleton (Hinck *et al.*, 1994). In this way, both β -catenin and γ -catenin link cell surface adhesion molecules to the cell architecture (see Figure 1.5).

The multiple functions of β -catenin are possible through a precise subcellular compartmentalization and the fine-tuning of its concentration in each compartment. This regulation is based on the observation that most of β -catenin's protein interacting motifs overlap such that interaction with one partner can block binding of another at the same time, for example, sequestering of β -catenin by APC prevents interaction with cadherin (Hulsken *et al.*, 1994; Rubinfeld *et al.*, 1995). Also a subtle change in the level of signalling-competent β -catenin may have a drastic impact on gene activation. For example, Larabell *et al.*, 1997, have shown that relatively small differences in free β -catenin on the dorsal side of *Xenopus* embryo resulted in axis formation.

Figure 1.5. Function of β -catenin in cellular adhesion

β -catenin and γ -catenin link cell surface adhesion molecules to the cell actin cytoskeleton. The cytoplasmic domains of E-cadherin bind either β -catenin or γ -catenin. Subsequently either catenin molecule is then complexed with α -catenin which in turn acts as a bridge to bind actin molecules making up the cytoskeleton (Ilyas and Tomlinson, 1997).



1.4 Adenomatous Polyposis Coli (APC)

APC is a tumour suppressor gene, first identified by virtue of its mutation in Familial Adenomatous Polyposis (FAP) (see section 1.4.1.2.1) (Groden *et al.*, 1991; Kinzler *et al.*, 1991). The previous section introduced APC as a member of the Wnt signalling pathway, however APC is a large multifunctional protein that can affect a variety of fundamental cellular processes. This section describes the *APC* gene including its structure and functions.

1.4.1 APC

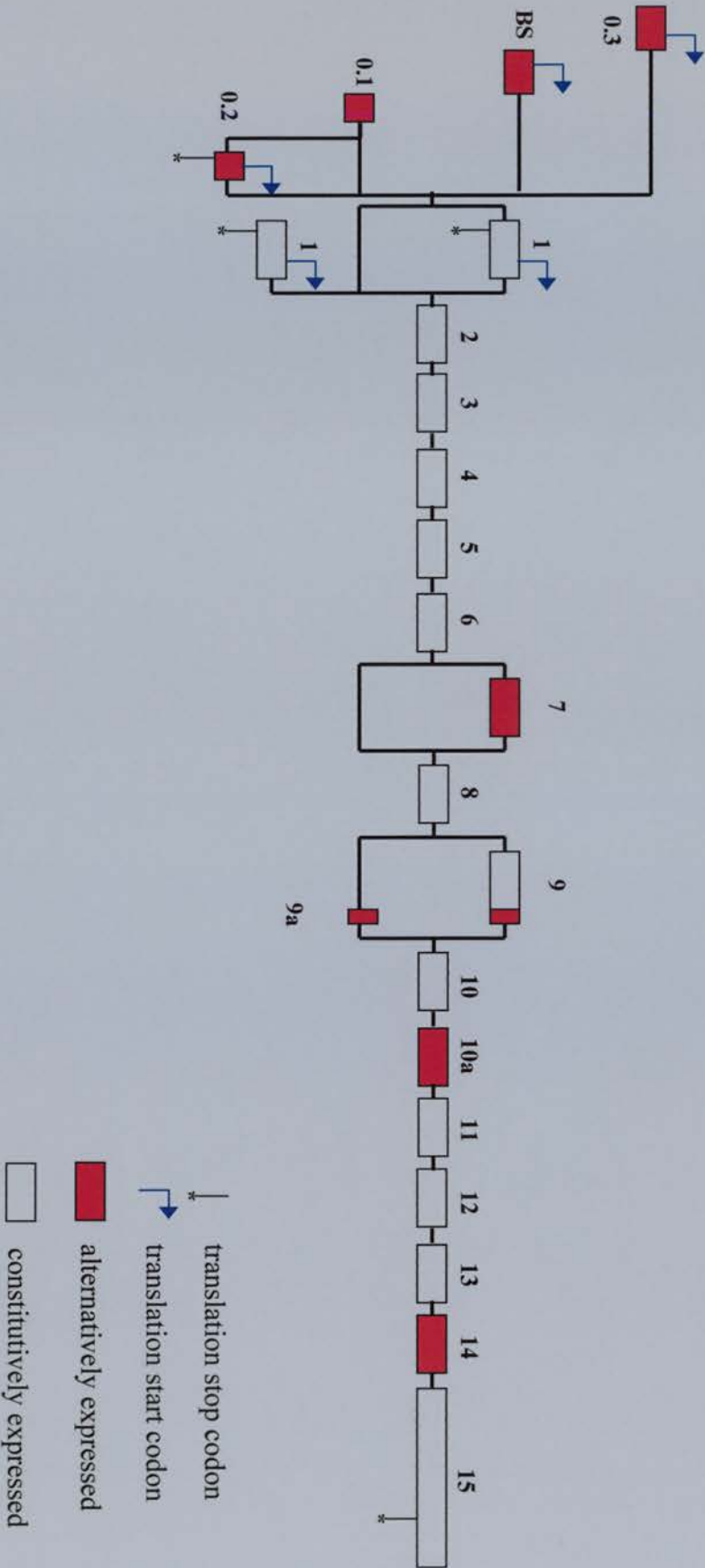
1.4.1.1 Genomic organisation in human and mouse

The *APC* gene is located at human chromosome 5q21 (Kinzler *et al.*, 1991), the mouse homologue is found on chromosome 18 (Luongo *et al.*, 1993). Originally, the *APC* gene was thought to be composed of 15 exons (Groden *et al.*, 1991), exons 1-14 combined occupy the NH₂ – terminal quarter whereas exon 15 alone occupies three quarters of the molecule at the COOH terminal (Groden *et al.*, 1995; Joslyn *et al.*, 1991). However, evidence has accumulated that the *APC* gene codes for a complex pattern of gene products that are generated on the basis of alternative splicing (Bardos *et al.*, 1997) (Fig. 1.6).

To date, at least 21 exons have been identified (Thliveris *et al.*, 1994; Horii *et al.*, 1993; Sulekova *et al.*, 1995), 17 of these are predicted to be coding exons due to their location downstream of an initiating methionine codon in exon 1. Four exons 5' to exon 1 have been identified and these have been termed (from 5' to 3') 0.3, BS (brain specific), 0.2 and 0.1. The BS exon, expression of which is now known not to be restricted to the brain (Pyles *et al.*, 1998) is the best characterised of these. Alternative *APC* isoforms containing BS do not include exon 1 and are found in differentiated tissues such as the brain (Santoro and Groden, 1997). Exon 1 contains a translation start codon for the known APC protein. Therefore transcripts lacking exon 1 must use alternative initiating codons to be translated into proteins. Four

Figure 1.6. Genomic structure of APC

The APC gene codes for a complex pattern of gene products that are generated on the basis of alternative splicing. To date, 21 exons have been identified to comprise the APC gene with 17 of these predicted to be coding exons due to locations downstream of translation start codons. The known APC protein is composed of 15 exons with translation starting in exon 1.



translation start codons have been identified, one each in exons 0.3, BS, 0.2 and 1, however three of these (0.3, BS, 0.2) are upstream of a stop codon in exon 1, suggesting that only alternative *APC* isoforms lacking exon 1 produce full length protein (Thliveris *et al.*, 1994; Santoro and Groden, 1997; Pyles *et al.*, 1998).

Oshima *et al.*, 1993 identified *APC* isoforms lacking exon 7, Horii *et al.*, 1993 reported alternative splicing in exon 9 and Sulekova *et al.*, 1995 identified a novel exon (exon 10A) located 1.6kb downstream from exon 10. In addition, skipping of exon 14, resulting in a novel exon 13/15 connection has been reported but this results in loss of *APC* exon 15 long open reading frame (Sulekova *et al.*, 1995). The coding regions for the human *APC* gene (exons 1-15) are highly conserved in the mouse *Apc* gene (86% identical at nucleotide level) (Su *et al.*, 1992) and most of the splice variants described in human *APC* have also been identified in murine *Apc* (Oshima *et al.*, 1993).

1.4.1.2 Mutations of the *APC* gene

Mutations of the *APC* gene have been identified in several species and the implications of these mutations are discussed in the following sections. Mice homozygous for the *Apc*^{MIN} mutation (truncated after residue 850, see section 1.5.1.1) display embryonic lethality (Moser *et al.*, 1995), while heterozygotes develop multiple adenomas of the intestine with progression to tumours (Moser *et al.*, 1990). Loss of function of a *Drosophila APC* homologue (*D-APC*) causes cell death in neuronal cells (Ahmed *et al.*, 1998) while mutation of another *Drosophila APC* (*E-APC*) results in adhesion defects and activation of Wnt target genes (Hamada *et al.*, 2002). In *C. elegans* mutations in *APR-1* (*APC* related gene) inhibit epithelial cell migration (Hoier *et al.*, 2000). However, mutations of the human *APC* gene are well documented and are discussed below.

1.4.1.2.1 Familial Adenomatous Polyposis (FAP)

The *APC* gene was initially identified by positional cloning of the Familial Adenomatous Polyposis (FAP) locus (Groden *et al.*, 1991; Kinzler *et al.*, 1991). FAP is an autosomal dominant disorder of humans characterised by the development of multiple adenomas of the colorectum and duodenum with progression to colorectal carcinoma in the third to fourth decade of life in an untreated individual (Groden *et al.*, 1991). Tumours arising in patients with FAP show loss of the remaining wild-type *APC* allele (Levy *et al.*, 1994; Luongo *et al.*, 1994). FAP patients also present tumours in other regions of the gastrointestinal tract, and extraintestinal cancers including tumours in the brain, thyroid, adrenal gland and pancreas (Burt *et al.*, 1991; Haggitt *et al.*, 1986). *APC* is also somatically mutated in the majority, (>80%), of sporadic colorectal tumours (Miyoshi *et al.*, 1992)

Almost all of the mutations of *APC*, both germline and somatic, result in the premature truncation of the gene product through nonsense or frameshift mutations (Miyoshi *et al.*, 1992). While mutations have been found throughout the length of the *APC* coding sequence the majority of mutations resulting in deleterious phenotypes, occur in the 5' portion of the coding sequence. Many of the somatic mutations are located in the central region of the gene termed the mutation cluster region (MCR) (Miyoshi *et al.*, 1992). Consequently mutations of the *APC* gene result in the expression of APC proteins lacking the C-terminal half of the molecule and unable to perform many of the normal protein interactions as described below (Kinzler *et al.*, 1996; Polakis, 2000; van Es *et al.*, 2001).

1.4.2. The APC tumour suppressor protein

1.4.2.1 Structure and protein interactions

The *APC* gene codes for a protein of 2843 amino acids, (~310 kDa) containing a number of distinct domains and repeated elements (see figure 1.3c) (Polakis, 1995;

Polakis, 1997). Many of the repeat elements of the APC protein have been recognized as motifs involved in interaction with other proteins. To date a large number of these interactions have been confirmed and explored.

Beginning with the amino terminal region of the protein the first recognized active region of the APC protein is an oligomerisation domain, believed to contain >95% α -helical conformation. This domain contains a series of heptad repeats, the most important of which is the first heptad repeat (amino acids 6-57) (Joslyn *et al.*, 1993; Su *et al.*, 1993). Immunoprecipitation experiments involving truncated and wild type proteins established that APC has the ability to bind to itself (Su *et al.*, 1993). The ability of the APC protein to oligomerise may be responsible for the observations of dominant-negative effects of mutant APC proteins made by some researchers (Dihlmann *et al.*, 1999). It is also possible that the protein products of certain splice variants of the *APC* gene may lack the oligomerisation domain, presumably creating a protein with altered activity or regulation (Samowitz *et al.*, 1995).

Moving towards the carboxy terminus of the APC protein, the next region is a series of armadillo repeats (residues 453-767) (Polakis, 1997). These repeats are homologous to 42 amino acid motifs found initially in the *Drosophila* armadillo protein, the homologue of the human β -catenin protein (Hatzfeld, 1999). This segment of the APC protein contains 7 armadillo repeats and the function of these repeats appears to be protein-protein interaction (Hirschl *et al.*, 1996). The armadillo region of APC has been shown to bind to the regulatory B56 subunit of protein phosphatase 2a (PP2A) a protein capable of interacting with and involved in the regulation of Axin, (Seeling *et al.*, 1999; Hsu *et al.*, 1999) and this interaction facilitates the nuclear import of APC (Galea *et al.*, 2001). The armadillo region is also known to bind to the APC-stimulated guanine nucleotide exchange factor (Asef), which acts as a guanine nucleotide exchange factor for the Rac GTP binding proteins. This interaction stimulates Asef activity, thereby regulating the actin cytoskeletal network and cell morphology (Kawasaki *et al.*, 2000). Additionally, APC interacts with the kinesin superfamily (KIF) 3A-KIF3B proteins, microtubule plus-end-directed motor proteins, through an association with the kinesin

superfamily-associated protein 3 (KAP3). The authors speculate that the interaction between APC and KAP3 functions to transport APC along microtubules (Jimbo *et al.*, 2003).

The pattern of somatic mutations indicates that the armadillo repeats are typically retained by the mutant APC proteins and therefore cannot independently convey tumour suppressor activity. In cases where mutation does cause a loss of some armadillo repeats from the APC protein the number of repeats lost shows a positive correlation with development of congenital hyperplasias of the retinas (Davies *et al.*, 1995; Wallis *et al.*, 1994; Wallis *et al.*, 1999). This may support the observations by some researchers of a potential partial dominant-negative effect of truncated APC protein (Dihlmann *et al.*, 1999).

Downstream of the armadillo repeat segment of the APC protein, are found three 15 amino acid repeats, responsible for the binding of β -catenin (amino acids 1020-1169) (Su *et al.*, 1993). These repeats are not homologous to the motifs found on other proteins which interact with β -catenin (T-cell factor (TCF)/Lymphocyte enhancer factor (LEF) transcription factors and cadherins for example) and need not be removed by truncation mutation to eliminate the tumour suppressor functions of the APC protein (Kintner, 1992; Ozawa *et al.*, 1995; Polakis, 1995; Beroud and Soussi, 1996).

Following the β -catenin binding repeats are a series of 7 relatively dispersed 20 amino acid motifs (amino acids 1324–2075) (Grodén *et al.*, 1991). These 20 amino acid repeats bear some resemblance to the 15 amino acid repeats found more N-terminal and were believed to play a role in the binding and subsequent degradation of β -catenin. This is in part supported by the fact that most tumourigenic truncation mutations of APC eliminate some or all of these motifs (Polakis, 1995). This may not be the whole story, however, as interspersed with these β -catenin binding and degradation domains are amino acid motifs, which bind Axin (Zeng *et al.*, 1997). Axin acts as a scaffold protein in the canonical Wnt signalling pathway bringing together a number of proteins in order to function as a regulator of free cellular β -

catenin levels and hence regulate transcription of *Wnt* target genes (see section: 1.3.4.1.). It may be that the tumourigenic potential of the truncated APC proteins is not entirely due to the loss of the 20 amino acid repeats but rather due to the loss of Axin interaction elements preventing the formation of protein complexes necessary for β -catenin degradation.

The next region of protein interaction is the basic domain, stretching approximately from amino acid 2200 to 2400, containing a higher proportion of the basic residues arginine and lysine (Groden *et al.*, 1991). This region of the APC protein enables it to bind to microtubules and full length APC is believed to be capable of promoting the polymerisation of tubulin *in vitro*, while mutant APC proteins are unable to encourage this reaction (Smith *et al.*, 1994; Munemitsu *et al.*, 1994). This ability to assemble and/or associate with microtubules may in part explain the localisation of APC to the leading edge of migrating cells, a region where microtubule assembly is required, and in addition may lend itself to the observations of disordered cell migration in models of APC overexpression and in animal models of FAP (Nathke *et al.*, 1996; Wong *et al.*, 1996; Mahmoud *et al.*, 1997; Mahmoud *et al.*, 1999).

Finally the C-terminal region of APC interacts with at least two other proteins, end-binding protein 1 (EB1) and Human Discs Large (hdlg). EB1 is a small microtubule binding protein and binds APC in the final 170 amino acids (Askham *et al.*, 2000). The binding site for PDZ domains (protein-protein interaction domains as found in the human homologue of the *Drosophila* Discs Large (dlg)) resides in the last 15 amino acids (Matsumine *et al.*, 1996). The hdlg protein is the human homologue of the *Drosophila* Discs Large (dlg) tumour suppressor protein which when lost in *Drosophila* results in neoplastic growth in the imaginal disc of the developing embryo (Bryant *et al.*, 1993).

In addition to the APC protein described above, a second related protein has been identified in a number of species. APCL in humans (Nakagawa *et al.*, 1998) and APC-2 in mouse (van Es *et al.*, 1999), which are both highly related and thus called APC-2/L. In *Drosophila* there are also two forms of APC, D-APC and E-APC

(Hayashi *et al.*, 1997; McCartney *et al.*, 1999; Yu *et al.*, 1999). D-APC which was the first *Drosophila* APC identified is expressed predominantly in the nervous system and negatively regulates Arm/ β -catenin signalling in the *Drosophila* eye. Loss of D-APC therefore, only has an effect in the larval photoreceptors and has no effect on Wg-dependent patterning at any developmental stage (Ahmed *et al.*, 1998). These observations suggested the existence of a second APC gene. E-APC is ubiquitously expressed, interacts directly with Arm and negatively regulates Wg signalling. Inactivation of E-APC results in the constitutive activation of Wg signalling but this is restricted to embryogenesis (Hayashi *et al.*, 1997; McCartney *et al.*, 1999; Yu *et al.*, 1999). In general these related proteins are shorter and lack some of the typical motifs of APC and thus vary in their ability to bind additional proteins, however they can all function in Wnt signalling (Nakagawa *et al.*, 1998; van Es *et al.*, 1999; Ahmed *et al.*, 2002).

1.4.2.2 Subcellular localisation

APC protein expression has been detected in four subcellular regions, cytoplasm, nucleus, associated with the plasma membrane, or associated with microtubule tips (Nathke *et al.*, 1996; Neufeld & White, 1997). APC protein can also shuttle between the nucleus and the cytoplasm by virtue of conserved and functional nuclear-export signals (NESs) (Rosin-Arbesfeld *et al.*, 2000; Henderson *et al.*, 2000; Neufeld *et al.*, 2000). Nuclear import of APC seems to be mediated by the amino terminal armadillo repeat domain (Rosin-Arbesfeld *et al.*, 2000; Galea *et al.*, 2001) and also by nuclear-localisation signals (NLSs) (Zhang *et al.*, 2000). The function of APC at each of these locations is detailed below.

1.4.3 Functions of APC

The role of APC in the prevention of tumour development, or more accurately the failure of truncated APC to prevent neoplastic transformation, has led to an intense

study of its role in normal and dysregulated cell functioning. Its main function as a tumour suppressor involves regulating β -catenin levels in the Wnt signalling pathway (Munemitsu *et al.*, 1995). In addition APC is linked directly to the cytoskeleton and plays a role in cytoskeletal regulation, cell migration, cell division and cell adhesion (Nathke, 1999; Dikovskaya *et al.*, 2001; Bienz, 2002).

1.4.3.1 APC in the Wnt signalling pathway

APC protein functions as a negative regulator of the canonical Wnt pathway by promoting the destabilisation of β -catenin. APC forms part of the multi-protein destruction complex that facilitates the phosphorylation of β -catenin by GSK3 β thereby targeting it for ubiquitination and subsequent destruction by the proteasome (Munemitsu *et al.*, 1995). This function is mediated in part through two distinct β -catenin binding domains of APC, but also through Axin binding to APC and this latter activity is crucial for APC's role as a tumour suppressor (Smits *et al.*, 1999; Rubinfeld *et al.*, 2001). This is supported by the fact that all three Axin-binding motifs are located downstream of the MCR, resulting in mutant APC that has lost the ability to bind Axin. Thus the tumourigenic potential of the truncated APC proteins is not entirely due to the loss of the 20 amino acid repeats but rather due to the loss of Axin interaction elements preventing the formation of protein clusters necessary for β -catenin degradation (Smits *et al.*, 1999).

The identification of APC as a shuttling protein has led to speculation that the nuclear-export function of APC controls the level or transcriptional activity of nuclear β -catenin (Henderson *et al.*, 2000). It was originally proposed that APC transports β -catenin directly out of the nucleus (Bienz, 1999). However it is also possible that APC, by binding β -catenin, blocks TCF/LEF transcriptional activation and shifts the equilibrium of β -catenin to the cytoplasm where it is then degraded (Neufeld *et al.*, 2000). Most mutant disease-linked truncated forms of APC lack the two central nuclear-localisation signals (NLSs) and certain NESs but retain nuclear-cytoplasmic shuttling activity via an N-terminal NES and nuclear import facilitation

by the N-terminal ARM domain (Galea *et al.*, 2001). However it is believed that this compromised nuclear-export activity is insufficient for full tumour suppressor function. Some studies have shown that an exogenous APC fragment that mimics typical APC cancer truncations had low nuclear export and failed to reduce TCF mediated transcription (Rosin-Arbesfeld *et al.*, 2000; Bienz, 2002).

1.4.3.2 APC and the cytoskeleton

APC associates with the cytoskeleton in at least two ways, directly binding microtubules (Smith *et al.*, 1994; Munemitsu *et al.*, 1994) and indirectly connecting with the actin cytoskeleton (Townesley *et al.*, 2000).

APC appears to interact with microtubules in at least three ways; the C-terminus basic domain directly binds microtubules (Munemitsu *et al.*, 1994) and an adjacent domain binds to End-binding protein 1 (EB1), a microtubule binding protein (Su *et al.*, 1995). Additionally, it has been reported that APC lacking the basic domain still associates with microtubules (Dikovskaya *et al.*, 2001; Mimori-Kiyosue *et al.*, 2000; Zumbunn *et al.*, 2001). An APC isoform lacking the EB1 binding site can bind EB3 (an EB1 family member) indicating that there may also be more than one binding site for EB1-like proteins (Nakagawa *et al.*, 2000). APC was discovered to localise at the distal tips ('plus ends') of microtubules that meet the plasma membrane in cellular protrusions of actively migrating cells (Nathke *et al.*, 1996). Here APC is involved in stabilizing microtubules (Zumbunn *et al.*, 2001) and there is a correlation between the dissociation of APC from growing microtubule ends and their subsequent depolymerization (Mimori-Kiyosue *et al.*, 2000). This function aids in the formation of cellular protrusions that are important for cell migration.

Defects in epithelial cell migration are apparent upon examination of adenomatous polyps from both mice and humans (Oshima *et al.*, 1995; Moss *et al.*, 1996; Oshima *et al.*, 1997) and overexpression of APC in gut epithelia of mice induced disordered cell migration in the intestinal epithelium (Wong *et al.*, 1996). Normally colonic

epithelial cells migrate upwards from the crypt base forming coherent columns, however in FAP patients one reason for polyp formation may be due to defective epithelial cell migration increasing both the time cells remain in the proliferative environment of the crypt and their exposure to toxins present in the gut. Mutations in *APR-1* inhibit epithelial cell migration in *C. elegans* (Hoier *et al.*, 2000).

Microtubules are important for the formation of mitotic spindles that mediate chromosome segregation during mitosis. In metaphase cells, when the spindle microtubules attach to kinetochores, APC is localised at microtubule tips (Kaplan *et al.*, 2001). APC directly binds to a kinetochore protein, Bub 1 thus APC could promote the growth of spindle microtubules toward the kinetochore, or attach the kinetochore to the spindle via Bub1 (a mitotic checkpoint kinase) (Kaplan *et al.*, 2001). EB1 also associates at the growing plus ends of cytoplasmic and spindle microtubules and is required for the APC-mediated attachment of microtubules to kinetochores (Fodde *et al.*, 2001).

Mutations in the *APC* gene cause chromosomal instability (CIN). Cells expressing mutant APC that lacks the C-terminal structural domains are prone to defects in chromosome segregation and develop aneuploidy (Kaplan *et al.*, 2001; Fodde *et al.*, 2001) and this has been shown to be an early event in colorectal cancer (Shih *et al.* 2001).

Studies in *Drosophila* show that APC isoforms that lack microtubule-binding sites (APC-2/E-APC) associate with actin indirectly (Townsend *et al.*, 2000) possibly through catenins and other actin-binding proteins such as Dlg (Matsumine *et al.*, 1996). This membrane associated APC has a function in cellular adhesion. Hamada & Bienz, 1999, show that E-APC containing a missense mutation becomes delocalised from the plasma membrane and results in adhesion defects at the phenotypic and ultrastructural levels.

1.5 The APC Tumour Suppressor Protein in Cancer

Genetic evidence from humans and mouse models suggest that *APC* is a classic tumour suppressor, requiring both alleles to be inactivated for tumour growth to develop (Luongo *et al.*, 1994; Levy *et al.*, 1994; Oshima *et al.*, 1995; Laird *et al.*, 1995). The type of germline mutation in *APC* determines the nature of the second hit, which is either allelic loss or truncation mutation. FAP patients with germline mutations close to codon 1300 tend to acquire a 'second hit' at *APC* by allelic loss, whereas those with germline mutations away from codon 1300 are more likely to have 'second hits' by truncating mutations in the MCR (Lamlum *et al.*, 1999). Thus different *APC* mutations provide cells with different selective advantages, which are reflected in the probability and rate of tumour growth (FAP patients with germline mutations around codon 1300 are known to have very severe colonic polyposis) (Nugent, *et al.*, 1994). In a mouse model of FAP, the *Min* mouse (see below), tumour formation also requires loss of the wild type *Apc* allele, most commonly by chromosome loss but also through somatic *Apc* truncation mutations that resemble those observed in human intestinal tumours (Luongo *et al.*, 1994).

As mentioned in section 1.4, mutational inactivation of the *APC* tumour suppressor gene initiates most hereditary and sporadic colon carcinomas. Both hereditary and sporadic human colorectal tumours evolve from adenomatous polyps to larger malignant carcinomas over the course of several decades (Groden *et al.*, 1991; Powell *et al.*, 1992). *APC* mutations are a very early event in sporadic colorectal tumourigenesis and associate with tumour initiation (Powell *et al.*, 1992). Patients with FAP typically develop hundreds to thousands of colorectal adenomas during their second and third decades of life and due to their large numbers some eventually progress to malignant carcinomas (Kinzler and Vogelstein, 1996). Both human germline and somatic *APC* mutations almost invariably produce truncated proteins lacking the C-terminal half of the molecule (Miyoshi *et al.*, 1992). Loss of Axin and some β -catenin binding sites in the APC C-terminus prevents the downregulation of β -catenin by APC resulting in its interaction with LEF/TCF transcription factors and activation of target genes that participate in cancer progression (Munemitsu *et al.*,

1995; He *et al.*, 1998). In support of this idea that β -catenin acts as an oncogene, mutations in β -catenin have been detected in human colon cancers (Morin *et al.*, 1997) and cancer cell lines (Rubinfeld *et al.*, 1997) that have wild-type *APC*. Additionally, mutations resulting in loss of APC microtubule binding domains results in defects in cell migration (Oshima *et al.*, 1995; Moss *et al.*, 1996; Oshima *et al.*, 1997), adhesion (Hamada & Bienz, 1999) and chromosomal instability (Fodde *et al.*, 2001), which are all features of colon cancer.

Importantly, mutations of the *APC* gene have been subsequently implicated in a large number of tumours derived from other tissues. These tumours, which include osteomas, desmoid tumours (Miyaki *et al.*, 1993; Davies *et al.*, 1995), brain tumours (Itoh *et al.*, 1993) and breast tumours (Furuuchi *et al.*, 2000; Virmani *et al.*, 2001; Jin *et al.*, 2001) were found to be missing alleles of *APC* and/or to contain mutated sequences coding for truncated versions of the APC protein. Desmoid tumours are defined as benign fibrous tumours that do not metastasise and are frequently observed in FAP patients after abdominal surgery (Miyaki *et al.*, 1993). FAP patients are 92 times more likely than the general population to develop medulloblastoma (Hamilton *et al.*, 1995). Medulloblastoma is a malignant invasive embryonal tumour of the cerebellum with a preferential manifestation in children. Turcot's syndrome, a condition characterised clinically by the concurrence of a primary brain tumour and multiple colorectal adenomas, is reportedly due to germline *APC* mutation. *APC* mutations have also been detected in a subset of sporadic medulloblastomas (Huang *et al.*, 2000). There is continuing debate over whether *APC* mutations play a causative role in breast cancer, a topic which is summarised below.

1.5.1 The APC tumour suppressor protein and breast cancer

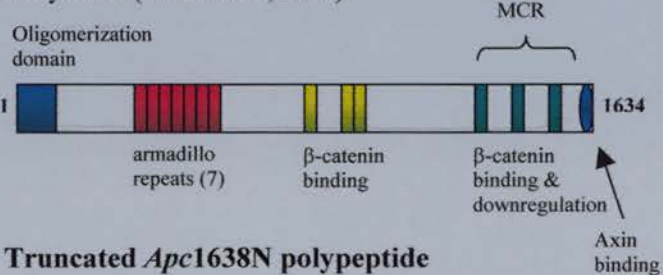
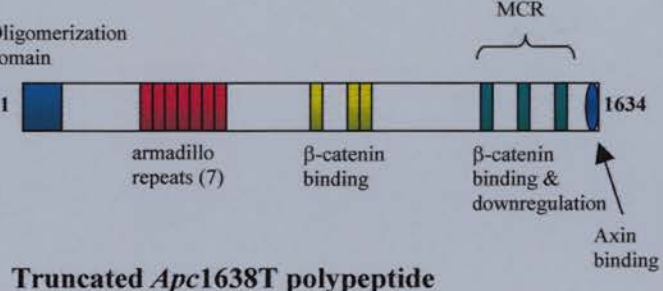
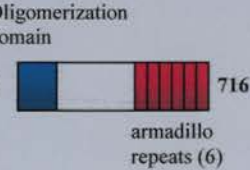
1.5.1.1 The *Min* (Multiple intestinal neoplasia) mouse

The first evidence that *APC* mutation may play a role in mammary cancer came from studies of the *Min* mouse. *Min* (multiple intestinal neoplasia) is an ethylnitrosourea (ENU)-induced mutation in the murine *Apc* gene (Moser *et al.*, 1990; Su *et al.*, 1992). ENU, a direct-acting alkylating agent, induces germline mutations that are usually single base pair changes (Moser *et al.*, 1990). *Min* is a nonsense mutation at codon 850 of *Apc* resulting in premature truncation of the protein just after the armadillo repeat region, therefore lacking the β -catenin regulatory domains (Su *et al.*, 1992). This mutation is analogous to that seen in humans with FAP (Joslyn *et al.*, 1991) and thus represents a mouse model of FAP. Table 1.5.1 summarises the other identified mouse models of FAP.

On the C57BL/6J (B6) background, *Min*/+ mice develop more than 50 adenomas throughout the intestinal tract and rarely survive beyond 120 days due to secondary effects of tumour growth including severe, chronic anaemia and intestinal blockage (Moser *et al.*, 1990). Tumour formation in these mice is invariably associated with somatic loss of the wild type (wt) *Apc* allele, most commonly by chromosome loss but also through somatic *Apc* truncation mutations that resemble those observed in human intestinal tumours (Luongo *et al.*, 1994; Shoemaker *et al.*, 1997). Mice homozygous for the *Min* mutation demonstrate early embryonic lethality at approximately 6.5 days post-coitum (Moser *et al.*, 1995).

Significantly, *Min*/+ female mice are also predisposed to spontaneous and carcinogen induced mammary tumours (Moser *et al.*, 1993). Approximately 5% of B6 *Min*/+ female mice spontaneously develop a single adenocanthoma, however both the incidence and multiplicity of mammary tumours are dramatically increased in *Min*/+ females by somatic treatment with ENU (Moser *et al.*, 1993). The hormonal stimulation of pregnancy and lactation were not necessary for *Min*-induced mammary cancer as most of the mice that developed mammary tumours were

Table 1.5.1 – Mouse models of FAP

<u>Mouse Model</u>	<u>Mutation</u>	<u>Phenotype</u>
<i>Apc</i> ^{1638N}	<p>Gene targeting in ES cells: PGK-neomycin gene introduction at codon 1638 in the opposite transcriptional orientation to that of <i>Apc</i>. The expected truncated <i>Apc</i> polypeptide (185kDa) was not always present, thus termed a leaky allele (Fodde et al., 1994).</p>  <p>Truncated <i>Apc</i>^{1638N} polypeptide</p>	<p><u><i>Apc</i>^{+/1638N} mice:</u></p> <ul style="list-style-type: none"> - Intestinal tumours - Desmoids - Cutaneous cysts (Fodde et al., 1994) <p><u><i>Apc</i>^{1638N/1638N} mice:</u></p> <ul style="list-style-type: none"> - Embryonic lethal (Kielman et al., 1999)
<i>Apc</i> ^{1638T}	<p>Gene targeting in ES cells: PGK-hygromycin cassette introduction at codon 1638 in the same transcriptional orientation as <i>Apc</i>. Results in the truncation of the <i>Apc</i> polypeptide (185kDa) (Smits et al., 1999)</p>  <p>Truncated <i>Apc</i>^{1638T} polypeptide</p>	<p><u><i>Apc</i>^{+/1638T} mice:</u></p> <ul style="list-style-type: none"> - No tumours or major abnormalities <p><u><i>Apc</i>^{1638T/1638T} mice:</u></p> <ul style="list-style-type: none"> - Survive to adulthood - Growth retardation - Reduced postnatal viability on B6 genetic background - Absence of prepubital glands - Formation of nipple associated cysts (Smits et al., 1999)
<i>Apc</i> ^{Δ716}	<p>Gene targeting in ES cells: introduction of a neomycin gene at <i>Apc</i> codon 716. This targeted mutation results in a truncated protein (Oshima et al., 1995).</p>  <p>Truncated <i>Apc</i>^{Δ716} polypeptide</p>	<p><u><i>Apc</i>^{+/Δ716} mice:</u></p> <ul style="list-style-type: none"> - Intestinal adenomas <p><u><i>Apc</i>^{Δ716/Δ716} mice:</u></p> <ul style="list-style-type: none"> - Embryonic lethal (Oshima et al., 1995).

virgins. Transplantation experiments, where mammary cells from *Min/+* female mice were transferred to wild type hosts demonstrated that tumour susceptibility is intrinsic to *Min/+* mammary tissue (Moser *et al.*, 1993). *APC* mutation had not been reported to be a feature of human breast cancer and this discovery was the first evidence that *Apc* mutation was involved in mammary cancer and thus prompted much research into the human condition.

1.5.1.2 APC and human breast cancer

Somatic mutations of the *APC* gene, although originally reported to be quite rare in human breast cancers (Sorlie *et al.*, 1998), were detected in 18% of primary breast cancers in a later study (Furuuchi *et al.*, 2000). Prior to this, frequent loss of heterozygosity (LOH) at 5q21 (Thompson *et al.*, 1993; Medeiros *et al.*, 1994; Kashiwaba *et al.*, 1994) and reduced or lost expression (40.7%) of the APC protein had been reported in human primary breast carcinomas (Ho *et al.*, 1999).

Aberrant methylation of the *APC* locus has been reported in about 18% of sporadic colorectal carcinomas (Hiltunen *et al.*, 1997; Esteller *et al.*, 2000) and is recognised as an alternative mechanism to gene mutations for the transcriptional silencing of many tumour suppressor genes (Baylin *et al.*, 1998). Hypermethylation of the *APC* promoter CpG island was detected in 30% of primary tumours in one study (Tamura *et al.*, 2001) and in 44% of breast cancer tumours and cell lines in another (Virmani *et al.*, 2001). The frequency of methylation in breast cancer increased with tumour stage and size and the authors suggest methylation status may be associated with poor prognosis (Virmani *et al.*, 2001).

Additionally, Laken *et al.*, 1997, reported a new mutation in the *APC* gene, I1307K, which is caused by a transversion of T-A in nucleotide 3920 creating a hypermutable tract. This mutation, which was found to be predominant in Ashkenazi Jews, predisposes to colorectal cancer and has been associated with an increased risk for breast cancer in the same population. This effect was mainly limited to women who

also carried *BRCA* mutations (Redston *et al.*, 1998). *BRCA1* and *BRCA2* are two breast-cancer-susceptibility genes and inherited mutations in either predisposes to breast, ovarian and other cancers (reviewed in Venkitaraman, 2002).

Finally, an *APC* mutation was identified in a human breast cancer cell line that resulted in the expression of truncated APC and was associated with increased β -catenin levels (Schlosshauer *et al.*, 2000). Although reports of overexpression of several WNTs, including WNT2, WNT4, WNT5A, WNT7B, and WNT10B in a proportion of breast tumours have been documented (Huguet *et al.*, 1994; Lejeune *et al.*, 1995; Dale *et al.*, 1996; Bui *et al.*, 1997) this discovery, that due to *APC* mutation β -catenin levels were dysregulated, was the first evidence linking Wnt signal activation to human breast cancer. This correlates with data proposing that high β -catenin activity is associated with poor prognosis of breast cancer patients (Lin *et al.*, 2000).

1.5.1.3 Wnt signalling and mouse mammary carcinomas

1.5.1.3.1 β -catenin overexpression

Over the past decade numerous transgenic mice have been generated, in which the Wnt pathway is activated in the mammary gland. As mentioned in section 1.1.3.1 molecules that activate the Wnt pathway have been expressed ectopically in mammary epithelium under the control of the MMTV-LTR, including *Wnt1* (Tsukamoto *et al.*, 1988) and *Wnt10b* (Lane and Leder, 1997) both of which result in mammary carcinoma. In addition stabilised forms of β -catenin have been overexpressed from the MMTV promoter in several studies (Michaelson and Leder, 2001; Imbert *et al.*, 2001). MMTV- Δ N90 β -catenin lacks the first 90 codons and mice expressing this transgene develop mammary gland hyperplasia and adenocarcinoma. The histopathology of tumours dissected from these mice is reportedly identical to that observed in tumours derived from MMTV-*Wnt1* and MMTV-*Wnt10b* mice (Michaelson and Leder, 2001). MMTV- Δ N89 β -catenin is deleted in the N-terminal 89 amino acids but retains cadherin/catenin binding and has greater stability in the

cytoplasmic pool (Imbert *et al.*, 2001; Munemitsu *et al.*, 1996). Female mice expressing this transgene display precocious lobuloalveolar development and premature differentiation, as determined by β -casein expression in the mammary gland. In addition, all transgenic females develop multiple aggressive adenocarcinomas, with tumours becoming visible in breeding females from 4 months of age and virgin females by 7 months (Imbert *et al.*, 2001).

1.5.1.3.2 Cyclin D1 overexpression

Cyclin D1 is a downstream target of the Wnt signalling pathway and is one of the most commonly overexpressed oncogenes in human breast cancer (Sutherland and Musgrove, 2002). Cyclin D1 plays a pivotal role in the regulation of progression from G₁ to S phase of the cell cycle through the formation of active enzyme complexes with cyclin-dependent kinases Cdk4 and Cdk6 (reviewed in Sutherland and Musgrove, 2002). In humans, *in situ* hybridisation studies suggest that cyclin D1 overexpression occurs at the transition from *in situ* to invasive carcinoma, and thus may represent a late event in tumourigenesis (Weinstat-Saslow *et al.*, 1995). In contrast, immunohistochemical studies demonstrate cyclin D1 overexpression in preneoplastic lesions consistent with an early role of cyclin D1 in mammary gland neoplasia (Alle *et al.*, 1998). Female mice overexpressing *cyclin D1* from the MMTV promoter display increased proliferation and precocious alveolar development in the virgin mammary gland (Wang *et al.*, 1994). These mice eventually developed mammary adenocarcinomas after 1 year of age. This data is consistent with cyclin D1 overexpression contributing to mammary gland hyperplasia.

1.6 Conditional gene targeting in the mouse mammary gland

One method for addressing the significance of gene deficiency *in vivo* is conditional gene targeting. Conditional gene targeting is an invaluable method for overcoming the high incidence of embryonic lethality observed in constitutive knockouts (for

example Apc), and for discerning the *in vivo* significance of gene deficiency in specific tissues. Two methods of conditional gene targeting, the *cre-loxP* and Flp-*frt* systems, are in existing use in mammals. Of these, the *cre-loxP* system has been used with the most frequent success.

1.6.1 Cre-*loxP* recombination system

The *cre-loxP* recombinase system evolved within bacteriophage P1 as a mechanism to maintain correct unit copy segregation of the prophage within host cells. Bacteriophage P1 encodes a 38-kDa *cre* recombinase that catalyses site-specific DNA recombination between 34-base pair repeats termed loci of recombination or '*loxP*' sites (Sauer and Henderson, 1988). *Cre* recombinase, expressed ectopically in mammalian cells, induces either deletion or inversion of the sequences flanked by the *lox* sites dependent upon *lox* site orientation (Figure 1.7). The *cre-loxP* system can function in a highly efficient manner in directing tissue-specific, site-specific, and heritable chromosomal DNA recombination events in transgenic mice *in vivo* (see Table 1.6.1). The ability to generate temporally and/or spatially restricted gene alterations largely resolves two of the main problems associated with conventional gene 'knock-outs', namely embryonic lethality and secondary effects of the targeting event, such as developmental compensation.

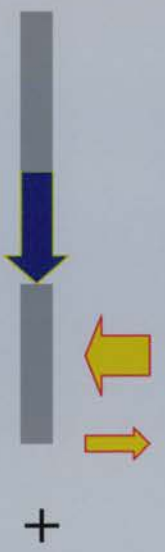
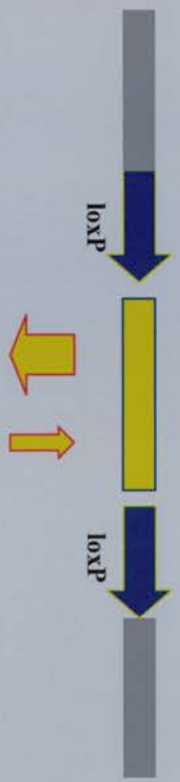
1.6.2 Conditional β -catenin overexpression

As mentioned previously (section 1.5.1.3.1), several studies have documented the pathological effect of dysregulated β -catenin in the mammary gland. A criticism of these studies is that overexpression of β -catenin from an ectopic promoter does not question the effect of endogenous β -catenin levels on mouse mammary gland development. Using *cre-loxP* technology Keiko Miyoshi's research group have manipulated endogenous β -catenin levels and have reported on the effects of this dysregulation on an assortment of cell types in the mammary gland (Miyoshi *et al.*,

Figure 1.7. A model describing the Cre-lox system of site directed recombination. Recombination of loxP sites is mediated by Cre recombinase (denoted by yellow arrows). Excision of the floxed allele is energetically favourable over the reverse reaction. Inversion is reversible in the continued presence of Cre.

Excision

Direct repeats of loxP flanking the gene of interest



Deleted allele, incorporating one loxP site

+

Recombined circular product, incorporating Excised allele and one loxP site

Inversion

Inverted repeats of loxP flanking the gene of interest



Inverted allele

Table 1.6.1 – Use of cre-loxP technology in the mouse

Tissue-specific cre

Adipose tissue (aP2-cre)	Barlow et al., 1997
Mammary gland (BLG-cre)	Selbert et al., 1998
Skin (Keratin-5-cre)	Tarutani et al., 1997
Cardiac muscle (α -MHC-cre)	Agah et al., 1997
Kidney (AQP2-cre)	Nelson et al., 1998
Pancreas (Rat Insulin-cre)	Ray et al., 1998
Cerebellum (GFAP-cre)	Gustafsson et al., 2001
Smooth Muscle (SM-MHC-cre)	Regan et al., 2000
T cell (Ick-cre)	Gu et al., 1994
CNS (Synapsin 1-cre)	Zhu et al., 2001

Inducible-cre

Tetracycline-inducible cre	St-Onge et al., 1996
Interferon α/β -inducible cre	Kuhn et al., 1995
4-hydroxytamoxifen-inducible cre	Feil et al., 1996; Zhang et al., 1996; Hayashi and McMahon, 2002

Chromosomal Translocations

Modelling the t(8;21) reciprocal translocation found in human acute myeloid leukaemia	Exploits Nestin-driven cre to overcome lethal effects in early embryogenesis Buchholz et al., 2000
Modelling the t(9;11) reciprocal translocation found in human leukaemia	Exploits ubiquitously expressed cre (deleter mice, Schwenk et al., 1995) Collins et al., 2000

2002). Two different cre transgenes, one using the mammary-specific whey acidic protein (WAP) gene promoter and the other exploiting MMTV-LTR, were used to conditionally excise exon 3 of a floxed β -catenin allele. Whereas WAP-cre is expressed in mammary alveolar epithelium transiently during oestrus and during pregnancy (Pittius *et al.*, 1988; Robinson *et al.*, 1995), MMTV-LTR driven cre is expressed in both ductal epithelium (during puberty) and in alveolar epithelium (during pregnancy) (Wagner *et al.*, 2001; Walton *et al.*, 2001). Deletion of exon 3 (amino acids 5-80) of the β -catenin gene removes the N-terminal region that is the target of GSK3 β phosphorylation and consequently renders the protein resistant to degradation by the proteasome (section 1.3.4.1) (Harada *et al.*, 1999; Miyoshi *et al.*, 2002). Stabilisation of β -catenin from WAP-cre resulted in the transdifferentiation of mammary epithelium into epidermal cells and squamous metaplasias during the first pregnancy. Squamous nodules are frequent dysplasias of the mouse mammary gland and are characterised by the presence of confluent keratin swirls and cells containing translucent nuclei (ghost cells). Transdifferentiation into epidermis was confirmed by the expression of keratins K1 and K5 in the hyperplastic structures and squamous cells, with expression patterns resembling those seen during epidermal differentiation. Early activation of β -catenin by MMTV-cre resulted in a similar phenotype with the notable exception that mice were unable to lactate. Significantly, in both experiments mice did not develop mammary adenocarcinomas (over a time period of 6 months) (Miyoshi *et al.*, 2002). The authors argue that the phenotypic differences observed differ from the previous transgenic studies due to biochemical differences between the two β -catenin proteins, the floxed mice lacking amino acids 5-80 as compared to the previous studies overexpressing $\Delta 89$ and $\Delta 90$ β -catenin (Imbert *et al.*, 2001; Michaelson and Leder, 2001). The authors additionally suggest this difference could be due to the cell types targeted and/or the expression levels of β -catenin in floxed β -catenin mice. That transgenic mice overexpressing $\Delta 89$ β -catenin/ $\Delta 90$ β -catenin from an MMTV promoter develop adenocarcinoma and MMTV-cre-*loxP*- $\Delta E3\beta$ -catenin mice do not argue against differences in cell type accounting for differences in phenotype. The issue of altered β -catenin levels in inducing mammary adenocarcinoma has yet to be fully understood.

1.6.3 Conditional inactivation of APC

Tetsuo Noda's research group have generated floxed *Apc* mice in which *loxP* sites were introduced into introns 13 and 14 of the *Apc* gene (see Figure 1.8) These transgenic mice thus have a conditionally targeted allele of *Apc*, which upon recombination mediated by the cre recombinase deletes a region of *Apc* encompassing exon 14 and induces a frameshift mutation at codon 580. This mutation results in a truncated protein where all of the β -catenin regulating motifs and four of the seven armadillo repeats are missing. Whereas mice heterozygous (*Apc*^{+/580S}) or homozygous (*Apc*^{580S/580S}) for this silent mutant allele were phenotypically normal, homozygotes displayed decreased *Apc* expression in the intestine. Using an adenovirus cre recombinase *Apc* inactivation was targeted to the colorectum of *Apc*^{580S/580S} mice. Homozygotes, but not heterozygous or wild type mice, subsequently developed colorectal adenomas within 4 weeks. PCR analysis of genomic DNA from these adenomas confirmed deletion of *Apc* exon 14 and established that loss of *Apc* function was mediated by cre-*loxP* recombination (Shibata *et al.*, 1997).

To specifically inactivate *Apc* in the mouse mammary gland the floxed *Apc* mice (*Apc*^{580S/580S}) mice were crossed to transgenic mice expressing a mammary gland specific cre recombinase (BLG-cre) (Gallagher *et al.*, 2002). This transgene (Figure 1.9) is driven from the ovine beta-lactoglobulin (*BLG*) promoter, which has been used successfully to target transgenes efficiently and reliably to secretory epithelial cells of the mammary gland (Whitelaw *et al.*, 1992; Farini *et al.*, 1995). The BLG-cre transgene has previously been shown to induce very efficient excision of floxed *DNA ligase I* in mice. Excision was specific to the mammary gland and was temporally regulated, predominantly occurring during lactation (Selbert *et al.*, 1998; Chapman *et al.*, 1999). Subsequent breeding of the BLG-cre transgenic mice to the cre ROSA reporter strain (Soriano, 1999) was used to measure the extent of cre-recombinase activity in the mammary gland. Cre ROSA mice carry a flox-STOP β -galactosidase cassette that facilitates measurement of cre activity. Wholemout and histological

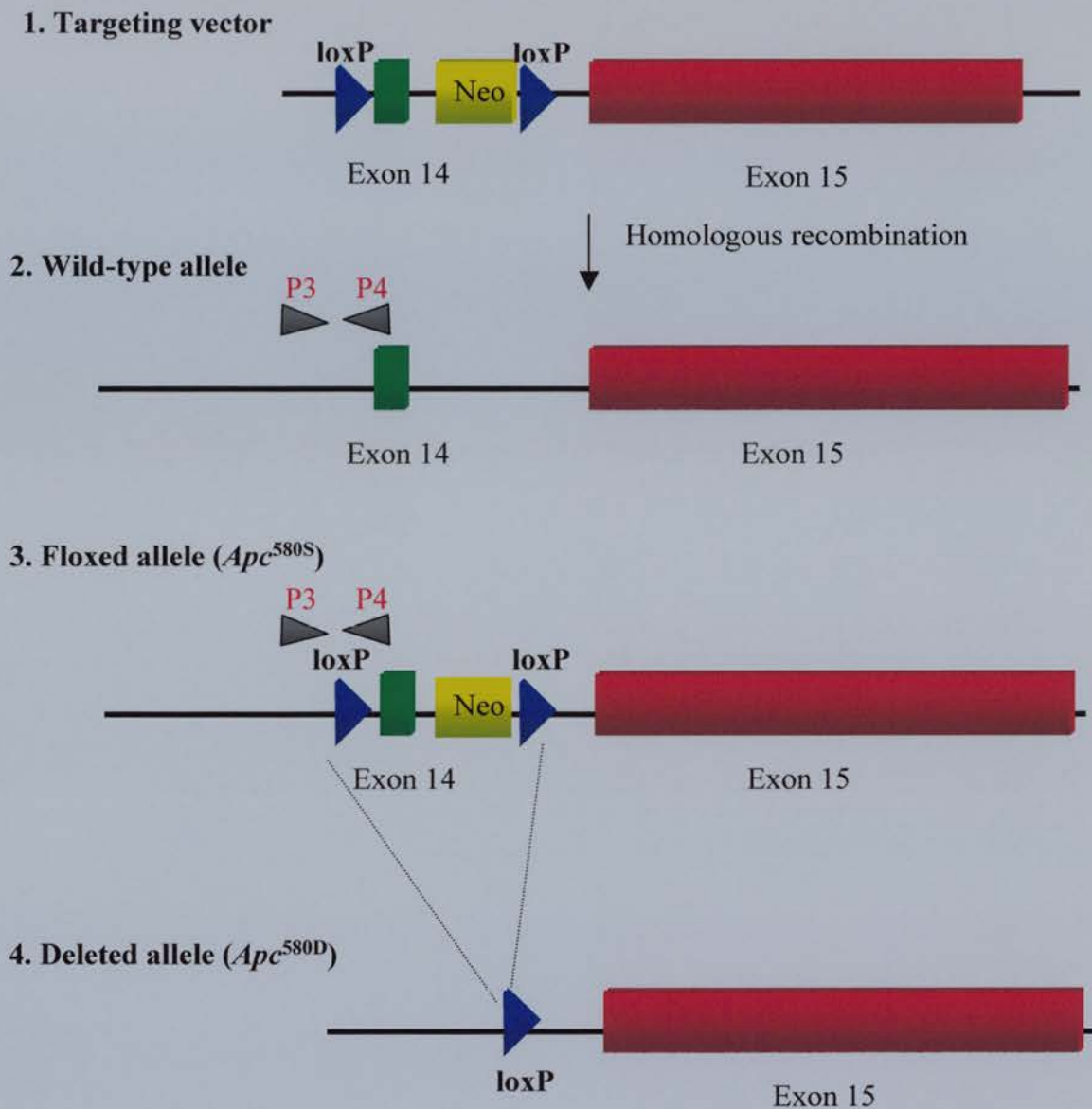


Figure 1.8. Establishment of a mutant mouse line carrying a conditionally targeted *Apc* allele (Shibata *et al.*, 1997). (1) Structure of the targeting vector which was introduced into ES cells. (2) Homologous recombination between the targeting vector and the wild-type allele creates the targeted allele. (3) The targeted allele (*Apc*^{580S}) has *loxP* sites flanking exon 14 of the *Apc* gene. (4) Recombination mediated by Cre recombinase produces the deleted allele *Apc*^{580D} lacking exon 14 of the *Apc* gene. The location of the genotyping primers P3 and P4 are shown.

Figure 1.9. Structure of the cre-transgene (Selbert *et al.*, 1998)

Cre recombinase was cloned into the *Eco* RV site of 4.2kb-BLG/SK+ plasmid. The start of translation is indicated by an arrow.

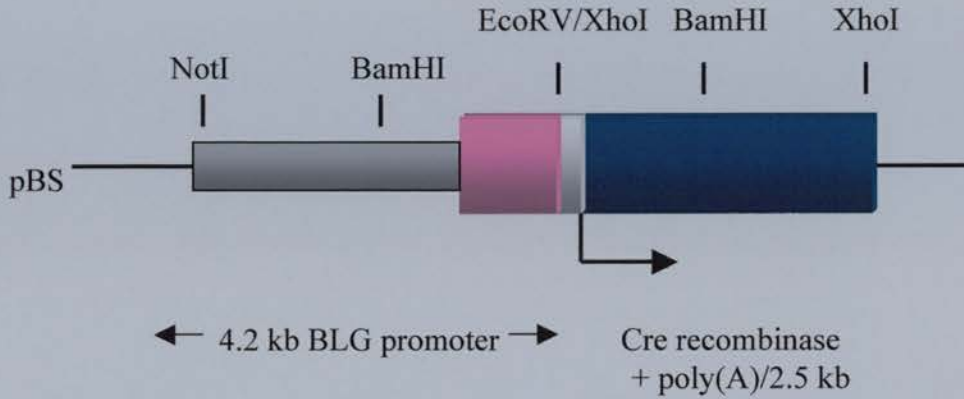
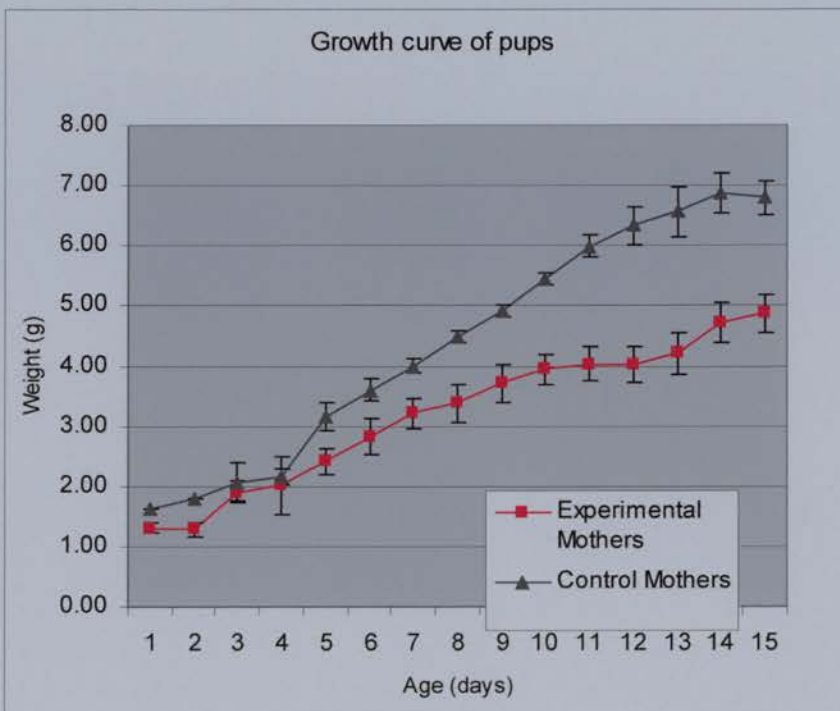


Figure 1.10. Growth of pups born to $cre^+ Apc^{580S/580S}$ females

Weights of pups born to experimental mothers with conditional inactivation of the *Apc* gene in the mammary gland ($cre^+ Apc^{580S/580S}$) were compared to those from littermate control mothers ($cre^+ Apc^{+/580S}$ and $cre^- Apc^{580S/580S}$).



analysis of *LacZ*-stained mammary glands showed widespread and highly efficient recombination throughout the epithelium of the virgin gland and thus indicated that the temporal expression of the BLG-cre transgene was not unique to lactation. By day 10 of lactation almost all epithelial cells had undergone recombination (Gallagher *et al.*, 2002). When crossed with floxed *Apc* mice, BLG-cre excises exon 14 in mammary gland secretory epithelial cells. All mice generated appeared to develop normally and litter sizes were comparable between $cre^+ Apc^{580S/580S}$, $cre^+ Apc^{+/580S}$ and $cre^- Apc^{580S/580S}$ females. However, we noted that the offspring from $cre^+ Apc^{580S/580S}$ females did not thrive (Figure 1.10) (Gallagher *et al.*, 2002). Analysis of wholemount virgin mammary gland preparations from these mice revealed that conditional inactivation of *Apc* leads to a marked delay in normal ductal development. Mammary glands from $cre^+ Apc^{580S/580S}$ females showed delayed ductal growth as compared with littermate control genotypes ($cre^+ Apc^{+/580S}$ and $cre^- Apc^{580S/580S}$) (Figure 1.11), however ductal growth does eventually succeed in reaching the end of the fat pad (Gallagher *et al.*, 2002). Lactating mammary glands from $cre^+ Apc^{580S/580S}$ females showed extensive metaplastic nodules (Figure 1.12). This phenotype was 100% penetrant and small areas of similar appearance were observed in virgin mammary gland sections. Metaplastic nodules consisted of tightly bound balls of epithelial cells emanating from ducts, which transdifferentiate into squamous cells as determined by histological criteria. Both keratinising squamous differentiation (characterised by the presence of keratohyaline granules) and non-keratinising squamous differentiation were observed, the latter being more frequent and resulting in the appearance of an eosinophilic material. These areas of metaplasia increased during lactation, remained after involution and increased in number and extent after two lactation cycles. Significantly, progression to neoplasia never occurred, even in mice that have been through up to 4 complete lactation cycles and one year after the initial lactation cycle (Gallagher *et al.*, 2002).

The observed phenotype of mice with conditional inactivation of the *Apc* gene ($cre^+ Apc^{580S/580S}$) highlights a critical role of *Apc* in both the growth and development of the mammary gland. Using the BLG-cre floxed *Apc* mice ($cre^+ Apc^{580S/580S}$) this thesis reports the exploration of the role of wild type *Apc* in the mouse mammary

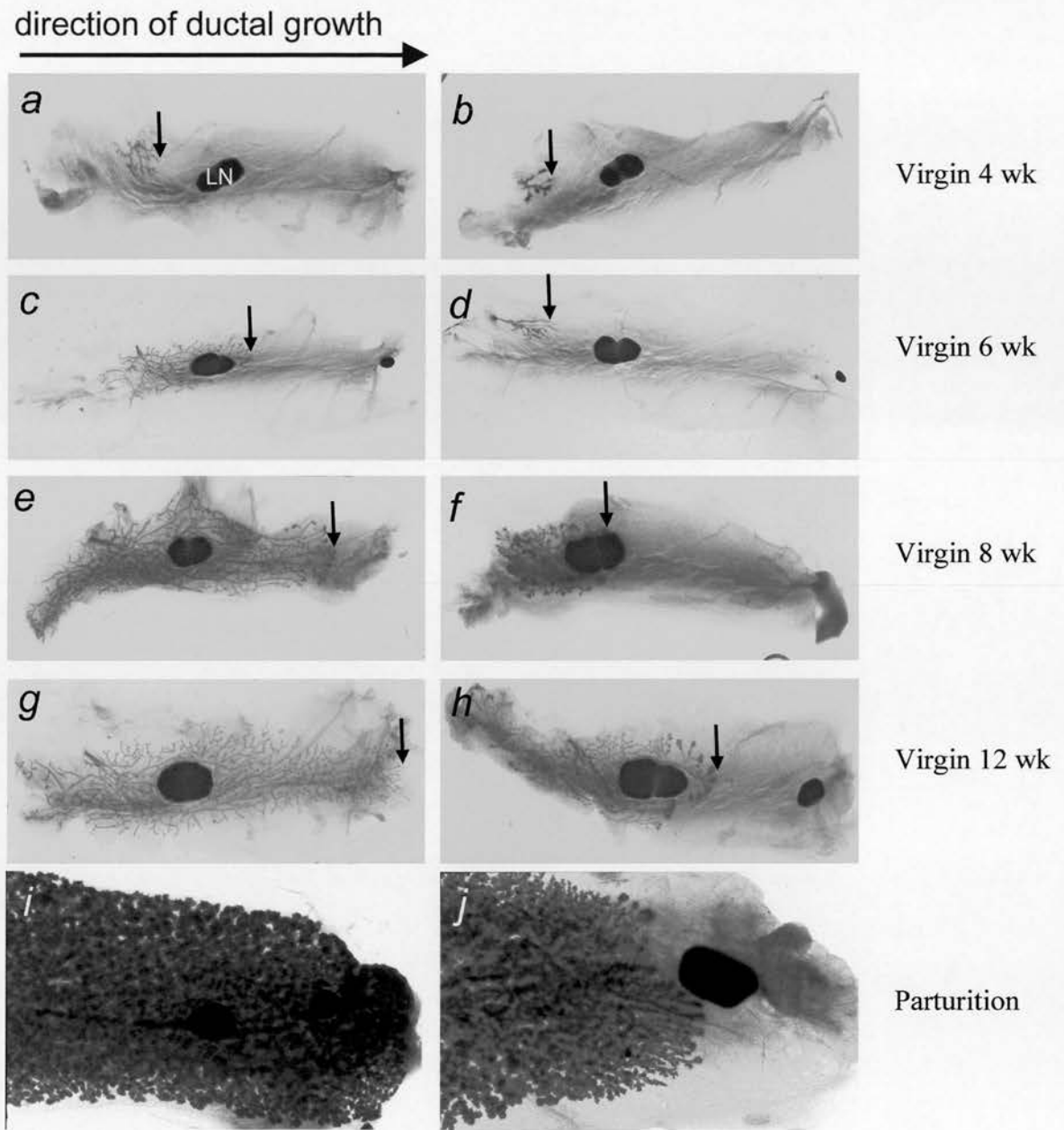


Figure 1.11. Mammary glands from $cre^+ Apc^{580S/580S}$ female mice displayed delayed ductal growth. Wholemount mammary preparations from control ($cre^+ Apc^{+/580S}$) female mice (**a,c,e,g,i**) and experimental $cre^+ Apc^{580S/58}$ littermates (**b,d,f,h,j**). Ductal growth initiates at the nipple end of the fat pad (left) and advances past the lymph node (LN) to completely fill the fat pad. The tip of the growing ductal network is marked by an arrow and at all stages remains delayed in experimental glands. Note that (i,j) show a 70 day mammary gland at parturition. Adapted from Gallagher *et al.*, 2002.

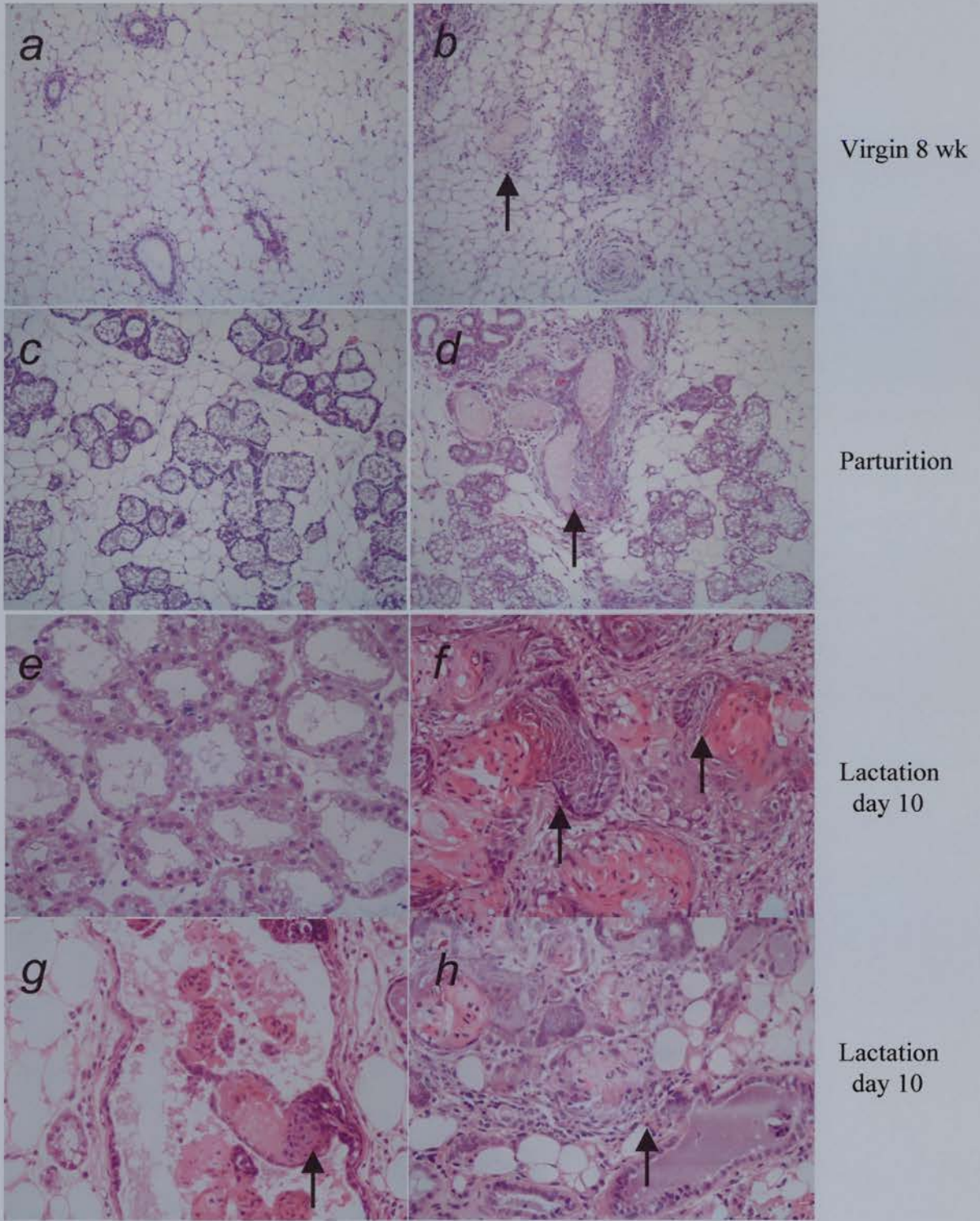


Figure 1.12. Mammary glands from experimental $cre^+ Apc^{580S/580S}$ female mice display extensive metaplastic lesions. Haematoxylin and eosin stained sections of mammary glands from control ($cre^+ Apc^{+/580S}$) female mice (a,c,e) and experimental $cre^+ Apc^{580S/580S}$ littermates (b,d,f,g,h). Metaplastic lesions are indicated by arrows and (g,h) show areas where metaplastic lesions extending into ducts. Magnification X20 for (a-d) and X40 (e-h). Adapted from Gallagher *et al.*, 2002.

gland. Initial characterisation, involving proliferation analysis (BrdU, TUNEL (TdT-mediated dUTP nick end labelling)) and immunohistochemical analysis of candidate proteins (Apc, β -catenin, cyclinD1), supported a role of *Apc* in canonical Wnt signalling in mammary gland secretory epithelial cells. DDRT-PCR was incorporated into this analysis as a means of investigating the effect of *Apc* deletion on expression levels of downstream genes. It was hypothesised that by using this non-candidate gene approach, it would be possible to isolate novel downstream targets of *Apc* in the mammary gland, thereby giving insight into this unexpected phenotype. This involved expression profiling at several critical stages of mouse mammary gland development, including mid-gestation, parturition, and lactation. Differentially displayed genes (including Casein, α 1 type IV collagen, Gm2a) were subsequently cloned and, where possible, identified. Three novel clones isolated from DDRT-PCR gels were subjected to cDNA library screening in an effort to characterise them further. Despite these efforts, the relationship between mammary gland metaplasia and *Apc* deficiency remains unclear. These observations highlight the complexity of *Apc* function in mouse mammary gland secretory epithelium.

1.7 AIMS

The aims of this thesis are the following:

- 1) Detailed phenotypic characterisation of the mammary gland of cre^+ *Apc*^{580S/580S} mice**
- 2) Differential Display Reverse Transcription Polymerase Chain Reaction (DDRT-PCR) analysis to identify transcriptional changes in response to loss of *Apc* in the mouse mammary gland**
- 3) Biochemical and functional analysis of two *Wnt* genes (*Wnt8b* and *Wnt10a*) cloned from mammary gland cDNA**

2 Materials and Methods

2.1 Basic Cloning Methodology

2.1.1 Agarose gel electrophoresis Of DNA

Agarose gel concentrations used varied from 0.5% to 2% w/v in Tris-borate EDTA (TBE) depending on the size of the DNA molecules to be resolved. TBE gels were prepared by boiling an appropriate mass of agarose powder (BioWhittaker Molecular Applications) in TBE buffer until dissolved and supplementing with 0.1mg/ml ethidium bromide (EtBr)(Fisher Scientific). DNA samples (volumes ranged from 2-50 μ l) were mixed with one-sixth volume of type III loading buffer (see Appendix A) and loaded directly onto the gel. Molecular weight markers, 1Kb or 100bp (New England Biolabs) were diluted in loading buffer and run parallel to DNA samples. Electrophoresis was carried out in 1X TBE at 50-100V for periods of 30 minutes to 2 hours, with the exception of genomic DNA which was performed at 40 Volts overnight, and visualised using UV light on a transilluminator (Dual Intensity Ultraviolet Transilluminator).

2.1.2 Restriction endonuclease digestion of DNA

All restriction endonucleases and appropriate buffers were purchased from Promega Ltd., Boehringer Mannheim, Roche or New England Biolabs. Suitable amounts of Plasmid DNA (1 μ g-5 μ g) were mixed with 0.1 volumes of 10X reaction buffer, 0.1 volumes of appropriate restriction endonuclease, and the volume made up to 20-50 μ l with ddH₂O. The digests were incubated for 90 minutes at 37°C. Double digests were performed in a buffer/temperature combination giving efficient digestion with both enzymes. Genomic DNA was digested as above however digests were incubated at 37°C overnight to ensure complete digestion of genomic DNA.

2.1.3 Phenol: chloroform extraction and ethanol precipitation of DNA

An equal volume of Phenol/Chloroform/Isoamylalcohol solution (P:C:I, 25:24:1, AMS Biotechnology) was added to the solution containing nucleic acid, gently vortexed and spun briefly at 13,000rpm for 5 minutes at 4°C. The upper aqueous phase was removed to a clean tube and an equal volume of chloroform was added and the sample vortexed and centrifuged as before. Nucleic acid was recovered from the upper aqueous phase by transferring to a clean tube and the addition of 0.1 volumes of 3M sodium acetate (pH 5.5) and 2.5 volumes of 100% ethanol. Following mixing by inversion several times the sample was incubated at -20°C for 1 hour to overnight. The nucleic acid precipitate was recovered by centrifugation at 13 000rpm for 20 minutes at 4°C. The ethanol was removed and the pellet washed with 200µl of 70% ethanol. A further centrifugation step was preformed at 13 000rpm for 5 minutes at 4°C. After removal of ethanol, the pellet was air dried at room temperature for 5 minutes and resuspended in an appropriate volume of dH₂O.

2.1.4 Extraction of DNA fragments from agarose gels

The QIAquick™ Gel Extraction Kit (Quiagen) was used for the purification of DNA fragments from agarose gels. DNA was digested with appropriate restriction endonucleases and electrophoresed on an agarose-TBE gel containing ethidium bromide. The bands were visualised with UV light and excised from the gel with a clean scalpel. The gel slice was weighed and 3 volumes of Buffer QG were added (eg. 100µl of buffer QG per 100mg of gel). The solution was heated to 50°C until the gel had completely dissolved. One gel volume of isopropanol was added to the solution, mixed briefly and applied to a Quiaquick spin column (placed in a 2ml collection tube) and centrifuged for 1 minute at 13 000rpm. The flow-through was discarded. To wash the DNA, 0.75ml of buffer PE was added to the column, centrifuged for 1 minute at 13 000rpm and the flow-through again discarded. To remove the last traces of buffer PE, the column was centrifuged once more then placed in a 1.5ml eppendorf tube. To the centre of the column 30µl of water was added and the column allowed to stand at room temperature for 1 minute. To elute

the DNA, the column was centrifuged at 13 000rpm for 1 minute and the elute transferred to a fresh 1.5ml eppendorf tube. DNA samples extracted from gels in this manner were electrophoresed to determine concentration and used immediately or stored at -20°C.

2.1.5 DNA ligation reactions

2.1.5.1 Dephosphorylation of vector DNA

Vector DNA linearised with a single restriction endonuclease was dephosphorylated with Calf Intestinal Phosphatase (CIP) (Boehringer Mannheim) prior to ligation with insert DNA to prevent re-ligation of vector DNA. Blunt end ligation omitted this step.

Following restriction digestion of an appropriate quantity of vector DNA (e.g. 5µg), the DNA was phenol/chloroform extracted and ethanol precipitated as previously described and resuspended in 16µl of water. To the DNA, 2µl (2units/µl) of CIP and 2µl of 10X reaction buffer was added, mixed and incubated at 37°C for 1 hour. To denature the CIP, the reaction was heated to 70°C for 10 minutes. The dephosphorylated DNA was purified by phenol/chloroform extraction and ethanol precipitation as previously described and resuspended in water to a final concentration of 10ng/ul and stored at -20°C. Typically 10-15ng/ul of vector DNA was used for ligation reactions. Ligation controls were also set up that contained no insert but only dephosphorylated vector.

2.1.5.2 Ligation reaction (pBluescript[®] II KS (+) (pBS)(Stratagene), pZErO[™]-2 (Invitrogen) and pGEM[®]-T Easy (Invitrogen))

The DNA to be used as insert in ligation reactions was first purified by agarose gel electrophoresis and quantified on an agarose gel. An approximate 3-5 fold molar excess of insert DNA was added to vector DNA (10-15ng/µl) and diluted to 8µl with water. To the solution 1µl of 10X ligation buffer was added followed by 1µl T4

DNA Ligase (1 U/ μ l; Boehringer Mannheim). The solution was incubated at 4°C overnight.

2.1.6 Transformation of competent bacteria

Aliquots of TOP10 One Shot™ ultracompetent *E. coli* K12 derived cells (Invitrogen) were removed from storage at -70°C and thawed on ice. Plasmid DNA was added directly onto the cells and then mixed by tapping the tube gently. The cells and the DNA were incubated on ice for 30 minutes, heat shocked in a water bath at 42°C for 30 seconds and returned to ice. 250 μ l of room temperature SOC media (Appendix A) was added to the tube, which was then incubated at 37°C for 1 hour in a shaking incubator at 225rpm. The transformed bacteria were plated onto LB-agar plates containing appropriate antibiotics that selected for transformants. Plates were inverted and incubated at 37°C overnight. However for routine transformations DH5 α *E. coli* cells were used. 200 μ l aliquots were removed from storage at -70°C and transformations were as above however heat shock was 42°C for 75 seconds followed by the addition of 400 μ l of 2XTY medium (Appendix A) and incubation at 37°C in a shaking incubator for 30 minutes before plating onto LB-agar plates containing appropriate antibiotics that selected for transformants.

2.1.7 Preparation of plasmid DNA

Small-scale preparations of plasmid DNA were purified from transformed bacterial cells with the QIAGEN QIAprep Spin Miniprep kits in accordance with the manufacturer's instructions. A single bacterial clone was picked from a LB-agar plate using a sterile toothpick. The clone was transferred to a Falcon 2059 tube containing 1.5 ml of LB (see Appendix A) supplemented with appropriate antibiotics and incubated in a shaking incubator (225rpm) at 37°C overnight. This overnight bacterial culture was poured in a 1.5ml Eppendorf microcentrifuge tube and spun at 13,000 rpm for 1 minute. The supernatant was discarded and bacterial pellets were resuspended in 250 μ l of resuspension buffer (50mM Tris-HCl, pH7.5, 10mM EDTA,

100µg/ml RNase A). RNase A was added to this solution to avoid RNA contamination in later nucleic acid purification steps. Bacterial lysis was accomplished by adding 250µl of lysis solution (0.2M NaOH, 35mM SDS) and mixed by inversion. The lysis reaction was subsequently neutralised by addition of 350µl of neutralisation buffer (1.32M potassium acetate, pH 4.8) and again mixing by inversion. This latter step produces a protein precipitate, subsequently removed by centrifugation at 13,000rpm for 10 minutes. Supernatants were transferred to QIASpin filter tubes and placed in collection tubes; the liquid was passed through the filter by centrifugation at 13,000rpm for 1 minute. 750µl of wash buffer (80mM potassium acetate, 8.3mM Tris-HCl pH 7.5, 40µM EDTA, 55% (v/v) ethanol) was added to the QIASpin filter tube followed by centrifugation for 1 minute at 13,000rpm. The collection tubes were emptied and the filter tubes spun again for 1 minute at 13,000rpm. QIASpin filter tubes were placed on fresh 1.5ml Eppendorf tubes and 50µl of water was added to each tube. The tubes were incubated at room temperature for 1 minute. The QIASpin/Eppendorfs were spun at 13,000rpm for 1 minute. The elute containing the DNA was used immediately or stored at -20°C.

In instances where quantities of plasmid DNA greater than that produced by the miniprep method were required, 'midipreps' were prepared using a midiprep kit, Qiagen Plasmid Midi Kit. The general protocol consists of inoculating a conical flask containing 50ml of LB or 2XTY, supplemented with the appropriate antibiotics with bacteria from suitable miniprep cultures. The bacteria were grown at 37°C for 12- 16 hours in a shaking incubator at 225 rpm, harvested by centrifugation (6,000g for 5 minutes at 4°C, Heraeus #3046 roter, in a Heraeus Biofuge centrifuge), resuspended and lysed and neutralised in manufacturer supplied solutions as for the miniprep method. Protein precipitate was removed by centrifugation at 20,000g for 30 minutes at 4°C (JA-25 rotor in a Beckman Avanti J-25 centrifuge). Supernatant was removed and re-centrifuged at 20,000g for 15 minutes at 4°C. Supernatants were added directly to equilibrated QIAGEN-tips, and allowed to pass through the DNA binding resin by gravity flow. Columns with bound DNA were washed with the supplied buffers twice prior to elution of DNA. DNA was removed from the column using a supplied elution buffer and 0.7 volumes of isopropanol were added. The

DNA was collected by centrifugation at 15,000g for 30 minutes at 4°C (JA-25 roter, in a Beckman Avanti J-25 centrifuge). DNA pellets were washed with 70% ethanol and recentrifuged. The final DNA pellet was dissolved in 100µl of water and stored at -20°C.

2.1.8 Preparation of bacterial glycerol stocks

Single clones were used to inoculate 1.5ml of LB supplemented with the appropriate antibiotic and grown overnight at 37°C in a shaking incubator. 500µl of this culture was added to 400µl of glycerol in a 1.5ml eppendorf and stored at -70°C. To resuscitate the recombinant bacteria when required, a scraping of frozen glycerol stock was transferred to 3ml of LB medium supplemented with the appropriate antibiotic and propagated overnight at 37°C as previously described.

2.1.9 ExSite™ PCR-based site-directed mutagenesis

Plasmid DNA (0.5pmol) was added to a 25µl PCR mixture containing the following reagents:

2.5µl	10X mutagenesis buffer
1µl	25mM dNTP mix
15pmol	Fwd primer
15pmol	Rev primer
dH ₂ O to 24µl	
1µl	ExSite DNA polymerase blend

Cycling conditions were as follows

94°C	-	4 minutes	} 8 cycles
50°C	-	2 minutes	
72°C	-	2 minutes	
94°C	-	1 minute	
56°C	-	2 minutes	
72°C	-	1 minute	

72°C - 5 minutes

Following completion of PCR two populations of plasmids exist. The first population contains the desired linear plasmids that contain the mutations in the double-stranded DNA. The second population includes the parental plasmids that have not incorporated the mutation. DNA was subsequently digested with 1µl of the restriction enzyme *Dpn I*, which cuts methylated DNA and will therefore only cut the parental plasmid and leaves the PCR product undigested. The undigested linear DNA was then end polished with 0.5µl of cloned *Pfu* DNA polymerase and the ends ligated by incubation at 37°C for 1 hour with 1µl of T4 DNA ligase. The ligated DNA was then ready to be transformed.

2.2 Differential Display RT-PCR

2.2.1 Isolation of total RNA from murine mammary glands

All mammary glands dissected were collected in sterile 1.5ml eppendorf tubes, flash frozen in liquid nitrogen and transferred to -70°C until required. The preparation of all total RNA during this project was performed using The RNAzol™ B method (AMS Biotechnology), based on the guanidinium thiocyanate phenol/chloroform extraction method of Chomczynski & Sacchi (1987). A variable speed polytron homogeniser was used for the homogenisation of tissue. To clean the homogeniser probe prior to homogenisation the probe was washed three times in 40ml of 0.2 M NaOH and three times in 40ml of water. RNAzol™ B (2ml per 100mg of tissue) was dispensed into 50ml tubes (Greiner Labortechnik Ltd), stored on ice, and the tissue transferred directly from liquid nitrogen. For homogenisation of mammary gland tissue, 4ml of RNAzol B was used per 100mg of tissue. The tissue was immediately homogenised and 1ml aliquots transferred to 2ml eppendorf tubes. To each homogenate, 100µl of chloroform was added, the tubes mixed by inversion several times and centrifuged at 13 000rpm for 15 minutes at 4°C. 500µl of the upper aqueous phase was removed and transferred to a fresh 2ml eppendorf tube. An equal volume of isopropanol was added and the tubes mixed by inversion several times. Samples were incubated on ice for 15 minutes then centrifuged at 13 000 rpm for

15minutes at 4°C. The RNA pellet was washed once with 75% ethanol, the last traces of which were removed using a P2 Gilson pipette. RNA was resuspended typically in 400µl of water by pipetting, 0.1 volumes of 3M sodium acetate and 2.5 volumes ethanol were added, the tubes vortexed briefly and stored as ethanolic precipitates at -20°C. Prior to use, the tubes were vortexed before removing an aliquot for preparation. To quantitate stock concentrations of total RNA, typically a 10µl aliquot was removed, centrifuged and quantified by spectrophotometry

2.2.2 Synthesis of first-strand cDNA

A volume, containing approximately 20µg RNA was centrifuged at 13 000rpm for 25 minutes at 4°C. The pellet was washed with 75% ethanol, dried at 45°C for 2 minutes and resuspended in 10µl of RNase-free water. A small portion (2µl) of each sample was used for spectrophotometric quantitation (an average of three readings were taken) and 5µg total RNA (in 5µl volume) was used to synthesise first-strand cDNA (First-strand cDNA synthesis kit; Amersham Pharmacia Biotech). Reactions contained 1µl DTT (200mM), 5µl of bulk first-strand mix (containing Moloney Murine Leukaemia Virus reverse transcriptase) and 4µl of either d(T)₁₂MA, d(T)₁₂MG, d(T)₁₂MC, d(T)₁₂MT primer (24µM; M = A, G or C). Reactions were mixed and incubated at 37°C for 1 hour and heated to 95°C for 10 minutes to inactivate reverse transcriptase. Reactions were then dispensed into 1µl aliquots on 0.5ml eppendorf tubes and stored at -20°C.

2.2.3 Differential Display PCR

For differential display PCR reactions, 1µl of aliquoted cDNA was diluted to 133µl with water and 10µl of this solution was used for each display PCR (equivalent to the amount of cDNA produced from 25ng RNA). To each 10µl of cDNA on ice, 2µl of arbitrary 10-mer primer (5µM) was added and the solution overlaid with 30µl mineral oil (Sigma). Master mix (8µl) containing 2µl 10X PCR buffer (Boehringer Mannheim), 2µl dNTPs (20µM; Amersham Pharmacia Biotech), 0.3µl Taq

polymerase (1.5U; Boehringer Mannheim), 2 μ l of d(T)₁₂MN (25 μ M), 1 μ l α^{35} S dATP and 0.7 μ l dH₂O was added to each tube. Tubes were centrifuged briefly and incubated in a Biometra Unoblock PCR machine at 94°C (2 minutes), followed by 40 cycles of 94°C denaturation (30 seconds), 40°C annealing (2 minutes) and 72°C extension (3- seconds), followed by a final extension step at 72°C for 5 minutes. Type III loading dye (4 μ l) was added to each tube and 8 μ l of each sample loaded onto a 6% non-denaturing HR-1000 GenomyxLR polyacrylamide gel (Beckman Instruments Ltd.), using GenomyxLR electrophoresis equipment. Samples were run for 2 hours 15 minutes at 2700V (50°C) on a GenomyxLR DNA analyser (Beckman Instruments Ltd.). The gels were transferred to 3MM blotting paper, dried and subjected to autoradiography. The sequence identities of all arbitrary and anchored oligonucleotides used for the DDRT-PCR analysis are listed in Appendix C.

2.2.4 Recovery of cDNA from dried polyacrylamide gels

Gel regions corresponding to bands representing candidate cDNAs were excised using sterile scalpels and transferred to sterile 0.5ml eppendorf tubes. GlogosTM autoradiograph markers (Stratagene) were used to align the gel with the autoradiograph and identical regions were excised from test and control lanes (e.g. Cre⁺APC^{580S/+} / Cre⁻APC^{580S/580S} or Cre⁺APC^{580S/580S}). The gel fragments were rehydrated by incubation at room temperature for 15 minutes in 100 μ l water, and the cDNA eluted at 99°C for 15 minutes before transfer of the liquid phase to fresh 0.5ml tubes. cDNA was precipitated by the addition of 1 μ l See-DNA (Amersham Pharmacia Biotech), 2.5 volumes ethanol, 0.1 volumes of 3M sodium acetate (pH 5.2) and stored on dry ice for 1 hour. Following centrifugation (13 000rpm, 25 minutes, 4°C) and washing with 75% ethanol the pellet was resuspended in 4 μ l of water.

2.2.5 Modified single-strand conformation polymorphism (mSSCP)

For the mSSCP-PCR reaction 4 μ l 10X PCR buffer (Boehringer Mannheim), 3.2 μ l dNTPs (2.5Mm dGTP, dCTP, dTTP; 0.025 mM dATP; Amersham Pharmacia

Biotech), 2.5 μ l anchored primer (20 μ M), 2.5 μ l arbitrary primer (20 μ M), 0.3 μ l Taq polymerase (1.5U; Boehringer Mannheim), 0.5 μ l [³³P] α -dATP was added to the DNA and the reaction volume adjusted to 40 μ l with water. PCR conditions were similar to those used for display-PCR, with exception that only 5 cycles were performed. After removing the mineral oil, PCR products were purified by phenol chloroform extraction. Pellets were washed, resuspended in 8 μ l of mSSCP loading buffer (see Appendix A) and denatured at 95°C for 10 minutes prior to loading onto a 0.5X MDE gel (Flowgen), cast using the GenomyxLR system. Samples were electrophoresed typically for 18 hours at 8W (25°C) in 0.6X TBE buffer. Following autoradiography, areas of the gel corresponding to candidate cDNAs were excised, cDNA eluted and precipitated as previously described.

2.2.6 PCR re-amplification of mSSCP-purified candidate cDNAs

A final reamplification of the recovered cDNA was performed. Instead of the original anchored and arbitrary primers, oligonucleotides were synthesised with additional 5' *Eco* RI restriction sites to aid cloning (herein referred to as extended primers). Also, only one anchored oligonucleotide was used to cover d(T)₁₂MA, GA, CA or TA. A full listing of oligonucleotides used is provided in Appendix C. The reaction contained 4 μ l mSSCP purified cDNA, 4 μ l 10X PCR buffer (Boehringer Mannheim), 3.2 μ l dNTPs (10mM each dATP, dCTP, dTTP, dGTP, Amersham Pharmacia Biotech), 2.5 μ l each extended primer (20 μ M), and 0.5 μ l Taq polymerase (1.5U; Boehringer Mannheim) in a 40 μ l volume. Cycling conditions were as follows

94°C	-	2 minutes	
94°C	-	30 seconds	} 1 cycle
40°C	-	2 minutes	
72°C	-	30 seconds	
94°C	-	30 seconds	
58°C	-	1 minute	} 5 cycles
72°C	-	30 seconds	
72°C	-	5 minutes	

4°C - Hold

PCR products were subjected to *EcoR*I restriction endonuclease digestion, prior to purification and cloning into the *EcoR*I site of pBluescript SKII⁺ (Stratagene).

2.2.7 'Cold' Southern blotting

The following procedure was performed for the rapid screening and validation of the candidate clones prior to northern blotting. To the remaining 16µl of the original completed DDRT-PCR reaction, 4µl of Type III loading dye was added, the tubes centrifuged briefly and 10µl loaded onto a 1% TBE-agarose gel. Electrophoresis was performed at 80V until the bromophenol dye had run approximately three-quarters of the gel length. The gel was subsequently soaked for 30 minutes in denaturing solution (1.5M NaCl/0.5M NaOH) and neutralised by soaking in 1.5M NaCl/0.5M Tris-HCL (Ph 7.5) for 30 minutes. DNA was transferred to Hybond[®]-N nylon membrane (Amersham Pharmacia Biotech) overnight by capillary action in 20 X SSC buffer. Membranes were rinsed briefly in 2 X SSC, UV crosslinked and baked at 120°C for 20 minutes. Probes were labelled as in section 2.7.4.2, and hybridisation was as in section 2.7.4.1.

2.3 Polyacrylamide Gel Electrophoresis

2.3.1 Preparation and pouring of polyacrylamide gels

The following procedure was used for the preparation of polyacrylamide gels to be used for electrophoresis of DDRT-PCR products, modified Single-Stranded Conformation Polymorphism (mSSCP) products and DNA sequencing products. The GenomyxLR electrophoresis system, GenomyxLR electrophoresis equipment and GenomyxLR DNA analyser (Beckman Instruments Ltd.) were used for all three electrophoresis protocols.

The casting plates were both washed thoroughly prior to preparation of the gel. Both plates were rinsed with water and the larger of the two plates was cleaned with 50ml

of 5 M Sodium hydroxide and then rinsed again with water. Both plates were then cleaned with 100% ethanol and the smaller of the two plates, or notched plate, was treated with a siliconising agent (Acrylgrease; Stratagene). The two plates were separated by 0.2mm spacers, held in place by bulldog clips and placed horizontally over a pouring tray. To the acrylamide solution to be poured, de-gassed under vacuum, 500µl of 10% Ammonium persulphate (Anachem) and 50µl of N,N,N',N'-Tetramethylethylenediamine (TEMED; Promega) was added and the solution mixed by swirling. Using a disposable 50ml syringe (Beckton Dickinson Ltd.), the acrylamide mix was poured between the glass plates, the appropriate combs placed in position, held in place by bulldog clips, and the gel allowed to completely polymerise over a period of 1 hour.

2.3.1.1 Non-denaturing polyacrylamide gels

Non-denaturing polyacrylamide gels were used for DDRT-PCR analysis. To prepare a non-denaturing 6% polyacrylamide gel the HR-1000 polyacrylamide matrix (Beckman Ltd.) was used. This was supplied as a 6% solution and required only brief de-gassing and the addition of ammonium persulphate and TEMED prior to pouring.

2.3.1.2 Denaturing polyacrylamide gels

Denaturing polyacrylamide gels were used for sequencing analysis. The HR-1000 polyacrylamide matrix was used. This was supplied as a 6% acrylamide/8M urea solution and required de-gassing and the addition of ammonium persulphate and TEMED prior to pouring.

2.3.1.3 MDE Polyacrylamide Gels

For mSSCP analysis, 0.5X MDE polyacrylamide (Flowgen) was used. To prepare this, 5.8ml of 10 X TBE and 18ml 2 X MDE solutions were mixed and diluted to 100mls with water. Immediately prior to pouring, ammonium persulphate and TEMED were added.

2.3.2 Drying of polyacrylamide gels

After electrophoresis was complete, the two glass plates were carefully separated so that the gel remained on the larger of the two plates. For native polyacrylamide gels, the gel was then transferred to an equal sized sheet of 3MM paper (Merck), and secured to the larger plate and dried directly in the GenomyxLR at 50°C for approximately 15 minutes. In the case of denaturing sequencing gels, the notched plate was carefully removed and the gel dried directly in the GenomyxLR apparatus for 15 minutes at 50°C. The gel was rinsed with 2 litres of water to remove urea and dried again. This cycle of drying and rinsing with water was repeated until all traces of urea were removed from the gel.

2.4 DNA sequencing

2.4.1 Fluorescent cycle sequencing of DNA (Automated Sequencing)

Plasmid DNA was prepared using the Qiaprep Spin Miniprep Kit (Qiagen) and sequenced using the ABI BigDyeTM Terminator Kit (Perkin Elmer Applied Biosystems). Reactions were set up as follows in 0.5ml eppendorf tubes; 1µg of Plasmid template (in a volume not greater than 5µl), 1µl of 10µM sequencing primer, 4µl of ready reaction mix (containing dye terminators, deoxynucleoside triphosphates, Ampli Taq DNA polymerase, magnesium chloride and buffer) and water to a final volume of 10µl. Tubes were placed in a thermal cycler and cycling conditions were as follows:

96°C -	1 minute	} 25 cycles
96°C -	30 seconds	
50°C -	15 seconds	
60°C -	1 minute	
4°C -	Hold	

Once cycling was complete the DNA was precipitated by the addition of 2 μ l 1.5M sodium acetate/ 250mM EDTA (pH= 8) and 50 μ l of ice cold absolute ethanol and placed on ice for 10 minutes. Samples were then centrifuged at 13 000rpm, 4°C for 30 minutes, the supernatant was removed and the pellet was rinsed briefly in 200 μ l of 75% ethanol. Following centrifugation at 13 000rpm, 4°C for 10 minutes, the supernatant was removed and the pellet air-dried. Samples were then posted to the DNA sequencing facility at the University of Oxford where automated fluorescence label sequencing was carried out, and the results were received by FTP within a week.

2.4.2 *Fmol* cycle sequencing (manual sequencing)

This protocol used the *Fmol* Cycle Sequencing Kit (Promega Ltd.) and is based on the chain termination method originally described by (Sanger *et al.*, 1977). For each DNA template four 0.5ml eppendorf tubes were labelled and placed on ice. To each tube, 2 μ l of the appropriate ddNTP was added. The reactions were set up as follows:

DNA template (1 μ g)	8 μ l
Sequencing primer (3pmol/ μ l)	2 μ l
Water	to a final volume of 10 μ l

To each primer/template sample, 5 μ l of sequencing buffer, 1 μ l of [³⁵S] α -dATP and 1 μ l of *fmol* sequencing enzyme mix was added and mixed. To the inside wall of each tube containing ddNTP, 4 μ l of the reaction mix was added. One drop of mineral oil (Sigma) was added to each tube and after a brief centrifugation step, the tubes were placed in a thermal cycler preheated to 95°C and the cycling conditions were as follows:

95°C -	2 minutes	} 40 cycles
95°C -	30 seconds	
55°C -	30 seconds	
70°C -	1 minute	
4°C -	Hold	

After the cycling program was complete, 3 μ l of STOP solution was added to each tube. Each sample was denatured at 70°C for 5 minutes immediately prior to loading on a 6% acrylamide/8M urea sequencing gel. In each lane, 3 μ l of sequencing was loaded in the order A, G, C, T. Using the GenomyxLR system, the upper and lower buffers were 0.5 X TBE and 1 X TBE respectively, and electrophoresis was performed at 2700 V at 50°C for 2 hours and 45 minutes. Reliable sequence reads of approximately 500bp were obtained.

2.5 Northern blotting

2.5.1 RNA formaldehyde gel electrophoresis

Northern analysis was used to confirm differential expression of the DDRT-PCR candidate genes. RNA was fractionated by gel electrophoresis through 1% denaturing formaldehyde agarose gels. To prepare the gels, 2g of RNase/DNase-free agarose (Boehringer Mannheim) was added to 166ml of 1X MOPS solution (see Appendix A) in a 250ml sterile conical flask. The agarose was dissolved by heating in a microwave on full power setting for 3 minutes. Once dissolved the solution was allowed to cool to 60°C. Meanwhile, the gel casting tray, electrophoresis unit and combs were cleaned with RNaseZAP (Invitrogen), followed by rinsing with water. In a fume hood, 34ml of Formaldehyde (Fisher Scientific) was added to the agarose solution, mixed and poured into the gel-casting unit. The combs were positioned and the gel allowed to set for approximately 30 minutes. An appropriate volume of RNA (corresponding to 10 μ g of total RNA) stored as an ethanolic precipitate, was prepared for gel electrophoresis by transferring to a 0.5ml eppendorf tubes on ice. RNA was pelleted by centrifugation at 13 000rpm for 20minutes at 4°C. The ethanol was removed by aspiration and the pellet washed with 100 μ l of ice cold 75% ethanol. Following a further centrifugation step for 5 minutes at 13 000rpm at 4°C the ethanol was removed by aspiration, and the tubes placed on ice. RNA was dissolved in 15 μ l of RNA sample buffer by pipetting. To denature the RNA the samples were placed in a Biometra Unoblock Thermal Cycler (Anachem) and heated

to 65°C for 10 minutes. To each sample, 1 µl of a 10 mg/ml stock of ethidium bromide and 4 µl of Type III loading buffer was added. The tubes were pulse centrifuged and placed on ice.

The combs were removed from the set agarose gel and the unit placed in the electrophoresis apparatus and submerged in 1X MOPS running buffer. The denatured RNA samples were loaded into the appropriate wells of the gel. Electrophoresis was performed at 60 Volts for approximately 3 hours. On completion of electrophoresis, the gel was photographed in an identical fashion to DNA agarose gels, with the exception that the UV transilluminator was first cleaned with RNaseZAP (Invitrogen) and rinsed with water.

2.5.2 Northern blotting of RNA

After completion of electrophoresis, the formaldehyde agarose gel was first rinsed in distilled water before submerging in 500 ml of transfer buffer (10X SSC) for approximately 1 hour. Meanwhile a sheet of Hybond[®]-N nylon membrane (Amersham Pharmacia Biotech) was briefly equilibrated in transfer buffer. RNA was transferred from the gel onto the membrane overnight. The membrane was subsequently rinsed in 2XSSC, UV crosslinked and baked at 120°C for 20 minutes. Membranes were stored between sheets of Whatman 3MM paper at room temperature until ready to probe, see protocol for screening cDNA library.

2.6 Southern Blotting

2.6.1 Preparation of genomic DNA

Genomic DNA was prepared from mouse liver using the Nucleon Kit (Amersham Life Sciences) for the extraction of genomic DNA from hard tissue. Briefly, 25 mg of liver was ground to a fine powder on dry ice using a pestle and mortar. This was then transferred to a 50 ml falcon tube and 12 ml of reagent B added. RNase solution was added to a final concentration of 400 ng/ml and the tube incubated in a water bath at

37°C for 30 minutes. Proteinase K was added to a final concentration of 50µg/ml and the tube was incubated at 50°C overnight. The tube was centrifuged at 2000g for 5 minutes and the supernatant removed to a new tube. 3ml of 5M Sodium Perchlorate was added and the tube inverted several times to mix, and then mixed on a rotary mixer for 10 minutes at room temperature. 11ml of chloroform was added and again mixed by inverting, followed by 10 minutes on a rotary mixer. The tube was then centrifuged at 800g for 1 minute and 1600µl of Nucleon resin added gently down the side of the tube. Taking care not to remix the phases, the tube was centrifuged at 1300g for 3 minutes. Without disturbing the Nucleon resin layer (brown in colour), the upper aqueous phase was removed to a new 50ml falcon tube and recentrifuged at 1300g for 3 minutes. The upper aqueous phase was again removed to a clean tube and 2 volumes of ice-cold ethanol added. The tube was gently mixed by inversion and the precipitated DNA was spooled out using a heat-sealed Pasteur pipette, washed briefly in 70% ethanol and transferred to 4mls of TE. Incubating overnight at 37°C with gentle agitation dissolved the genomic DNA. DNA was quantified by measuring the optical density, under UV light at a wavelength of 260nm, (based on the fact that an OD of 1 equates to a concentration of 50µg/ml for DNA). 20µg of genomic DNA was digested with restriction enzyme overnight at 37°C.

Following digestion, all samples were electrophoresed on a 0.8% agarose gel at low voltage (40V) overnight (~16 hours). The gel was ethidium bromide stained and images of the electrophoresed DNA were captured on a UV transilluminator (see above) for later comparison. Transfer of the DNA to the nylon membrane was improved by partial depurination ('acid nick') of the DNA prior to transfer. Partial depurination was achieved by soaking the gel for 30 minutes in 0.2M HCl. The gel was then soaked in 500ml of southern denaturation buffer for 30 minutes to denature the DNA. After a brief rinse with water the gel was submerged in 500ml of southern neutralisation buffer for 30 minutes. Meanwhile a sheet of Hybond[®]-N nylon membrane (Amersham Pharmacia Biotech) was briefly equilibrated in transfer buffer (10X SSC). DNA was transferred from the gel onto the membrane overnight. The membrane was subsequently rinsed in 2XSSC, UV cross linked and baked at 120°C

for 20 minutes. Membranes were stored between sheets of Whatman 3MM paper at room temperature until ready to probe, see protocol for screening cDNA library.

2.7 Screening a phage cDNA library

2.7.1 Titration of genomic phage library

The lambda phage library (lactation day 10 mammary gland library) was titrated by inoculating a known quantity of VCS257 *E. coli* host strain (Stratagene) with a serial dilution of the library master stock, followed by culture in top agar to determine the number of plaque forming units per ml (pfu/ml). The VCS257 *E. coli* host strain cells were prepared by inoculating 50mls of lambda broth, supplemented with maltose to 0.2% and culturing overnight at 37°C. The bacteria for infection were grown in the presence of maltose so as to optimise the efficiency of infection due to the fact that phage attach to the maltose receptor on the bacterial surface. The culture was then centrifuged at 6000g for 15 minutes, the pellet resuspended in 25mls of 100mM MgSO₄ and stored at 4°C. MgSO₄ is also required for phage attachment. The phage library was kindly supplied by Dr. Christine Watson and was reported to have a titre of 10⁶ pfu/ml. A set of serial dilutions of the library stock were prepared (10⁻², 10⁻⁴, 10⁻⁶ and 10⁻⁸ in SM buffer), and 100ul of *E. coli* cells added to 10µl and 100µl of each dilution. Tubes were mixed gently and placed in a 37°C water bath for 15 minutes to allow the phage to absorb to the bacteria. Lambda Top-Agar was melted in a microwave and cooled to 47°C. 3mls of the molten top-agar was added to each tube and swirled to mix, then poured onto the centre of a lambda agar plate (pre-warmed in a 37°C oven). Plates were allowed to stand for 5 minutes to allow top agar to set, then incubated overnight at 37°C. The plaques were counted and the pfu/ml calculated.

$$\text{pfu/ml} = \frac{(\text{no. of plaques}) \times (\text{dilution factor}) \times (1 \times 10^3)}{(\text{no. of } \mu\text{l dilution used})}$$

2.7.2 Plating of genomic phage library

To get an appropriate representation of all the genes in the library ~1 million plaques were plated out on a suitable number of 20cm x 20cm plates. The minimum number of microlitres of library stock needed per plate to achieve this density of plaques was calculated from the pfu/ml determined for the stock. For each plate, a 600µl aliquot of an overnight culture of VCS257 *E.coli* cells was inoculated with the desired amount of library master stock (diluted with SM buffer (Appendix A)) and placed in a 37°C water bath for 15minutes. Lambda Top-Agar was melted in a microwave and cooled to 47°C. The infected culture was mixed with 25mls of Lambda Top-Agar and supplemented to 10mM MgSO₄, and poured quickly onto 20cm x 20cm Lambda Agar plates (pre-warmed in a 37°C incubator). When the agar had set, the plates were inverted and incubated at 37°C until plaques had formed (~7 hours). Plates were then Saran wrapped and stored at 4°C until needed.

2.7.3 Phage DNA Lifts

The library DNA was transferred from the plaque plates onto nylon membrane, Hybond-N⁺ (Amersham) for screening by hybridisation. Duplicate lifts were taken for each plate and following hybridisation only plaques that were positive on both filters were picked. The corners of the membrane were marked for orientation purposes and the membrane placed onto the agar surface. The plate was marked in alignment with the marks on the membrane and after 1 minute the membrane was removed from the agar to Whatman filter paper soaked in denaturing solution and left for 30 seconds (DNA side facing up). During this time the second membrane was placed onto the agar surface and marked in alignment with the marks on the plate and after 1 minute removed to denaturing solution for 30 seconds. The membranes were then removed to Whatman filter paper soaked in neutralising solution and left for 2 minutes after which time they were placed onto Whatman filter paper, UV cross-linked and baked at 120°C for 20 minutes. Membranes were stored between Whatman filter paper at room temperature.

2.7.4 Primary screen of cDNA library

2.7.4.1 Prehybridisation

The prepared membrane was rolled between two hybridisation meshes in a hybridisation tube (Hybaid) and 25mls of Church Hybridisation buffer (see Appendix A), preheated to 65°C, was added, salmon sperm DNA was also added to a final concentration of 0.1mg/ml to reduce background hybridisation. Membrane and buffer were incubated with rotation at 65°C for 3 hours in a hybridisation oven (Hybaid) to allow the membrane to equilibrate. Multiple membranes may be probed in the same tube so long as sufficient meshes were used to allow even fluid flow.

2.7.4.2 Generation of radiolabelled probes

25-ng of clean probe DNA in 11µl of dH₂O (gel extracted restriction fragment or PCR product) was radiolabelled with ³²P-dCTP using High Prime enzyme (Boehringer Mannheim) by addition of 4µl of enzyme and 5µl of ³²P-dCTP followed by incubation at 37°C for 10 minutes. The reaction was stopped by the addition of 2µl 0.2M EDTA (pH8). Labelled probe was separated from unincorporated nucleotides using a Sephadex G50 column (Amersham Pharmacia Biotech). The column is equilibrated by centrifugation at 3000rpm for 1 minute. The radiolabelled probe solution volume was made up to 50µl with dH₂O and added to the column, centrifuged at 3000rpm for 2 minutes and the elute containing the radiolabelled probe was collected in a 1.5ml Eppendorf tube. Unincorporated nucleotides remained in the column and it was discarded. The radiolabelled probe was denatured by placing in a hot block at 100°C for 10 minutes, cooled rapidly in an ice/ethanol bath for 1 minute and placed on ice.

2.7.4.3 Hybridisation

Following prehybridisation, the Church buffer was removed and 10mls of fresh church buffer, preheated to 65°C and containing salmon sperm DNA, was added to

the hybridisation tube. The radiolabelled probe was then added and the membrane was incubated with rotation overnight at 65°C. The membrane was washed four times for 30 minutes each in Church Wash (see Appendix A) at 65°C. Following these washes the membrane was removed from the hybridisation tube, sealed in Saran wrap and exposed to MR X-ray film (Kodak) in an autoradiography cassette. Autoradiography cassettes were stored at -70°C for 2-5 days, depending on signal strength. Autoradiography films were developed (Hyperprocessor, Amersham) and primary and secondary filters compared for overlapping signals.

2.7.5 Secondary screen of phage clones

Positive plaques from the 1° screen were then subjected to a further round of screening so as to achieve single homogenous clones. The positive plaques were excised from the agar master plates and introduced into a 1.5ml eppendorf tube containing 500µl of SM buffer and 20µl of chloroform. The phage DNA was left to elute at 4°C overnight. This eluent was used to infect VCS257 (*) *E.Coli* cells at a suitable density for well spread plaques to form on 10cm² lambda agar plates. Duplicate membrane lifts were then made and screened as for the 1° screen. Positive individual clones were then identified and excised as before.

2.7.5.1 Preparation of phage DNA

Phage DNA was isolated using the Rapid Excision Kit (Stratagene) following manufacturers instructions. Briefly, 5µl of lambda phage (~1000pfu), 100ul of XPORT cells at OD₆₀₀ of 1.0 and 10µl of 704 helper phage (10⁸ pfu/ml) were mixed and 3mls of NZY top agar was added to each sample. The entire sample was plated separately onto NZY agar plates and incubated overnight at 37°C. The XPORT cells support growth of the lambda phage, 704 helper phage and phagemid DNA, whereas the XLOLR cells support only growth of the excised phagemid particles. Plaques contain lambda phage, 704 helper phage, excised pBluescript® phagemid particles and infected XLOLR cells. Turbid plaques were picked by touching with a toothpick and grown overnight in LB-tetracycline-ampicillin broth. Only XLOLR cells

containing phagemids with the ampicillin antibiotic resistance gene grew and the DNA was then minipreped.

2.8 *In vitro* synthesis of capped mRNA

Ambions mMESSAGE mMACHINE™ kit was used for the *in vitro* synthesis of capped mRNA (mimics most eukaryotic mRNAs *in vivo*, because it has a 7-methyl guanosine cap structure at the 5' end) for subsequent injection into *Xenopus* embryos. 10µg of plasmid DNA (*Wnt* genes 1, 8b and 10a in the *Xenopus* expression vectors pSP64TBX or pSP64TXB) was linearised by restriction digestion. The linearised DNA was ethanol precipitated and resuspended at 1µg/µl. The transcription reaction was set up as follows:

Linear template DNA	1µg
2X NTP/Cap	10µl
10x reaction buffer	2µl
Enzyme mix	2µl
Nuclease-free water	5µl

The transcription reaction was incubated at 37°C for 4 hours. 1µl of DNase 1 was then added and the reaction incubated for a further 15 minutes. The RNA was recovered by ethanol precipitation and quantified by denaturing gel electrophoresis alongside an aliquot of RNA of known concentration.

2.9 *Xenopus* embryo injections

RNA transcribed *in vitro* (10ng/µl) was microinjected ventrally into two-cell stage *Xenopus* embryos. *Xenopus* injections were performed by Dr. Stefan Hoppler. Embryos were then cultured, at 18°C for 24 – 48 hours, and their development monitored. Embryos were then fixed for 30 minutes in fresh 4% paraformaldehyde and washed four times in 1X PBS before photographing with a Leica digital camera.

2.10 Histological analysis

5µm sections were cut from paraffin embedded mammary glands and floated onto vectabond-coated slides. Slides were stained with haematoxylin and eosin for histological analysis.

2.10.1 Immunohistochemistry

Immunohistochemistry was carried out using either the DAKO EnVision plus system (cat. no. K4006) or the ImmunoCruz staining system (Santa Cruz Biotechnology Inc. cat. no. sc-896K) following the manufacturer's instructions. The Dako EnVision plus system was used for β - catenin and cyclin D1 detection. β - catenin was detected using a mouse monoclonal antibody (Transduction laboratories, cat. no. C19220). Antigen retrieval used 10mM citrate buffer, pH 6 and the slides were microwaved three times at 700Watts for 5 minutes. The antibody was titrated and used at an optimal concentration of 1 in 50 dilution overnight at 4°C. Cyclin D1 was detected using a mouse monoclonal antibody (Nova Castra cat. no. DCS-6). Antigen retrieval used Dako high pH target retrieval solution (Dako Corporation, cat. no. S3308) and the slides were incubated in preheated solution in a water bath at 95-99°C for 30 minutes, the slides were then removed from the water bath and allowed to cool in solution for 20 minutes. Following antibody titre the optimal concentration was 1 in 100 dilution overnight at 4°C. The DAKO EnVision kit comes with a peroxidase labelled polymer conjugated to goat anti-mouse immunoglobulins. Staining is visualised with 3,3'-diaminobenzidine (DAB) +substrate-chromagen which results in a brown-coloured precipitate at the antigen site. The ImmunoCruz staining system was used for APC and α 1 type IV collagen detection. Antigen retrieval for both was 10mM citrate buffer, pH 6. Slides were heated in solution at 95°C for 5 minutes, fresh buffer was added and heated again for 5 minutes at 95°C. Slides were then left to cool in buffer for 20 minutes. APC was detected using a c-terminus antibody (Midgeley C.A. et. al., 1997), at 1 in 100 dilution overnight at 4°C. α 1 type IV collagen was detected using a rabbit polyclonal antibody (Santa Cruz Biotechnology Inc. cat. no. sc-11360), at 1 in 100 dilution overnight at 4°C. The ImmunoCruz

staining system employs a biotinylated goat anti-rabbit secondary antibody, followed by HRP-streptavidin complex and staining is visualised as before using DAB. Immunohistochemical techniques were also used to detect BrdU and TUNEL (TdT-mediated dUTP nick end labelling) staining. Animals were injected with BrdU (70µg in sterile saline, i.p.), 2 hours before sacrifice. Antigen retrieval used 0.1% trypsin in 0.1% calcium chloride for 20 minutes in 37°C water bath, followed by IM HCL for 10 minutes in 60°C water bath. Detection of BrdU incorporation was by an anti-bromodeoxyuridine-peroxidase antibody (Roche cat. no. 1585 860), at 1 in 10 dilution for 45 minutes at room temperature. The rest of the protocol used the DAKO EnVision plus system as above. The ApopTag Peroxidase *In Situ* Apoptosis Detection Kit (Intergen Company, cat. no. S7101) was used for TUNEL detection.

2.11 General tissue culture

2.11.1 Human embryonic kidney (HEK 293) cells

Human embryonic kidney (HEK 293) cells were obtained from European Cell Culture Collection. To thaw cell lines for culture, aliquots of cells stored in CryoTube™ vials (Nunc) were thawed with agitation in a prewarmed 37°C water bath. The rapidly thawed cell suspensions were then dispersed into 25mls of culture media, RPMI 1640 medium (Invitrogen) supplemented with 10%(w/v) foetal calf serum (FCS), 20mM L- Glutamine (Sigma), 20U/ml Penicillin (Sigma) and 20µg/ml Streptomycin (Sigma). Cells were incubated at 37°C in an atmosphere of 5% CO₂ in Sanyo CO₂ incubators. Cells were cultured in disposable sterile plastic ware (flasks and petri dishes) supplied by Nalge-Nunc or Greiner.

2.11.2 Trypsinisation of cells (T75 flask)

The medium was aspirated off the cells. A few mls of PBS buffer was added and the flask gently swirled to wash the cells. PBS was then aspirated off and approximately 1ml of Trypsin solution was added and gently swirled over the surface of the cells.

The flask was incubated at 37°C until cells started to come off the culture flask when gently tapped, typically 2-3 minutes. 2mls of culture medium was added to the flask and a Pasteur pipette was used to break up the cell clumps and wash the surface of the flask. All of the liquid was transferred into a 15ml centrifuge tube containing 8ml of culture medium, mixed by pipetting and centrifuged for 5 minutes at 1000rpm. The medium was aspirated off and the bottom of the tube tapped to loosen the pellet. The pellet was resuspended in 10mls of PBS and centrifuged again for 5 minutes at 1000rpm. PBS was aspirated off and the bottom of the tube tapped to loosen the pellet. The cells were then either split into fresh medium by resuspending in 1-2mls of medium and plated at a density of 2.5×10^6 cells/ml. Alternatively, frozen stocks of cells were made by resuspending the pellet in 1-2 mls of freezing mix to a concentration of $3-5 \times 10^6$ cells/ml.

2.11.3 Lipid based transfection with FuGene™6 transfection reagent

Tissue culture cells were transfected with exogenous DNA using FuGene™6 transfection reagent (Boehringer-Mannheim), which forms DNA/lipid conjugates. FuGene™6 contains a novel blend of lipids that do not form liposomes and which have a very low level of cytotoxicity. The reagent can be used in the presence of serum and yields a high level of transfection efficiency over a broad range of DNA concentrations. On the day prior to transfection each well of a 6-well plate was plated with 1×10^5 HEK 393 cells. Each well was therefore approximately 50-80% confluent upon transfection. 100µl of serum free medium (RPMI 1640) was aliquoted into a sterile 1.5ml eppendorf tube, one tube per transfection. Following the addition of 3-6µl of FuGene™6, ensuring that the pipette does not touch the sides of the tube, the tubes were incubated at room temperature for 5 minutes. During this incubation step, the DNA (0.5 – 1.5µg) to be transfected was aliquoted into separate sterile 1.5ml tubes. The FuGene™6/medium mix was added directly to the DNA and tapped to mix. This was incubated at room temperature for 15 minutes after which time the entire FuGene™6/medium/DNA mix was added to the corresponding well of a 6-well plate and swirled to mix. Cells were incubated as before, at 37°C in an atmosphere of 5% CO₂ in Sanyo CO₂ incubators.

2.11.4 Isolation of stably transfected clones

HEK 293 cells were transfected with a series of *Wnt* genes (*Wnt1*, *Wnt8b* and *Wnt10a*) in two different expression vectors (Cags and PGK). Both of these expression vectors carry a second antibiotic resistance gene for Hygromycin B. In order to select for stably transfected clones the medium was changed after 24 hours to one which contained Hygromycin B at a concentration of 100µg/ml. Fresh Hygromycin B containing medium was added after 48 hours so as to remove any of the dead untransfected cells. The stable clones were grown for about 1 week, after which time the wells was 100% confluent. Cells were now ready to be split into fresh Hygromycin B containing medium or to be frozen down as stocks.

2.11.5 Tunicamycin treatment

Tunicamycin (Calbiochem) is an inhibitor of N-linked glycosylation and was added to subconfluent stably transfected HEK 293 cells at either 1µg/ml overnight or at 5µg/ml for 6 hours prior to protein isolation and electrophoresis.

2.11.6 C57MG mouse mammary epithelial cells

C57MG mouse mammary epithelial cells were grown in DMEM (Invitrogen) supplemented with 10%(w/v) foetal calf serum (FCS), 20U/ml Penicillin (Sigma), 20µg/ml Streptomycin (Sigma) and 10µg/ml insulin (Sigma). Cells were incubated at 37°C in an atmosphere of 5% CO₂ in Sanyo CO₂ incubators. Because the parental cell line exhibits spontaneous morphological alterations, limited dilution cloning isolated a subline that more stably maintains a flat morphology. Cells were split as for section 2.9.2 and stable transfection of *Wnt* expressing plasmids was performed as for sections 2.9.3 and 2.9.4. Stably transfected clones were pooled and after 24hours the medium was changed to one that was serum free as the morphological changes induced by *Wnt* genes are more readily observed in this medium. The

morphology was assessed and cells photographed at confluence with a Leica digital camera and inverted microscope.

2.11.7 Harvesting cells for protein (T75)

Cells to be harvested for protein analysis were washed twice with ice-cold PBS after removal of culture media. Cells were removed from the plastic surface in 10 mls of PBS using a cell-scraper (Nalge-Nunc) and the resulting suspension was collected in a 15ml centrifuge tube. This was then centrifuged at 1000rpm for 5 minutes and all of the PBS aspirated off. The pellet was resuspended in 200 μ l of TENT buffer (Appendix A) containing 1mM Pefabloc, 10mg/ml Aprotinin, 2mg/ml Leupeptin and 1mg/ml Pepstatin. Cells were lysed by incubation on ice for 20 minutes. Cells were then centrifuged at 10 000rpm, 4°C for 10 minutes. The protein containing supernatant was then aliquoted into 20 μ l samples and stored at -70°C.

2.12 Protein quantification

Quantification of protein concentration in tissue lysates was carried out using the BCA protein Assay Kit (Pierce). Briefly, fifty parts BCA reagent A were mixed with one part BCA reagent B (see Appendix A) to create the working BCA reagent solution. A protein concentration standard curve was generated by preparing a set of dilutions, (2, 1.5, 1.0, 0.750, 0.5, 0.25, 0.125, 0.025 and 0 mg/ml) of Bovine Serum Albumin (BSA, supplied) in sterile test tubes. 10 μ l of each standard and unknown sample to be assayed was placed in a test tube. 200 μ l of the working BCA reagent solution was added to each test tube, mixed and incubate at 37°C for 30 minutes. At the end of this incubation the tubes were cooled to room temperature and the absorbance at 562nm of each solution determined relative to a water blank. A standard curve was generated from the 562nm absorbance of the known BSA concentration samples and the protein content of each of the unknown tissue lysates determined by comparison to the standard curve.

2.13 Endoglycosidase treatment

Endoglycosidase H (Endo H) (New England Biolabs) treatment of protein samples, prior to electrophoresis, removes the N-linked carbohydrates and converts proteins to their unglycosylated forms. Protein samples (20µg) were denatured in 1X denaturing buffer (0.5% SDS, 1% β-mercaptoethanol) by incubation at 100°C for 10 minutes. 1/10th volume of 10X G5 reaction buffer (50mM Sodium Citrate (pH 5.5 at 25°C)) and 2.5µl of Endo H were added and the samples incubated at 37°C for 1hr/4hr/24hr prior to protein electrophoresis.

2.14 Western Blotting

2.14.1 Protein electrophoresis

SDS-polyacrylamide gel electrophoresis was accomplished on precast 10% Tris-Glycine gels in an Xcell *SureLock*TM mini cell tank (Novex). A volume of sample containing 20µg of total protein (5-20µl) was made up to a total volume of 20µl with TENT Buffer. 5µl of 4x SDS-Sample Loading buffer (Novex) and 2.5µl of 10x Sample Reducing agent were added to the protein samples. The samples were heated to 95°C for 5 minutes and then centrifuged briefly. Gel wells were then loaded with samples and electrophoresed at 150V in parallel with a molecular weight marker (Multimark from Invitrogen) in MOPS SDS running buffer (Novex) at room temperature for 3 hours.

2.14.2 Protein transfer

Protein was transferred onto PVDF membrane (Bio-Rad Laboratories) via electrophoresis at a constant current of 250mA (I did 50volts) over night in transfer buffer (Appendix A). Transfer was carried out at 4°C in an XCell IITM blot module which fits into the Xcell *SureLock*TM mini cell tank (Novex). Following transfer gels were stained in GelCode (Pierce) to determine transfer efficiency and to check

loading levels in the individual wells. Gels were placed in 15 ml of stain solution in a Coplin jar and gently rocked for 1-2 hours then destained in dH₂O for 2-6 hours. Destained gels were placed on 3MM Whatman filter paper and dried in a vacuum apparatus. PVDF membranes were stained in Ponceau S (Sigma) to ensure that the protein transfer was efficient and even throughout. Membranes were placed in 10mls of stain solution in a Coplin jar and incubated for up to one hour with gentle agitation, then the background removed by rinsing in distilled water. The stain could be completely removed from the protein bands by continued washing.

2.14.3 Antibody incubation

Protein blots were transferred to 50ml centrifuge tubes with 10ml of blocking solution (10% non-fat dried milk powder (w/v)(Marvel, Nestlé, UK) in TBST (Appendix A) and placed on a roller mixer. Blots were blocked in this solution for 3 hours at room temperature. Following blocking, a 1/500 dilution of primary antibody solution (HA-Probe, rabbit affinity-purified polyclonal antibody raised against a peptide mapping to an internal region of the influenza hemagglutinin (HA) protein (Santa Cruz Biotechnology, Inc.)), was added to the blocking solution and the blots incubated in the same manner for 2 hours at room temperature. The primary antibody solution was then poured off and the blot washed 3 times for 10 minutes in 10ml TBST at room temperature. The blot was then incubated with a 1/5000 dilution of HRP-conjugate secondary antibody solution (HRP anti-rabbit IgG, Diagnostics Scotland) in 10ml of 10% Marvel (Nestlé, UK) in TBST at room temperature for 1 hour. The blot was washed as above prior to signal detection.

2.14.4 Signal detection

Signals were detected using the ECLTMPlus Chemiluminescent detection system (Amersham Pharmacia Biotech). For each blot detection solutions A and B were mixed in a ratio of 40:1 (eg. 2ml solution A and 50µl solution) just prior to application. The blot was placed on a sheet of SaranWrapTM, protein upwards, and the mixed reagent solution pipetted onto its surface. The reagents were left in contact

with the blot for 5 minutes at room temperature then poured off. The blot was then placed between 2 acetate transparencies, and transferred to an x-ray film cassette. While in a dark room, the blot was then overlaid with ECLTM film (Amersham) for periods of 30 seconds to 10 minutes, depending on signal intensity. Films were developed (Hyperprocessor, Amersham), digitally scanned (DeskScan II, Hewlett Packard) and bands quantified with densitometry software (Aida, Microsoft).

2.15 Animal work

2.15.1 Isolation of genomic DNA from murine tissues

All mice used were genotyped from tail or ear biopsies. The following protocol was used to isolate genomic DNA from mouse ear biopsies and quantities were doubled for tail biopsies. Ear biopsies were supplied in a 1.5ml eppendorf tube and 250µl of Lysis buffer (Appendix A) was added. Tubes were incubated for 3 hours (if tail biopsy then overnight) in a 55°C shaking water bath. An equal volume of phenol chloroform was added to each sample and inverted several times to mix, and centrifuged at 13 000rpm for 1 minute. The upper aqueous phase was transferred to a fresh 1.5ml eppendorf tube and the DNA precipitated by the addition of 1/10th volume of 3M NaOAc and 2.5 volumes of 100% ethanol. The tubes were vortexed to mix and incubated at -20°C for at least 1 hour. DNA was pelleted by centrifugation at 13000rpm for 15 minutes, and 150µl of ddH₂O added to each tube. To remove all traces of ethanol and to dissolve the DNA the tubes were incubated in a PCR block at 55°C for 45 minutes. The samples were vortexed to mix then pulse centrifuged to collect the sample in the bottom of the tube. DNA was then ready to be used in a PCR reaction to determine the genotype of the mouse.

2.16 Gene specific PCR

Standard PCR amplification of specific DNA fragments was performed using *Taq* thermostable DNA polymerase (Promega) and accompanying 10 X reaction buffer

(Appendix A) and magnesium chloride (25mM). 25 μ M dNTP's (Amersham Pharmacia Biotech) were used at a concentration of 10mM (2.5mM each of dATP, dCTP, dGTP and dTTP) and unless otherwise stated all primers were used at a concentration of 10 μ M. (Genotyping primer pairs and reaction conditions were taken from the referenced publications and for all other reactions primers were chosen from a number of primer pair options supplied by Primer3, a web base primer design software program (<http://www.genome.wi.mit.edu/cgi-bin/primer/primer3.cgi>)) Reaction volumes of 20 μ l were used and reactions were carried out in 0.5ml thin-walled microcentrifuge eppendorf tubes in a standard thermocycler (Peltier Thermal Cycler). Unless otherwise stated, all PCR reactions were set up as follows:

DNA template	x μ l
10X PCR buffer	2 μ l
dNTP's (10 mM)	0.4 μ l
Primers (10 μ M)	0.25 μ l
MgCL ₂ (25mM)	1.2 μ l
Taq DNA polymerase (5U/ μ l)	0.2 μ l
Water to a final volume of	20 μ l

Typically a master mix containing all the above reagents was prepared, on ice and an appropriate volume added to 0.5 ml eppendorf tubes containing DNA template. Table 2.1 summarises the conditions in which PCR was accomplished.

Table 2.1 PCR reaction primers and conditions

PCR Reaction	Primer pair (5'-3')	Product size	Cycle Parameters
Genotyping; APC	P4: CACTCAAACGCTTTTGAGGGTTGATT P3: GTTCTGTATCATGGAAAGATAGGTGGT	314bp floxed allele 226bp wt allele	94°C - 3 minutes 94°C - 30 seconds 55°C - 30 seconds 72°C - 40 seconds 34 cycles
Genotyping; BLG	BLG Fwd: CTTCTGGGGTCTACCAGG BLG Rev: TCGTGCTTCTGAGCTCTG	180bp	94°C - 3 minutes 94°C - 30 seconds 55°C - 30 seconds 72°C - 40 seconds 34 cycles
Probe: APC exon 14	APC14Rev: GTCTGGCTCCGGTAAGTGAG APC14Fwd: TTGATGGAATGTGCTTTGGA	164bp	94°C - 2minutes 94°C - 30 seconds 60°C - 30 seconds 72°C - 40 seconds 40 cycles
Probe + Library PCR: Novel 2	Novel 2 Fwd: GCTGTGTGATTAAGACTAACATTTGAA Novel 2 Rev: CCACACACCCTCCCTAAAGA	590bp	94°C - 1 minute 94°C - 30 seconds 55°C - 30 seconds 72°C - 40 seconds 39 cycles
Library PCR: Novel 2 (nested)	Novel 2 nst Fwd: TGCAAGTTATTTAACCACCAATG Novel 2 Rev: CCACACACCCTCCCTAAAGA	210bp	94°C - 1 minute 94°C - 30 seconds 55°C - 30 seconds 72°C - 40 seconds 39 cycles
Library PCR: Novel 2 (nested)	Novel 2 nst Rev: CATTGGTGGTTAAATAACTTGCAT Novel 2 Fwd: GCTGTGTGATTAAGACTAACATTTGAA	402bp	94°C - 1 minute 94°C - 30 seconds 55°C - 30 seconds 72°C - 40 seconds 39 cycles
Probe: 3'UTR	3'UTR Fwd: TGGAAGAGGGGATATTGCAC 3'UTR Rev: GTCTTGTGGTGGGACTGGAT	973bp	94°C - 3 minutes 94°C - 30 seconds 55°C - 30 seconds 72°C - 40 seconds 34 cycles

Library PCR: 3'UTR (nested)	3'UTR nst Fwd: AAAGATCCTGTTCCATTGAA 3'UTR Rev: GTCTTGTGGTGGGACTGGAT	577bp	94°C - 3 minutes 94°C - 30 seconds 55°C - 30 seconds 72°C - 40 seconds 34 cycles
Library PCR: 3'UTR (nested)	3'UTR Fwd: TGGAAGAGGGGATATTGCAC 3'UTR nst Rev: GGATGAGCATTCTTTGAAAGC	497bp	94°C - 3 minutes 94°C - 30 seconds 55°C - 30 seconds 72°C - 40 seconds 34 cycles
Probe: Alpha gene	Alpha Fwd: AATTGTGATAGTTCAGCTTGAATG Alpha Rev: AAATTGGTAGCTTTCATTGCT	300bp	94°C - 3 minutes 94°C - 30 seconds 50°C - 30 seconds 72°C - 40 seconds 34 cycles
Probe: cDNA 1	cDNA 1 Fwd: AAGGCCAAAAAGCAAACCT cDNA 1 Rev: AGTGCTGGGTGGGAATGTAG	223bp	94°C - 3 minutes 94°C - 30 seconds 55°C - 30 seconds 72°C - 40 seconds 34 cycles
Probe: cDNA 2	cDNA 2 Fwd: CTACATCCCACCCAGCACT cDNA 2 Rev: TTTGGCCTAATCACAGACCC	261bp	94°C - 3 minutes 94°C - 30 seconds 55°C - 30 seconds 72°C - 40 seconds 34 cycles
Probe: cDNA 3	cDNA 3 Fwd: CACTTGTGGGGAGACCTTGT cDNA 3 Rev: TGAAAGAATCAAGCAGCAGT	288bp	94°C - 3 minutes 94°C - 30 seconds 55°C - 30 seconds 72°C - 40 seconds 34 cycles
Probe: cDNA 4	cDNA 1 Fwd: AAGGCCAAAAAGCAAACCT cDNA 3 Rev: TGAAAGAATCAAGCAGCAGT	813bp	94°C - 3 minutes 94°C - 30 seconds 55°C - 30 seconds 72°C - 40 seconds 34 cycles
Probe: 18S	18S Fwd: AGCTCTTCTCGATTCCGTG 18S Rev: GGGTAGACACAAGCTGAGCC	255bp	94°C - 3 minutes 94°C - 30 seconds 55°C - 30 seconds 72°C - 40 seconds 34 cycles

Table 2.2 Primers to PCR novel genes out of library

Vector Primers	Novel gene Primers	Cycle Parameters
Lib_Fwd: TTAAGTTGGGTAACGCCAGG Lib_Rev: TGTGGAATTGTGAGCGGATA Lib_nst_Fwd: GTTTTCCCAGTCACGACGTT Lib_nst_Rev: GCCAAGCTCGAAATTAACCC	EST Fwd: GTTGGTGGGCAGCTACCTTA EST_Rev: TTTTTCAGACATATTACTCACCA	94°C - 3 minutes 94°C - 30 seconds 55°C - 30 seconds 72°C - 40 seconds 34 cycles 70°C - 10 minutes

Table 2.3 Sequencing Primers

<i>Wnt8b</i> <i>Wnt8b/10a</i>	Seq8b_Fwd	TTCTCTTGCTCGCCATAG
	Seq8b_Rev	GCTACCTTGGTGTGTAAG
	Wnt8bFwd	CGGGAAAGAACTCCTAAG
	WnT8Brev	GCTTCGAAGTCCACCAT
	Glo5	TGCTGGTTGTTGTGCTGT
	Glo3	ACCACCTTCTGATAGGCA
<i>XWnt5a</i>	<i>XWnt5a</i> -Fwd	CACAATAATGAGGCCGGAAG
	<i>XWnt5a</i> -Rev	GCGCTGTCGTATTTCTCCTT
	<i>XWnt5a2</i> Fwd	GCTGCTACGTCAAATGCAAA
	<i>XWnt5a2</i> Rev	GCGACTCACTGCCTTCACTA
Standard sequencing primers	Sp6	ATTAACCCTCACTAAAG
	T7	GTAATACGACTCACTATAGGGC
	M13 rev	GGAAACAGCTATGACCATG
	M13 fwd	GGAAACAGCTATGACCATG

3 Characterisation of $cre^+ Apc^{580S/580S}$ mice

3.1. Introduction

Section 1.6.3 introduced a method of conditional inactivation of *Apc* in the mouse mammary gland. Briefly, mice harbouring a floxed allele of *Apc* ($Apc^{580S/580S}$) were crossed to transgenic mice expressing a transgene that drives expression of cre recombinase specifically in the mammary gland (BLG-cre), and the progeny, BLG-cre floxed *Apc* mice ($cre^+ Apc^{580S/580S}$), underwent specific inactivation of mammary *Apc* (Gallagher *et al.*, 2002). The authors identified a role of *Apc* in the normal growth of virgin mammary glands by observing that mutant ($cre^+ Apc^{580S/580S}$) glands grow more slowly than controls ($cre^+ Apc^{+/580S}$ and $cre^- Apc^{580S/580S}$) (Figure 1.11). In addition, $cre^+ Apc^{580S/580S}$ mice develop numerous small areas of metaplasia in the ductal epithelium as a consequence of loss of *Apc*. Pregnancy in these mice results in multiple extensive metaplastic nodules, however none of these lesions progress to neoplasia (Figure 1.12) (Gallagher *et al.*, 2002).

A variety of approaches were taken to investigate these interesting phenotypes. To determine the extent of *Apc* deletion in $cre^+ Apc^{580S/580S}$ mouse mammary glands, a combination of Southern and northern blot analysis was used to identify levels of both *Apc* excision and expression in dissected mammary gland extracts. In addition, the distribution of APC protein was examined using a C-terminal antibody (Pab3161) (Midgley *et al.*, 1997). Considering the function of APC in the canonical Wnt signalling pathway (Munemitsu *et al.*, 1995), an immunohistochemical study of candidate Wnt signalling proteins was incorporated into this analysis in combination with proliferation analysis (BrdU, TUNEL) as a means of further characterising the metaplastic lesions.

3.2 Results

Control genotypes $cre^+ Apc^{+/580S}$ and $cre^- Apc^{580S/580S}$ gave the same result and thus only one control image is shown from either genotype.

3.2.1 *Apc* excision and expression levels in cre^+ *Apc*^{580S/580S} mouse mammary glands

Although it was originally anticipated that in driving *cre* expression from the promoter of a milk protein gene (BLG) the effects of *cre* mediated *Apc* deletion would be found primarily in the lactating mammary gland, substantial *cre* activity was observed at earlier stages of mammary gland development (Gallagher *et al.*, (2002). In order to confirm BLG-*cre* recombinase mediated *Apc* excision and determine the temporal deletion of *Apc* in cre^+ *Apc*^{580S/580S} mouse mammary glands, Southern blot analysis of whole mammary gland extracts (minus lymph node) from these mice was performed. Genomic DNA extracted from littermate control (cre^+ *Apc*^{+/580S} and cre^- *Apc*^{580S/580S}) and mutant (cre^+ *Apc*^{580S/580S}) mouse mammary glands at four stages of development (mid-gestation, parturition, lactation day 2 and lactation day 4) was digested overnight with the restriction enzyme *Xba*I (see section 2.2.1). Digested DNA was subsequently electrophoresed on a 0.8% agarose gel, blotted onto a nylon membrane, and incubated overnight with radiolabelled probe (Probe A, Shibata *et al.*, 1997) (see Figure 3.1). Autoradiographs of the Southern blot displayed two major bands in mutant (cre^+ *Apc*^{580S/580S}) lanes (the probe failed to detect the floxed allele in control samples). The predominant band resolved at approximately 9.0kb, close to the expected size of the floxed allele. The excised allele resolved at 7.0kb and was observed from parturition. Excision levels appeared to increase in lactating mice however due to the weak signal quantitation was not possible (Figure 3.1). Therefore, alternative methods of calculating *Apc* deletion in cre^+ *Apc*^{580S/580S} mouse mammary glands were employed. Nevertheless, this data confirms BLG-*cre* recombinase activity in the mouse mammary gland prior to lactation.

Northern analysis was used to examine *Apc* expression levels in both control (cre^+ *Apc*^{+/580S} and cre^- *Apc*^{580S/580S}) and cre^+ *Apc*^{580S/580S} mouse mammary glands. Total RNA isolated from both control and mutant mouse mammary glands at four stages of development (as above) was electrophoresed through a 1% denaturing formaldehyde

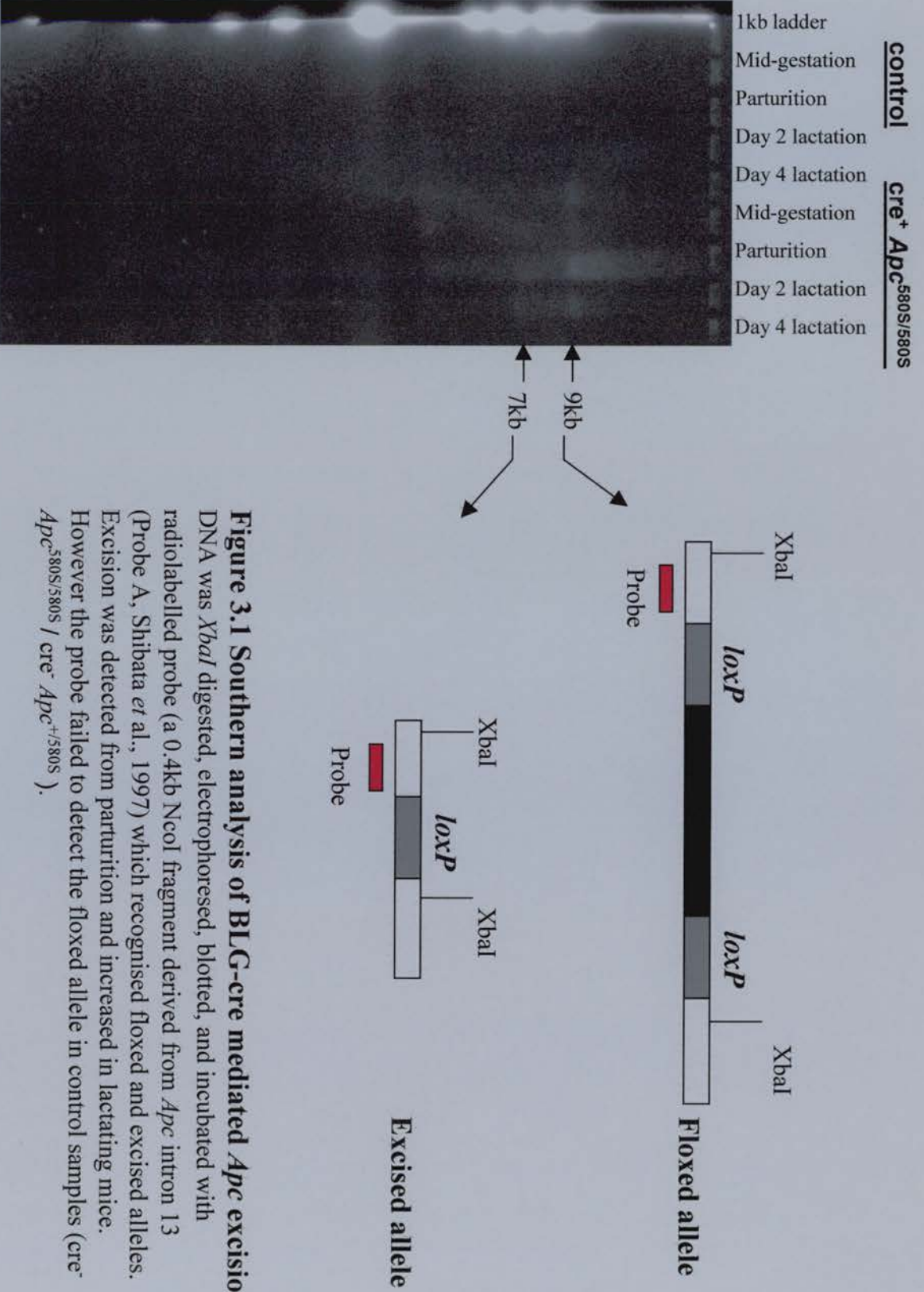


Figure 3.1 Southern analysis of BLG-cre mediated *Apc* excision
 DNA was *Xba*I digested, electrophoresed, blotted, and incubated with radiolabelled probe (a 0.4kb *Nco*I fragment derived from *Apc* intron 13 (Probe A, Shibata *et al.*, 1997) which recognised floxed and excised alleles. Excision was detected from parturition and increased in lactating mice. However the probe failed to detect the floxed allele in control samples (*cre*⁻ *Apc*^{580S/580S} / *cre*⁻ *Apc*^{+/580S}).

agarose gel, blotted onto a nylon membrane and incubated overnight with radiolabelled probe (see section 2.5). A probe designed against a 160bp region of *Apc* exon 14 (the exon deleted during BLG-cre mediated recombination) hybridised with the transcript derived from the floxed allele of $cre^+ Apc^{580S/580S}$ mice. Autoradiographs demonstrated decreased *Apc* mRNA levels in $cre^+ Apc^{580S/580S}$ mice from mid gestation relative to controls. A second smaller band was observed which followed a similar expression pattern albeit at lower levels which may represent an alternative splice variant of *Apc* in the mammary gland (Figure 3.2).

3.2.2 Characterisation of metaplastic lesions from $cre^+ Apc^{580S/580S}$ mouse mammary glands

As described in section 1.6.3, the phenotype of mice with conditional inactivation of the *Apc* gene ($cre^+ Apc^{580S/580S}$) in the mammary gland includes the formation of metaplastic nodules. To further characterise these lesions immunohistochemical staining for *Apc*, β -catenin, and cyclin D1 was performed on sections of day 10 lactation control ($cre^+ Apc^{+/580S}$ and $cre^- Apc^{580S/580S}$) and mutant ($cre^+ Apc^{580S/580S}$) mouse mammary glands. In addition analysis of BrdU incorporation and TUNEL were used to monitor cell proliferation and death in both normal and metaplastic epithelium. It was anticipated that this analysis may provide clues as to the molecular events underlying metaplasia in $cre^+ Apc^{580S/580S}$ mouse mammary glands.

3.2.2.1 *Apc*

Apc protein distribution in both control ($cre^+ Apc^{+/580S}$ and $cre^- Apc^{580S/580S}$) and mutant ($cre^+ Apc^{580S/580S}$) mouse mammary glands was examined using a C-terminal *Apc* antibody (Pab3161), kindly supplied by Dr. Inke Nathke (Figure 3.3a) (Midgley *et al.*, 1997). Immunohistochemical staining of sections from control day 10 lactating mammary glands ($cre^+ Apc^{+/580S}$ and $cre^- Apc^{580S/580S}$) demonstrated *Apc* expression within the alveoli. At high magnification, staining appeared predominantly cytoplasmic and was concentrated towards the apical surface. Sections from day 10 lactating $cre^+ Apc^{580S/580S}$ mammary glands displayed similar *Apc* expression in

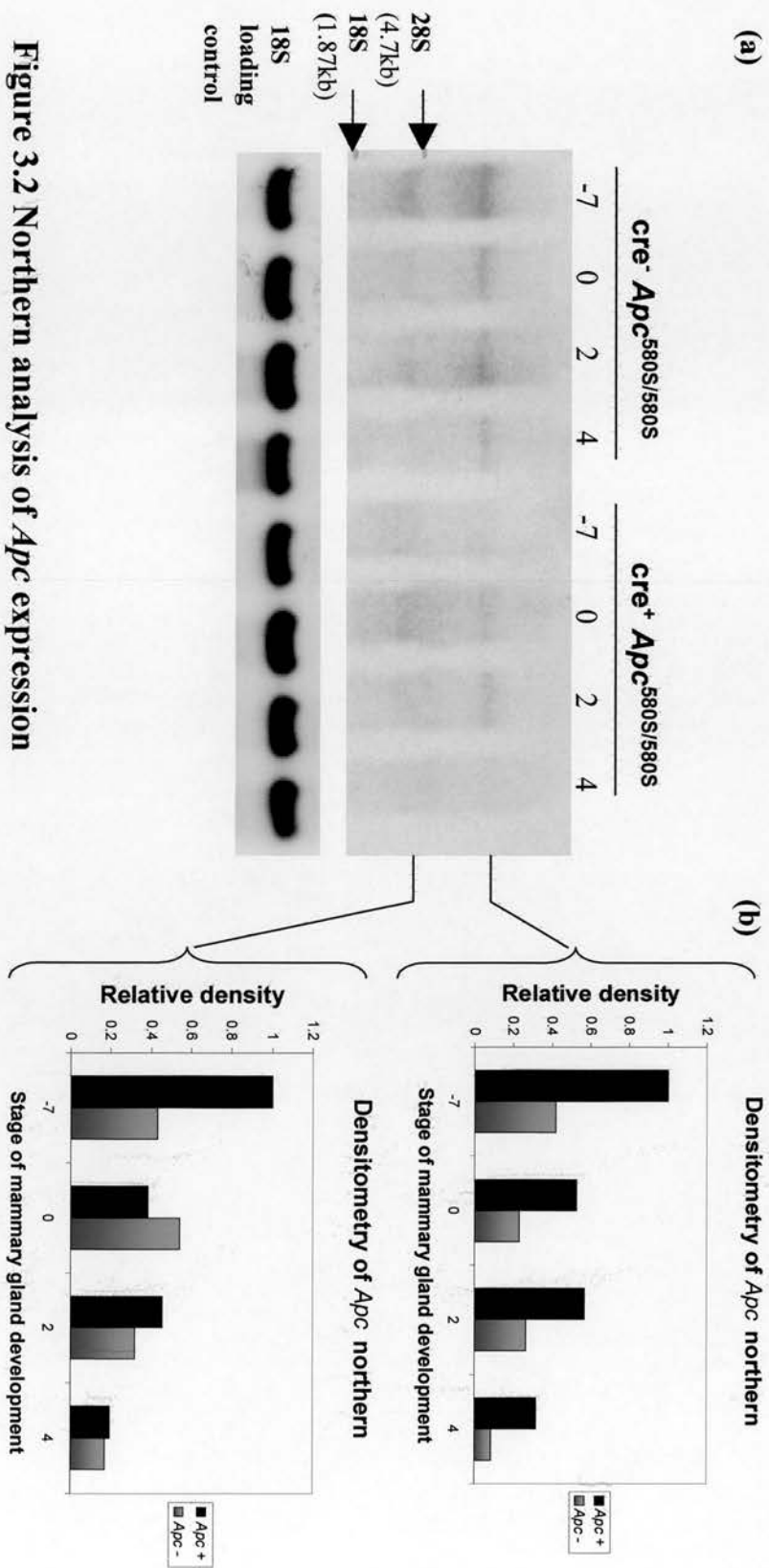
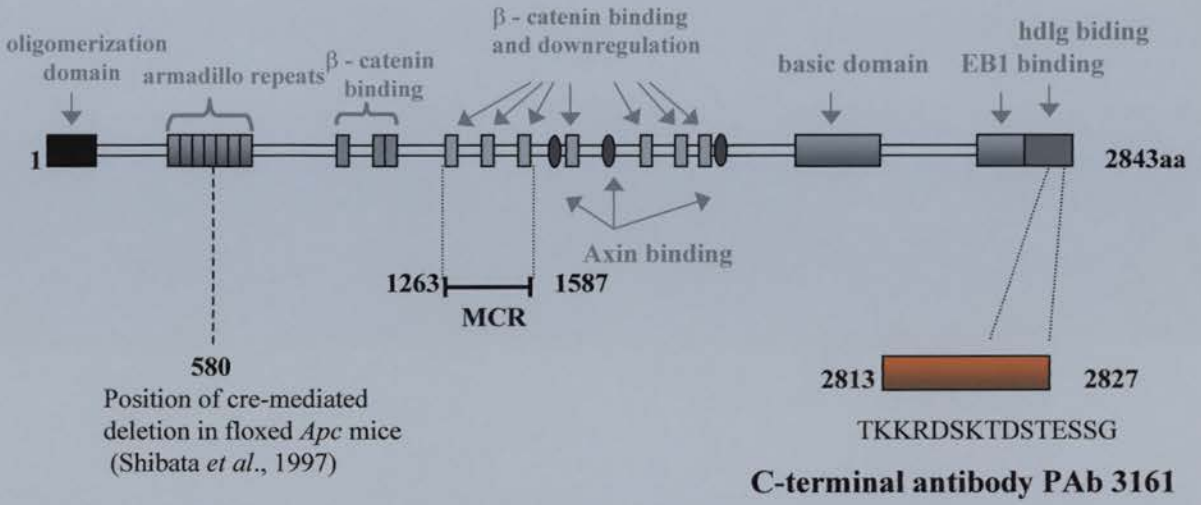


Figure 3.2 Northern analysis of *Apc* expression

(a) RNA isolated from both control and mutant mouse mammary glands at four stages of development was electrophoresed through a 1% denaturing formaldehyde agarose gel, blotted, and incubated overnight with radiolabelled probe (a 160bp fragment of *Apc* exon 14 (the exon deleted during BLG-cre mediated recombination)). Probe hybridised with the transcript derived from the floxed allele of *cre*⁺ *Apc*^{580S/580S} mouse. Two *Apc* transcripts were observed, with *Apc* mRNA levels in *cre*⁺ *Apc*^{580S/580S} mice decreased from mid gestation relative to controls confirming loss of *Apc* mRNA expression. 18S probing controlled for loading. **(b)** Densitometry analysis of *Apc* northern blot.

(a) APC



(b)

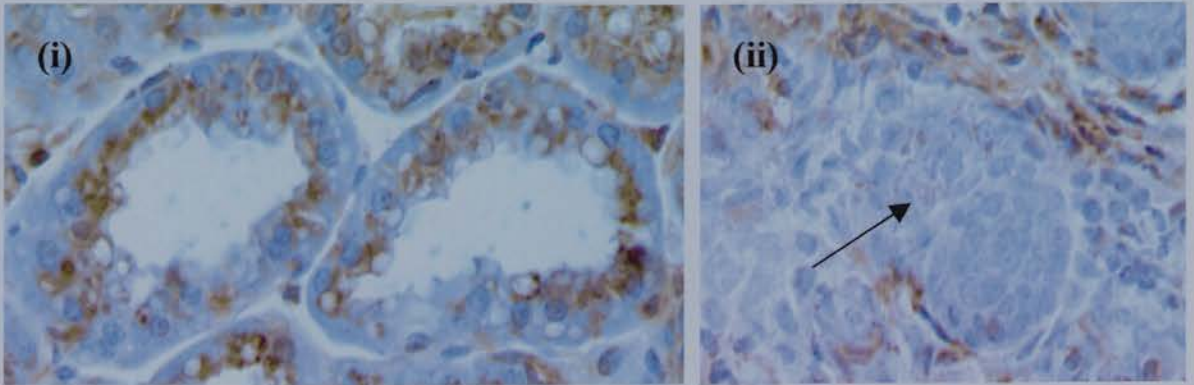


Figure 3.3 Immunohistochemical analysis of Apc expression

(a) Structural features of the APC tumour suppressor protein. The region recognised by the C-terminal APC antibody is indicated (Midgley *et al.*, 1997).

(b) Immunohistochemical analysis of Apc expression in (i) control ($cre^- Apc^{580S/580S}$) and (ii) experimental ($cre^+ Apc^{580S/580S}$) lactation day 10 mouse mammary glands. Brown staining, representing Apc expression, is located cytoplasmically within the alveoli in control mammary glands. Arrow identifies metaplastic lesion which has lost Apc expression.

normal epithelium but exhibited a significant loss of Apc protein within the metaplastic lesions (see Figure 3.3b).

3.2.2.2 β -catenin

β -catenin (see section 1.3.4.2) functions to mediate cellular adhesion through interactions with E-cadherin and additionally as a key regulator in the control of gene expression through the Wnt/Wingless pathway (Gumbiner *et al.*, 1995; Aberle *et al.*, 1996). Immunohistochemistry was used to examine whether β -catenin was dysregulated as a consequence of *Apc* deletion in $cre^+ Apc^{580S/580S}$ mouse mammary glands (see section 2.8.1). Normal mammary acinar epithelium stained only at the cell membrane where β -catenin was found in adherens junctions (Figure 3.4(i)). In contrast, balls of metaplastic squamous epithelium stained strongly for β -catenin throughout the cell cytoplasm and nucleus (Figure 3.4(ii)). However little or no β -catenin expression was observed in the mature squamous epithelium (Figure 3.4(ii)).

3.2.2.3 Cyclin D1

Expression of cyclin D1 (see section 1.5.1.3.2), a putative target gene activated by the β -catenin-TCF/LEF pathway, was analysed by immunohistochemistry in control ($cre^- Apc^{580S/580S}$) and mutant ($cre^+ Apc^{580S/580S}$) mouse mammary glands (see section 2.8.1). Expression of cyclin D1 was infrequent (<2%) in normal mouse mammary epithelium (Figure 3.5(i)). In contrast, increased levels of cyclin D1 (~10%) were detected in the nuclei of metaplastic lesions (Figure 3.5(ii)).

3.2.2.4 Proliferation analysis

In order to investigate whether the metaplastic areas were composed of cycling cells, BrdU incorporation assay was used to identify cells that had undergone S phase. Animals were injected with BrdU (70ug/g in sterile saline, i.p.) 2 hours before sacrifice. Paraffin-embedded mammary glands were sectioned and stained with an anti-BrdU antibody (see section 2.8.1). In contrast to the control mammary gland

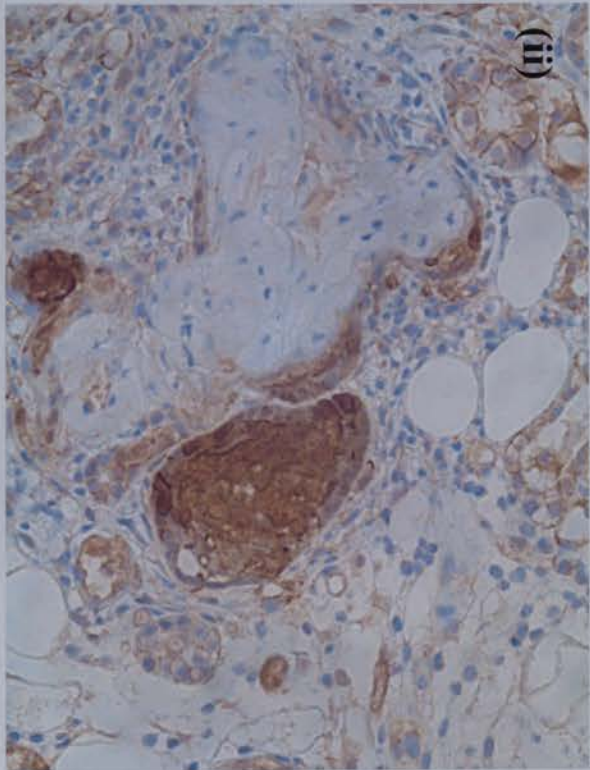
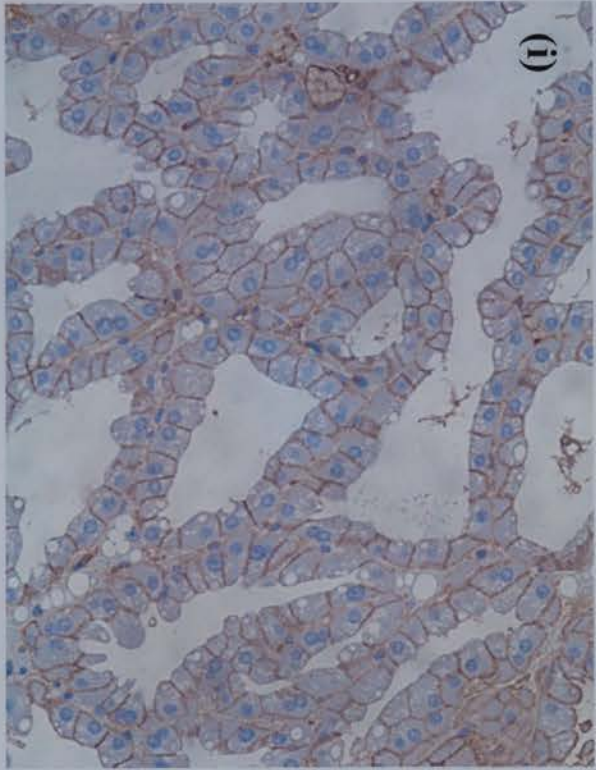


Figure 3.4 Immunohistochemical staining for β -catenin

β - catenin was detected using a mouse monoclonal antibody (Transduction laboratories, cat. no. C19220) and is represented by brown staining. (i) Control ($cre^+ Apc^{+/580S}$) mouse mammary gland section at day 10 lactation showing β - catenin staining at the cell membrane. (ii) Apc deleted ($cre^+ Apc^{s80S/580S}$) mouse mammary glands at day 10 lactation showing strong β - catenin staining within the metaplastic lesions.

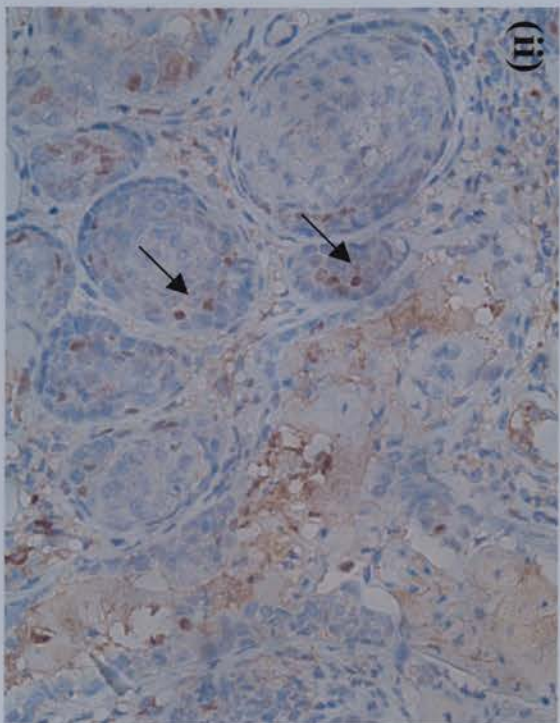
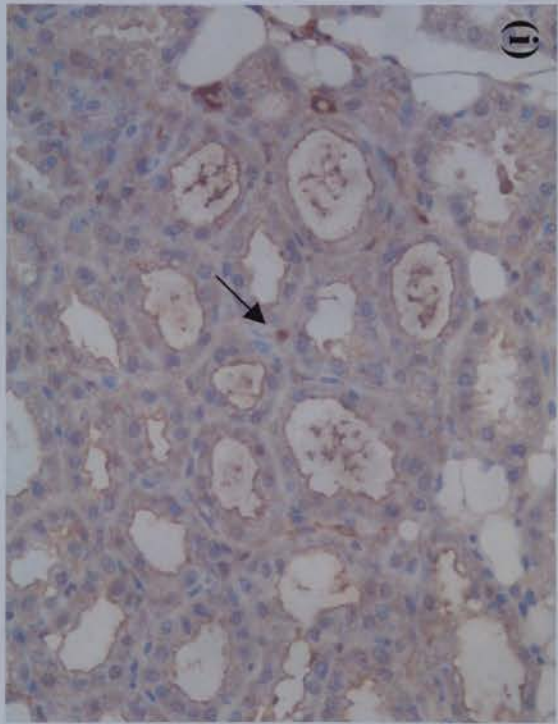


Figure 3.5 Immunohistochemical staining for cyclin D1

Cyclin D1 was detected using a mouse monoclonal antibody (Nova Castra cat. no. DCS-6) and is represented by brown staining. (i) Control ($cre^{-} Apc^{580S/580S}$) mouse mammary gland section at day 10 lactation showing infrequent cyclin D1 staining. (ii) *Apc* deleted ($cre^{+} Apc^{580S/580S}$) mouse mammary glands at day 10 lactation showing increased levels of cyclin D1 staining within the metaplastic lesions. Arrows indicate cyclin D1 positive nuclei.

epithelium (where low level BrdU staining was observed)(Figure 3.6(i)), cre^+ $Apc^{580S/580S}$ mouse mammary glands displayed an obvious increase of BrdU labelled cells in the metaplastic lesions (Figure 3.6(ii)). TUNEL analysis was used to identify cell death within the metaplastic nodules (see section 2.8.1). Squamous cells within the metaplastic lesions were found to be weakly TUNEL positive (Figure 3.6(iii)). This observation may reflect a process of anucleation within these cells, which ultimately results in the formation of ‘ghost’ nuclei and open spaces (Figure 3.4g).

3.3 Discussion

3.3.1 *Apc* inactivation dysregulates Wnt signalling in mouse mammary gland metaplastic lesions

Apc mutation is associated with mammary tumourigenesis in both humans (Furuuchi *et al.*, 2000) and mice (Moser *et al.*, 1993). Hyperplasia and malignant transformation have previously been reported in mouse mammary epithelium when *Wnt1*, *Wnt10b*, *cyclin D1* or truncated forms of β -catenin ($\Delta N89$ and $\Delta N90$) are overexpressed (Tsukamoto *et al.*, 1988; Edwards *et al.*, 1992; Wang *et al.*, 1994; Imbert *et al.*, 2001; Michaelson and Leder, 2001). The phenotype of cre^+ $Apc^{580S/580S}$ mice, which have undergone conditional inactivation of *Apc* from the mammary gland, involves the development of small areas of metaplasia in the ductal epithelium which increase in size and number during pregnancy but do not progress to neoplasia. Immunohistochemical staining confirms loss of *Apc* expression within the metaplastic lesions. In addition, lesions stain strongly for β -catenin throughout the cell cytoplasm and nucleus, consistent with a critical role of *Apc* in regulating β -catenin levels. Stabilised β -catenin translocates to the nucleus and interacts with TCF/LEF transcription factors resulting in the activation of target genes, including cyclin D1 (Behrens *et al.*, 1996; Molenaar *et al.*, 1996; Hsu *et al.*, 1998). Consequently, metaplastic lesions displayed an increase in cyclin D1 staining, a feature which correlated with an increase in cell proliferation as determined by the BrdU incorporation assay. It is possible that the metaplastic lesions arising due to

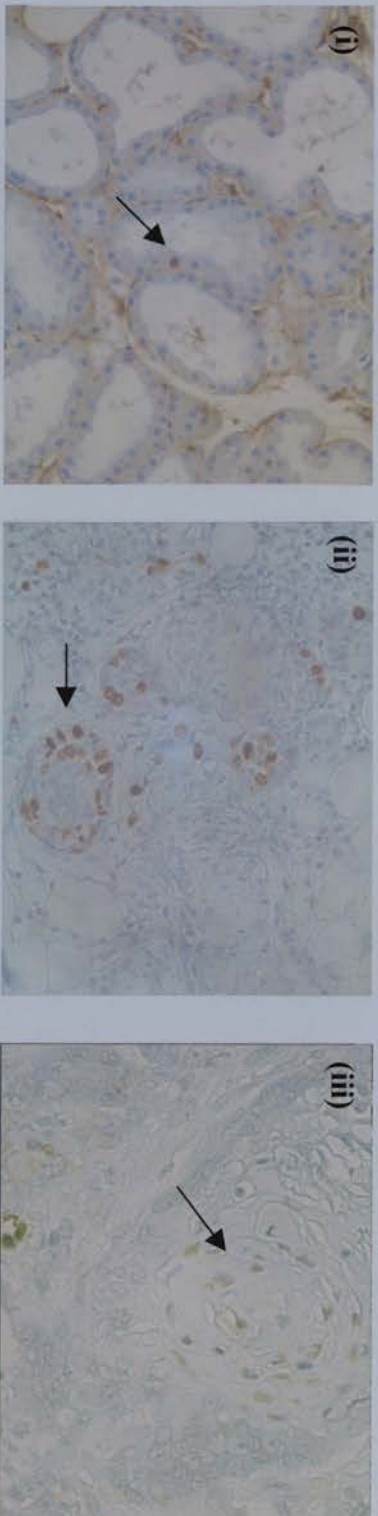


Figure 3.6 BrdU and TUNEL analysis

Detection of BrdU incorporation was by an anti-bromodeoxyuridine-peroxidase antibody (Roche cat. no. 1585 860) and is represented by brown staining. Panels (i) and (ii) show sections from control ($cre^+ Apc^{+/580S}$) and *Apc* deleted ($cre^+ Apc^{580S/580S}$) mouse mammary glands at day 10 lactation respectively. (i) BrdU staining was infrequent in control sections, (ii) but increased in metaplastic lesions. Arrows indicate BrdU positive nuclei. (iii) TUNEL staining of *Apc* deleted ($cre^+ Apc^{580S/580S}$) mouse mammary gland section at day 10 lactation. Arrow indicates a group of weakly TUNEL positive squamous cells within a metaplastic lesion.

Apc deletion represent an increase in the numbers of a specific cell type, for example squamous cells. Importantly, in this study dysregulated *Wnt* signalling (due to conditional inactivation of *Apc* from the mouse mammary gland) did not result in neoplasia. In this respect it is noteworthy that TUNEL analysis confirmed the presence of apoptosis in the metaplastic lesions and may represent one mechanism by which tumourigenesis is suppressed in these mice.

3.3.2 *Apc* deletion and mouse mammary gland tumourigenesis

Failure to observe mammary gland malignancy in the absence of *Apc* in cre^+ *Apc*^{580S/580S} mice contrasts with previous experiments overexpressing *Wnt1*, *Wnt10b*, *cyclin D1* and mutant forms of β -catenin in the mammary epithelium of transgenic mice (Tsukamoto *et al.*, 1988; Edwards *et al.*, 1992; Wang *et al.*, 1994; Imbert *et al.*, 2001; Michaelson and Leder, 2001). There are several possible explanations why the effects of inactivating *Apc* appear to differ from the effects of ectopic Wnt signalling or overexpression of stabilised β -catenin, and these can be subdivided into 4 categories: 1) cell type-specific effects, 2) levels of β -catenin, 3) effects of *Apc* mutation and 4) cytoskeletal effects.

First, the transgenes may be expressed in different cell types. The adult mammary gland contains a population of stem cells that are able to give rise to complete functional mammary glands (Kordon and Smith, 1998) and it has been suggested that MMTV-induced mammary tumours arise from infection of these stem cells (Callahan and Smith, 2000). Thus one possibility was that the BLG promoter was failing to drive deletion within those stem cells that can give rise to tumours. However, subsequent breeding of BLG- cre^+ *Apc*^{580S/580S} mice onto a *Tcf-1* null background resulted in the formation of mammary tumours, confirming that BLG- cre can drive tumour formation (Gallagher *et al.*, 2002). Specifically, the authors report the development of mammary adenocanthomas by 4 weeks of age in cre^+ *Apc*^{580S/580S} *Tcf-1* mice compared with a latency of 7 months in *Tcf-1* null mice. Thus it appears that

the BLG promoter is clearly driving loss of Apc in cells (mammary secretory epithelial cells), which can form tumours.

Secondly, levels of β -catenin may be a critical determinant in mammary gland tumourigenesis. Specifically, there may be a threshold level of β -catenin above which tumourigenesis is triggered. Two groups report that expression of a truncated β -catenin (Δ N89 and Δ N90) in virgin mammary glands induces inappropriate lobuloalveolar development, hyperplasia and progression to adenocarcinoma, with tumour latency decreasing with pregnancy (Imbert *et al.*, 2001; Michaelson and Leder, 2001). Imbert *et al.* (2001) have argued that β -catenin levels are not relevant, as both high and low-expressing lines of their MMTV- Δ N β -catenin transgenic mice display the same phenotype, with low expressors showing a longer latency. However, a criticism of these studies is that overexpression of β -catenin from an ectopic promoter produces at least threefold more β -catenin from the transgene than the endogenous locus (Imbert *et al.*, 2001), and therefore does not question the effect of endogenous β -catenin levels on mouse mammary gland development. To overcome this, Miyoshi *et al.* (2002) used cre-*loxP* technology to conditionally excise exon 3 of β -catenin from mouse mammary epithelium. Deletion of exon 3 of the β -catenin gene removed the N-terminal region that is the target of GSK3 β phosphorylation and consequently rendered the protein resistant to degradation by the proteasome (Harada *et al.*, 1999; Miyoshi *et al.*, 2002). Stabilisation of β -catenin induced squamous metaplasia during the first pregnancy. Importantly, these mice did not develop mammary adenocarcinomas (Miyoshi *et al.*, 2002). Similar observations have been reported in cre⁺ *Apc*^{580S/580S} mice where β -catenin dysregulation due to *Apc* deletion directs the formation of metaplastic lesions but not neoplasia (Gallagher *et al.*, 2002). It is noteworthy that when bred onto a *Tcf-1* null background these mice developed mammary tumours by 4 weeks of age. Thus, because tumourigenesis is a phenotype of cre⁺ *Apc*^{580S/580S} *Tcf-1* null mice, it remains possible that deficiency of *Apc* alone was insufficient to result in complete deregulation of β -catenin (Gallagher *et al.*, 2002). Additionally, mutant forms of β -catenin may have different properties to wild type β -catenin, and removal of either the 89 or 90 N-terminal amino acids may affect

more than β -catenin stability. It has been reported that amino acid alterations of the N-terminus of β -catenin affects signalling independent of any effect on β -catenin levels (Guger and Gumbiner, 2000).

Thirdly, the nature of the mutation at the *Apc* allele may determine the phenotype. Several *Apc* mutations have been described (see table 1.5.1) and these have different phenotypes. However despite the fact that cre-mediated deletion of *Apc*^{580S} in colonic epithelium leads to the formation of colorectal adenomas (Shibata *et al.*, 1997), direction of this mutation to the mammary gland epithelium does not result in tumourigenesis. One possibility is that the mammary gland epithelium may require higher levels of β -catenin for malignant transformation (Gallagher *et al.*, 2002). An alternative possibility is that an *Apc*-independent method of β -catenin regulation, such as feedback repression by Tcf-1, may prevail in the mammary gland. Tcf-1 is activated by β -catenin/Tcf-4 and acts within a feedback repressor pathway, where Tcf-1 isoforms lacking a β -catenin interaction domain bind to DNA target sequences but fail to mediate gene activation (Roose *et al.*, 1999) The authors argue that *Tcf-1* co-operates with *Apc* and that the combination of the two activities is particularly important for the prevention of mammary neoplasia in mice.

Finally, the truncated *Apc* protein, produced following BLG-cre mediated deletion of exon 14, has lost all of the C-terminal domains necessary for cytoskeletal regulation (Shibata *et al.*, 1997). APC associates with the cytoskeleton in at least two ways, directly binding microtubules (Smith *et al.*, 1994; Munemitsu *et al.*, 1994) and indirectly connecting with the actin cytoskeleton (Townesley *et al.*, 2000). These interactions are important for cell migration, adhesion and cell division (section 1.4.3.2). Thus, conditional inactivation of *Apc* from mouse mammary epithelial cells may result in migration or cytoskeletal defects. This could explain the observation of delayed ductal growth in the mammary glands of cre⁺ *Apc*^{580S/580S} female mice (Gallagher *et al.*, 2002). Disruption of the cytoskeleton in the absence of *Apc* could lead to a decreased ability of the tip of the growing duct to invade or grow through the fat pad. Consistent with this, Imbert *et al.* (2001) report a mild retardation in ductal extension in mice overexpressing Δ N89 β -catenin. N-terminal deleted β -

catenin has been suggested to interfere with *Apc*'s ability to bundle microtubules at the tips of cell extensions (Nathke *et al.*, 1996; Pollack *et al.*, 1997).

In conclusion, conditional inactivation of *Apc* from mouse mammary epithelial cells leads to dysregulated ductal growth and the formation of squamous metaplastic lesions but not neoplasia. Metaplastic lesions are characterised by dysregulation of β -catenin and activation of cyclin D1 and may represent preneoplastic lesions. One possibility is that in the mouse mammary gland additional gene mutations/deletions are required for full progression to neoplasia. In support of this, recent reports on the combined effect of *Apc* and *Tcf-1* deletion in mouse mammary epithelium highlight the critical effect of other genes on *Apc* tumourigenesis in the mammary gland.

4 Differential Display RT-PCR analysis of gene expression in the cre^+ $Apc^{580S/580S}$ mouse mammary gland

4.1 Introduction

4.1.1 Differential analysis of gene expression in the mammary gland of cre^+ $Apc^{580S/580S}$ mice

Conditional inactivation of *Apc* in the mouse mammary gland (cre^+ $Apc^{580S/580S}$ mice) produced a phenotype of delayed ductal growth in virgin animals and induced the formation of metaplastic lesions (section 1.6.3.2). These areas of metaplasia increased in size and number with pregnancy, remained after involution, but did not progress to neoplasia (Gallagher *et al.*, 2002). In an effort to understand the relationship between mammary gland metaplasia and *Apc* deficiency a method of differential analysis was used to identify transcriptional changes in response to loss of *Apc* in the mouse mammary gland. Several widely used techniques exist for the identification, and subsequent isolation, of differentially expressed genes and include differential screening, subtractive hybridisation, and differential display reverse transcription PCR (DDRT-PCR). In this analysis, DDRT-PCR was the method of choice, for reasons that are summarised below.

4.1.1.1 Differential Screening

Differential screening involves the use of deoxyoligonucleotide primers (such as $d(T)_n$) or random hexamers to prepare two single-stranded cDNA probes by reverse transcription of a poly(A)⁺ RNA template (from test and control tissue) in the presence of radiolabelled nucleotide. These probes, which are representative of the total mRNAs present in the sample tissue, are then used to screen cDNA libraries

prepared from test and control RNA. Differentially expressed clones, identified by changes in signal strength, are picked and subsequently re-screened to confirm their differential expression. This method of isolating differentially expressed genes has several drawbacks. Specifically, the over-representation of moderate to highly abundant mRNAs, whereby cDNAs of the most abundant mRNAs contribute most of the radioactivity present in the probe while cDNA copies of less abundant and rare mRNAs contribute a much smaller fraction. Accordingly, signals corresponding to such low copy mRNAs may be indistinguishable from background hybridisation. In addition, large quantities of poly(A)⁺ RNA starting material are required for this technique and correspondingly it is useful for the study of only a very small number of samples (for example, test and control).

4.1.1.2 Subtractive Hybridisation

Subtractive hybridisation represents a variation of differential screening designed to overcome much of the problem of sensitivity of mRNA detection inherent in differential screening. This method involves initial subtraction of all cDNAs shared between two samples (test and control). Subtraction involves hybridisation of control cDNA with an excess of biotinylated test cDNA. Biotinylated DNA is subtracted by avidin binding, and the remaining cDNAs are used to generate subtracted cDNA libraries for screening or alternatively as probes to screen libraries differentially. This method offers a slight increase in sensitivity of mRNA detection relative to conventional differential screening (section 4.1.1.1), but nonetheless has disadvantages. Complete subtraction of all common cDNAs is not possible, thus this method produces a significant number of false positives. Furthermore, due to the use of excess biotinylated subtraction cDNA, transcripts that are subtly differentially expressed, or alternatively differentially expressed homologous transcripts, may be subtracted. Finally, as with differential screening, only a small number of samples (test and control) can be studied, requiring large amounts of RNA starting material.

4.1.1.3 Differential Display RT-PCR

The DDRT-PCR technique essentially allows the direct comparison of genes expressed in multiple samples by the creation of an “RNA fingerprint” for each sample (Liang and Pardee, 1992). Isolated total RNA is fractionated into specific subpopulations of cDNA using modified deoxyoligonucleotide (T)₁₂MN primers for reverse transcription (where M = A, G or C and N = A, G, C or T). This fractionated RNA, represented as cDNA, is then used as a template in low annealing temperature PCR reactions with the original 3' d(T)₁₂MN primer and an additional 5' 10-mer of arbitrary but defined sequence. Incorporation of a radiolabelled nucleotide into the display PCR reactions allows the resulting PCR products (RNA fingerprints) to be visualised by autoradiography following standard polyacrylamide gel electrophoresis. Visual comparison of the banding pattern across gel lanes readily identifies any differentially expressed transcripts on the basis of band intensity. In comparisons of multiple samples (for example developmental stages), the majority of transcripts displayed should appear identical in intensity in all lanes, while a small percentage, representing developmentally regulated genes, should vary in intensity across lanes but display an identical profile in test and control lanes. Both of these types of expression pattern act as internal controls, and individual transcripts that differ in expression profile between test and control can be selected with confidence. Regions corresponding to bands of interest are excised from the dried gel, and the cDNA is recovered. Recovered cDNA is then reamplified using the appropriate primer combination (those used to display it) and cloned into an appropriate vector for further analysis.

In this analysis, DDRT-PCR offers several advantages over alternative techniques as the method of choice for a comparison of gene expression due to: (1) the low quantity of starting material required (frequently 1-5µg of total RNA), (2) the ability to simultaneously analyse multiple samples (limited only by the number of lanes on the gel electrophoresis equipment), (3) the sensitivity of the procedure (being PCR based, low copy number transcripts are included in the analysis), (4) the speed of the procedure (from extraction of RNA to sequenced clones can be achieved in less than

one and a half weeks), and (5) the extremely high reproducibility of the technique. However, criticisms of the technique include reports of significantly high false positive rates, where expression studies using isolated clones have failed to replicate the differential expression patterns seen on the original display gel (Li *et al.*, 1994; Sun *et al.*, 1994). Indeed, clones derived from an apparently single display band frequently represent a number of different cDNA species, making the identification of the true candidate cDNAs a time consuming and laborious task (Callard *et al.*, 1994; Li *et al.*, 1994). Miele *et al.* (1998 and 1999) have outlined two methods whereby these problems can be resolved, (1) mSSCP and (2) a 'cold' southern blot technique, both of which were used in this analysis (see methods section 2.2.5 and 2.2.7).

4.1.1.3.1 Modified Single-Strand Conformation Polymorphism (mSSCP)

Single-strand conformation polymorphism (SSCP) is an electrophoresis protocol designed to separate single-stranded DNA on the basis of conformation rather than size. Under standard conditions (Hayashi, 1991), SSCP will separate individual strands of a DNA duplex. The modified SSCP (mSSCP) protocol described in Miele *et al.* (1998) was designed to differentiate between similarly sized fragments of completely different sequence, thus aiding identification of the excised display candidate cDNA of interest from potential co-migrating cDNA species. The mSSCP procedure is performed after first excising gel regions corresponding to DDRT-PCR bands that represent differentially expressed cDNAs. In addition to recovering cDNA from display band regions representing a candidate of interest, cDNA is also isolated from the corresponding 'negative' region to allow identification of co-migrating cDNAs after mSSCP (Miele *et al.*, 1998). The eluted cDNA is PCR reamplified for an optimal number of cycles and the products are subjected to mSSCP electrophoresis. Miele *et al.* (1998) established that 5 cycles amplifies mouse brain cDNA sufficiently to permit detection without distorting the relative levels of different cDNA species recovered (see methods section 2.2.5).

4.1.1.3.2 'Cold' Southern Blotting

Miele *et al.* (1999) describe a Southern blotting procedure that can be used prior to labour intensive expression studies to validate that a particular isolated cDNA clone does represent the original band of interest. This can be achieved by simple electrophoresis of DDRT-PCR products through agarose gels, followed by standard Southern blotting to nylon membranes and the use of isolated cDNAs as hybridisation probes. Clones representing the candidate DDRT-PCR cDNAs of interest produce a pattern of hybridisation mirroring the original DDRT-PCR profile and are detectable after very short exposure times (< 2hours) (see methods section 2.2.7). Clones can then be used as probes to confirm differential expression using techniques such as northern blot analysis or *in situ* hybridisation.

4.1.2 DDRT-PCR analysis of gene expression in the mammary gland of $cre^+ Apc^{580S/580S}$ mice

One aim of this thesis was to identify transcriptional changes in response to loss of *Apc* in the mouse mammary gland, thus gaining insight into the relationship between *Apc* deficiency and the phenotype of mammary gland metaplasia observed in $cre^+ Apc^{580S/580S}$ mice. However a method of identifying differentially expressed genes that allowed comparison of multiple samples simultaneously was required. Reasoning for this was that BLG-cre recombinase mediated deletion of *Apc* was originally expected to take place exclusively during lactation occurred prior to lactation, and thus by comparing gene expression at several stages of mammary gland development it was hypothesised that this would profile gene expression before, during, and after *Apc* deletion. DDRT-PCR was the method chosen as it is a highly reproducible technique and allows the analysis of multiple samples simultaneously. In addition by incorporating the mSSCP and 'cold' Southern blotting steps the likelihood of identifying false positives was greatly reduced. Clones were subsequently identified by cloning and DNA sequencing and used as probes to confirm differential expression in northern blot analysis (see Figure 4.1).

Mammary glands (*Apc*⁺ and *Apc*⁻)
(multiple developmental stages).

↓
RNA extraction.

↓
CDNA synthesis.

↓
DDRT-PCR and Electrophoresis

↓
Isolation of candidate cDNA
(from test and control lanes).

↓
mSSCP purification
(5 cycles PCR).

↓
Isolation of mSSCP cDNA.

↓
5 cycles PCR re-amplification
(primers containing *Eco*RI
restriction sites).

↓
Cloning into *Eco*RI site of
de-phosphorylated vector.

↓
Sequencing and identification

↓
Verification of authenticity of
cloned cDNA by 'cold'
southern blotting.

↓
Northern analysis confirms
Differential expression

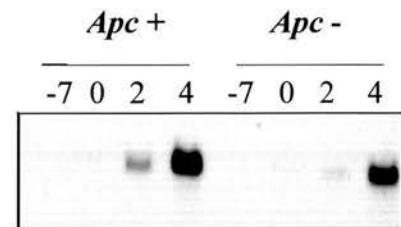
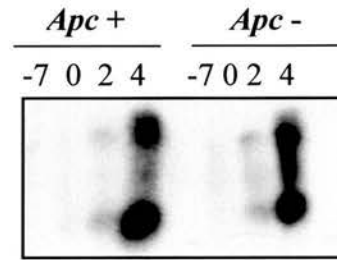
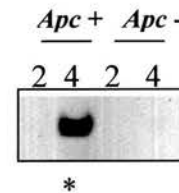
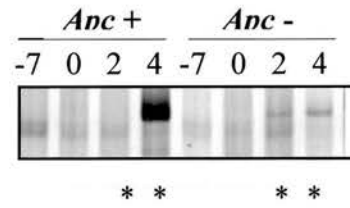
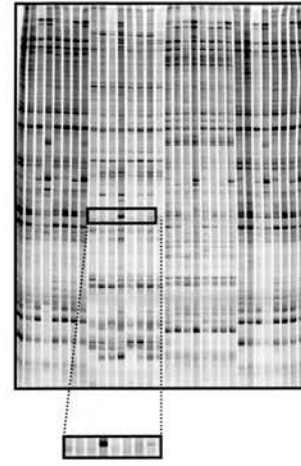


Figure 4.1 Overview of the strategy used to identify differentially transcribed genes in response to loss of *Apc* in the mouse mammary gland

Figure key (applies to all figures in Chapter 4)

Control ($cre^+ Apc^{+/580S}$ and $cre^- Apc^{580S/580S}$)	<i>Apc</i> ⁺
Mutant ($cre^+ Apc^{580S/580S}$)	<i>Apc</i> ⁻
Mid-gestation	-7
Parturition	0
Day 2 lactation	2
Day 4 lactation	4

4.2 Results

4.2.1 DDRT-PCR experimental design

In order to ensure that any transcript differences on the DDRT-PCR gels was due to *Apc* loss and not effects of genetic background variation it was important that the control and *Apc* deleted mice were as genetically similar as possible. See Appendix B for mouse breeding and mammary gland collection data, note at each time point five mammary glands were collected and pooled in order to minimise the effects of genotypic variation. Mammary glands were collected from littermate control genotype ($cre^+ Apc^{+/580S}$ and $cre^- Apc^{580S/580S}$) and mutant ($cre^+ Apc^{580S/580S}$) mice at 4 stages of mammary development, mid-gestation, parturition, day 2 lactation and day 4 lactation. Mammary glands were dissected and snap frozen in liquid nitrogen and stored at -70°C . Once all the samples had been collected RNA extraction and DDRT-PCR analysis were performed in Dr. Mike Clinton's laboratory at Roslin Institute, Roslin.

As a first step, it was necessary to estimate the number of DDRT-PCR primer combinations that would be required to achieve full coverage of gene expression in the mammary gland. Liang and Pardee (1992) estimate that twenty arbitrary DDRT-PCR 10-mer primers in conjunction with all anchored oligonucleotides should be sufficient to provide coverage of 12 000 - 24 000 transcripts in homogenous cell

lines. Assuming that 10 000 - 15 000 genes are expressed in any particular cell type at any one time (Liang and Pardee, 1992; Bauer *et al.*, 1994) and assuming that one DDRT-PCR band represents an individual transcript, this would be sufficient to examine most expressed genes. However due to constraints of time and resources it was only possible to perform a quarter of this analysis using only one of the four cDNA sub-fractions (i.e. d(T)₁₂MC). DDRT-PCR was performed on this cDNA sub-fraction using a total of 34 individual arbitrary 5' 10-mer primers (see Appendix C for DDRT-PCR primers) (Figure 4.2). Assuming a resolution of an average 200-300 DDRT-PCR bands per primer combination, this equates to a total visualisation of approximately 6 800 – 10 200 individual bands. On the basis that one DDRT-PCR band represents an individual transcript, the analysis presented in this thesis provides visualisation of between 6 000-10 200 individual expressed genes in the mouse mammary gland.

4.2.2 Gene expression in control ($cre^+ Apc^{+/580S}$ and $cre^- Apc^{580S/580S}$) and Apc deleted ($cre^+ Apc^{580S/580S}$) mouse mammary glands

The majority of DDRT-PCR autoradiographs presented in this thesis (Figure 4.2) display four individual “RNA fingerprints” between control and mutant ($cre^+ Apc^{580S/580S}$) mice mammary glands. As can be seen from Figure 4.3, the consistency of banding patterns within a particular primer combination was extremely high and the reproducibility between the developmental timepoints of control ($cre^+ Apc^{+/580S}$ and $cre^- Apc^{580S/580S}$) and mutant ($cre^+ Apc^{580S/580S}$) mammary material was excellent for each primer combination. Additionally the expression profiles of at least half of the transcripts did not change throughout the developmental period of study, while about 25%, representing developmentally regulated genes, displayed the same differential expression profile in the control and mutant mammary gland samples. Both types of expression profile act as internal controls, and individual transcripts that differ between control ($cre^+ Apc^{+/580S}$ and $cre^- Apc^{580S/580S}$) and mutant ($cre^+ Apc^{580S/580S}$) mammary glands can be selected with confidence.

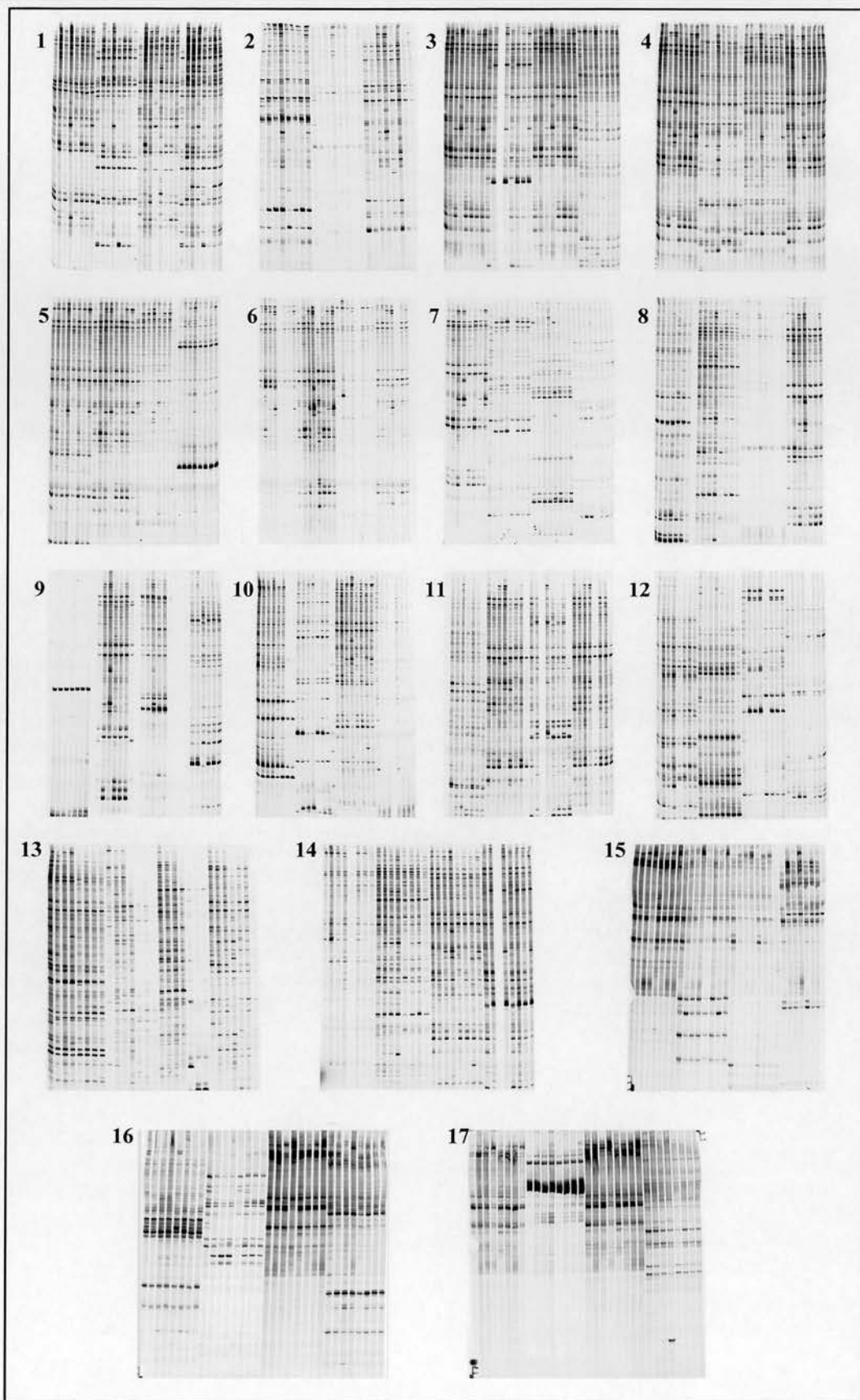


Figure 4.2 DDRT-PCR autoradiographs

All DDRT-PCR gels produced using the primer $d(T)_{12}MC$ with 34 individual arbitrary 5' 10-mer primers. These are presented in greater detail in Appendix D.

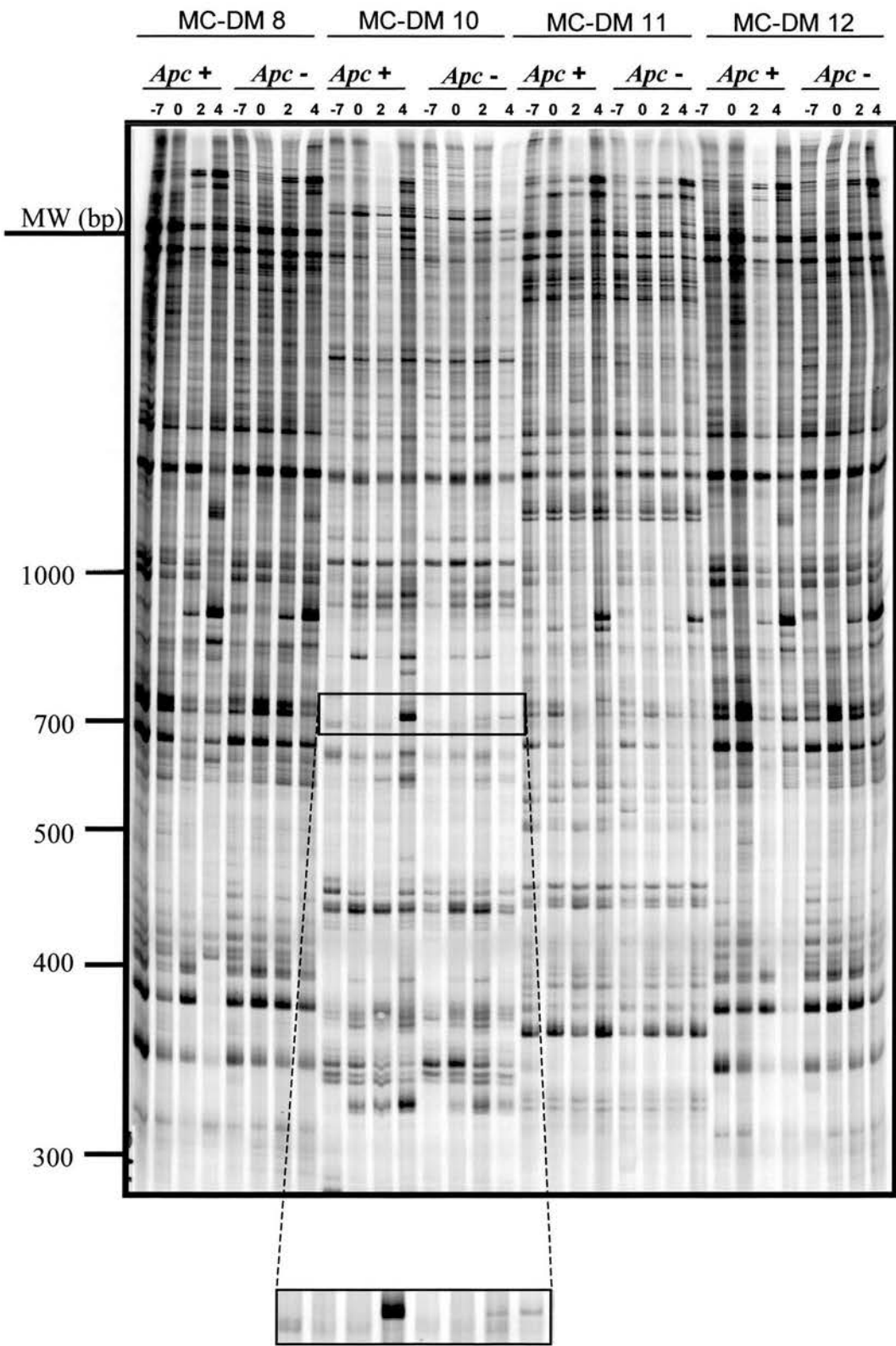


Figure 4.3 Identification of candidate 1 by DDRT-PCR

DDRT-PCR autoradiograph illustrating the results of DDRT-PCR with primer pairs d(T)₁₂MC and DM 8, 10, 11 and 12. The primer pair d(T)₁₂MC and DM 10 resulted in the identification of cDNA candidate 1, representing a transcript downregulated in mutant (*cre*⁺ *Apc*^{580S/580S}) mammary glands.

From an estimated maximum visualisation of 10 200 transcripts in control and *Apc* deficient mouse mammary glands, only thirteen individual transcripts were identified as being differentially expressed during the course of this screen. Of these, six were successfully cloned and are discussed individually in the following sub-sections of this chapter.

4.2.3 Transcripts identified as being differentially expressed between control ($cre^+ Apc^{+/580S}$ and $cre^- Apc^{580S/580S}$) and mutant ($cre^+ Apc^{580S/580S}$) mammary glands

From the comprehensive DDRT-PCR analysis (Figure 4.2), several bands representing potentially differentially expressed transcripts were selected for further analysis. These isolated cDNAs represent six individual expressed genes. The isolation, identification and verification of these are presented below.

4.2.3.1 Candidate 1 (Clone 3.4)

As can be seen from Figure 4.3, the d(T)₁₂MC/DM 10 DDRT-PCR primer combination resulted in the identification of a cDNA candidate (candidate 1), representing a transcript which although developmentally regulated (with expression being exclusive to lactation) appeared dramatically down regulated in mutant ($cre^+ Apc^{580S/580S}$) mammary glands. Although the intensity of all *Apc* deleted-day 4 lactation cDNAs generated using this primer combination appears to be slightly lower this does not account for the dramatic differential expression seen. This, together with the reproducibility of this apparent differential expression on several different occasions provides confidence that this particular transcript is differentially expressed in $cre^+ Apc^{580S/580S}$ mammary glands. This cDNA was recovered and subjected to mSSCP analysis to allow identification of co-migrating cDNAs. Figure 4.4, illustrates the mSSCP protocol and confirms the presence of several potential co-migrating cDNAs. Following mSSCP purification, the cDNA was recovered, PCR

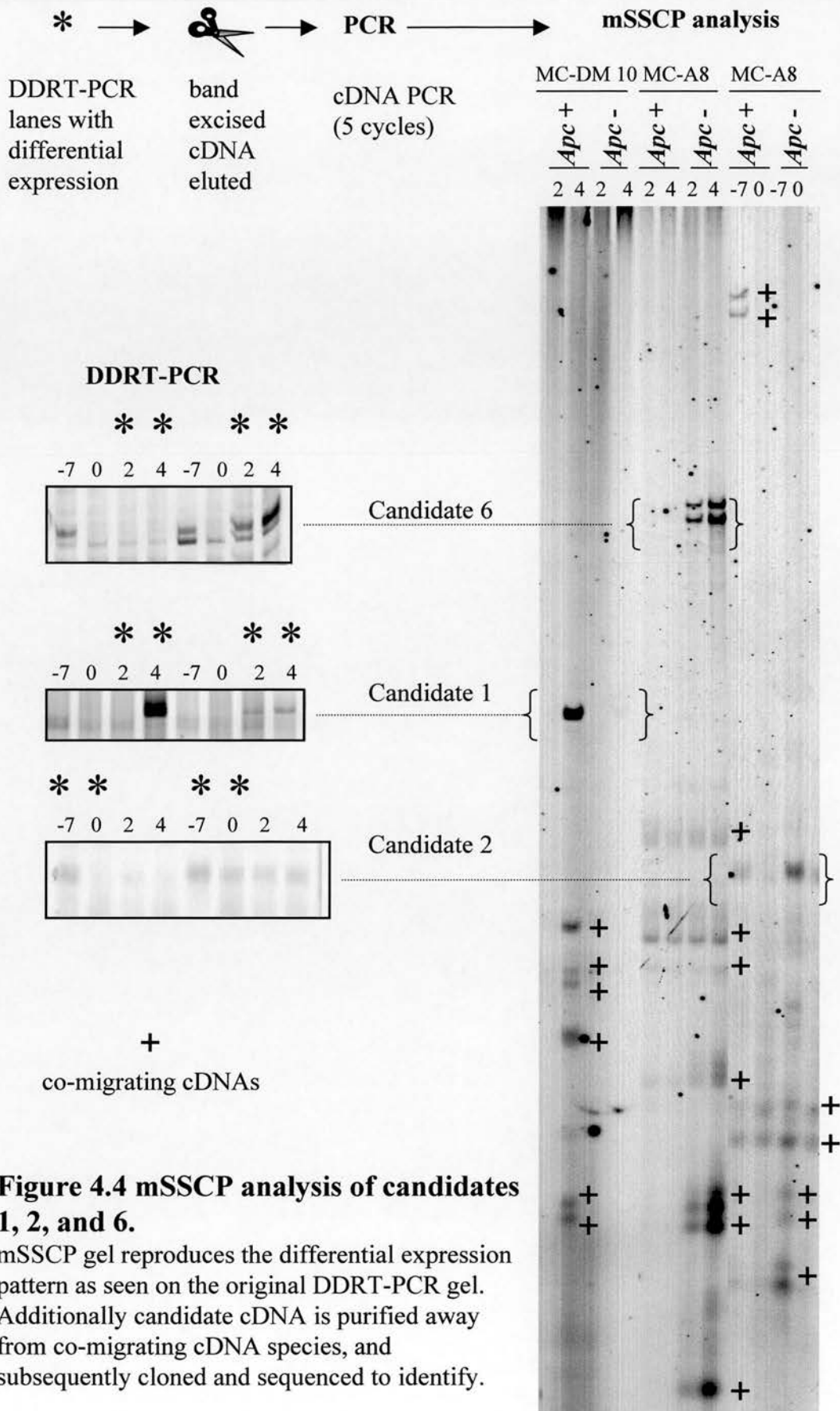


Figure 4.4 mSSCP analysis of candidates 1, 2, and 6.

mSSCP gel reproduces the differential expression pattern as seen on the original DDRT-PCR gel. Additionally candidate cDNA is purified away from co-migrating cDNA species, and subsequently cloned and sequenced to identify.

reamplified and subsequently cloned (section 2.2.6). Plasmid DNA from two transformants was sequenced and both were found to be identical. As shown in Figure 4.5, computer-assisted homology search (BlastN) of the non-redundant nucleic acid databases revealed that candidate 1 cDNA sequence, 143bp in length, matched from positions 477 - 615 of Murine *casein delta* mRNA. 'Cold' Southern blotting confirmed that candidate 1 (*casein delta*) represents the original differentially expressed transcript by producing a pattern of hybridisation that mirrored the original DDRT-PCR profile (Figure 4.6b). Finally, although capable of detecting extremely slight differences in gene expression between samples DDRT-PCR gives no indication as to the absolute level of expression, nor can it be used to quantitate the extent of the observed differences. For these reasons northern analysis was carried out to confirm differential gene expression. DDRT-PCR comparison of gene expression between control ($cre^+ Apc^{+/580S}$ and $cre^- Apc^{580S/580S}$) and mutant ($cre^+ Apc^{580S/580S}$) mouse mammary glands identified *casein delta* as being downregulated in $cre^+ Apc^{580S/580S}$ mammary glands. The *casein delta* fragment isolated by DDRT-PCR was used as a probe in northern hybridisation studies of *casein* expression in control and mutant mouse mammary glands (section 2.5). As shown in Figure 4.6c, use of this radiolabelled cDNA as a probe to mammary gland RNA replicates the general profile of expression observed by DDRT-PCR and confirms *casein delta* downregulation in $cre^+ Apc^{580S/580S}$ mouse mammary glands.

(a) Candidate 1 (143bp)

GCAGACCTAACACATTCAATGGAAATGTACAAGACTAGAAGATA
CTCTGGAACTATTTTGGAGCATTCTGTTGGTTTACCACTTCTGTAT
CATTTATACATCTATCCCAATATGTTGGTAATGAGAAGTAATTAC
AGCAAAAA

(b)

Sequences producing significant alignments:	Score (bits)	E Value
gi 20342009 ref XM_109430.1 Mus musculus casein delta (Csn...	276	7e-72
gi 12000467 gb AC074046.9 Mus musculus 5 BAC RP23-...	276	7e-72
gi 12862198 dbj AK021337.1 Mus musculus 10 days lactation,...	276	7e-72
gi 7106272 ref NM_009973.1 Mus musculus casein delta (Csnd...	268	2e-69
gi 50770 emb V00740.1 MMECAS Mouse messenger RNA for epsilo...	268	2e-69
gi 192982 gb J00379.1 MUSECA mouse epsilon casein mrna	268	2e-69

>gi|20342009|ref|XM_109430.1| **Mus musculus casein delta** (Csnd), mRNA
Length = 719

Score = 276 bits (139), Expect = 7e-72
Identities = 139/139 (100%)

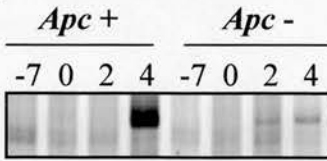
Query: 1 gcagacctaacacattcaatggaaatgtacaagactagaagataactctggaactatTTTg 60
|||||
Sbjct: 615 gcagacctaacacattcaatggaaatgtacaagactagaagataactctggaactatTTTg 556

Query: 61 gagcattctgttggtttaccacttctgtatcatttatacatctatcccaatatgTTggta 120
|||||
Sbjct: 555 gagcattctgttggtttaccacttctgtatcatttatacatctatcccaatatgTTggta 496

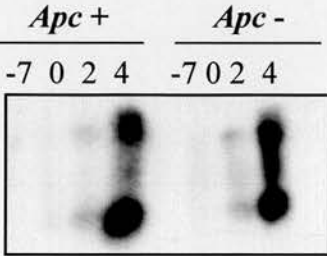
Query: 121 atgagaagtaattacagca 139
|||||
Sbjct: 495 atgagaagtaattacagca 477

Figure 4.5 BlastN comparison of candidate 1 cDNA sequence against non-redundant nucleic acid databases cDNA representing the transcript presented in Figure 4.3 (candidate 1) was cloned, transformed and plasmid DNA from two transformants sequenced. **(a)** Candidate 1 cDNA sequence. **(b)** Computer assisted homology search of the non-redundant nucleic databases (BlastN) revealed the sequence was 100% identical to positions 477-615 of the *Mus musculus casein detla* gene.

(a) DDRT-PCR



(b) 'cold' Southern



(c) Northern

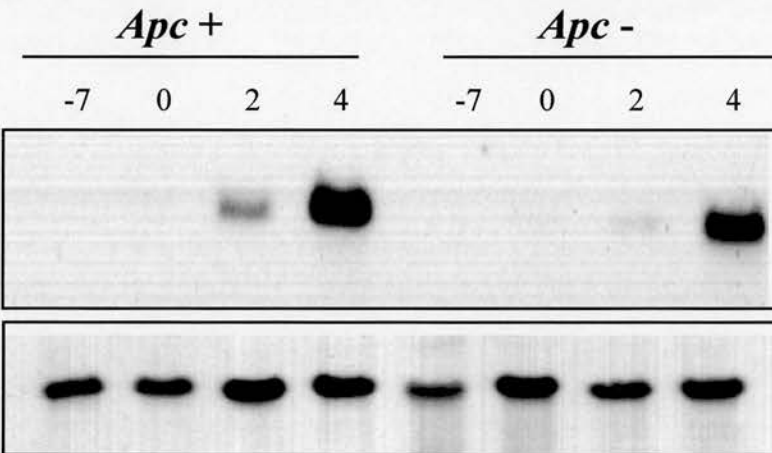


Figure 4.6 'Cold' Southern and Northern analysis of candidate 1 (Casein delta) (a) DDRT-PCR differentially expressed transcript. (b) Use of cloned cDNA as a probe to Southern-blotted DDRT-PCR products formally proves that the correct cDNA clone has been isolated by producing a pattern of hybridisation that mirrored the original DDRT-PCR profile. (c) Northern blot of 10 μ g total RNA from control ($cre^+ Apc^{+/580S}$ and $cre^- Apc^{580S/580S}$) and mutant ($cre^+ Apc^{580S/580S}$) mammary glands hybridised with the *casein* cDNA probe and exposed to MR X-ray film (Kodak) for 24 hours at $-70^\circ C$. Blots were stripped and re-probed with an 18S rDNA probe to allow normalisation for loading variations.

4.2.3.2 Candidate 2 (Clone 7.4)

The d(T)₁₂MC/A8 DDRT-PCR primer combination was used on several occasions throughout the entire DDRT-PCR analysis and resulted in the identification of three separate candidate cDNAs 2, 4 and 6. In the first instance use of this primer combination identified a transcript (candidate 2) that appears to be developmentally downregulated in control mammary glands but expression of which remains constant in mutant ($cre^+ Apc^{580S/580S}$) mouse mammary glands (Figure 4.7). This cDNA was recovered and subjected to mSSCP purification to remove any co-migrating cDNAs (Figure 4.4). The purified cDNA was recovered, PCR reamplified and cloned (section 2.2.6). Plasmid DNA was subsequently isolated from six transformants and the cloned cDNA sequenced. Computer-based homology search (BlastN) of the non-redundant nucleic acid databases revealed that candidate 2 cDNA sequence, 82bp in length, matched from positions 5681 – 5762 of the *Mus musculus alpha-1 type IV collagen* gene (Figure 4.8). ‘Cold’ Southern blotting confirmed that the cDNA (candidate 2 (*alpha-1 type IV collagen*)) isolated from the DDRT-PCR gel corresponds to the differentially expressed transcript by producing a pattern of hybridisation that mirrored the original DDRT-PCR profile (Figure 4.9b). Northern analysis confirmed differential *alpha-1 type IV collagen* gene expression in mutant ($cre^+ Apc^{580S/580S}$) mouse mammary glands (Figure 4.9c).

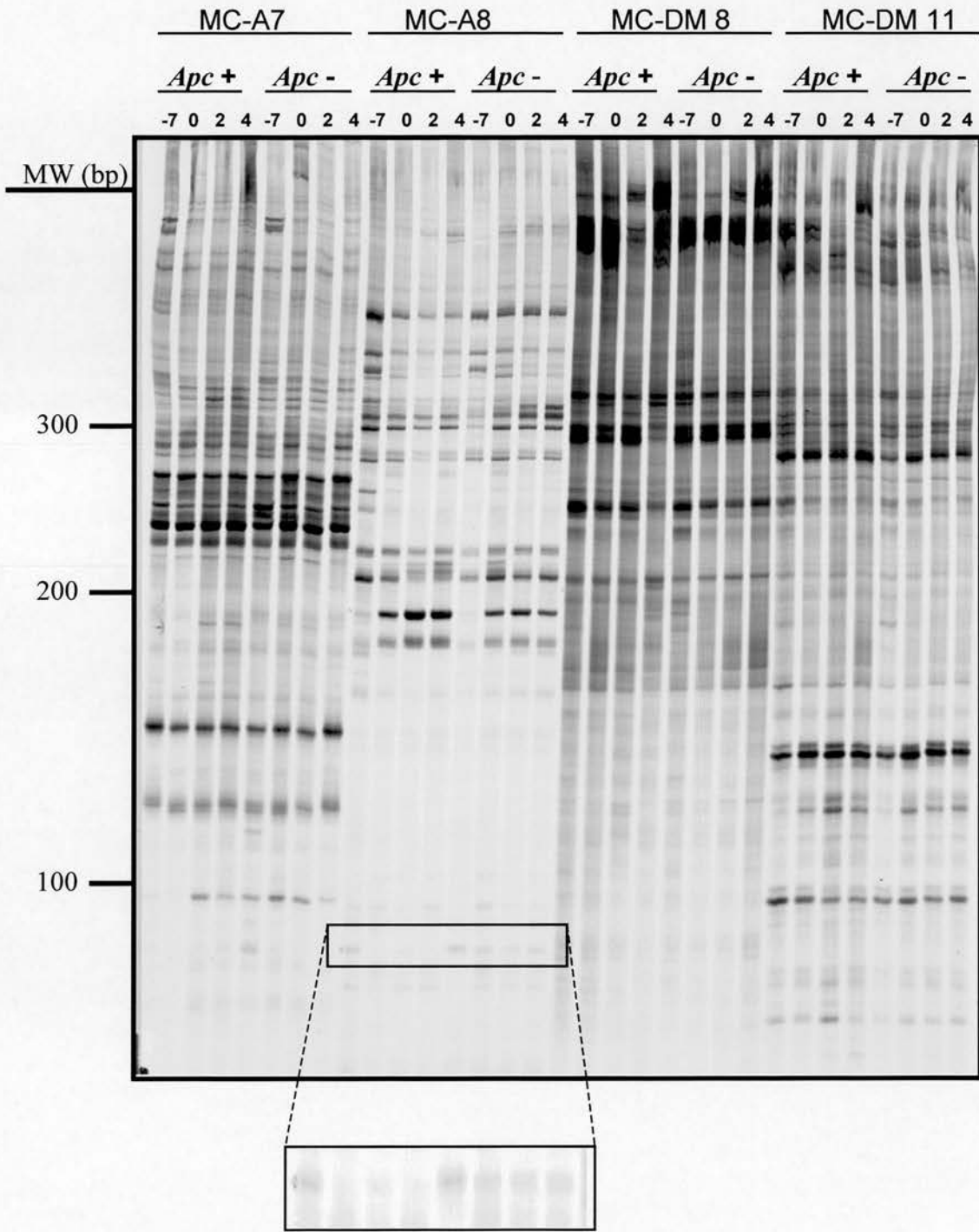


Figure 4.7 Identification of candidate 2 by DDRT-PCR

DDRT-PCR autoradiograph illustrating the results of DDRT-PCR with primer pairs d(T)₁₂MC and A7, A8, DM 8 and DM 11. The primer pair d(T)₁₂MC and A8 resulted in the identification of cDNA candidate 2, representing a transcript differentially regulated in mutant (*cre*⁺ *Apc*^{580S/580S}) mammary glands.

(a) Candidate 2 (82bp)

CCTGTGTGGTACTATGCAGCTGCTTTTGTGGAAGTCATGGCTTCCTGTG
GAATAAAGATGGTCCAAAGGTTAGATGGAAAAA

(b)

Sequences producing significant alignments:	Score (bits)	E Value
gi 556296 gb J04694.1 MUSCOL1A4A Mus musculus alpha-1 type ...	147	2e-33
gi 20859991 ref XM_134042.1 Mus musculus procollagen, type...	147	2e-33
gi 1045208 emb X92439.1 MMCOL4A1G M.musculus mRNA for alpha...	147	2e-33
gi 50233 emb X02201.1 MMC4A1NC Mouse mRNA fragment for base...	147	2e-33

>gi|556296|gb|J04694.1|MUSCOL1A4A **Mus musculus alpha-1 type IV
collagen (Col4a-1) mRNA, complete cds**

Length = 6512

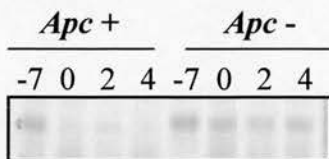
Score = 147 bits (74), Expect = 2e-33
Identities = 81/82 (98%), Gaps = 1/82 (1%)

Query: 1 cctgtgtggtactatgcagctgcttttgtggaagtcatggc-ttcctgtggaataaagat 59
|||||
Sbjct: 5681 cctgtgtggtactatgcagctgcttttgtggaagtcatggc-ttcctgtggaataaagat 5740

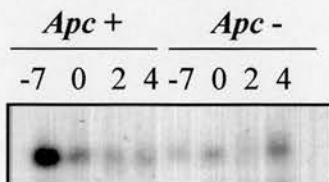
Query: 60 ggtccaaaggttagatggaaaa 81
|||||
Sbjct: 5741 ggtccaaaggttagatggaaaa 5762

Figure 4.8 BlastN comparison of candidate 2 cDNA sequence against non-redundant nucleic acid databases cDNA representing the transcript presented in Figure 4.7 (candidate 2) was cloned, transformed and plasmid DNA from six transformants sequenced. **(a)** Candidate 2 cDNA sequence. **(b)** Computer assisted homology search of the non-redundant nucleic databases (BlastN) revealed the sequence was 98% identical to positions 5681 - 5762 of the *Mus musculus alpha-1 type IV collagen* gene.

(a) DDRT-PCR



(b) 'cold' Southern



(c) Northern

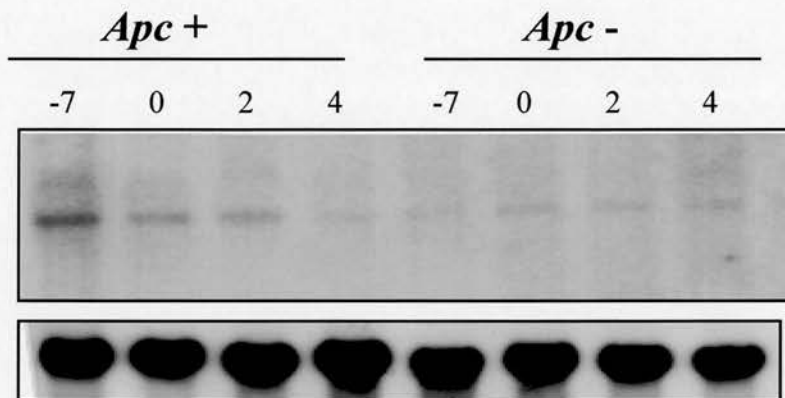


Figure 4.9 'Cold' Southern and Northern analysis of candidate 2

(alpha-1 type IV collagen) (a) DDRT-PCR differentially expressed transcript.

(b) Use of cloned cDNA as a probe to Southern-blotted DDRT-PCR products formally proves that the correct cDNA clone has been isolated by producing a pattern of hybridisation that mirrored the original DDRT-PCR profile. (c) Northern blot of 10µg total RNA from control ($cre^+ Apc^{+/580S}$ and $cre^- Apc^{580S/580S}$) and mutant ($cre^+ Apc^{580S/580S}$) mammary glands hybridised with the *alpha-1 type IV collagen* cDNA probe and exposed to MR X-ray film (Kodak) for 24 hours at $-70^\circ C$. Blots were stripped and re-probed with an 18S rDNA probe to allow normalisation for loading variations.

4.2.3.3 Candidate 3 (Clone 9.1)

The d(T)₁₂MC/MAX 3 DDRT-PCR primer combination resulted in the identification of a cDNA candidate (candidate 3) which represents a transcript specific to lactation in mutant ($cre^+ Apc^{580S/580S}$) mouse mammary glands (Figure 4.10). The observation that other cDNAs generated using this primer combination appeared almost identical in intensity between control and mutant provided confidence that this transcript was differentially expressed in $cre^+ Apc^{580S/580S}$ mouse mammary glands. Candidate 3 cDNA was therefore isolated and subjected to mSSCP analysis although in this particular instance there appeared to be no co-migrating cDNAs (Figure 4.11). This cDNA was recovered, PCR reamplified and cloned. Plasmid DNA was subsequently isolated from five transformants and sequenced. As illustrated in Figure 4.12, computer-based homology search (BlastN) of the non-redundant nucleic acid databases revealed that this particular candidate cDNA, 182bp in length, matched from positions 1818 – 1994 of *Mus musculus GM2 ganglioside activator protein (Gm2a)* mRNA. Use of cloned cDNA as a probe to Southern-blotted DDRT-PCR products produced a pattern of hybridisation that mirrored the original DDRT-PCR profile thus confirming isolation of the correct cDNA clone (Figure 4.13b). However northern analysis revealed expression of three *Gm2a* transcripts, only one of which appears differentially regulated (Figure 4.13c). This transcript was specific to $cre^+ Apc^{580S/580S}$ mouse mammary glands and may represent the differential transcript identified by DDRT-PCR.

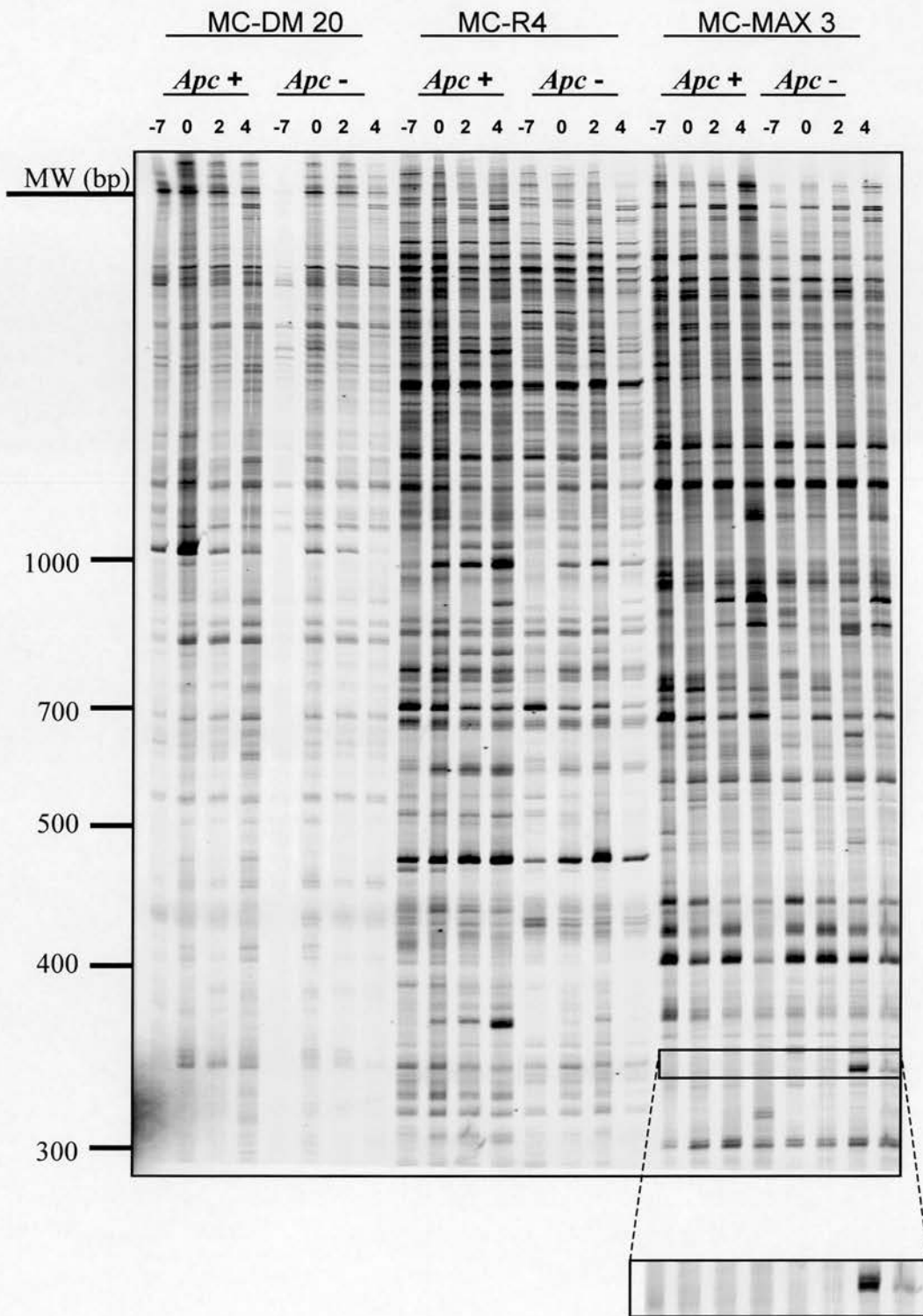


Figure 4.10 Identification of candidate 3 by DDRT-PCR

DDRT-PCR autoradiograph illustrating the results of DDRT-PCR with primer pairs d(T)₁₂MC and DM 20, R4 and MAX 3. The primer pair d(T)₁₂MC and MAX 3 resulted in the identification of cDNA candidate 3, representing a transcript specific to mutant (*cre*⁺ *Apc*^{580S/580S}) mammary glands.

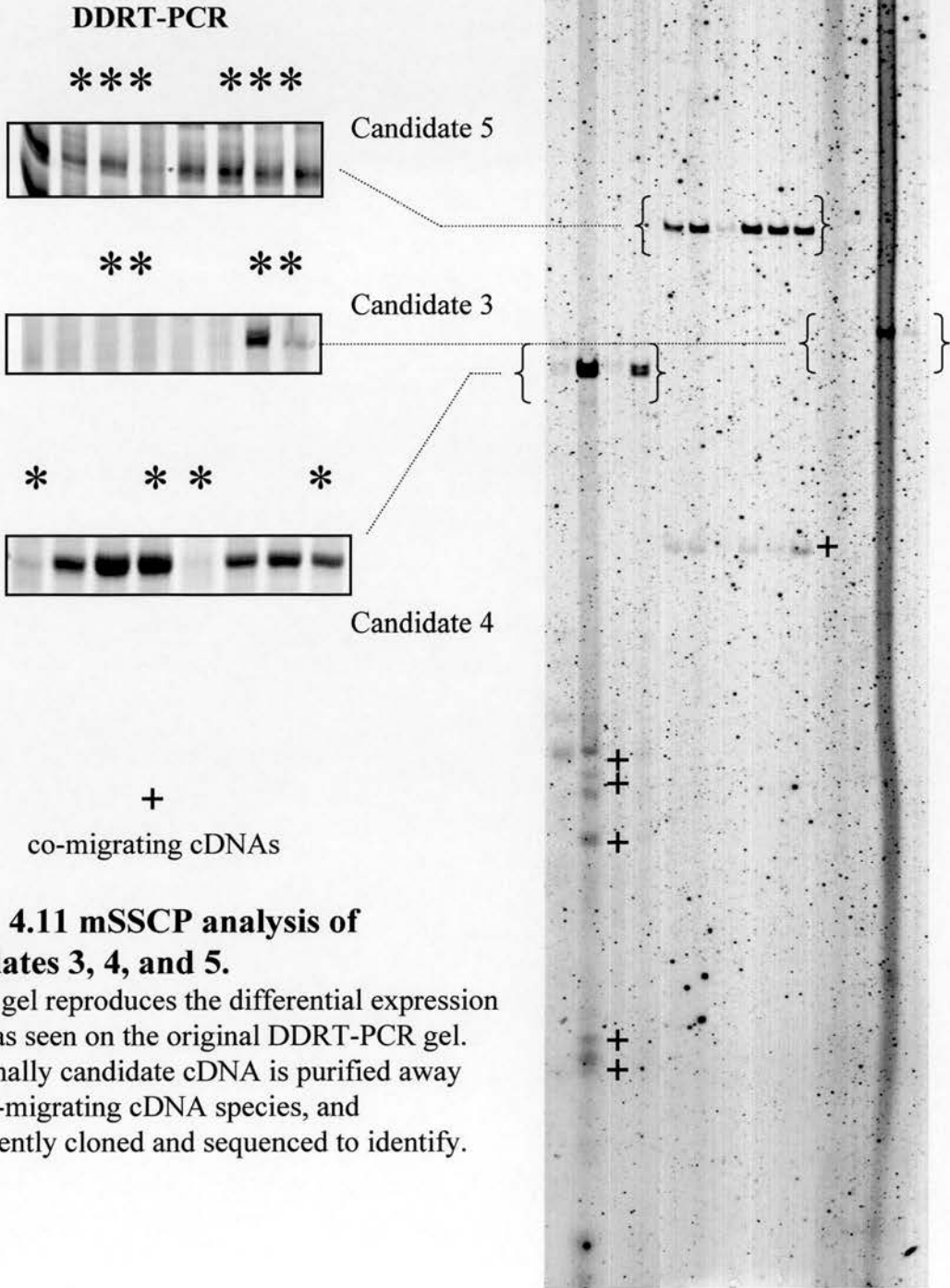
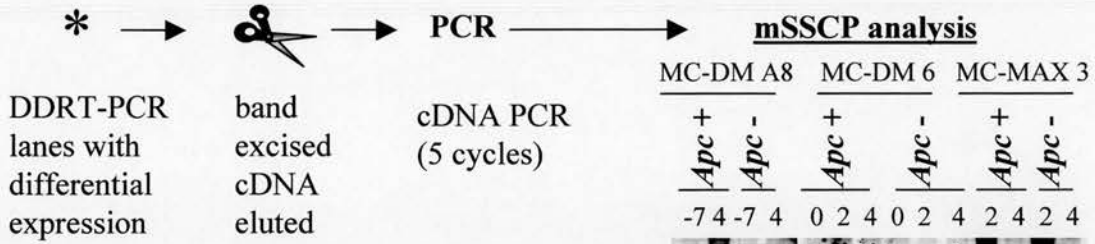


Figure 4.11 mSSCP analysis of candidates 3, 4, and 5.

mSSCP gel reproduces the differential expression pattern as seen on the original DDRT-PCR gel. Additionally candidate cDNA is purified away from co-migrating cDNA species, and subsequently cloned and sequenced to identify.

(a) Candidate 3 (182bp)

TTTTTGCAAGTTAAAAAGA TTTATTGCCAGACCAGTGTGTAGTCCAGAACCT
GGGCTGTCCGAGGAGGCTCAGGAAGTTGTCATGGTGCAACCTGATGTGGGAC
CCACTCTCTTCACAGGACCCCTGTTCCACGTGGTGGCTGCTAGGTGGGATCTA
CTCCAGTGTGAACCCCTCTACTCT

(b)

Sequences producing significant alignments:			Score	E
			(bits)	Value
gi 13435547 gb BC004651.1	Mus musculus, GM2 ganglioside ac...		335	1e-89
gi 22474421 emb AL772357.8	Mouse DNA sequence from clone R...		335	1e-89
gi 540017 gb U09816.1 MMU09816	Mus musculus GM2 activator p...		335	1e-89
gi 16507969 ref NM_000405.2	Homo sapiens GM2 ganglioside a...		44	0.058
gi 18559761 ref XM_041978.3	Homo sapiens GM2 ganglioside a...		44	0.058

gi|13435547|gb|BC004651.1| **Mus musculus, GM2 ganglioside activator protein**, clone MGC:5949 IMAGE:3482848, mRNA, complete cds
Length = 2024

Score = 335 bits (169), Expect = 1e-89
Identities = 175/177 (98%)

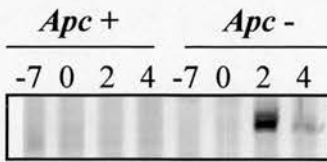
```
Query: 1   gcaagttaaaaagattttattgccagaccagtgtgttagtccagaacctgggctgtccgag 60
          |||
Sbjct: 1994 gcaagttaaaaagattttattgccagaccagtcttcttagtccagaacctgggctgtccgag 1935

Query: 61   gaggctcaggaagttgtcatggtgcaacctgatgtgggaccactctcttcacaggaccc 120
          |||
Sbjct: 1934 gaggctcaggaagttgtcatggtgcaacctgatgtgggaccactctcttcacaggaccc 1875

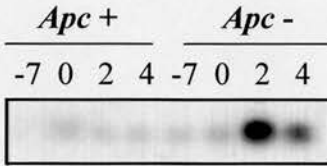
Query: 121  ctgttccacgtggtggctgctaggtgggatctactccagtgtgaaccctctactct 177
          |||
Sbjct: 1874 ctgttccacgtggtggctgctaggtgggatctactccagtgtgaaccctctactct 1818
```

Figure 4.12 BlastN comparison of candidate 3 cDNA sequence against non-redundant nucleic acid databases cDNA representing the transcript presented in Figure 4.10 (candidate 3) was cloned, transformed and plasmid DNA from five transformants sequenced. **(a)** Candidate 3 cDNA sequence. **(b)** Computer assisted homology search of the non-redundant nucleic acid databases (BlastN) revealed the sequence was 98% identical to positions 1818 - 1994 of the *Mus musculus* GM2 ganglioside activator protein clone MGC: 5949.

(a) DDRT-PCR



(b) 'cold' Southern



(c) Northern

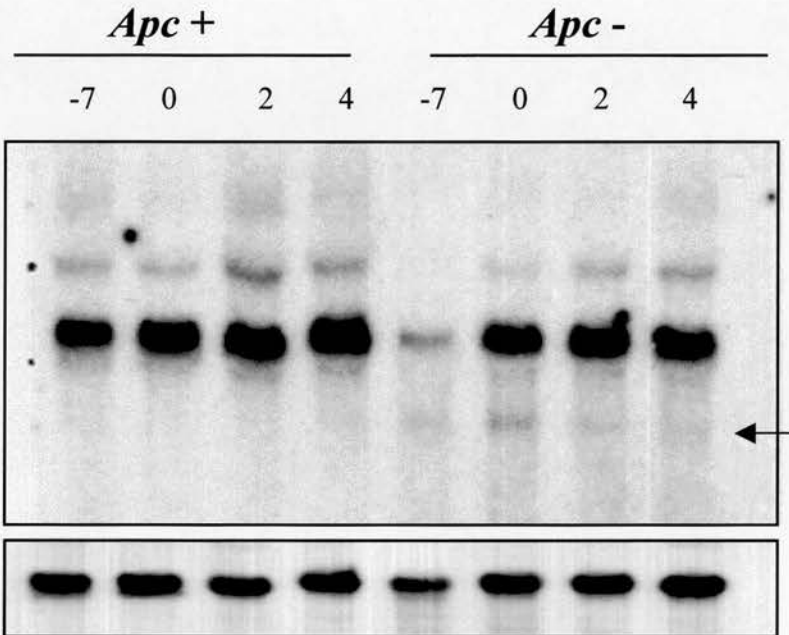


Figure 4.13 'Cold' Southern and Northern analysis of candidate 3 (GM2 ganglioside activator protein) (a) DDRT-PCR differentially expressed transcript. (b) Use of cloned cDNA as a probe to Southern-blotted DDRT-PCR products formally proves that the correct cDNA clone has been isolated by producing a pattern of hybridisation that mirrored the original DDRT-PCR profile. (c) Northern blot of 10 μ g total RNA from control ($cre^+ Apc^{+/580S}$ and $cre^- Apc^{580S/580S}$) and mutant ($cre^+ Apc^{580S/580S}$) mammary glands hybridised with the GM2 ganglioside activator cDNA probe and exposed to MR X-ray film (Kodak) for 24 hours at $-70^\circ C$. Arrow indicates transcript specific to mutant mammary glands. Blots were stripped and re-probed with an 18S rDNA probe to allow normalisation for loading variations.

4.2.3.4 Candidate 4 (Clone 11.2)

Candidate 4 cDNA represents the second cDNA differentially expressed when the DDRT-PCR primer combination d(T)₁₂MC/A8 was used (Figure 4.14). This transcript appears to be very subtly differentially regulated in mutant mouse mammary glands. Specifically, candidate 4 appears to be developmentally upregulated in control ($cre^+ Apc^{+/580S}$ and $cre^- Apc^{580S/580S}$) but remains constant in mutant ($cre^+ Apc^{580S/580S}$) mouse mammary glands. This cDNA was recovered and mSSCP analysis confirmed the presence of several potential co-migrating cDNAs (Figure 4.11). Following mSSCP purification, the cDNA was recovered, PCR reamplified and cloned. Plasmid DNA from six transformants was sequenced and computer-assisted homology search (BlastN) of the non-redundant nucleic acid databases revealed that candidate 4 cDNA sequence, 176bp in length, matched from positions 1 – 33 of *Mus musculus* clone MBI-32 miscellaneous RNA (Figure 4.15). This cDNA was termed 'novel 1' as MBI-32 encodes a novel, small, non-messenger RNAs (Huttenhofer *et al.*, 2001). Additionally, 'Cold' Southern blotting confirmed that *novel 1* represents the original differentially expressed transcript by producing a pattern of hybridisation that mirrored the original DDRT-PCR profile (Figure 4.16b). However northern analysis did not confirm the pattern of differential expression represented by the DDRT-PCR gel. Use of *novel 1* cDNA as a probe to northern blotted mammary gland RNA from control and *Apc* deficient mammary glands revealed expression of an alternative differentially expressed transcript that appears to be specifically upregulated in mutant ($cre^+ Apc^{580S/580S}$) mouse mammary glands (Figure 4.16c).

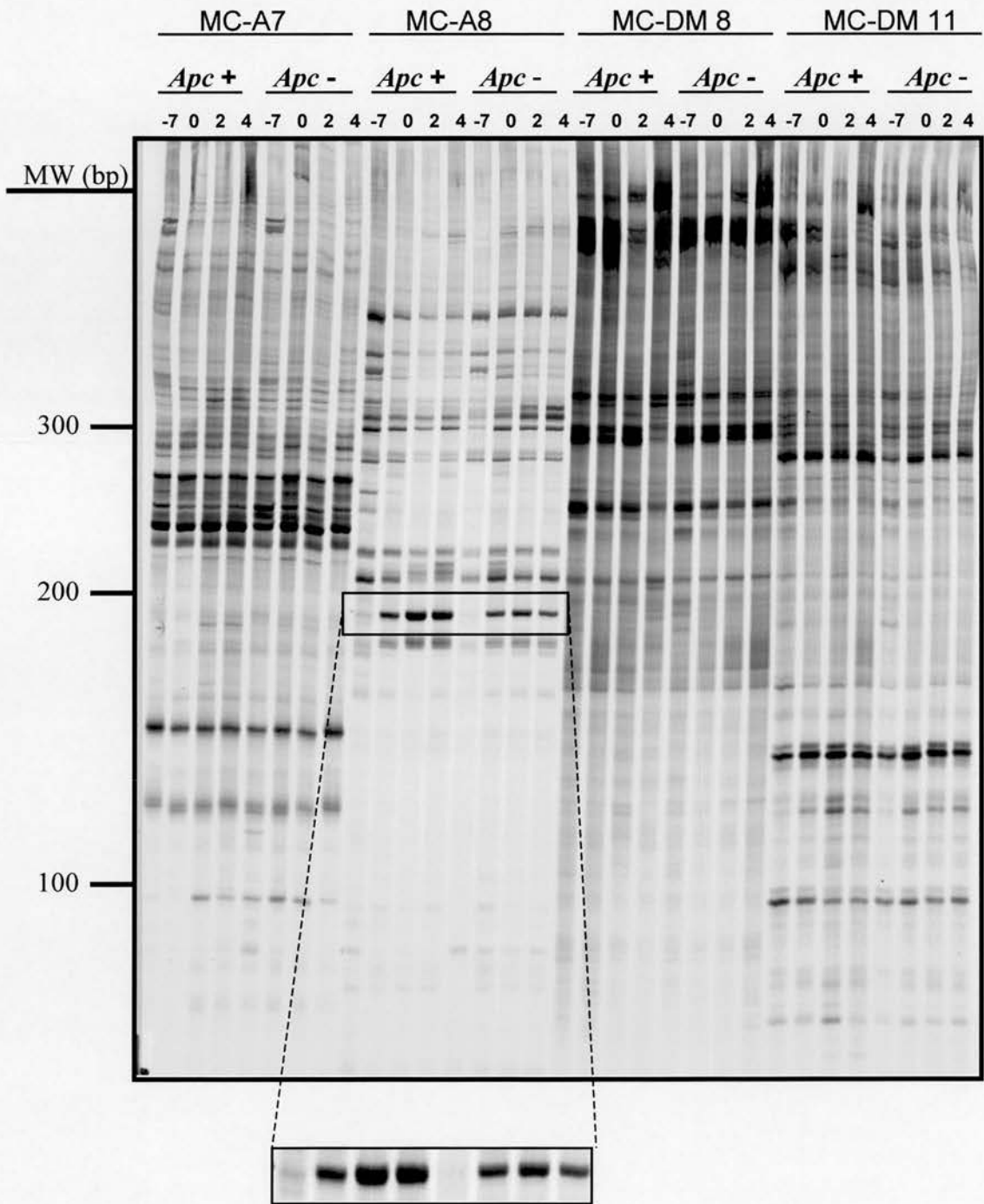


Figure 4.14 Identification of candidate 4 by DDRT-PCR

DDRT-PCR autoradiograph illustrating the results of DDRT-PCR with primer pairs d(T)₁₂MC and A7, A8, DM 8 and DM 11. The primer pair d(T)₁₂MC and A8 resulted in the identification of cDNA candidate 4, representing a transcript developmentally upregulated in control mammary glands but remains constant in mutant (*cre*⁺ *Apc*^{580S/580S}) mammary glands.

(a) Candidate 4

CGNTGTGTGGCAAGAATCAAGCAAGCAGTATTGTATCGAGACCAAAGTGG
TATCATGGTCGGTTTTGATTAGCAGTGGGGACTACCCTACCGTAACACCTT
GTTGGAATTGAAGCATCCAAAGAAAATACTTGAGAGGCCCTGGGCTTGTTT
TAACATCTGGAAAAAAAAAAAAAAAA

(b)

Sequences producing significant alignments:	Score (bits)	E Value
gi 14277082 gb AF357487.1 AF357487 Mus musculus clone MBI-3...	66	2e-08

>gi|14277082|gb|AF357487.1|AF357487 **Mus musculus clone MBI-32
miscellaneous RNA**, partial sequence
Length = 181

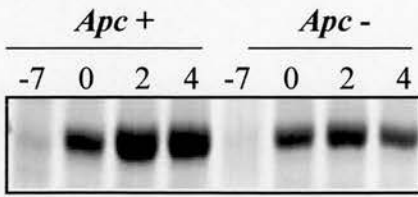
Score = 65.9 bits (33), Expect = 2e-08
Identities = 33/33 (100%)

```
Query: 130 cttgagaggccctgggcttggttttaacatctgg 162
          |||
Sbjct: 1   cttgagaggccctgggcttggttttaacatctgg 33
```

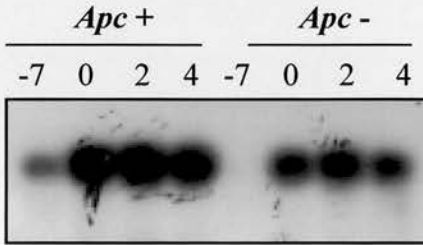
Figure 4.15 BlastN comparison of candidate 4 cDNA sequence against non-redundant nucleic acid databases

cDNA representing the transcript presented in Figure 4.14 (candidate 4) was cloned, transformed and plasmid DNA from six transformants sequenced. **(a)** Candidate 4 cDNA sequence. **(b)** Computer assisted homology search of the non-redundant nucleic databases (BlastN) revealed the sequence was 100% identical to positions 1 - 33 of the *Mus musculus clone MBI-32* miscellaneous RNA.

(a) DDRT-PCR



(b) 'cold' Southern



(c) Northern

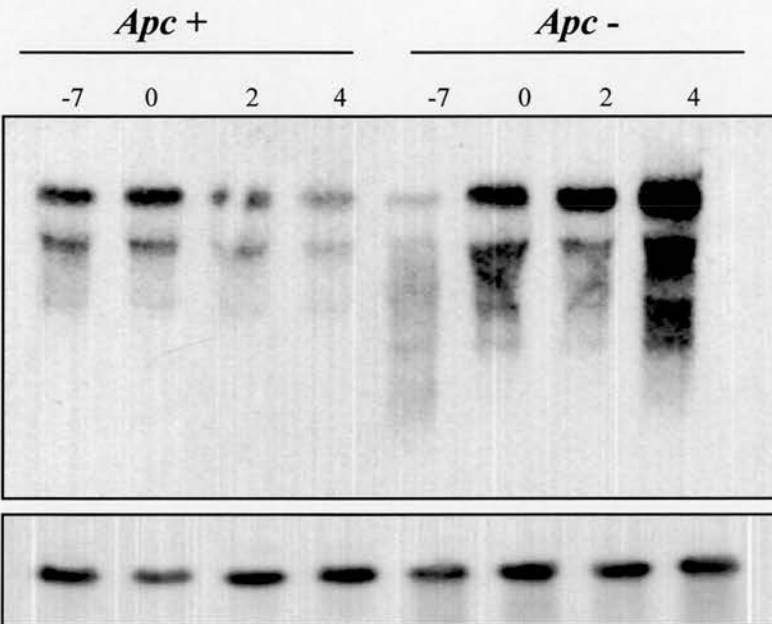


Figure 4.16 'Cold' Southern and Northern analysis of candidate 4 (novel 1) (a) DDRT-PCR differentially expressed transcript. (b) Use of cloned cDNA as a probe to Southern-blotted DDRT-PCR products formally proves that the correct cDNA clone has been isolated by producing a pattern of hybridisation that mirrored the original DDRT-PCR profile. (c) Northern blot of 10 μ g total RNA from control (*cre*⁺ *Apc*^{+/580S} and *cre*⁻ *Apc*^{580S/580S}) and mutant (*cre*⁺ *Apc*^{580S/580S}) mammary glands hybridised with the candidate 4 cDNA probe and exposed to MR X-ray film (Kodak) for 24 hours at -70°C. Blots were stripped and re-probed with an 18S rDNA probe to allow normalisation for loading variations.

4.2.3.5 Candidate 5 (Clone 12.3)

The d(T)₁₂MC/DM6 DDRT-PCR primer combination resulted in the identification of a cDNA candidate (candidate 5) which represents a transcript that appears to be developmentally downregulated in control mammary glands but expression of which remains constant in mutant (*cre*⁺ *Apc*^{580S/580S}) mouse mammary glands (Figure 4.17). Candidate 5 cDNA was isolated and subjected to mSSCP analysis which identified one co-migrating cDNA species (Figure 4.11). The purified cDNA was recovered, PCR reamplified and cloned. Plasmid DNA was subsequently isolated from five transformants and sequenced. Computer-based homology search (BlastN) of the non-redundant nucleic acid databases revealed that candidate 5 cDNA sequence, 436bp in length, matched from positions 19006 – 19233 of *Mus musculus chromosome 15* clone RP24-116K14 (Figure 4.18). Thus, candidate 5 cDNA was renamed *novel 2* as it encoded an unknown gene. ‘Cold’ Southern blotting confirmed that *novel 2* cDNA isolated from the DDRT-PCR gel corresponds to the differentially expressed transcript by producing a pattern of hybridisation similar to the original DDRT-PCR profile (Figure 4.19b). Northern analysis revealed differential expression of a transcript, however the pattern was not identical to that observed by DDRT-PCR (Figure 4.19c).

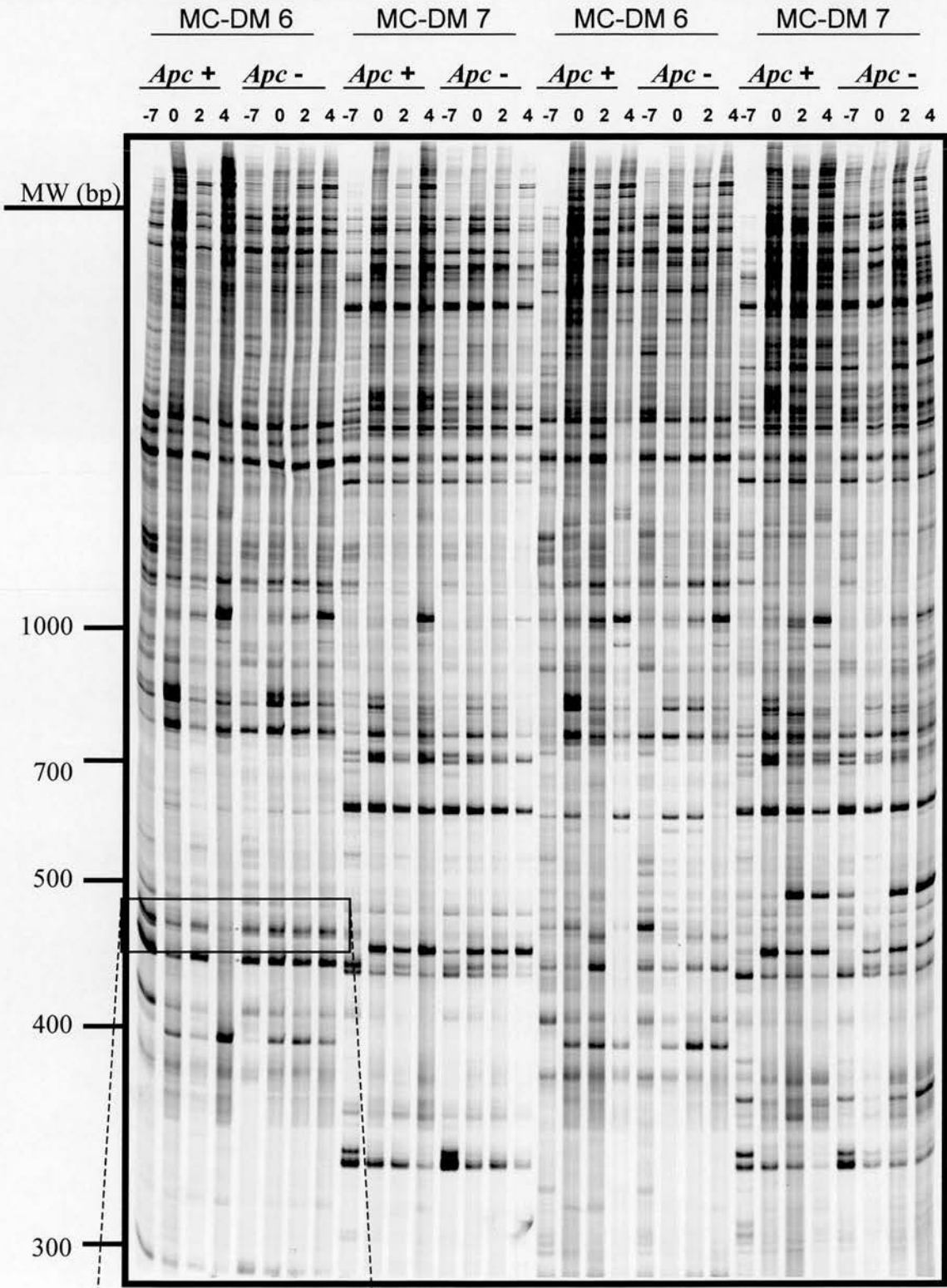


Figure 4.17 Identification of candidate 5 by DDRT-PCR DDRT-PCR autoradiograph illustrating the results of DDRT-PCR with primer pairs $d(T)_{12}MC$ and DM 6 and DM 7. The primer pair $d(T)_{12}MC$ and DM6 resulted in the identification of cDNA candidate 5, representing a transcript differentially regulated in mutant ($cre^+ Apc^{580S/580S}$) mammary glands.

(a) Candidate 5 (436bp)

GAATTCCTTTTTTTTTTTTTTTTGCAGACATATTACTCACCAGTGGGTCTACCTA
TAATTAAGTTTCATGTATTGGTAAATAAGACTAGATTTAAATCTATGAAA
GAATAGTAAGAGATGAAATAAATTCCCAGTAGAGTCTGACATGTTTGATTC
AAAATGTTAGTCTTAATCACACAAGCTTCTGATTGCTAACAATAAAATCC
TGTCTTTCTCTTTCTCGTCCTGTGAAATGAAAGCCTTTGTGGAAAAAAAAA
AAAAAGAATTC

(b)

Sequences producing significant alignments:	Score (bits)	E Value
gi 22748533 gb AC112158.4 Mus musculus chromosome 15 clone...	436	e-120

>gi|22748533|gb|AC112158.4| **Mus musculus chromosome 15 clone
RP24-116K14**, complete sequence
Length = 175171

Score = 436 bits (220), Expect = e-120
Identities = 226/228 (99%)

Query: 21 gcagacatattactcaccagtgggtctacctataaattaaagtttcatgtattggtaaata 80
|||||
Sbjct: 19233 gcagacatattactcaccagtgggtctacctataaattaaagtttcatgtattggtaaata 19174

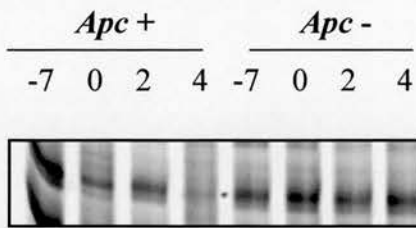
Query: 81 agactagatttaaactctatgaaagaatagtaagagatgaaataaattcccagtagagtct 140
|||||
Sbjct: 19173 agactacatttaaactctatgaaagaatagtaagagatgaaataaattcccagtagagtct 19114

Query: 141 gacatgtttgattcaaaatgtagtcttaatcacacaagcttctgattgctaacaattaa 200
|||||
Sbjct: 19113 gacatgtttgattcaaaatgtagtcttaatcacacaagcttctgattgctaacaattaa 19054

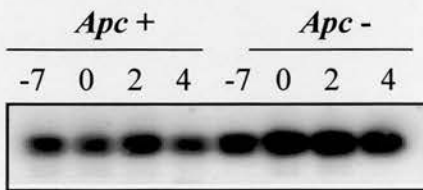
Query: 201 aatcctgttcttttcttttctcgtcctgtgaaatgaaagcctttgtgg 248
|||||
Sbjct: 19053 aatcctgttcttttcttttctcgtcctgtgaaatgaaagcctttgtgg 19006

Figure 4.18 BlastN comparison of candidate 5 cDNA sequence against non-redundant nucleic acid databases cDNA representing the transcript presented in Figure 4.17 (candidate 5) was cloned, transformed and plasmid DNA from five transformants sequenced. **(a)** Candidate 5 cDNA sequence. **(b)** Computer assisted homology search of the non-redundant nucleic acid databases (BlastN) revealed the sequence was 99% identical to positions 19006 - 19233 of the *Mus musculus* chromosome 15 clone RP24-116K14.

(a) DDRT-PCR



(b) 'cold' Southern



(c) Northern

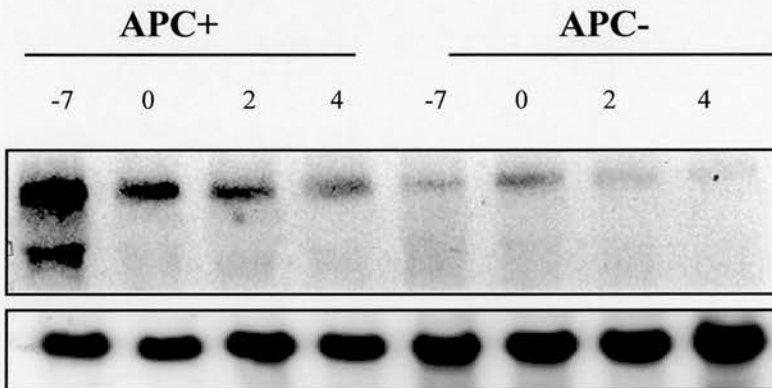


Figure 4.19 'Cold' Southern and Northern analysis of candidate 5 (novel 2) (a) DDRT-PCR differentially expressed transcript. (b) Use of cloned cDNA as a probe to Southern-blotted DDRT-PCR products formally proves that the correct cDNA clone has been isolated by producing a pattern of hybridisation that mirrored the original DDRT-PCR profile. (c) Northern blot of 10 μ g total RNA from control ($cre^+ Apc^{+/580S}$ and $cre^- Apc^{580S/580S}$) and mutant ($cre^+ Apc^{580S/580S}$) mammary glands hybridised with the candidate 5 cDNA probe and exposed to MR X-ray film (Kodak) for 24 hours at $-70^\circ C$. Blots were stripped and re-probed with an 18S rDNA probe to allow normalisation for loading variations.

4.2.3.6 Candidate 6 (Clone 13.4)

Candidate 6 cDNA represents the final cDNA differentially expressed when the DDRT-PCR primer combination d(T)₁₂MC/A8 was used (Figure 4.20). This transcript appears to be expressed at mid-gestation in both control ($cre^+ Apc^{+/580S}$ and $cre^- Apc^{580S/580S}$) and mutant ($cre^+ Apc^{580S/580S}$) mouse mammary glands, but becomes differentially regulated during lactation when *Apc* has been deleted. Candidate 6 cDNA was isolated and subjected to mSSCP analysis, which separated out several co-migrating cDNAs (Figure 4.4). Subsequently, the purified cDNA was PCR reamplified and cloned. Plasmid DNA from four transformants was sequenced and computer-assisted homology search (BlastN) of the non-redundant nucleic acid databases revealed that candidate 6 cDNA sequence, 187bp in length, matched from positions 752 – 901 of *H.sapiens* mRNA for the 3'UTR of an unknown protein (Figure 4.21). However despite exhaustive attempts, use of cloned candidate 6 cDNA (*novel 3*) to probe either Southern blotted DDRT-PCR products or northern blot of control and mutant RNA have been unsuccessful.

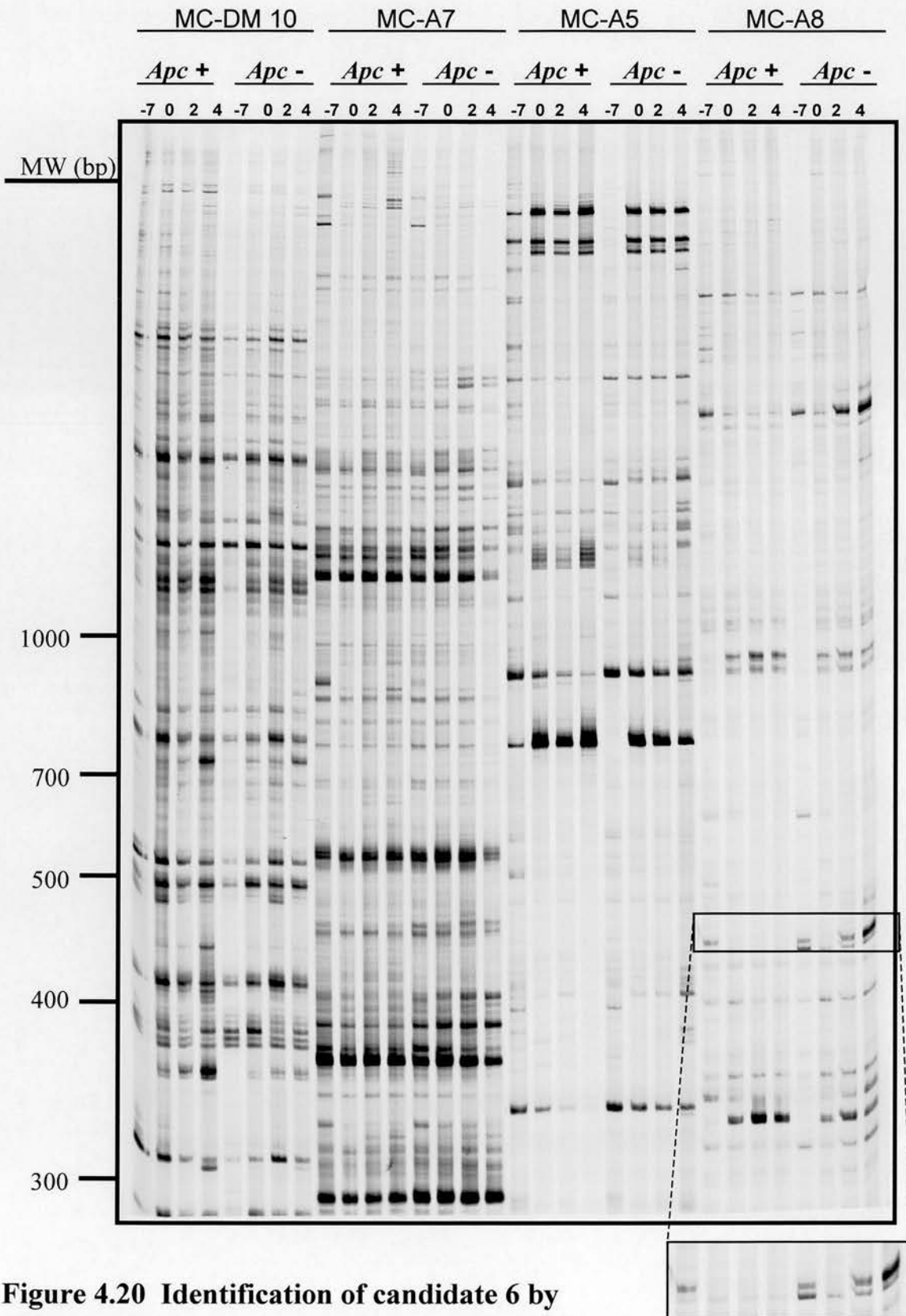


Figure 4.20 Identification of candidate 6 by DDRT-PCR DDRT-PCR autoradiograph illustrating the results of DDRT-PCR with primer pairs $d(T)_{12}MC$ and DM10, A7, A5 and A8. The primer pair $d(T)_{12}MC$ and A8 resulted in the identification of cDNA candidate 6, representing a transcript differentially regulated in mutant ($cre^+ Apc^{580S/580S}$) mammary glands.

(a) Candidate 6 (187bp)

TTTTTTTTTTTTTGCACCTTCAGATTTAGAAGAAACGATCCTGTTTCCATTTG
 AAAGGAACTGTAAAGCTTTTTTATCATTAAACCAACTGAACAACACACCA
 AAAGCAGCCTAGGGATGAGCACTTCTTTGAAGGCGATTAGGTTATTCCACC
 TGGTATTAATAACTATTTTCTATGGAAAAAAAAAAAAA

(b)

Sequences producing significant alignments:	Score	E
	(bits)	Value
gi 1743253 emb Y09836.1 HS3UTRUNK H.sapiens mRNA for 3'UTR ...	218	2e-54
gi 23273179 gb BC033486.1 Homo sapiens, clone IMAGE:519336...	218	2e-54
gi 21306641 gb AC012609.7 Homo sapiens chromosome 5 clone ...	218	2e-54

>gi|1743253|emb|Y09836.1|HS3UTRUNK **H.sapiens mRNA for 3'UTR of unknown protein**
 Length = 1420

Score = 218 bits (110), Expect = 2e-54
 Identities = 144/153 (94%), Gaps = 3/153 (1%)

```

Query: 16  cttcagatttagaagaacgatcctgtttccatttgaaaggaactgtaaagcttttttat 75
          |||
Sbjct: 752  cttcagatttagaagaaagatcctgtttccatttgaaaggaactgtaa-gctttt--at 808

Query: 76  catttaaccaactgaacaacacacacaaaagcagcctagggatgagcacttctttgaaggc 135
          | |||
Sbjct: 809  ctttaaccaactgaacaatacacacaaaagcagcctagggatgagcatttctttgaaagc 868

Query: 136 gattaggttattcacctggtattaaaactattt 168
          |||
Sbjct: 869 aattaggttattcacctggtattaaaactattt 901
  
```

Figure 4.21 BlastN comparison of candidate 6 cDNA sequence against non-redundant nucleic acid databases

cDNA representing the transcript presented in Figure 4.20 (candidate 6) was cloned, transformed and plasmid DNA from four transformants sequenced. **(a)** Candidate 6 cDNA sequence. **(b)** Computer assisted homology search of the non-redundant nucleic databases (BlastN) revealed the sequence was 94% identical to positions 752 - 902 of the *H.sapiens* mRNA for the 3'UTR of an unknown protein.

4.3 Discussion

DDRT-PCR comparison of gene expression between control ($cre^+ Apc^{+/580S}$ and $cre^- Apc^{580S/580S}$) and mutant ($cre^+ Apc^{580S/580S}$) mouse mammary glands identified six differentially expressed transcripts. A comprehensive and detailed study to isolate and identify these six candidate cDNAs was undertaken. Genes identified through this screen included *casein delta*, $\alpha 1$ type IV collagen, *Gm2a* and three novel genes, each of which are discussed below (and summarised in Table 4.3.1).

4.3.1 Candidate 1/ *Casein delta*

Candidate 1 cDNA when cloned and sequenced was identified to be 100% identical to *Mus musculus casein delta* mRNA. The caseins are the predominant proteins in milk. They are synthesised in great abundance in the mammary gland during gestation and lactation and are regulated by a variety of factors including peptide and steroid hormones (Prolactin and glucocorticoid hormones), cell-cell and cell-extracellular matrix interactions (Doppler *et al.*, 1990; Boudreau *et al.*, 1995). Hennighausen and Sippel (1982) report the identification of seven murine caseins, encoded by five mRNAs, designated $\alpha 1$, $\alpha 2$, $\beta 1$, $\beta 2$, γ , δ , and ϵ . DDRT-PCR identified expression *casein delta* as being exclusive to lactation, which correlates nicely with its identification as a milk protein gene (Figure 4.3). *Casein delta* appeared downregulated in mutant ($cre^+ Apc^{580S/580S}$) mammary glands and this differential expression was verified by subsequent northern analysis using the isolated *casein delta* cDNA as a probe (Figure 4.6c). Therefore, *Apc* deleted ($cre^+ Apc^{580S/580S}$) mouse mammary glands produce less milk than controls. One explanation for this may be the presence of extensive areas of metaplasia throughout the lactating gland of $cre^+ Apc^{580S/580S}$ mice resulting in less functional secretory epithelium (Figure 1.12). These metaplastic nodules consisted of tightly bound balls of epithelial cells emanating from ducts, which transdifferentiate into squamous cells as determined by histological criteria. Both keratinising and non-keratinising squamous differentiation occur within these lesions with the latter being more

Table 4.3.1 – Summary of DDRT-PCR results

<u>Differentially expressed gene</u>	<u>Function</u>	<u>Expression in cre⁺Apc^{580S/580S} mammary glands</u>
(1) <i>Mus musculus casein delta</i> mRNA	Milk protein gene	Casein expression was downregulated in cre ⁺ Apc ^{580S/580S} mammary glands during lactation.
(2) <i>Mus musculus alpha-1 type IV collagen</i>	Type IV collagen is a major structural component of mammary gland basement membrane	Alpha-1 type IV collagen expression was not developmentally downregulated in cre ⁺ Apc ^{580S/580S} mammary glands, as it is in controls.
(3) <i>Mus musculus GM2 ganglioside activator protein (Gm2a)</i> mRNA	Gm2a is a cofactor for the lysosomal degradation of GM2 ganglioside by hexosaminidase A	Three Gm2a mRNA transcripts were observed by northern analysis, only one of which was differentially expressed, with expression being specific to cre ⁺ Apc ^{580S/580S} mammary glands.
(4) <i>Novel 1 / alpha gene</i>	Function unknown	Novel 1 expression was upregulated in cre ⁺ Apc ^{580S/580S} mammary glands.
(5) <i>Novel 2 / mus musculus chromosome 15</i>	Function unknown	Novel 2 expression was downregulated in cre ⁺ Apc ^{580S/580S} mammary glands.
(6) <i>Novel 3 / H.sapiens</i> mRNA for the 3'UTR of an unknown protein	Function unknown	Novel 3 expression was upregulated during lactation in cre ⁺ Apc ^{580S/580S} mammary glands. However it most likely represents a false positive of DDRT-PCR.

frequent and resulting in the appearance of an eosinophilic material. These areas of metaplasia increased during lactation, remained after involution and increased in number and extent after two lactation cycles (Gallagher *et al.*, 2002). One possibility is that *Apc* deletion from the secretory epithelium of $cre^+ Apc^{580S/580S}$ mouse mammary glands disrupts normal function and consequently less milk is produced. The observation that offspring from $cre^+ Apc^{580S/580S}$ females did not thrive supports this hypothesis (Figure 1.10). These observations highlight the effectiveness of DDRT-PCR as a method for identifying differentially expressed transcripts in $cre^+ Apc^{580S/580S}$ mouse mammary glands.

4.3.2 Candidate 2 | *Mus musculus alpha-1 type IV collagen*

Sequencing revealed that candidate 2 cDNA was 98% identical to the *Mus musculus alpha-1 type IV collagen* gene. Type IV collagen is a major structural component in basement membrane and is a known component of mammary gland basement membrane (section 1.1.1) (Muthukumaran *et al.*, 1989; Hennighausen *et al.*, 2001). Collagen IV consists of two chains, $\alpha 1(IV)$ and $\alpha 2(IV)$, which are 43% identical. The $\alpha 1$ chain of mouse collagen IV is 1669 amino acids in length, including a putative 27-residue signal peptide, which is cleaved to produce the mature protein (Muthukumaran *et al.*, 1989). Initial identification of this cDNA transcript by DDRT-PCR indicated that its expression was specific to the mid-gestation time point in control mouse mammary glands and was consistent throughout all time points in *Apc* deleted ($cre^+ Apc^{580S/580S}$) mouse mammary glands (Figure 4.7). Northern analysis confirmed that while *alpha-1 type IV collagen* was expressed at mid gestation in control mammary glands its expression was developmentally downregulated through parturition and lactation to almost undetectable levels at day 4 lactation. In agreement with this another study reports that collagen IV expression in the mouse mammary gland peaks at mid-pregnancy with subsequent downregulation to almost undetectable levels in the lactating gland (Keely *et al.*, 1995). However, $cre^+ Apc^{580S/580S}$ mice, having undergone conditional inactivation of *Apc* from the mammary gland, express *alpha-1 type IV collagen* at equivalent levels

throughout all developmental time points examined (Figure 4.9c). This observation may detail a role of collagen in metaplasia formation in $cre^+ Apc^{580S/580S}$ mouse mammary glands. Further analysis of the relationship between collagen and metaplastic lesions is discussed in Chapter 5.

4.3.3 Candidate 3 / *Mus musculus* GM2 ganglioside activator protein mRNA

Candidate 3 cDNA was identified to be 98% identical to *Mus musculus* GM2 ganglioside activator protein (*Gm2a*) mRNA. The GM2 activator protein is an essential component for the lysosomal degradation of GM2 ganglioside by hexosaminidase A. Gangliosides are glycosphingolipid constituents of the outer surface of most cell membranes, hydrolysis of which requires three gene products. Whereas two of these proteins are the alpha- (HEXA gene) and beta- (HEXB) subunits of the lysosomal enzyme β -N-acetylhexosaminidase A, the third gene GM2A encodes the human GM2 activator protein. A deficiency in any one of these proteins leads to the storage of the ganglioside, primarily in the lysosomes of neuronal cells, and one of the three forms of GM2 gangliosidosis, Tay-Sachs disease, Sandhoff disease or the AB-variant form (Bellachioma *et al.*, 1993; Mahuran, 1999). DDRT-PCR identified the *Gm2a* cDNA transcript as one specific to lactation in mutant ($cre^+ Apc^{580S/580S}$) mouse mammary glands (Figure 4.10). It was hypothesised that due to this expression pattern, candidate 3 cDNA may represent a gene activated in the mouse mammary gland as a consequence of *Apc* deletion during lactation. Northern analysis using the cloned *Gm2a* cDNA as a probe revealed that this was not strictly accurate. Three *GM2 activator protein* mRNA transcripts were observed by northern analysis, two of which were expressed at equivalent levels across all time points in both control ($cre^+ Apc^{+/580S}$ and $cre^- Apc^{580S/580S}$) and mutant ($cre^+ Apc^{580S/580S}$) mouse mammary glands. The final and smallest of the three transcripts was specific to $cre^+ Apc^{580S/580S}$ mouse mammary glands and may represent the differential transcript identified by DDRT-PCR. The role of *Gm2a* expression in the mouse mammary gland was further examined in Chapter 5.

4.3.4 Candidate 4 / Novel 1

Sequencing and subsequent computer-assisted homology search (BlastN) of the non-redundant nucleic acid databases revealed that candidate 4 cDNA sequence, 176bp in length, was 100% identical to a 33bp sequence of *Mus musculus clone MBI-32* miscellaneous RNA. This small RNA was isolated in a screen for the detection of novel, small, non-messenger RNAs from two mouse brain cDNA libraries (generated from small RNA molecules)(Huttenhofer *et al.*, 2001). The authors concluded that *MBI-32* represented one of several novel, small, non-messenger RNAs that may represent degradation products of unknown human RNAs (Huttenhofer *et al.*, 2001). Thus candidate 4 cDNA represented a novel gene and was termed '*novel 1*'. DDRT-PCR identified *novel 1* cDNA transcript as one subtly differentially regulated in mutant mouse mammary glands. While *novel 1* appears to be developmentally upregulated in control ($cre^+ Apc^{+/580S}$ and $cre^- Apc^{580S/580S}$) mouse mammary glands expression remained constant in mutants ($cre^+ Apc^{580S/580S}$). Northern analysis did not confirm the DDRT-PCR expression pattern expected, revealing instead a contradictory differential expression pattern that appears to be specifically upregulated in mutant ($cre^+ Apc^{580S/580S}$) mouse mammary glands (Figure 4.16c). Several possible explanations exist for this apparent difference and are discussed in turn. First, the cDNA isolated off the DDRT-PCR gel and cloned did not represent the candidate of interest. However, the results of both mSSCP purification and 'cold' Southern analysis argue that this was unlikely. mSSCP analysis confirmed the presence of several potential co-migrating cDNAs and made capable the isolation of candidate 4 cDNA (Figure 4.11). 'Cold' Southern blotting confirmed that candidate 4 (*novel 1*) represents the original differentially expressed transcript by producing a pattern of hybridisation that mirrored the original DDRT-PCR profile (Figure 4.16b). Thus, the correct cDNA was isolated from the DDRT-PCR gel, cloned, sequenced and used to probe both Southern blotted DDRT-PCR products and northern blotted control and mutant RNA. A second explanation why northern analysis revealed an alternative differentially expressed transcript may be the existence of alternatively spliced family members which appear identical in size by northern analysis and mask

the differential expression pattern expected. Finally, there is also the possibility that a different member of the same gene family was being detected. This subject, and further characterisation of *novel 1* are described in Chapter 5.

4.3.5 Candidate 5 / *Novel 2*

Candidate 5 cDNA when cloned and sequenced was identified to be 99% identical to positions 19006 – 19233 of *Mus musculus chromosome 15* clone RP24-116K14. Therefore, this cDNA represented an unknown gene and was termed '*novel 2*'. DDRT-PCR identified *novel 2* cDNA as representing a transcript that appears to be developmentally downregulated in control mammary glands but expression of which remains constant in mutant ($cre^+ Apc^{580S/580S}$) mouse mammary glands (Figure 4.17). It was confirmed by 'Cold' Southern blotting that this cDNA (*novel 2*) isolated from the DDRT-PCR gel corresponds to the differentially expressed transcript by producing a pattern of hybridisation similar to the original DDRT-PCR profile (Figure 4.19b). However northern analysis revealed a discrepancy as the pattern of hybridisation observed following use of *novel 2* cDNA as a probe was different from that observed by DDRT-PCR (Figure 4.19c). Although different the pattern of hybridisation displayed similarities with the DDRT-PCR profile. Specifically, the northern blot showed a marked downregulation of *novel 2* mRNA expression. Further characterisation of *novel 2* is described in Chapter 5.

4.3.6 Candidate 6 / *Novel 3*

Sequencing and subsequent computer-assisted homology search (BlastN) of the non-redundant nucleic acid databases revealed that candidate 6 cDNA sequence was 94% identical to positions 752 – 901 of *H.sapiens* mRNA for the 3'UTR of an unknown protein. This cDNA, identified by DDRT-PCR, represented a transcript that becomes differentially regulated during lactation as a consequence of *Apc* deletion ($cre^+ Apc^{580S/580S}$ mice)(Figure 4.20). Despite exhaustive attempts, use of cloned candidate

6 cDNA (*novel 3*) to probe either Southern blotted DDRT-PCR products or northern blot of control and mutant RNA proved unsuccessful. Chapter 5 details further analysis of *novel 3*.

5 Further analysis of differentially expressed transcripts in $cre^+ Apc^{580S/580S}$ mouse mammary glands

5.1 Introduction

Chapter 4 described the identification of six transcripts differentially expressed in $cre^+ Apc^{580S/580S}$ mouse mammary glands. These included *casein delta*, *$\alpha 1$ type IV collagen*, *Gm2a* and transcripts from three presumed novel genes. In this chapter, I describe further investigation of the roles of these genes in the mouse mammary gland. It was anticipated that this information may help to understand the relationship between mammary gland metaplasia and *Apc* deficiency. Casein delta represents one of seven murine caseins, which are the major proteins in milk (Hennighausen and Sippel, 1982). DDRT-PCR identified *casein delta* as a gene downregulated in $cre^+ Apc^{580S/580S}$ mouse mammary glands during lactation and this was confirmed by northern blot analysis (section 4.2.3.1). The observation that *Apc* deleted mouse mammary glands ($cre^+ Apc^{580S/580S}$) produced less milk than controls although interesting, is not surprising when one considers that these glands at lactation show extensive metaplasia resulting in less functional secretory epithelium (Figure 1.12). This is further supported by the observation that offspring from $cre^+ Apc^{580S/580S}$ females did not thrive (Figure 1.10). Further analysis of *casein delta* was not pursued in this thesis, as its differential expression in $cre^+ Apc^{580S/580S}$ mouse mammary glands was considered most likely a consequence of metaplasia.

Gm2a encodes the murine *ganglioside activator protein* gene. This gene bears several hallmarks of a housekeeping gene including a highly GC rich 5' portion and several common putative promoter elements, Sp1, AP1 and AP2. Consistent with this, *Gm2a* expression has been observed in a wide variety of tissues including placenta, bone marrow, brain, spleen, mammary gland, lung, heart, and pancreas, albeit at varying transcript levels (Beccari *et al.*, 2001). The Gm2a activator protein

functions in lysosomal metabolism and is specifically required for the hydrolysis of GM2 ganglioside by the lysosomal enzyme β -N-acetylhexosaminidase A (Mahuran, 1998). DDRT-PCR identified *Gm2a* expression specifically during lactation in mutant ($cre^+ Apc^{580S/580S}$) mouse mammary glands. However subsequent northern analysis revealed three *Gm2a* mRNA transcripts, two of which were expressed at equivalent levels across all time points in both control ($cre^+ Apc^{+/580S}$ and $cre^- Apc^{580S/580S}$) and mutant ($cre^+ Apc^{580S/580S}$) mouse mammary glands. The third *Gm2a* transcript was specific to $cre^+ Apc^{580S/580S}$ mouse mammary glands and may represent the differential transcript identified by DDRT-PCR. A specific role of *Gm2a* in the mouse mammary gland has not been identified, however it has been reported that *Gm2a* is also a secretory protein and thus it is conceivable it has a function in mammary gland secretory epithelium (Rigat *et al.*, 1997). Several *Gm2a* transcripts have been identified and are reported to result from alternative splicing (Klima *et al.*, 1991; Nagarajan *et al.*, 1992). In addition, a processed pseudogene (*Gm2a*-related sequence) has been identified (Yamanaka *et al.*, 1994). Consequently, further analysis of *Gm2a* function in the mammary gland is complex and has no immediately obvious association with mammary gland development and/or metaplasia. Therefore, no further analysis of *Gm2a* in the mouse mammary gland was undertaken.

The remaining genes identified in Chapter 4 (*$\alpha 1$ type IV collagen*, and novel genes 1-3) are further analysed in the mouse mammary gland and are discussed in turn below.

5.2 *alpha-1 type IV collagen*

5.2.1 Introduction

Type IV collagen is a major structural component in basement membrane (a thin sheet of highly specialised extracellular matrix present at the epithelial/mesenchymal interface of most tissues) and is a known component of mammary gland basement membrane (section 1.1.1) (Muthukumaran *et al.*, 1989; Hennighausen *et al.*, 2001). It is considerably different from fibrillar collagens, types I-III, for example, unlike

fibrillar collagens nonhelical regions creating flexibility frequently interrupt the triple helical domain of type IV collagen (Sakurai *et al.*, 1986). Collagen IV consists of two chains, $\alpha 1(\text{IV})$ and $\alpha 2(\text{IV})$, which are 43% identical at the amino acid level (Muthukumaran *et al.*, 1989). *Type IV collagen* mRNA expression in the mammary gland is well documented with levels peaking at mid-pregnancy and falling to almost undetectable levels in the lactating gland (Keely *et al.*, 1995). Expression was localised to the stroma and the cells of the connective tissue sheath surrounding the mammary epithelium. The authors suggest that this temporal and spatial localisation of *type IV collagen* is consistent with a role in triggering epithelial cells to switch from ductal formation to alveolus formation (Keely *et al.*, 1995). In agreement with the *type IV collagen* expression pattern observed by Keely *et al.* (1995), northern analysis (section 4.2.3.2) revealed that *alpha-1 type IV collagen* mRNA expression in control mouse mammary glands, although high at mid-gestation, was developmentally downregulated through parturition and lactation to almost undetectable levels at day 4 lactation. However, in *Apc* deleted ($\text{cre}^+ \text{Apc}^{580\text{S}/580\text{S}}$) mouse mammary glands *alpha-1 type IV collagen* expression was consistent at all time points. It was hypothesised that *alpha-1 type IV collagen* plays a role in metaplastic lesion formation, following specific inactivation of *Apc* in the mouse mammary gland. To further investigate *alpha-1 type IV collagen* expression in metaplastic lesions, *alpha-1 type IV collagen* immunohistochemistry was performed.

5.2.2 Results

$\alpha 1$ type IV collagen protein distribution in both control ($\text{cre}^+ \text{Apc}^{+/580\text{S}}$ and $\text{cre}^- \text{Apc}^{580\text{S}/580\text{S}}$) and mutant ($\text{cre}^+ \text{Apc}^{580\text{S}/580\text{S}}$) mouse mammary glands was examined using a rabbit polyclonal antibody against the carboxy terminus of human $\alpha 1$ type IV collagen (amino acids 1452-1685)(see section 2.8.1). Immunohistochemical staining of sections from control day 10 lactating mammary glands ($\text{cre}^+ \text{Apc}^{+/580\text{S}}$ and $\text{cre}^- \text{Apc}^{580\text{S}/580\text{S}}$) demonstrated weak $\alpha 1$ type IV collagen expression in the stromal cells and the cells of the connective tissue sheath surrounding the mammary epithelium (Figure 5.1i). Sections from day 10 lactating $\text{cre}^+ \text{Apc}^{580\text{S}/580\text{S}}$ mammary glands

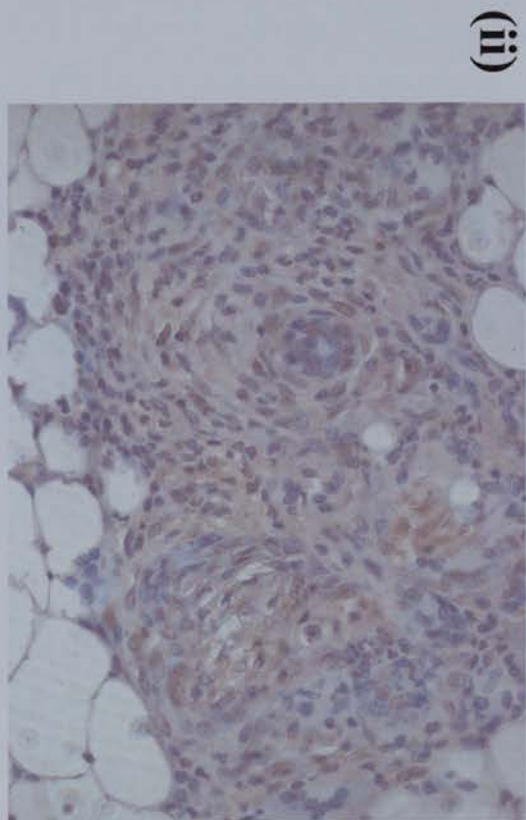
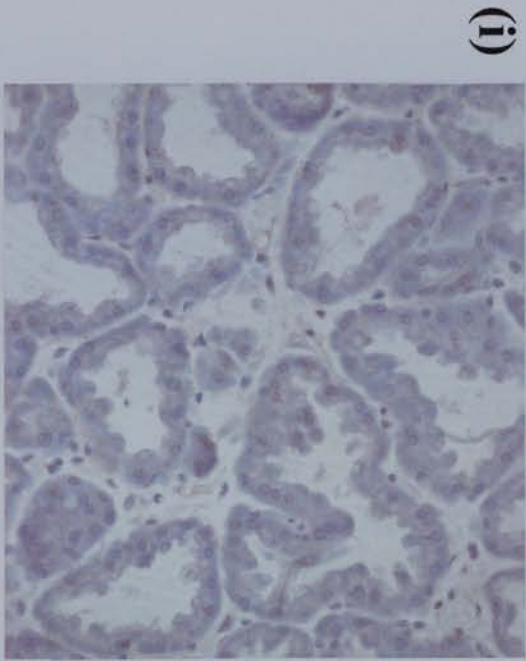


Figure 5.1 Immunohistochemical staining for $\alpha - 1$ type IV collagen

$\alpha - 1$ type IV collagen was detected using a mouse monoclonal antibody (Transduction laboratories, cat. no. C19220) and is represented by brown staining. (i) Control ($cre^{-} Apc^{580S/580S}$) mouse mammary gland section at day 10 lactation showing weak $\alpha - 1$ type IV collagen staining in the ECM surrounding the secretory epithelial cells. (ii) Apc deleted ($cre^{+} Apc^{580S/580S}$) mouse mammary glands at day 10 lactation showing strong $\alpha - 1$ type IV collagen staining within the metaplastic lesions.

displayed extensive $\alpha 1$ type IV collagen protein deposition within the metaplastic lesion (Figure 5.1ii).

5.2.3 Discussion

As introduced in chapter 1 (section 1.1.1), the mammary gland comprises stromal and epithelial cells that communicate with each other through a basement membrane composed of extracellular matrix (ECM) proteins. These interactions begin during the embryonic development of the mammary gland and in combination with steroid and peptide hormones are necessary for proper ductal morphogenesis throughout all stages of mammary gland development (Hennighausen *et al.*, 2001; Wiseman and Werb, 2002). One of the major structural components of the basement membrane is type IV collagen and its synthesis by mammary cells (stromal/mesenchymal) is important for the growth and/or survival of the mouse mammary epithelium. There is considerable evidence indicating that collagen production is tightly coupled to a mitogenic response in mammary epithelial cells. Significantly, Salomon *et al.* (1981) found that the ability to synthesise and accumulate type IV collagen was important for the proliferation of rat mammary epithelial cells. In the latter studies, cells maintained on plastic or collagen type I required epidermal growth factor and glucocorticoids to promote the accumulation of type IV collagen necessary for attachment and growth. However, cells grown on type IV collagen did not require these factors for proliferation thus highlighting the important role of type IV collagen in growth and development of the mammary epithelium. In breast cancer increased synthesis and degradation of ECM components has been observed and is associated with tumour progression and invasion (Liotta *et al.*, 1983; Lochter and Bissell, 1995). Additionally, a study by Nerlich *et al.* (1997) detailing gene expression and protein deposition of major basement membrane components in human breast cancer reported that mammary carcinomas show enhanced mRNA synthesis for major basement membrane proteins including fibronectin and type IV collagen. In all mammary carcinomas investigated, regardless of the degree of tumour cell differentiation, both tumour and stromal cells displayed strong mRNA expression for type IV collagen as

opposed to normal breast tissue where weak expression was observed (Nerlich *et al.*, 1997). In this study upregulation of $\alpha 1$ type IV collagen protein expression was observed in the mouse mammary gland following conditional inactivation of *Apc* ($cre^+ Apc^{580S/580S}$ mice). This upregulation was localised to the metaplastic lesions that arise following *Apc* loss, and is indicative of a dysregulated basement membrane within these lesions. It is unclear how *Apc* deletion in $cre^+ Apc^{580S/580S}$ mouse mammary glands leads to an upregulation of $\alpha 1$ type IV collagen expression, however the spatial and temporal expression of $\alpha 1$ type IV collagen is consistent with a possible role in metaplastic lesion formation.

5.3 Novel genes

5.3.1 Introduction

As described in Chapter 4, DDRT-PCR identified three novel genes differentially expressed in *Apc* deleted mouse mammary glands ($cre^+ Apc^{580S/580S}$ mice). These genes were termed 'novel' as sequencing and subsequent computer-assisted homology search (BlastN) of the non-redundant nucleic acid databases revealed they had no significant match to any known gene. In this analysis these novel cDNAs were used as probes to screen a mouse mammary gland day 10 lactation cDNA library with the aim of isolating full-length clones. It was anticipated that with increased sequence information the novel genes may match known genes in the non-redundant nucleic acid databases or alternatively have sequence motifs that may provide clues as to the functions of the novel genes.

5.3.2 Results

A lambda phage cDNA library prepared from lactation day 10 mouse mammary gland mRNA was kindly supplied by Dr. Christine Watson. Approximately 1 million plaques were plated out on a total of six 20cm x 20cm plates, sufficient to represent

all the genes in this library. Following plaque formation library DNA was transferred onto nylon membrane for screening by hybridisation with probes specific for each of the novel genes (section 2.7.3). Duplicate lifts were taken from each plate and following hybridisation only plaques that were positive on both filters were picked and subjected to a further round of screening in an effort to achieve single homogenous clones (section 2.7.5). Again, duplicate lifts were taken from each plate and hybridised in turn with each of the novel genes. Phage DNA was isolated from positive plaques (on both filters) and sequenced (section 2.7.5.1). The results for each novel gene are discussed in turn below.

5.3.2.1 Characterisation of transcript 'Novel 1'

In chapter 4, a 33bp region in *novel 1* cDNA (176bp) was shown to be 100% identical to the first 33bp of the *Mus musculus clone MBI-32* miscellaneous RNA (section 4.3.4). Prior to cDNA library screening, the 176bp sequence of *novel 1* was subjected to computer-assisted homology search (BlastN) of the expressed sequence tagged (EST) databases. *Novel 1* significantly matched a mouse cDNA clone with GenBank accession no. BG298761, which had been originally cloned from a murine retina cDNA library (Figure 5.2). This EST clone was obtained from the MRC UK HGMP Resource centre and was sequenced in an attempt to add to the 715bp of sequence already in the EST database. This sequence (1017bp), when subjected to BlastN search, displayed significant matches with the *Mus musculus* cDNA clone *MBI-32* miscellaneous RNA (100% identical over 181bp)(Figure 5.3) and the *Homo sapiens alpha* gene sequence (85% identical over 239bp and 87% identical over 118bp)(Figure 5.4).

Novel 1 was then used to probe the mouse mammary gland day 10 lactation cDNA library and following a primary screen 12 positive plaques were identified (Figure 5.5a). In order to achieve single homogenous clones, these were each plated out and subjected to a secondary screen, which identified 16 positive plaques (Figure 5.5b). Phage DNA was recovered from six of these and sequenced. The sequences

(a) *Novel 1* (176bp)

CGNTGTGTGGCAAGAATCAAGCAAGCAGTATTGTATCGAGACCAAAGTGG
TATCATGGTTCGGTTTTGATTAGCAGTGGGGACTACCCTACCGTAACACCTT
GTTGGAATTGAAGCATCCAAAGAAAATACTTGAGAGGCCCTGGGCTTGTTT
TAACATCTGGAAAAAAAAAAAAAAAA

(b)

Sequences producing significant alignments:	Score (bits)	E Value
gi 13063738 gb BG298761.1 BG298761 602396687F1 NIH_MGC_94 M...	315	9e-84
gi 2811800 gb AA762053.1 AA762053 vv49h04.r1 Soares_thymus_...	315	9e-84
gi 1776644 gb AA190040.1 AA190040 mt91h05.r1 Soares mouse l...	315	9e-84

>gi|13063738|gb|BG298761.1|**BG298761** 602396687F1 NIH_MGC_94

Mus musculus cDNA clone IMAGE:4511445 5'.

Length = 838

Score = 315 bits (159), Expect = 9e-84

Identities = 159/159 (100%)

```
Query: 4   tgtgtggcaagaatcaagcaagcagtattgtatcgagaccaaagtggatcatggtcggt 63
          |||
Sbjct: 172 tgtgtggcaagaatcaagcaagcagtattgtatcgagaccaaagtggatcatggtcggt 231

Query: 64   tttgattagcagtggggactaccctaccgtaaacaccttgttgaattgaagcatccaaag 123
          |||
Sbjct: 232 tttgattagcagtggggactaccctaccgtaaacaccttgttgaattgaagcatccaaag 291

Query: 124  aaaatacttgagagggccctgggcttgttttaacatctgg 162
          |||
Sbjct: 292  aaaatacttgagagggccctgggcttgttttaacatctgg 330
```

Figure 5.2 BlastN comparison of *novel 1* cDNA sequence against the EST databases

(a) *Novel 1* cDNA sequence. (b) Computer assisted homology search of the EST databases (BlastN) revealed that *novel 1* cDNA was 100% identical to positions 172 - 330 of the *Mus musculus* cDNA clone with GenBank accession number BG298761.

(a) cDNA clone BG298761 (1017bp)

CCACGCGTCCGCTGGTAATCTAGTGTTGAATCCTCTCCAGCTTCATGCTGGAGCAGCTAGCATGTGATGTAA
TGTTGGCCTTGGGGTGGAGGGGTGAGGTGGGCGCTAAGCCTTTTTTTAAGATTTTTTCAGGTACCCCTCACTA
AAGGCACTGAAGGCTTAATGTAGGACAGCGGAGCCTTCCTGTGTGGCAAGAATCAAGCAAGCAGTATTGT
ATCGAGACCAAAGTGGTATCATGGTCGGTTTTGATTAGCAGTGGGGACTACCCTACCGTAACACCTTGTTG
GAATTGAAGCATCCAAAGAAAATACTTGAGAGGCCCTGGGCTTGTTTTAACATCTGGAAAAAAGGCTGTTT
TTATAGCAGCGGTTACCAGCCCAAACCTCAAGTTGTGCTTGCAGGGGAGGGAAAAGGGGGAAAAGCGGGCA
ACCAGTTTCCCAGCTTTCCAGAATCCTGTTACAAGGTCTCCCCACAAGTGATTTCTCTGCCACATCGCCA
CCATGGGCCTTTGGCCTAATCACAGACCTTCACCCCTCACCTTGATGCAGCCAGTAGCTGGATCCTTGAGG
TCACGTTGCATATCGGTTTCAAGGTAACCATGGTGCCAAGGTNCTGTGGGTTGCACCAGAAAAGGCATCAA
TTTTCCCTTGCCTGTAATTAACATTAACCATAGCTAGATGTTTATCATAGCACCTATCAGAGTAAACAAACC
AGTATGGTATAGATGTTGAACCAGTCTGGTGGAATGAGGAAGTCGATAAAACAAGCTTGNAGAAGTGTGG
GNGATGAAAATNTTGTAACCTTTTAGTGCATACAATTGCCACTGCTNTANGAACAAATNNTNGTNGGTTAAG
TTTTTCTGAAACACTTGTGTTAGTTTGTGTTGCTTCTACTTAAAAAANNAACCTGGGTGATCTGTTTCAGACG
GTATTCTNGGGTTNTTATTANTNAGCTAATTTTGGGNTAAGNTNGTGGNNTATTGACCCCCCNNT
TAAAANNTNTNNCCANNT

(b)

Sequences producing significant alignments:	Score (bits)	E Value
gi 14277082 gb AF357487.1 AF357487 Mus musculus clone MBI-3...	359	5e-96
gi 2529712 gb AF001540.1 AF001540 Homo sapiens clone alpha1...	172	6e-40
gi 6979641 gb AF203815.1 AF203815 Homo sapiens alpha gene s...	170	2e-39

>gi|14277082|gb|AF357487.1|AF357487 **Mus musculus clone MBI-32**
miscellaneous RNA, partial sequence
Length = 181

Score = 359 bits (181), Expect = 5e-96
Identities = 181/181 (100%)

Query: 310 cttgagaggccctgggcttggttttaacatctggaaaaaggctgtttttatagcagcgg 369
|||||
Sbjct: 1 cttgagaggccctgggcttggttttaacatctggaaaaaggctgtttttatagcagcgg 60

Query: 370 taccagcccaaacctcaagttgtgcttgcaggggagggaaaaggggaaagcgggcaacc 429
|||||
Sbjct: 61 taccagcccaaacctcaagttgtgcttgcaggggagggaaaaggggaaagcgggcaacc 120

Query: 430 agtttcccagcttttccagaatcctgttacaaggtctccccacaagtgatttctctgcc 489
|||||
Sbjct: 121 agtttcccagcttttccagaatcctgttacaaggtctccccacaagtgatttctctgcc 180

Query: 490 a 490
|
Sbjct: 181 a 181

Figure 5.3 BlastN comparison of mouse cDNA clone BG298761 against non-redundant nucleic acid databases

(a) Mouse cDNA clone BG298761 sequence. **(b)** Computer assisted homology search of the non-redundant nucleic acid databases (BlastN) revealed that the cDNA clone BG298761 was 100% identical to the *Mus musculus clone MBI-32* miscellaneous RNA.

(a)

>gi|6979641|gb|AF203815.1|AF203815 *Homo sapiens alpha gene sequence*
Length = 8586

Score = 170 bits (86), Expect = 2e-39
Identities = 205/239 (85%) Gaps = 8/239 (3%)

Query: 374 agcccaaacctcaagttgtgcttgccagggaggaaaggggaaagcgggcaaccagtt 433
||||||| ||||| ||||| ||||||||| ||||||||| ||||| ||
Sbjct: 7073 agcccaaactcaagcgggtgcttgaagggaggaaaggggaaagcgggcaaccact 7131

Query: 434 tcccc-agcttttccagaatcctgtta----caaggtctccccacaagtgatttctctgc 488
| ||| ||||||||| ||||| ||||||||| ||||| | |||||
Sbjct: 7132 ttccctagcttttccagaagcctgttaaaagcaaggtctccccacaagcaacttctctgc 7191

Query: 489 cacatcgccaccatgggcctttggcctaatacacagacccttcaccctcaccttgatgca 548
||||||| | ||||| | | ||||||||| ||||| |||||
Sbjct: 7192 cacatcgccaccccgctgctttgatctagcacagacccttcaccctcacctcgatgca 7251

Query: 549 gccagtagc-tggatccttgagggtcacgttgcacat-atcggtttcaaggtaacatgggtg 605
||||||| ||||||||| || || | | ||| ||||||||| |||||
Sbjct: 7252 gccagtagccttggatccttggggcatgatccataatcggtttcaaggtaacgatgggtg 7310

(b)

Score = 125 bits (63), Expect = 1e-25
Identities = 103/118 (87%) Gaps = 3/118 (2%)

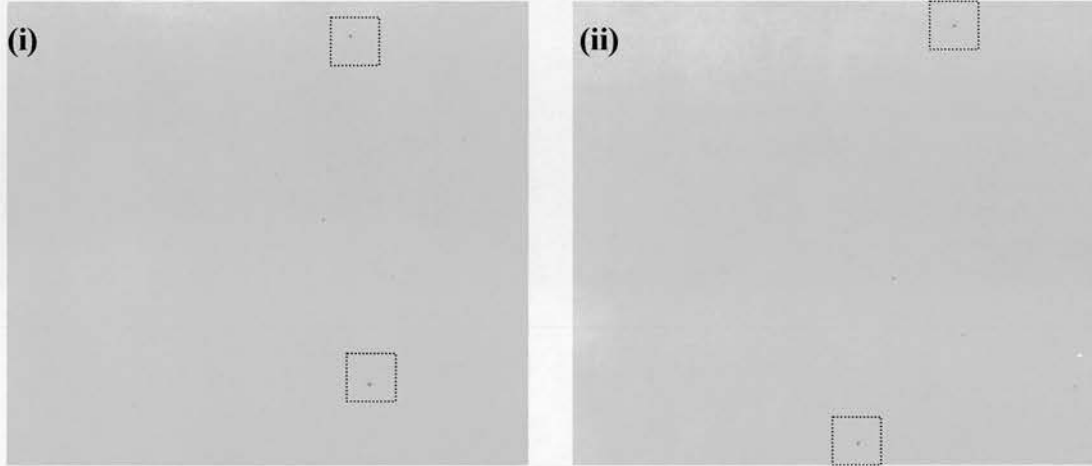
Query: 73 tgttggccttgggggtggaggggtgaggtggggcctaagcnnnnnnaagatttttcagg 132
||||||| | ||||||||| ||||||||| ||||||||| |||||
Sbjct: 6764 tgttggcgtgggggtggaggggtgaggtggggcctaagccttttttaagatttttcagg 6823

Query: 133 taccctcactaaaggcactgaaggcttaatgtaggacagc---ggagccttctctgtg 187
||||||||| ||||||||| ||||||||| ||||||||| | |||||||||
Sbjct: 6824 taccctcactaaaggcaccgaaggcttaagtaggacaacatggagccttctctgtg 6881

Figure 5.4 BlastN comparison of mouse cDNA clone BG298761 against non-redundant nucleic acid databases

Computer assisted homology search of the non-redundant nucleic acid databases (BlastN) revealed that the cDNA clone BG298761 was had two regions identical to *Homo sapiens alpha* gene sequence (a) region one was 85% identical over 239bp and (b) region two was 87% identical over 118bp.

(a)



(b)

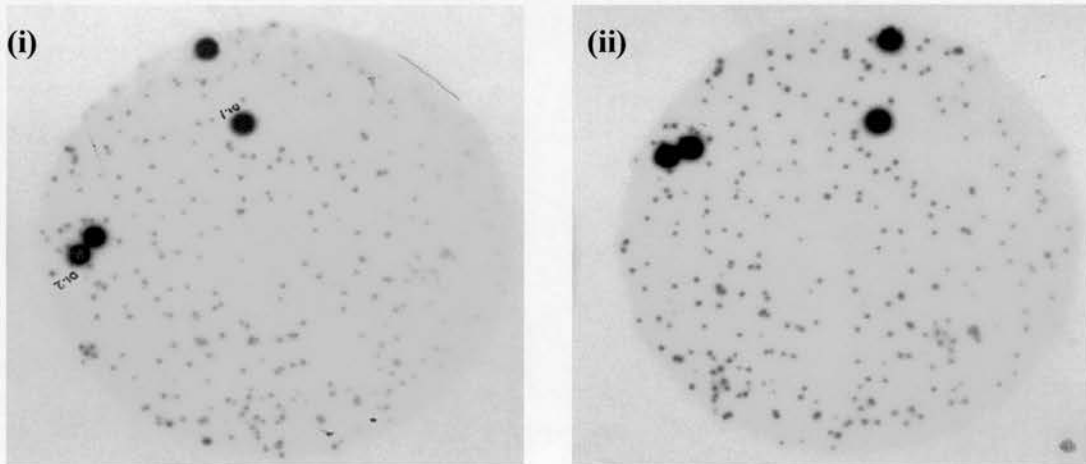


Figure 5.5 Isolation of *novel 1* cDNA positive clones from a mouse mammary gland cDNA library (a) i and ii are typical primary screen autoradiographs identifying *novel 1* positive plaques. Duplicate lifts were taken and only plaques that were positive on both filters were picked. (b) (i) Secondary screen autoradiograph with 4 *novel 1* positive plaques (intense black spots). The multiple spots of weaker intensity represent background hybridisation. (ii) Duplicate autoradiograph confirming that the 4 plaques are *novel 1* positive.

(~1200bp in length) were found to be identical. As shown in Figure 5.6, BlastN search of the non-redundant nucleic acid databases revealed that this longer *novel 1* cDNA sequence (*novel 1*^{1243bp}) was 100% identical to the entire 181bp of the *Mus musculus* clone MBI-32 miscellaneous RNA. Additionally, *novel 1*^{1243bp} cDNA matched the *Homo sapiens alpha* gene sequence in two regions, the first was 85% identical over 185bp and the second was 87% identical over 239bp (Figure 5.7). Figure 5.8 summarises the above information and details that whilst the *novel 1* sequence obtained from DDRT-PCR has sequence identity with the cDNA clone (BG298761) and the clone isolated from the cDNA library screen (*novel 1*^{1243bp}) it does not share any similarity with *alpha* gene. However both the cDNA clone (BG298761) and *novel 1*^{1243bp} have two regions that share sequence identity with *alpha* gene. Consequently, it was unclear whether the DDRT-PCR clone (*novel 1*) represented a fragment of *alpha* gene. Two methods, northern and Southern blotting, were used to attempt to decipher the relationship between *novel 1* and *alpha* gene.

Northern analysis was used in an effort to determine if *novel 1* and *alpha* gene represent the same gene. Figure 5.9 details five probes designed against various regions of *novel 1*^{1243bp}, which either do or do not have sequence identity with regions of *alpha* gene. Probes 1-4 were generated by PCR using specific primers designed against the *novel 1*^{1243bp} template. An additional probe (probe 5) was designed against a region of *alpha* gene way downstream from the region in question (4192-4492bp). It was hypothesised that if these probes hybridised to different transcripts then it remained possible that *novel 1* was not derived from the *alpha* gene locus. Hybridisation of these probes to northern blotted mammary gland RNA from control (*cre*⁺ *Apc*^{+580S} and *cre*⁻ *Apc*^{580S/580S}) and *Apc* deleted (*cre*⁺ *Apc*^{580S/580S}) mouse mammary glands revealed similar patterns of hybridisation (Figure 5.10 and Figure 5.11). On closer examination, (Figure 5.11), it was determined that although different in intensity the patterns of hybridisation were identical and the transcript hybridising to each probe was the same size. This data is consistent with all five probes hybridising to the same transcript - *alpha* gene. To rule out the possibility of more than one gene hybridising a Southern analysis approach was used.

(a) Novel *I*^{1243bp} (cDNA library clone) (1243bp)

```
GAGTATTTGGNNCGTTTGCTTAGGNCGAATTGGGTTCCGGGCCCCCCTCGAGTTTTTTTTTTTTTTTTTAAAGC
TAGGGAAAGGCCAAAAAGCAAAACCTGAGAAAACAAAAGGTTGTTTTCTCAGGAAAAGAAAAACCTTTACAAC
CCTACTGACGAATCTGCTTCCACTAAGATGCTAGCTTGGCCAAGTCTGTTATGTCCACCTGAAAAAGTCTTAGCA
GAGAATTTTTCGAATCCACCCCAACAACCTCCTACAAAAGGCTTGCCTTTCATCCGACTTCTACATTTCCACCC
AGCACTGGTATCAAACATACTATAACCATACTGGTTTGTACTCTGCATAGGTGCTATGTATAAAAACATCTTAG
CTATGGTTTTAATGTTAAATTACAGGCAAGGGGAAAAATTGATGGCCTTTTCTGGTGCAACCCACAGGACCTTGG
CACCATGGTTACCTTGAAACCGATATGCAACGTGACCTCAAGGATCCAGCTACTGGCTGCATCAAGGTGAGGGG
TGAAGGGTCTGTGATTAGGCCAAAGGCCCATGGTGGCGATGTGGCAGAGAAATCACTTGTGGGGGAGACCTTGT
AACAGGATTCTGGAAAAGCTGGGGAAACTGGTTGCCCGCTTTCCCCCTTTCCCTCCCCTGCAAGCACAACTTG
AGGTTTGGGCTGGTAAACCGCTGCTATAAAAACAGCCTTTTTTCCAGATGTTAAAACAAGCCAGGGCCTCTCAA
GTATTTTCTTTGGATGCTTCAATTCCAACAAGGTGTTACNGNAGGGTAGTCCCCTGNTNATCAAAAACCGACC
ATGATACCACTTTGGTCTCGATACATACTGCTGCTTGTATTCTGCACACAGGAAGNTTCGCTGNCTACATAAGCC
TNAGTGCTTTAGTGNGGGTCTGAAAATTTAAAAAAGGTTAGCGCCACCTACCCTTACCCAAGGCACATACAT
ACATNTAGCTGTTCANATGAACTGGGNGGATCACCTNGATNCATGCTATNTTACAGAAAGNTCGTCCCNNTGGC
TATTTGGCNTGNGATTTAATNACNGGACTTTNCGTTGANCNTTNAGANAGGTTCCACCCCTNAAGNGGTT
TTTTTTTTNTNAAAAAGGGTTTTNTGGGGGNNTTTTCCCAAAAAAATNTGNNAANATCCNNAAAAAACNNGG
GGGGGACNNCNAANTTTNACCNNGGAAANNCCNGAAATTAAGNTNGTTTT
```

(b)

Sequences producing significant alignments:	Score	E
	(bits)	Value
gi 14277082 gb AF357487.1 AF357487 Mus musculus clone MBI-3...	359	6e-96
gi 6979641 gb AF203815.1 AF203815 Homo sapiens alpha gene s...	186	5e-44
gi 4884449 emb AL050210.1 HSM800507 Homo sapiens mRNA; cDNA...	186	5e-44
gi 17425224 dbj AP000769.4 Homo sapiens genomic DNA, chrom...	186	5e-44
gi 2529712 gb AF001540.1 AF001540 Homo sapiens clone alphal...	178	1e-41

```
>gi|14277082|gb|AF357487.1|AF357487 Mus musculus clone MBI-32  
miscellaneous RNA, partial sequence  
Length = 181
```

```
Score = 359 bits (181), Expect = 6e-96  
Identities = 181/181 (100%)
```

```
Query: 564 tggcagagaaatcacttgtggggagaccttgaacaggattctggaaaagctggggaaac 623  
|||||  
Sbjct: 181 tggcagagaaatcacttgtggggagaccttgaacaggattctggaaaagctggggaaac 122
```

```
Query: 624 tggttgcccgctttccccctttccctcccctgcaagcacaacttgaggtttgggctggt 683  
|||||  
Sbjct: 121 tggttgcccgctttccccctttccctcccctgcaagcacaacttgaggtttgggctggt 62
```

```
Query: 684 aaccgctgctataaaaaacagcctttttccagatgttaaacaagcccagggcctctcaag 744  
|||||  
Sbjct: 61 aaccgctgctataaaaaacagcctttttccagatgttaaacaagcccagggcctctcaag 1
```

Figure 5.6 BlastN comparison of cDNA library clone *novel I*^{1243bp} against non-redundant nucleic acid databases

(a) Mouse cDNA clone *novel I*^{1243bp} sequence. **(b)** Computer assisted homology search of the non-redundant nucleic acid databases (BlastN) revealed that *novel I*^{1243bp} 100% identical to the *Mus musculus clone MBI-32* miscellaneous RNA.

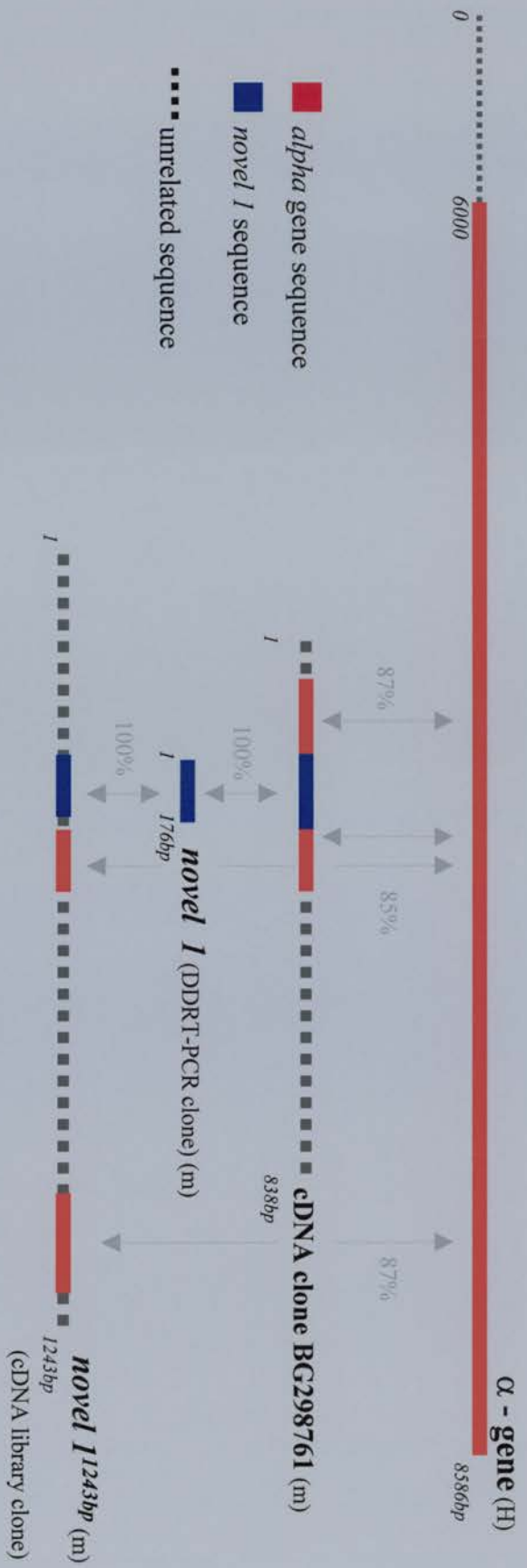


Figure 5.8 Schematic representation of regions identical to *alpha* gene

Novel I is 100% identical to both the mouse cDNA clone BG298761 and the cDNA clone isolated from the mouse cDNA library, *novel I*^{1243bp}. Both the cDNA clone BG298761 and *novel I*^{1243bp} have two regions identical to the human *alpha* gene sequence. They both share one region which is 85% identical to *alpha* gene and they each have an alternative region that is 87% identical.

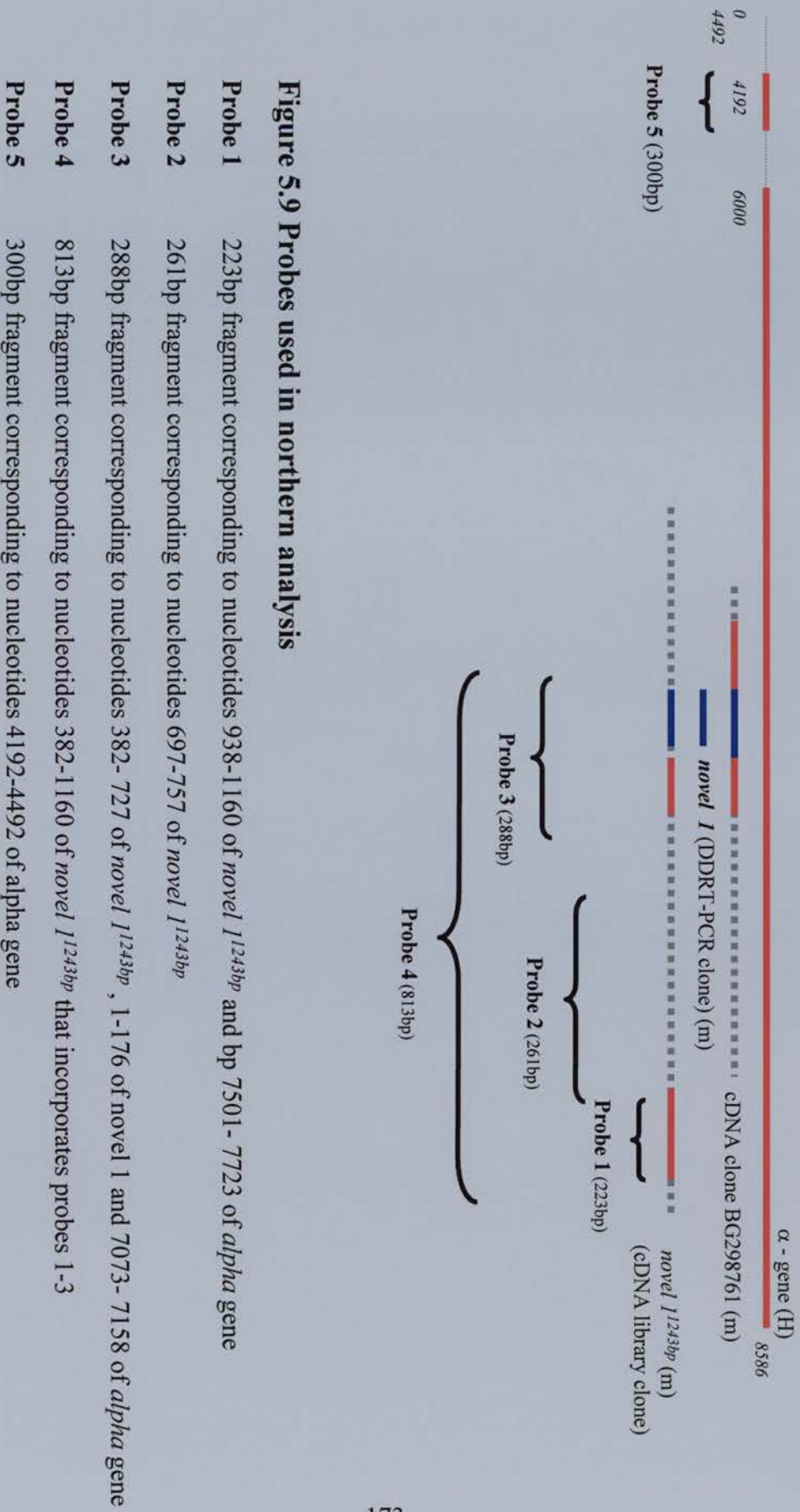


Figure 5.9 Probes used in northern analysis

- Probe 1** 223bp fragment corresponding to nucleotides 938-1160 of *novel 1*^{1243bp} and bp 7501-7723 of *alpha* gene
- Probe 2** 261bp fragment corresponding to nucleotides 697-757 of *novel 1*^{1243bp}
- Probe 3** 288bp fragment corresponding to nucleotides 382-727 of *novel 1*^{1243bp}, 1-176 of *novel 1* and 7073-7158 of *alpha* gene
- Probe 4** 813bp fragment corresponding to nucleotides 382-1160 of *novel 1*^{1243bp} that incorporates probes 1-3
- Probe 5** 300bp fragment corresponding to nucleotides 4192-4492 of *alpha* gene

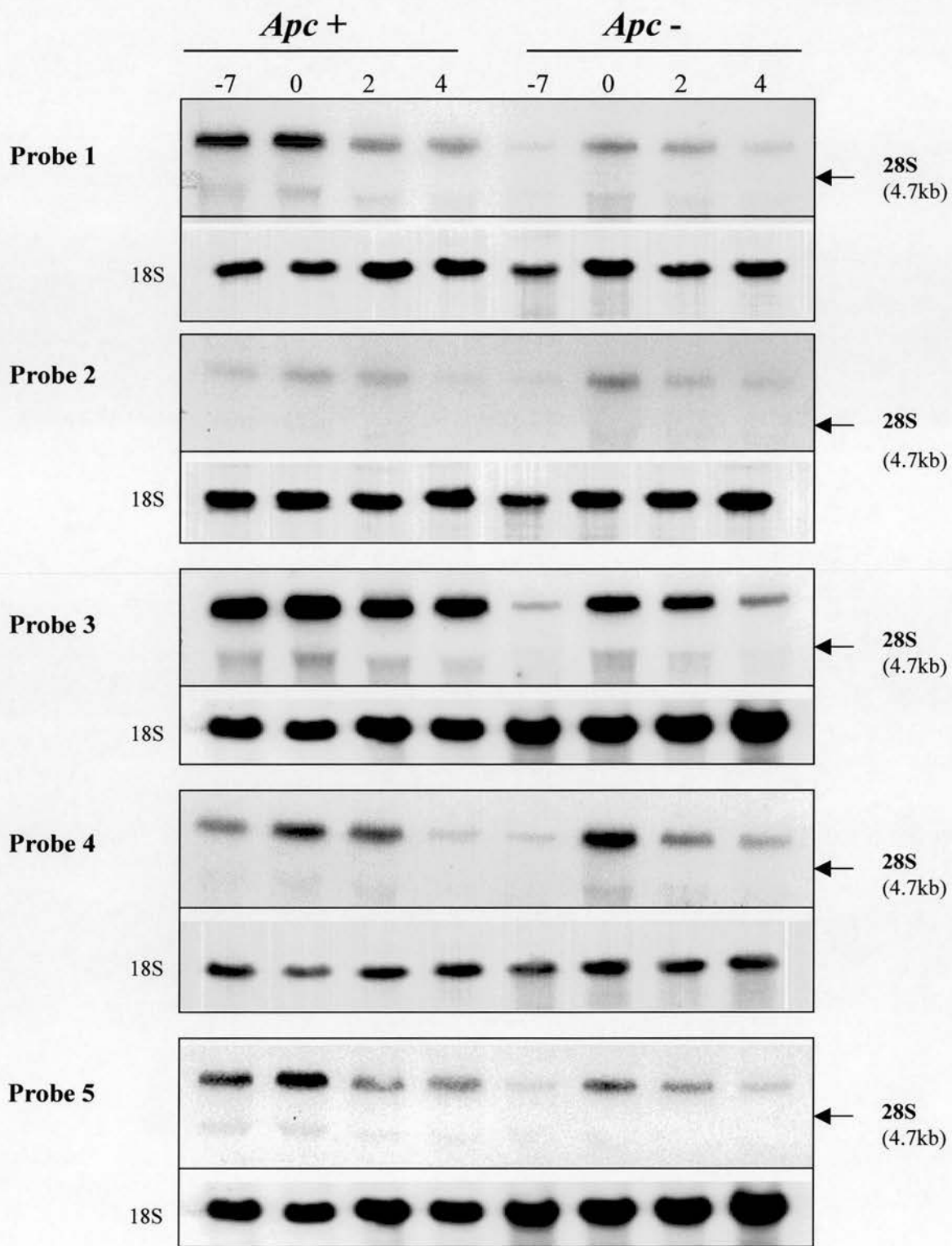


Figure 5.10 Northern analysis to identify if *novel 1* cDNA and *alpha* gene represent the same gene Probes 1-4 were generated by PCR using specific primers to *novel 1*^{1243bp} cDNA, and probe 5 was generated by PCR using specific primers against *alpha* gene. Blots were stripped and re-probed with an 18S rDNA probe to allow normalisation for loading variations.

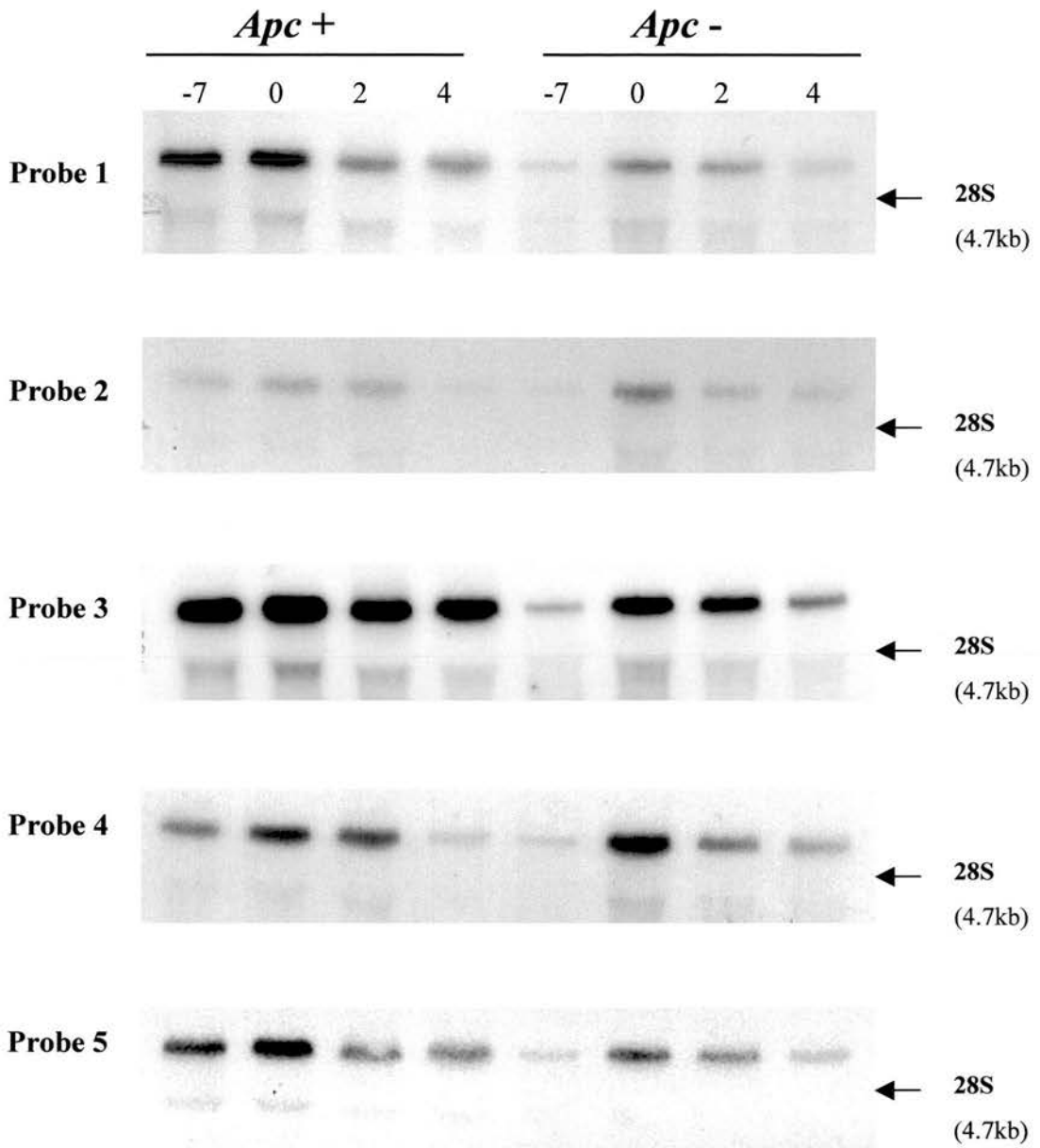


Figure 5.11 Northern analysis to identify if *novel 1* cDNA and *alpha* gene represent the same gene Northern results as for Figure 5.10 but without the loading controls so as to allow direct comparison of the patterns of hybridisation for each probe. All probes hybridised to a transcript of the same size and produced similar patterns of hybridisation.

Southern analysis was performed on mouse genomic DNA digested with 9 different restriction enzymes (*BamHI*, *EcoRI*, *HindIII*, *NcoI*, *PstI*, *PvuII*, *ScaI*, *StuI* and *XbaI*). Digested DNA was electrophoresed on a 0.8% agarose gel, blotted onto a nylon membrane, and incubated overnight with one of three radiolabelled probes (cDNA clone BG298761, *novel 1* or probe 4) (Figure 5.12). There were similarities between blots labelled with all three probes, for example consistently one *HindIII* band, one *XbaI* band, and one *NcoI* band were observed on all three autoradiographs. Significantly, the pattern of hybridisation between the DDRT-PCR probe (*novel 1*) and probe 4 (*novel 1*^{1243bp}) were identical except for the *PstI*-digested DNA which displays an additional band when labelled with probe 4, reflecting the longer length of probe 4. The results of Southern analysis argue towards the existence of only one gene.

5.3.2.2 *Novel 1* Discussion

Mouse mammary gland cDNA library screening, using *Novel 1* (176bp) as a probe, identified a longer length positive clone of 1217bp termed *novel 1*^{1243bp}. Following BlastN search of the non-redundant nucleic acid databases it was discovered that *novel 1*^{1243bp} was 100% identical to the entire 181bp of the *Mus musculus* clone MBI-32 miscellaneous RNA. As mentioned in section 4.3.4, *Mus musculus* clone MBI-32 represents a novel, small, non-messenger RNA that does not exhibit any sequence or structural motifs that would make it possible to assign a genomic location or a specific function to this RNA. Thus, it was hypothesised that *clone MBI-32* represents a degradation product of an unknown human RNA (Huttenhofer *et al.*, 2001). Additionally, *novel 1*^{1243bp} cDNA matched the *Homo sapiens alpha* gene sequence in two regions, the first of which was 231bp in length and 85% identical to *alpha* gene and the second region was 173bp long and 87% identical. Despite the name, *alpha* gene represents a transcript of unknown function. *Alpha* gene was identified during the construction of a transcript map for the 2.8-Mb region containing the multiple endocrine neoplasia type I (MEN1) locus (Guru *et al.*, 1997). (MEN1 is an inherited cancer syndrome in which affected individuals develop multiple parathyroid,

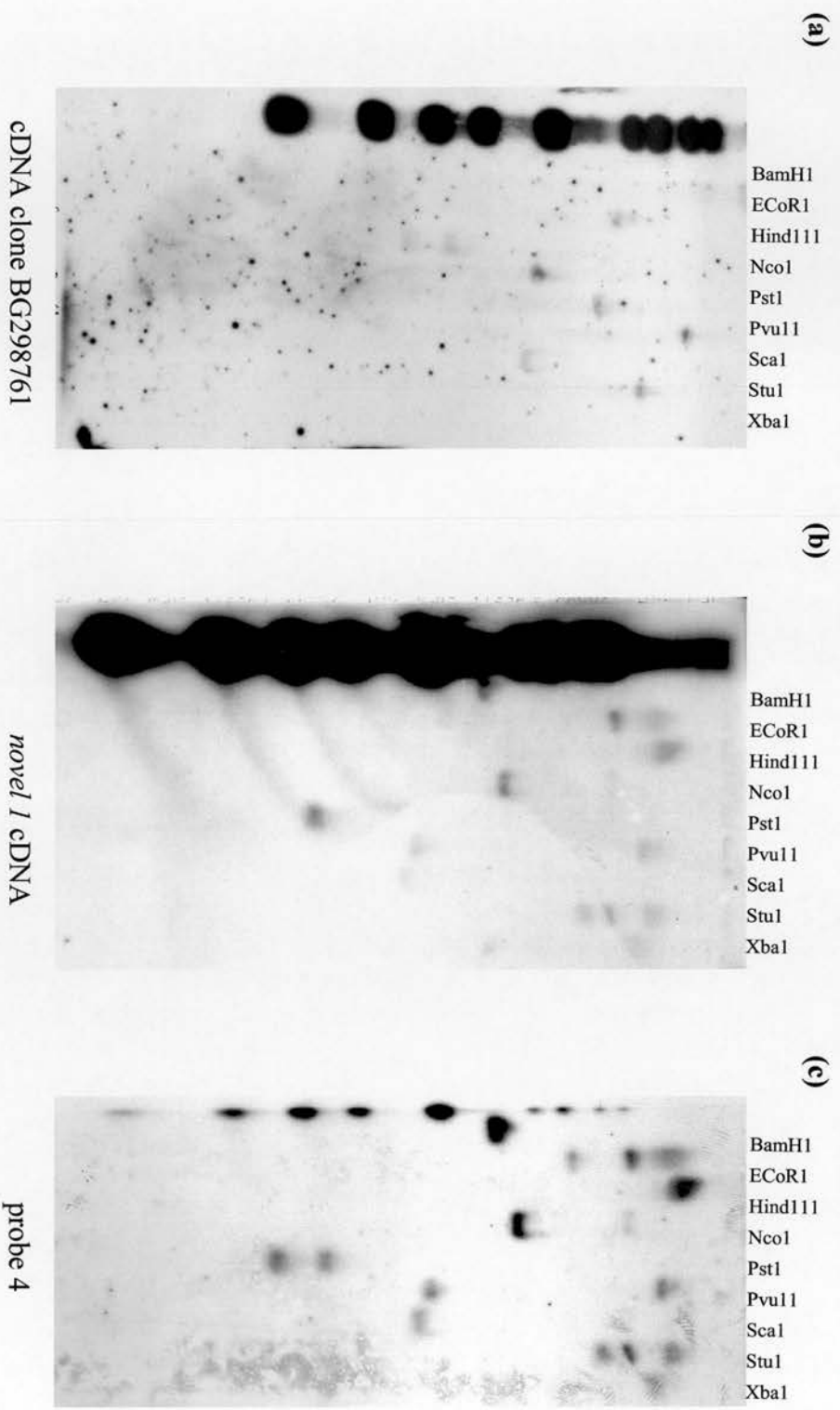


Figure 5.12 Southern analysis to determine if the novel 1 cDNA probe hybridises to more than one gene
 Mouse genomic DNA was digested with nine different restriction enzymes, digested DNA was electrophoresed on a 0.8% agarose, gel blotted onto a nylon membrane, and incubated overnight with one of three radiolabelled probes (a) cDNA clone BG298761 (b) novel 1 cDNA (c) probe 4.

pancreatic, and pituitary tumours. The *MEN1* gene is tightly linked to the PYGM (muscle glycogen phosphorylase) locus on human chromosome 11q13 and linkage analysis has placed the *MEN1* gene within a 2-Mb interval of this locus (Larsson *et al.*, 1988). To aid in the cloning of the *MEN1* gene a 2.8-Mb clone contig, from which 33 transcripts are predicted, was generated (Guru *et al.*, 1997). *Alpha* gene was identified as one of twelve transcripts of unknown function that mapped to the contig and each was named with sequential Greek letters (Guru *et al.*, 1997). Although *novel I*^{1243bp} has two sections of significant homology with *alpha* gene, the DDRT-PCR clone (*novel 1*) had no sequence similarity to *alpha* gene, thus it was unclear whether *novel 1* represented a fragment of *alpha* gene. Northern analysis using four different probes derived from *novel I*^{1243bp} and one probe derived from *alpha* gene, revealed identical patterns of hybridisation to a transcript of identical size, thus it remained likely that *novel 1* represented a fragment of *alpha* gene. Southern analysis was used to determine if there was more than one *alpha* gene family member as it was possible that the probes were hybridising to different members of the same gene family. However these results argued against the presence of a second gene. Finally in chapter 4 it was observed that northern analysis using the *novel 1* DDRT-PCR fragment did not confirm the DDRT-PCR expression pattern expected, revealing instead a contradictory differential expression pattern that appears to be specifically upregulated in mutant (*cre*⁺ *Apc*^{580S/580S}) mouse mammary glands (Figure 4.16). Two reasons why this may have occurred were detailed in chapter 4 (either the existence of an alternatively spliced family member which appeared identical in size by northern analysis and masked the differential expression pattern expected or a different member of the same gene family was being detected). As mentioned above, the results of Southern analysis argue against there being two genes present, thus it remains possible that the *novel 1* DDRT-PCR fragment hybridised to an alternatively spliced transcript.

The identification of a mouse homologue of *alpha* gene has not yet been reported, and it remains possible that the novel gene, *novel 1*, identified in this thesis represents this gene. Thus areas of sequence divergence could be explained due to species difference. Unfortunately there is no published information on the expression or

functions of human *alpha* gene and consequently speculations as to its role in the mouse mammary gland cannot be made.

5.3.2.3 Characterisation of transcript '*Novel 2*'

A BlastN search of the non-redundant nucleic acid databases revealed that *novel 2* cDNA (436bp) had a 228bp region 99% identical to positions 19006 – 19233 of *Mus musculus chromosome 15* clone RP24-116K14 (section 4.3.5). When *novel 2* cDNA sequence was subjected to computer-assisted homology search of the EST databases, 172bp of this same region was found to be 98% identical to the *Mus musculus* cDNA clone with GenBank accession no. BE916654 (Figure 5.13). The cDNA clone (BE916654) had originally been isolated from a virgin mouse mammary cDNA library generated from a tumour biopsy sample. This EST clone was obtained from the MRC UK HGMP Resource centre and sequencing added 326bp to the known sequence of 617bp. BlastN search of this cDNA clone (BE916654, 943bp) identified a region of 587bp that was 97% identical to positions 19040 – 19626 of *Mus musculus chromosome 15* clone RP24-116K14 (Figure 5.14).

Novel 2 was then used to probe the mouse mammary gland day 10 lactation cDNA library and following a primary screen only 2 positive plaques were identified. In order to achieve single homogenous clones, these were each plated out and subjected to a secondary screen, which unfortunately failed to identify any positive plaques. A PCR approach was used to confirm whether the mouse mammary gland cDNA library contained clones with homology to *novel 2*. PCR of an aliquot of the cDNA library with primers against the *novel 2* cDNA sequence and the cDNA clone (BE916654) produced PCR products of the expected size (Figure 5.15). This result established that clones with *novel 2* identical sequence were present in the mouse mammary gland cDNA library. However, due to the failure of the cDNA library screen to isolate any of these *novel 2* identical clones a different approach was undertaken. It was anticipated that by performing PCR reactions on an aliquot of the cDNA library with one primer against the vector arm and the other against the *novel*

(a) Novel 2 (436bp)

GAATTCTTTTTTTTTTTTTTGCAGACATATACTCACCAGTGGGTCTACCTA
TAATTAAGTTTCATGTATTGGTAAATAAGACTAGATTTAAATCTATGAAA
GAATAGTAAGAGATGAAATAAATCCAGTAGAGTCTGACATGTTTGATTC
AAAATGTTAGTCTTAATCACACAAGCTTCTGATTGCTAACAATAAAATCC
TGTTCTTTCTCTTTCTCGTCCTGTGAAATGAAAGCCTTTGTGGAAAAAAAA
AAAAAGAATTC

(b)

```
Sequences producing significant alignments:                               Score      E
                                                                           (bits) Value

gi|10417510|gb|BE916654.1|BE916654  601667260F1 NCI_CGAP_Mam.. 301      2e-79
```

```
>gi|10417510|gb|BE916654.1|BE916654  601667260F1 NCI_CGAP_Mam1
Mus musculus cDNA clone IMAGE:3967167 5'.
```

```
Length = 617
Score = 301 bits (152), Expect = 2e-79
Identities = 169/172 (98%), Gaps = 2/172 (1%)
```

```
Query: 21  gcagacatattactcaccagtgggtctacctataaattaaagtttcatgtattggtaaata 80
          |||
Sbjct: 170 gcagacatattactcaccagtgggtctacctataaattaaagtttcatgtattggtaaata 111
```

```
Query: 81  agactagatttaaactctatgaaagaatagtaagagatgaaataaattcccagtagagtct 140
          |||
Sbjct: 110 agactacatttaaactctatgaaagaatagtaagagatgaaataaattcccagtagagtct 51
```

```
Query: 141 gacatgtttgattcaaaatgtagtcttaatacacacaagcttctgattgcta 192
          |||
Sbjct: 50  gacatgtttgattc-aaatgtagtcttaatacacac-agcttctgattgcta 1
```

Figure 5.13 BlastN comparison of novel 2 cDNA sequence against the EST databases

(a) Novel 2 cDNA sequence. **(b)** Computer assisted homology search of the EST databases (BlastN) revealed that novel 2 cDNA was 98% identical to positions 1-170 of the *Mus musculus* cDNA clone with GenBank accession number BE916654.

(a) CDNA clone BE916654 (943bp)

```
GNNNNCGNGNTNNTGAANCGTGGACANAAAGCGGCTGGTACCGGTCGGAATTCCC GGGATA
TCGTCGACCCACGCGTCCGAAAAGAACAGGATTTAATTGTTAGCAATNAGAAGCTTGTGTGA
TTAAGACTAACATTTTGAATCAAACATGTCAGACTCTACTGGGAATTTATTTTCATCTCTACTA
TTCTTTTCATAGATTTAAATGTAGTCTTATTTACCAATACATGAAACTTTAATTATAGGTAGACC
CACTGGTGAGTAATATGTCTGCAAAAAGTAATTTCTTATTGGAGTTAAGGATTTCCATGTGATT
TAAATAGACAGCTTCCTTCTTTTATATTCTTGCTTGTGTTTGGAAATACCTAAAATCTTAACTATC
CTTAGGCCTCCAAGTCAATCTTTGATGTATAAAAATGGACACTCTTGAGAACTAACATATTTTG
GTGAGGATTGCTATGTTAAGTTTCTATTAATATGAATGATTCTTAACATTAATGCAAGTTATT
TAACCACCAATGNTCATATTAGTCAATGNTTAGTTCAACGATTAAGCATTAGGTATTAGAGCA
GAACTCANAGAACGGNATGTAGAAAGNCTGGNTGGTGGGCAGCTACCTTATTGNAGTGAGCC
TTTCTGGAGGAGAAAAGGAGAGACTGAGTAAGNTGGGGAGGNAGAGAACTNTTTAAGGAGG
GGNGGTGGAGAAGCAGACTGGACTTAAAGAGTNTAATGTNCCAGTCTAACACCCAGAGAAT
GGTTATTTGGACATTACTTTNGAACTTGCTGCTGGNNCCACACTGGGGGACTGAATGNACNGA
ACTACCCCTGTNCTTCCGAAANCCGGAATTNTCTGTGCTGTAACNNNACCAAGCGGCATGAC
CCAGTAAGGAGGGGGGGGGGGGNNNNNNNNNNNNNNNNNNNNNNNNNNNNNGGGGGNNNTNN
```

(b)

```
Sequences producing significant alignments:                               Score   E
                                                                           (bits) Value

gi|22748533|gb|AC112158.4| Mus musculus chromosome 15 clone... 1068   0.0
gi|13124448|gb|AF172398.2|AF172398 Homo sapiens junctional ...   98    3e-17

>gi|22748533|gb|AC112158.4| Mus musculus chromosome 15 clone
RP24-116K14, complete sequence
Length = 175171
Score = 1068 bits (539), Expect = 0.0
Identities = 575/587 (97%), Gaps = 2/587 (0%)

Query: 82      aaaagaacaggattttaattgtagcaatnagaagcttgtgtgattaagactaacatttt 141
              |||
Sbjct: 19040  aaaagaacaggattttaattgtagcaatcagaagcttgtgtgattaagactaacatttt 19099

Query: 142     gaatcaaacatgtcagactctactgggaatttatttcatctcttactattcctttcataga 201
              |||
Sbjct: 19100  gaatcaaacatgtcagactctactgggaatttatttcatctcttactattcctttcataga 19159

Query: 202     tttaaatgtagtcttatttaccatacatgaaactttaattataggtagaccactggtg 261.....
              |||
Sbjct: 19160  tttaaatgtagtcttatttaccatacatgaaactttaattataggtagaccactggtg 19219...

.....Query: 622  attgnagtg-agcctttctgga-ggagaaaaggagagactgagtaag 666
              ||| ||| ||| ||| ||| |||
.....Sbjct: 19580 attgcagtgaagccttctctggaggagaaaaggagagactgagtaag 19626
```

Figure 5.14 BlastN comparison of mouse cDNA clone BE916654 against non-redundant nucleic acid databases

(a) Mouse cDNA clone BE916654 sequence. (b) Computer assisted homology search of the non-redundant nucleic acid databases (BlastN) revealed that the cDNA clone BE916654 was 97%% identical across 587bpto the *Mus musculus chromosome 15* clone.



Figure 5.15 PCR based identification of *Novel 2* identical sequence in the mouse mammary gland cDNA library

(a) Schematic representation of *novel 2* cDNA and the mouse mammary cDNA clone BE916654 detailing the 170bp region of homology. Primers used to PCR the mouse mammary gland cDNA library are represented by coloured arrows. (b) Agarose gel electrophoresis of the primary PCR product resulting from the *novel 2* Fwd and *novel 2* Rev primer combination. (c) Agarose gel electrophoresis of the nested PCR products resulting from the *novel 2* Fwd and *novel 2* nested Rev primer combination and the *novel 2* nested Fwd and *novel 2* Rev primer combination.

2 cDNA or the cDNA clone (BE916654), the PCR products would represent full-length *novel 2* clones. The mouse mammary gland cDNA library is in the Lambda Zap express vector and primers were designed to the vector arms on either side of the multiple cloning site (Figure 5.16a). PCR reactions were performed in both directions, as the orientation of the *novel 2* cDNA within the cDNA library was not known and the results show only the primer combinations that generated PCR products (Figure 5.16b). DNA was recovered from four PCR products (ranging in size from 600-1000bp) by gel purification, but only one (clone 2.1) was successfully cloned into the pGEM[®]-T Easy vector. Sequencing of clone 2.1 (659bp), followed by computer-assisted homology search (BlastN) of the non-redundant nucleic acid databases revealed that the first 20bp were identical to positions 19561-19580 of the mouse chromosome 15 clone. However, this sequence represented the primer (EST Fwd) used to PCR clone 2.1 out of the mouse mammary cDNA library (Figure 5.17). Thus BlastN failed to identify any sequences of significant homology.

5.3.2.4 *Novel 2* Discussion

Novel 2 (436bp), the DDRT-PCR cDNA isolated as described in chapter 4, has a 228bp region 99% identical to positions 19006 – 19233 of *Mus musculus chromosome 15* clone. Additionally, when *novel 2* cDNA sequence was subjected to BlastN of the EST databases, a cDNA clone (BE916654) which was 98% identical was isolated and when sequenced this cDNA clone was also identical to *Mus musculus chromosome 15* clone (97% identical over a 587bp region). Unfortunately, *novel 2* screening of the mouse mammary gland cDNA library failed to identify any *novel 2* positive plaques. One reason for this failure was the possibility that this mouse mammary gland cDNA library, which was specific for lactation day 10, did not contain any *novel 2* homologous clones. Nevertheless, PCR reactions using the mouse mammary gland cDNA library as a template and with primers specific for the *novel 2* cDNA and the cDNA clone BE916654, established that clones with *novel 2* identical sequence were present in the mouse mammary gland cDNA library. However, a subsequent PCR method of isolating these clones had a very low success

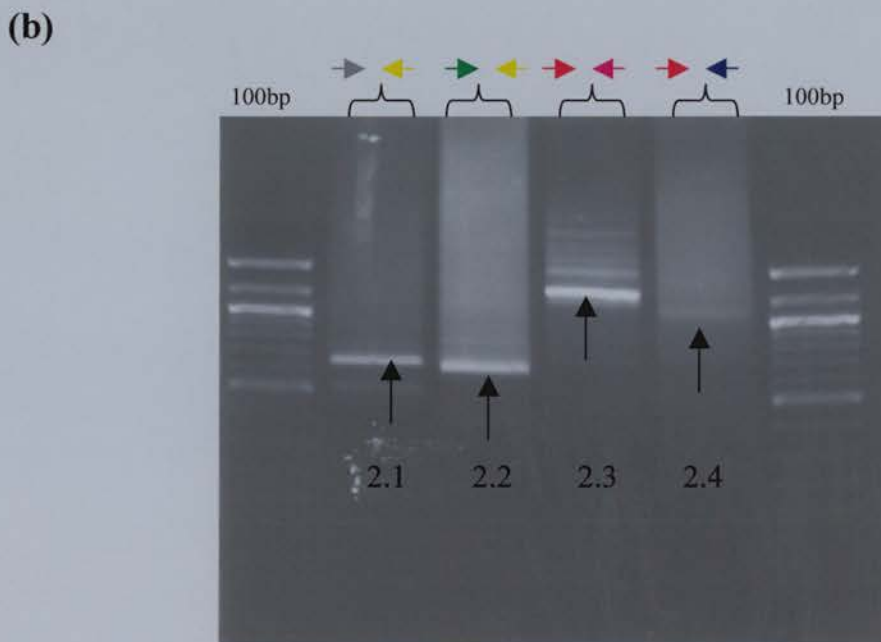
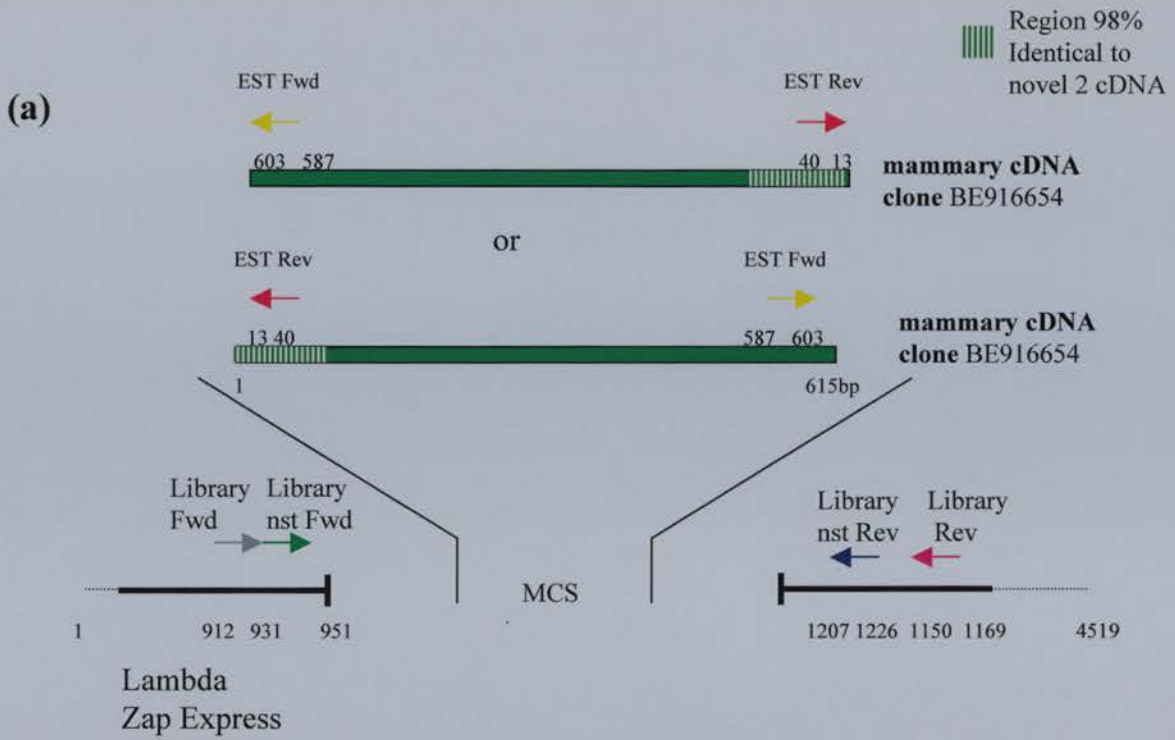


Figure 5.16 Isolation of full-length clones with homology to *novel 2* cDNA from the mouse mammary gland cDNA library

(a) Schematic representation of the Lambda Zap Express vector and the primers (represented by coloured arrows) used to PCR full length clones out of the library. The cDNA clone BE916654 is shown in two orientations. (b) Agarose gel electrophoresis detailing the PCR reactions that produced products. The arrows indicate the bands from which DNA was recovered and these were numbered 2.1 – 2.4.

(a) CDNA library clone 2.1 (659bp)

```
GTTGGTGGGCAGCTACCTTAATGCCCAAACCAACGCCGCCGCCAGTCCGGCAGA
CTTTGCGGCTGATCCTCGCTTCCCGGATGATGTTGCCTTACCTTCAATGTCAGCCATCC
TGCTGCGCAGACTGCCTTCATCCTTAGCATCAGGTTCCGGCAGGCTTATCGGAGGGCGC
GGTTGCGCCTTTACCTTCGATTTCCGGCCATTCTGCTGCGCAGATCGTTGCTTTCATCGG
TCATTGGAAAAGCTCCACAATAACAGATTTCTGATTGCCGAGGCGCAGTGGCCATTGC
TGCGATGTGCCGCTGACGCGAACAATCCGGCCATCCATGCTTTGAGAGTTGACGCTGC
GCTCACGCCCGCCGTCACCTTGAAGACAGCGGGAACGGGGCAATTTTCGCGGAATCT
GAAATACGTGAATGCACCATCATCCAGATTGCGGTTGGGGTGATTTTCGCTGCTGGCG
CTGACGCCATAGTTGGTATTCGCGGCTGTCCGAACCGGCGTCGTCCCGGCTTGTTGAC
GTGCCCGTGCAGGATAGGAGAAGCGGACAACATAGAACGGGGTGGCAGTCTCTTTGA
CGTGAAATAGTAACTCCGCCGATCCGTGTAGACCGTACGTTGGTTTCAACATCACT
GGCCGTCGTTTTACAAGGGC
```

(b)

```
Sequences producing significant alignments:                               Score      E
                                                                           (bits) Value

gi|22748533|gb|AC112158.4| Mus musculus chromosome 15 clone...      40      0.006

>gi|22748533|gb|AC112158.4| Mus musculus chromosome 15 clone
RP24-116K14, complete sequence
Length = 175171

Score = 40.1 bits (20), Expect = 0.006
Identities = 20/20 (100%)

Query: 1      gttggtgggcagctacctta 20
             |||
Sbjct: 19561 gttggtgggcagctacctta 19580
```

Figure 5.17 BlastN comparison of cDNA library clone 2.1 against non-redundant nucleic acid databases

(a) Mouse cDNA library clone 2.1 sequence. **(b)** Computer assisted homology search of the non-redundant nucleic acid databases (BlastN) revealed that the first 20bp of this cDNA clone 2.1 were 100% identical to positions 19561 – 19580 of the *mus musculus* chromosome 15 clone

rate. There are several possible reasons for this, firstly, the mouse mammary gland cDNA library represented a very 'dirty' DNA template (i.e. impurities may be present (due to the nature of the sample) which inhibit PCR) and even though the PCR reactions used a *Taq* polymerase with increased sensitivity (TITANIUM™ *Taq*), it remains possible that the level of primers annealing was not at a maximum. Additionally, DNA isolated from PCR products that were generated was of very low concentration resulting in poor ligation efficiency into the pGEM®-T Easy vector. One clone (2.1) was successfully isolated from the cDNA library but subsequent BlastN of the non-redundant nucleic acid databases failed to identify any sequences of significant homology. Thus *novel 2* cDNA represents a small section of the mouse chromosome 15 DNA clone (1-175171bp) and may represent a novel gene.

5.3.2.5 Characterisation of transcript 'Novel 3'

Sequencing and subsequent computer-assisted homology search (BlastN) of the non-redundant nucleic acid databases revealed that *novel 3* cDNA sequence (187bp) was 94% identical to positions 752 – 901 of *H.sapiens* mRNA for the 3'UTR of an unknown protein (section 4.2.3.6). In an attempt to acquire a *novel 3* cDNA sequence longer than 187bp, *novel 3* cDNA was used to probe the mouse mammary gland day 10 lactation cDNA library. Following a primary screen only 2 positive plaques were identified. In order to achieve single homogenous clones, these were each plated out and subjected to a secondary screen, which unfortunately failed to identify any positive plaques. Thus, as for *novel 2* cDNA, the library screen failed and so as to ensure that the mouse mammary gland cDNA library contained clones with homology to *novel 3*, PCR was used. Primers were designed against the *novel 3* cDNA and the human 3'UTR sequence for an unknown protein (Figure 5.18a). The primary PCR reaction, using the mouse mammary gland cDNA library as a template, and with primers specific to the human 3'UTR (spanning the region homologous to *novel 3*) produced a product of the expected size (Figure 5.18b). However when these primary PCR products were used in a nested PCR reaction the results were less definitive, showing several bands of varying intensity (Figure 5.18c). Finally, a probe

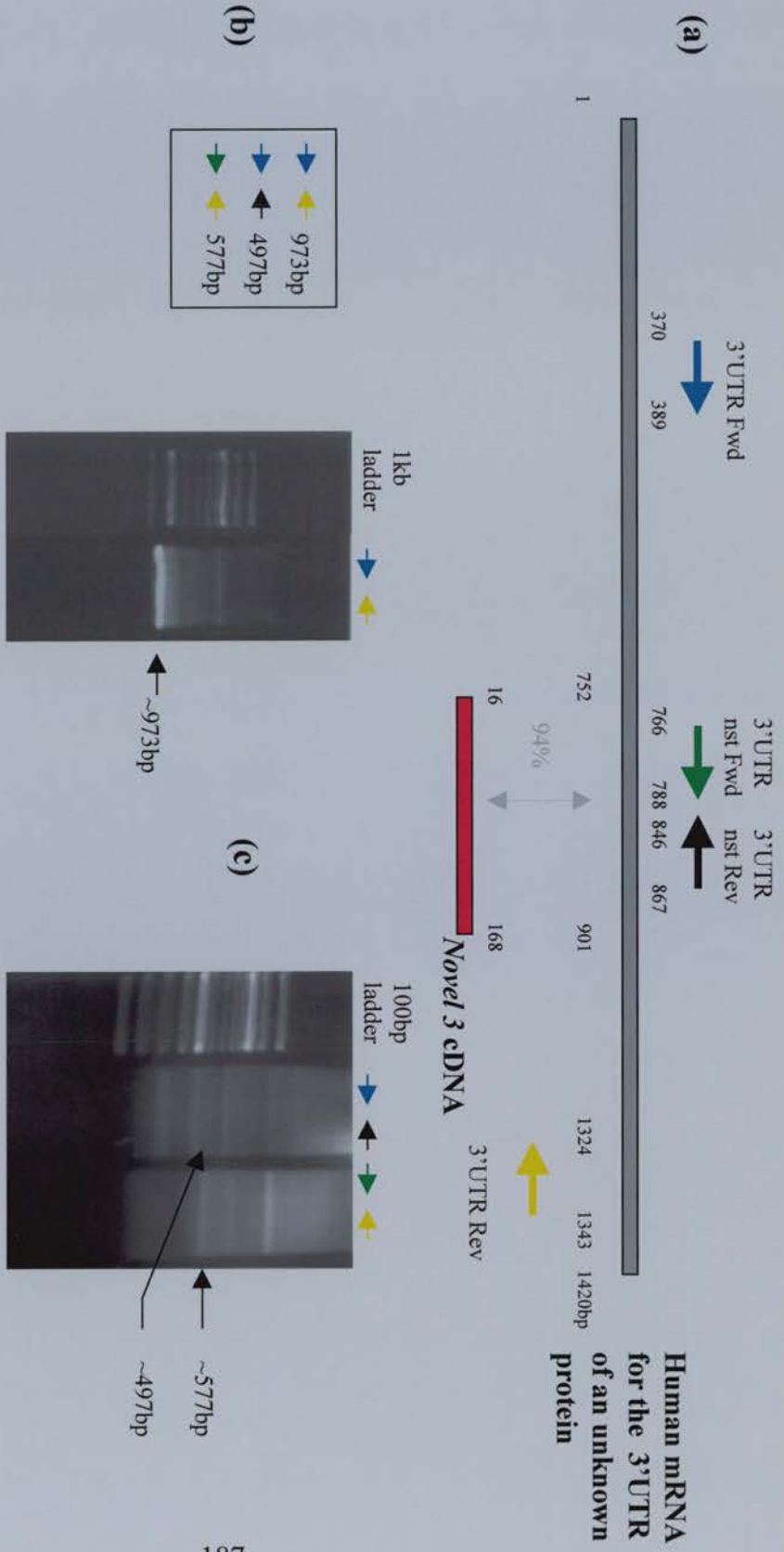


Figure 5.18 PCR based identification of *Novel 3* identical sequence in the mouse mammary gland cDNA library

(a) Schematic representation of *novel 3* cDNA and the human mRNA for the 3'UTR of an unknown protein detailing the 153bp region of homology. Primers used to PCR the mouse mammary gland cDNA library are represented by coloured arrows. **(b)** Agarose gel electrophoresis of the primary PCR product resulting from the 3'UTR Fwd and 3'UTR Rev primer combination. **(c)** Agarose gel electrophoresis of the nested PCR products resulting from the 3'UTR Fwd and 3'UTR nst Rev primer combination and the 3'UTR nst Fwd and 3'UTR Rev primer combination.

designed against the human 3'UTR of an unknown protein was hybridised to northern blotted mammary gland RNA from control ($cre^+ Apc^{+/580S}$ and $cre^- Apc^{580S/580S}$) and *Apc* deleted ($cre^+ Apc^{580S/580S}$) mouse mammary glands. This probe represented the primary PCR product of 976bp, equivalent to positions 370 to 1343 of the human 3'UTR of an unknown protein. It was anticipated that if the DDRT-PCR expression pattern was replicated it would indicate that *novel 3* cDNA represented a fragment of the human 3'UTR of an unknown protein. However, northern analysis revealed that this probe did not hybridise to any specific transcript (data not shown).

5.3.2.6 *Novel 3* Discussion

Novel 3 cDNA (186bp) was identified as a transcript differentially expressed during lactation in *Apc* deleted ($cre^+ Apc^{580S/580S}$) mouse mammary glands (Figure 4.20). However, despite exhaustive attempts neither 'cold' Southern analysis or northern blotting confirmed this expression pattern. This could be due to the decreased ability to radioactively label DNA fragments shorter than 200bp or alternatively *novel 3* cDNA may represent a false positive. These two reasons further explain why the cDNA library screen, using *novel 3*, failed to identify *novel 3* positive plaques. In a final attempt to obtain additional sequence information for the *novel 3* cDNA, a PCR based approach was used. Although the primary PCR reaction identified a fragment of the expected size, when this was used in a nested PCR reaction with primers specific for *novel 3* cDNA sequence the results were not definitive. Thus it was unclear whether the cDNA library contained clones with *novel 3* identical sequences. Finally, northern analysis using a 976bp probe (100% identical to positions 370 to 1343 of the human 3'UTR of an unknown protein, and 94% identical to positions 16 to 168 of *novel 3* cDNA) revealed high levels of background hybridisation, which after high stringency washing failed to expose any transcript hybridisation. Thus, despite exhaustive attempts to confirm that *novel 3* cDNA represents a real differentially expressed transcript in *Apc* deleted ($cre^+ Apc^{580S/580S}$) mouse mammary

glands, these results indicate that *novel 3* cDNA most likely represents a false positive produced by DDRT-PCR.

5.4 Summary

This chapter aimed to further investigate the roles of the six genes (*casein delta*, $\alpha 1$ type IV collagen, *Gm2a* and three presumed novel genes), identified by DDRT-PCR, in the mouse mammary gland. It was anticipated that this information may help to understand the relationship between mammary gland metaplasia and *Apc* deficiency.

$\alpha 1$ type IV collagen is a known component of mammary gland basement membrane and its upregulation was localised to the metaplastic lesions that arise following *Apc* loss. This expression pattern is indicative of a dysregulated basement membrane within these lesions. Although it is unclear how *Apc* deletion in $cre^+ Apc^{580S/580S}$ mouse mammary glands leads to an upregulation of $\alpha 1$ type IV collagen expression, the spatial and temporal expression of $\alpha 1$ type IV collagen is consistent with a role in metaplastic lesion formation.

Despite exhaustive attempts to identify the novel genes only one had sequence homology with a known gene. *Novel 1* may represent the mouse homologue of the human *alpha* gene. However, there is no published information on the expression or functions of human *alpha* gene and consequently speculations as to its role in the mouse mammary gland cannot be made. Thus it remains possible that the functions of the novel genes (*novel 1* and *novel 2*) may be related to metaplasia formation.

6 A preliminary characterisation of two *Wnt* genes (*Wnt8b* & *Wnt10a*) identified from mouse mammary gland cDNA

6.1 Introduction

The previous chapters concentrated on the analysis of the functions of the *Apc* gene in mouse mammary secretory epithelium using a conditional knockout mouse (cre^+ *Apc*^{580S/580S}). In a separate but related study, a biochemical and functional analysis of two *Wnt* genes identified from mouse mammary gland cDNA was initiated. *Wnt* genes and the *Wnt* signalling pathway are described in detail in section 1.3. Briefly, *Wnt* genes constitute one of the major families of developmentally significant signalling molecules with a number of actions in a wide variety of organisms, including defining segment polarity in *Drosophila* and controlling early lineage and gut development in *C. elegans*. (Nusslein-Volhard and Roth, 1989; McMahon and Moon, 1989; McMahon and Moon, 1989; Nusslein-Volhard, 1991; Han, 1997). The mouse *Wnt* gene family comprises at least 18 members, each of which encodes a secretory glycoprotein of between 350 and 380 amino acids in length and containing a characteristically spaced pattern of cysteine residues. Both spontaneous mutations and gene knockout studies have demonstrated the importance of a number of these *Wnt* genes in normal mouse development (reviewed by Cadigan and Nusse 1997). Specifically, *Wnt1* knockout mice have defects in mid- and hindbrain development (McMahon and Bradley, 1990; Thomas *et al.*, 1991), *Wnt2* mutants die perinatally owing to placental defects (Monkley, 1996) and *Wnt4* mutant mice fail to form kidneys (Stark *et al.*, 1994) and have defects in mammary gland morphogenesis during pregnancy (Briskin *et al.*, 2000). *Wnt* genes have been subdivided into two distinct classes, the *Wnt1* class, including: *Wnt1/3/3a/8*, and the *Wnt5a* class, including *Wnt4/5a* and *Wnt6* (see Table 6.1.1). This classification is based on two assays of *Wnt* gene function, the first of which uses mammary epithelial cells and the second requiring *Xenopus* embryos, both of which are discussed below.

Table 6.1.1 Wnt assays

Wnt genes have been subdivided into two distinct classes (*Wnt1* class and *Wnt5a* class) based on two assays of *Wnt* gene function, (1) the ability to induce morphological transformation and altered growth characteristics of mammary epithelial cell lines (C57 or RAC311C mammary epithelial cells) and (2) the overexpression of *Wnts* in *Xenopus* embryos through mRNA injection.

	<u><i>Wnt</i> Gene</u>	<u>Transformation of C57 or RAC mammary epithelial cells</u>	<u><i>Xenopus</i> axis duplication</u>
<u><i>Wnt1</i> class</u>	<i>Wnt1</i>	Yes (Brown <i>et al.</i> , 1986)	Yes (McMahon <i>et al.</i> , 1989)
	<i>Wnt3</i>	Yes (Shimizu <i>et al.</i> , 1997)	
	<i>Wnt3a</i>	Yes (Wong <i>et al.</i> , 1994)	Yes (Wolda <i>et al.</i> , 1993)
	<i>Wnt8</i>		Yes (Sokol <i>et al.</i> , 1991)
<u><i>Wnt5a</i> class</u>	<i>Wnt4</i>	No (Wong <i>et al.</i> , 1994)	No (Du <i>et al.</i> , 1995)
	<i>Wnt5a</i>	No (Wong <i>et al.</i> , 1994)	No (Moon <i>et al.</i> , 1993)
	<i>Wnt6</i>	No (Wong <i>et al.</i> , 1994)	

Wnt genes can be divided into three groups (highly transforming (*Wnt1/3/3a/7a/8*), transforming (*Wnt2/5b/7b*) and non-transforming (*Wnt4/5a/11*) depending on their ability to induce morphological transformation and altered growth characteristics of mammary epithelial cell lines, either C57 mammary epithelial cells (C57MG cells) or RAC311C mammary epithelial cells (Wong *et al.*, 1994; Rijsewijk *et al.*, 1987). C57MG cells, an epithelial cell line derived from normal mouse mammary tissue (Vaidya *et al.*, 1978), grow in a monolayer with a regular, cuboidal appearance at confluence. However, *Wnt1* expression causes the cells to become refractile and elongated, growing over other cells in a disorganised pattern. This transformation is considered partial (semi-transformation) because cells are unable to form tumours in syngeneic host animals (Brown *et al.*, 1986). In contrast, RAC311C mammary epithelial cells, derived from a mammary tumour that has lost its tumorigenic capacity, are fully transformed by *Wnt1* exhibiting morphological transformation *in vitro* and tumour formation *in vivo* (Rijsewijk *et al.*, 1987). In the mouse, a subset of *Wnt* genes are involved in the development of the mammary gland, *Wnt2*, *Wnt4*, *Wnt5a*, *Wnt5b*, *Wnt6*, *Wnt7b*, and *Wnt10b* (see section 1.2) (Weber-Hall *et al.*, 1994; Lane and Leder, 1997) and aberrant expression of those *Wnt* genes normally silent or expressed at low levels in this tissue induces mammary gland carcinoma. Accordingly, mouse *Wnt 1*, *Wnt 3* and *Wnt 10b* have been shown to function as mammary oncogenes during MMTV-insertional carcinogenesis (section 1.1.3)(Nusse and Varmus, 1982; Roelink *et al.*, 1990; Lane and Leder, 1997). Interestingly, the *Wnt* genes *Wnt4* and *Wnt5a*, which are normally expressed in the mammary gland, are incapable of inducing morphological transformation and deregulated growth of C57MG cells. In the case of *Wnt4*, this may be because its function in mammary gland development is well defined. *Wnt4* has an essential role in side branching during early pregnancy (Briskin *et al.*, 2000). Thus, transformation is not due to simply overexpressing a *Wnt* protein, but rather appears to depend on the interaction of specific *Wnt* protein with its specific Frizzled receptor, which in the case of *Wnts 4* and *5a* may not be present on the surface of C57MG cells (Wong *et al.*, 1994).

The second assay of *Wnt* gene function involves the overexpression of *Wnts* in *Xenopus* embryos through mRNA injection (Moon *et al.*, 1993a). Ectopic expression

of the *Wnt1* class in *Xenopus* embryos causes anterior duplication of the embryonic axis, whilst the *Wnt5a* class perturbs gastrulation but does not result in axial duplication (McMahon and Moon, 1989; Moon *et al.*, 1993b). Sokol *et al.*, (1991) propose that this axis duplication arises due to *Wnt1* induction of a new ectopic organiser (Spemann organiser). Thus one set of dorsal axial structures in the injected embryos is initially specified in the embryo, while *Wnt1* induces the other. However, there is no data concerning an endogenous *Wnt* in induction of the primary axis as no known *Wnt* is expressed at the time when mesoderm induction begins (early blastula stages). McMahon and Moon, (1989) hypothesise that the *Wnt1* class of proteins are acting on a receptor for a yet unidentified member of the *Wnt* family, which is normally active in dorsal axis formation *in vivo*. Consistent with this model is the observation that *Wnt5a* induced axis duplication and an ectopic Spemann organiser when coexpressed with the human *frizzled5* *Wnt* receptor. Thus it is possible that the *Wnt5a* class of *Wnt* genes are non-duplicating due to a lack of *Wnt5a* receptors during axis formation (He *et al.*, 1997).

This chapter focuses on the biochemical and functional analysis of two *Wnt* genes originally identified in a PCR screen designed to amplify novel members of the *Wnt* gene family from 11-day lactating mouse mammary gland. Degenerate oligonucleotides, designed to correspond to the conserved amino acid motifs CKCHG [5'-GGGGCTGAGTG(CT)AA(AG)TG(CT)CA(CT)GG-3'] and FHWCC [5' -GGAATCTAGA(AG)CA(AG)CACCA(AG)TG(AG)AA-3'], resulted in the identification of fragments of two novel *Wnt* genes – *Wnt8b* and *Wnt10a*. Subsequently, full length *Wnt8b* sequence was compiled from a clone isolated from a mouse embryonic cDNA library screen and an EST sequence derived from a dbEST database search (Richardson *et al.*, 1999). *Wnt8b* is expressed in the developing forebrain of chicks, mice and humans (Hollyday *et al.*, 1995; Lako *et al.*, 1998; Richardson *et al.*, 1999). Full length *Wnt10a* cDNA was isolated from a rat brain cDNA library. *Wnt10a* is expressed in the murine adult pituitary, thymus, spleen and embryonic liver (Wang and Shackleford, 1996). *Wnt* proteins are secreted glycoproteins and during synthesis the primary translation product has an N-terminal hydrophobic signal peptide, which is cleaved by signal peptidase, the resulting

protein then being sequentially glycosylated at up to 4 sites. N-linked glycosylation, involving the attachment of carbohydrate groups to the side chain of the amino acid asparagines, is a common post-translational modification of secretory signal peptides, however site-directed mutagenesis has shown that in the case of *Wnt1* no single glycosylation is required for biological activity or secretion (Papkoff, *et al.*, 1987; Mason *et al.*, 1992). In this study, western analysis was used to identify the presence of *Wnt8b* and *Wnt10a* protein and their respective glycosylation status in stably transfected HEK293 (human embryonic kidney) cells. The functional assays described above (C57 mammary epithelial cell transformation and axis duplication in *Xenopus*) were then performed with the aim of classifying *Wnt8b* and *Wnt10a*. These experiments produced some interesting preliminary observations however shortage of time prevented a complete analysis.

6.2 Results

6.2.1 Biochemical analysis of *Wnt8b* and *Wnt10a*

In the absence of effective anti-*Wnt* antibodies, epitope tagged *Wnts* were generated. This involved cloning of the HA epitope tag (57bp sequence encoding an internal region of the influenza haemagglutinin antigen (Appendix E) into a pBluescript plasmid, and subsequent insertion of the *Wnt8b*, *Wnt10a*, or *Wnt1* (used as a positive control) cDNA sequences. Site directed mutagenesis was used to recombine the *Wnt* cDNA and HA sequences (Figure 6.1). The HA-tagged *Wnt* cDNAs were then cloned into the phosphoglycerate kinase (PGK) mammalian expression vector (pHPmPGKpS-BstX1(+Svori)) (a gift from Dr. I. Chambers, Centre for Genome Research, University of Edinburgh) which carries a hygromycin B antibiotic resistance gene and thus permits selection of stably transfected clones. These three epitope tagged *Wnt* cDNA expression vectors (PGK *Wnt1*-HA, PGK *Wnt8b*-HA, and PGK *Wnt10a*-HA (Appendix E)) were then stably transfected into HEK293 cells.

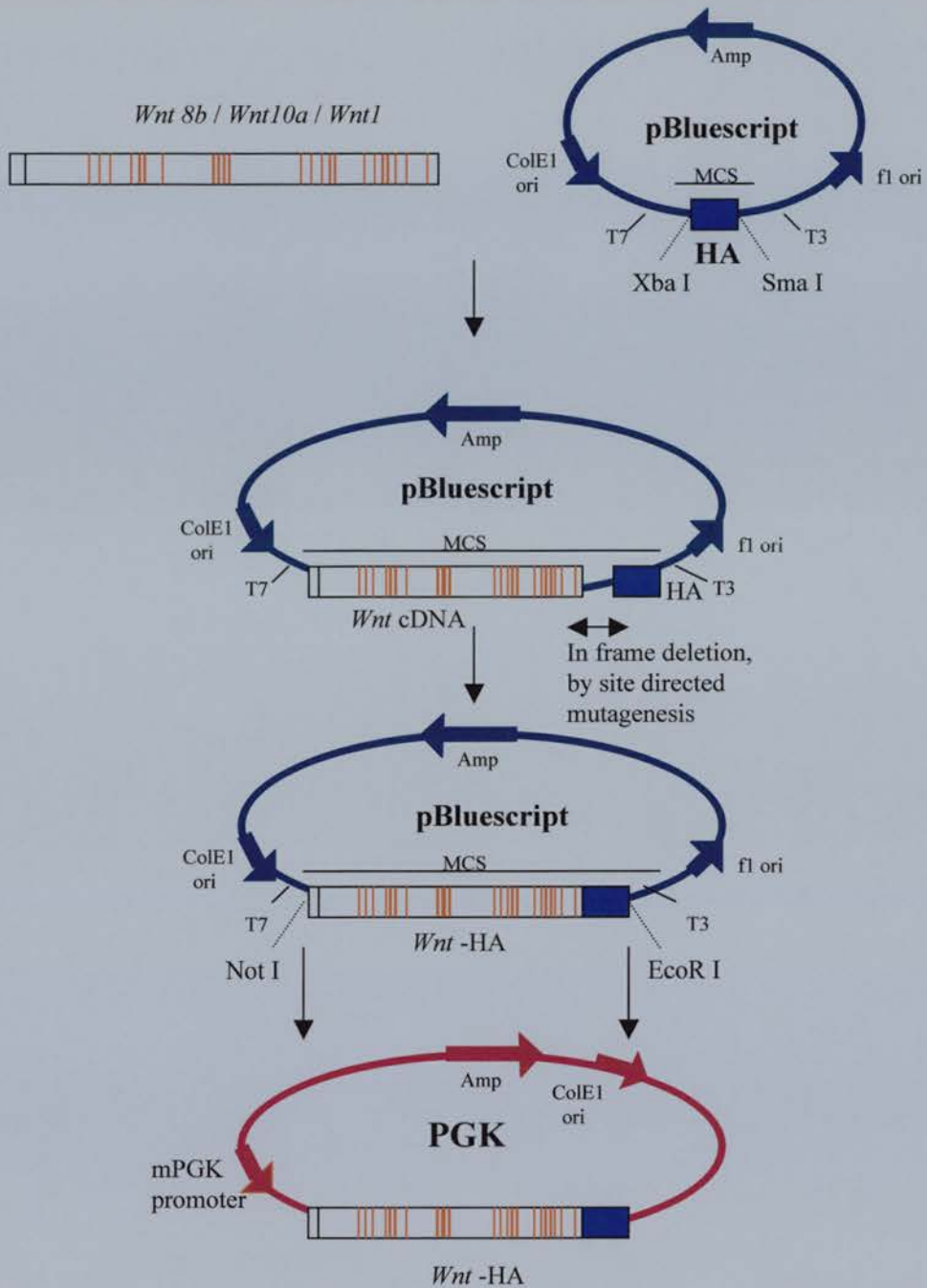


Figure 6.1 Generation of HA epitope tagged Wnt cDNA expression vectors

Wnt8b, *Wnt10a*, or *Wnt1* cDNA sequences were cloned into a pBluescript plasmid containing an HA epitope tag. Site directed mutagenesis was used to fuse in frame the *Wnt* cDNA and HA sequences. The HA-tagged *Wnt* cDNAs were then cloned into the phosphoglycerate kinase (PGK) mammalian expression vector (pHPmPGKpS-BstX1(+Svori)) which carries a hygromycin B antibiotic resistance gene. See Appendix E for vector maps.

Protein was harvested, quantified and subjected to SDS-polyacrylamide gel electrophoresis. The protein was then transferred onto PVDF membrane and Ponceau S staining confirmed both equal loading and efficient transfer of protein samples. Wnt proteins were detected upon incubation with an anti-HA antibody (a rabbit affinity-purified polyclonal antibody raised against a peptide mapping to an internal region of the influenza haemagglutinin (HA) protein). Figure 6.2a details schematic representations of the Wnt1, 8b and 10a proteins. The results of western analysis for each of these Wnt proteins are detailed below.

Western analysis identified two of the five reported Wnt 1 protein species (Figure 6.2b). Wnt1 has four potential N-linked glycosylation sites producing five different protein species of 36, 38, 40, 42 and 44 kDa (Brown *et al.*, 1987; Papkoff *et al.*, 1987). In this analysis two bands resolving at 38kDa and 40kDa were observed with the 40kDa band being present in greater abundance.

The predicted Wnt8b protein is 350aa in length and contains 22 cysteines. Signal sequence cleavage is predicted to occur between amino acids 21 and 22, and there are two potential N-linked glycosylation sites. Thus, Wnt8b is predicted to produce up to three different protein species at around 36kDa. All three Wnt8b protein species were identified (37kDa, 40kDa and 42kDa) although the sizes were greater than predicted using a peptide molecular weight calculator. The 40kDa band was expressed at significantly higher levels than the 37kDa and 42 kDa bands.

The predicted Wnt10a protein consists of 417 amino acids, with cleavage of the N-terminal signal sequence predicted to occur between amino acids 35 and 36. There are 23 cysteine residues and two potential N-linked glycosylation sites, which predict three different Wnt10a protein species at around 42kDa. Only one Wnt10a protein species was identified by western analysis, which resolved at approximately 40kDa.

Two methods were used to determine the size of the unglycosylated forms of Wnt8b and Wnt10a. Tunicamycin is an inhibitor of N-linked glycosylation and was added to subconfluent stably transfected HEK 293 cells at either 1µg/ml overnight or at

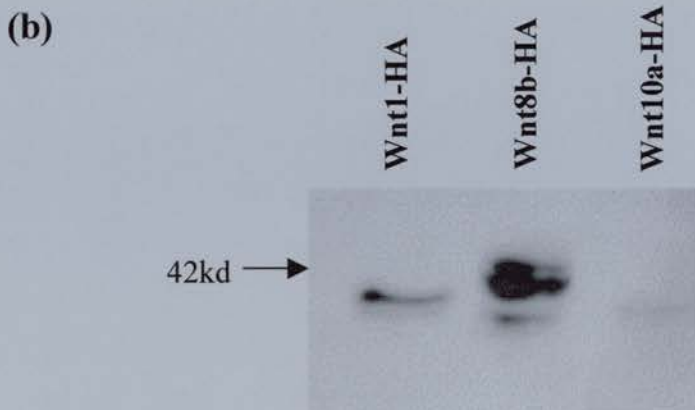
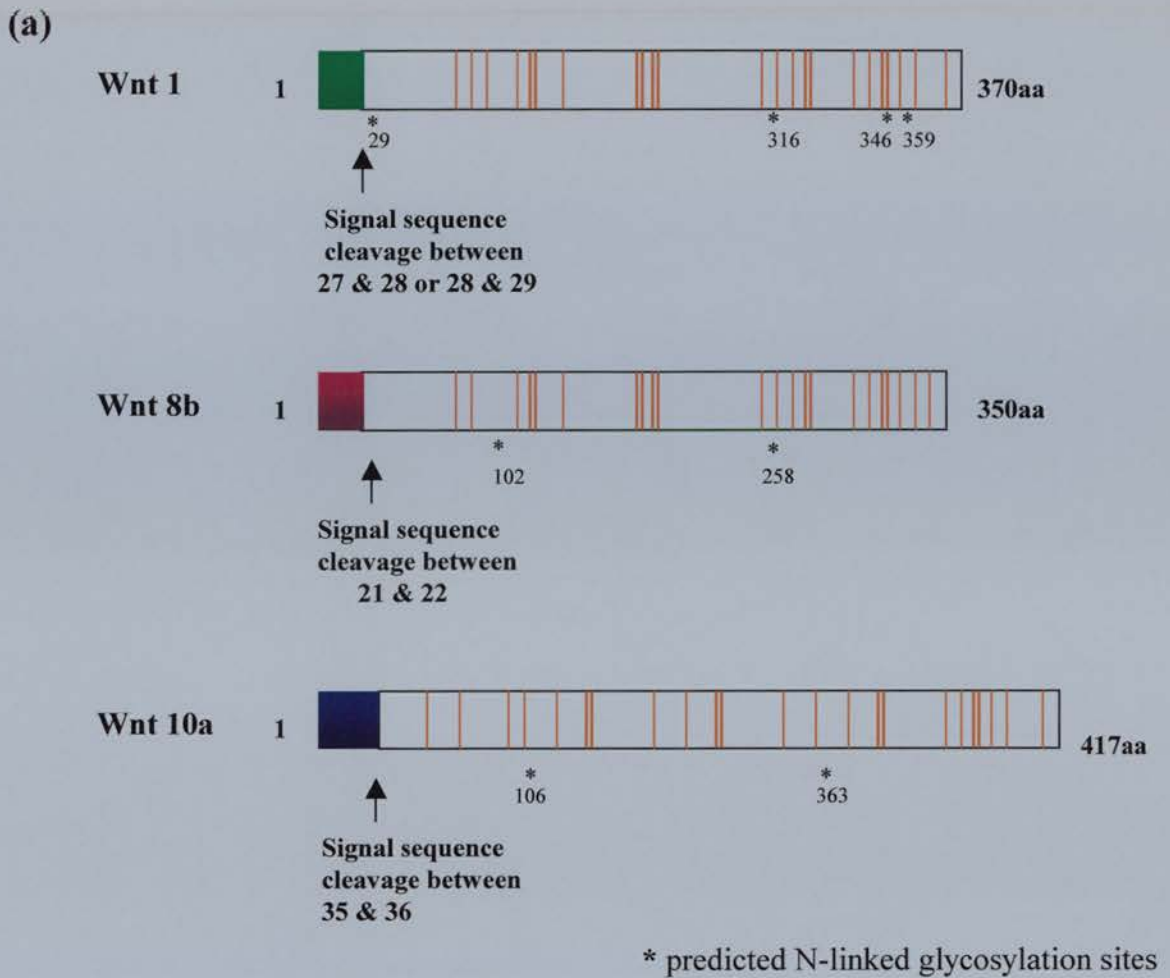


Figure 6.2 Western analysis of Wnt8b and Wnt10a

(a) Schematic representation of Wnt1, Wnt8b and Wnt10a proteins detailing the site of signal sequence cleavage and sites of potential N-linked glycosylation. (b) Western analysis of stably transfected HEK 293 cells using an anti-HA antibody. Wnt1-HA transfected HEK 293 cells were used as a positive control and displayed two of the five known Wnt1 protein species (38 and 40kDa). Wnt8b-HA transfected HEK 293 cells displayed three protein species of approximately 37, 40 and 42kDa. Wnt10a transfected HEK 293 cells displayed only one protein species of approximately 40 kDa

5µg/ml for 6 hours prior to protein isolation. Tunicamycin treatment did not effectively eliminate all glycosylation (data not shown), thus an alternative method exploiting Endoglycosidase H (Endo H) was incorporated into this study. Endo H is a glycosidase that cleaves the chitobiose core of high mannose and some hybrid oligosaccharides from N-linked glycoproteins. Thus Endo H treatment of protein samples, prior to electrophoresis, removes the N-linked carbohydrates and should convert Wnt1, Wnt8b and Wnt10a to their respective unglycosylated forms. Wnt1, Wnt8b and Wnt10a protein samples (20µg) were treated with Endo H for 1, 4 or 24 hours and subsequent western analysis revealed a single band representing the unglycosylated form of the protein (Figure 6.3a). However, complete removal of all N-linked carbohydrates was detected after 1 hour (Figure 6.3b). Endo H treatment reduced the two Wnt1 protein species (resolving 38kDa and 40kDa) to one unglycosylated form resolving at approximately 36kDa. The Wnt8b protein was not reduced to a single unglycosylated band. In this experiment only two Wnt8b protein species were observed (42kDa and 37kDa) and the larger 42kDa band was reduced to 38kDa, while the 37kDa band was reduced to 32kDa. The Wnt10a protein, which resolved at 40kDa, was reduced to a single unglycosylated form that resolved at approximately 38kDa following Endo H treatment.

6.2.2 Functional analysis of Wnt8b and Wnt10a

Having established that the Wnt8b-HA and Wnt10a-HA expression vectors produce proteins of the expected sizes, these were then used in two functional assays - C57 mammary epithelial cell transformation and axis duplication in *Xenopus* - with the aim of identifying whether these *Wnts* belong to the *Wnt1* class or *Wnt5a* class of *Wnt* genes. Despite these experiments resulting in interesting observations, this data remains a preliminary study, as there was insufficient time to complete this analysis.

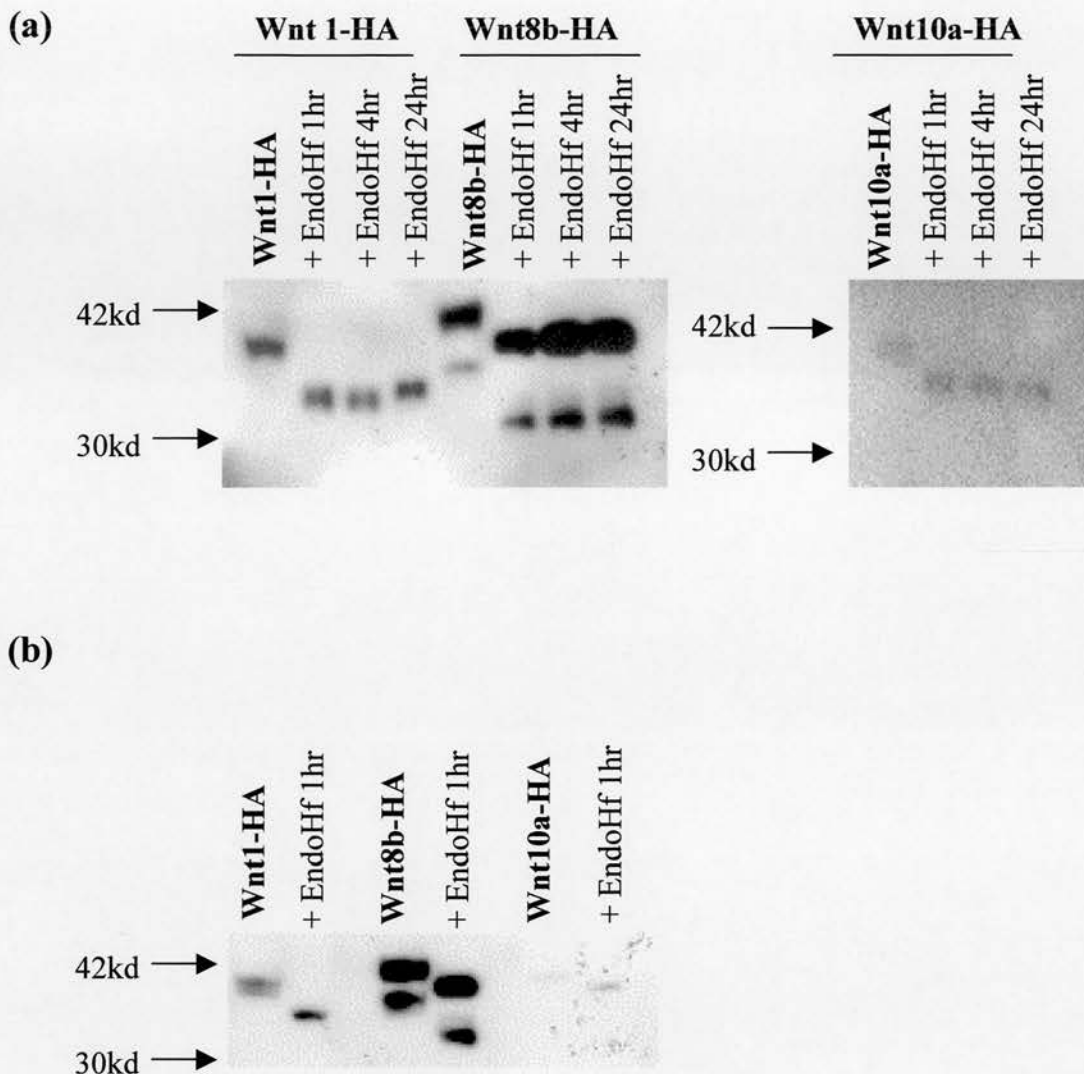


Figure 6.3 Western analysis of Endo H treated Wnt8b and Wnt10a

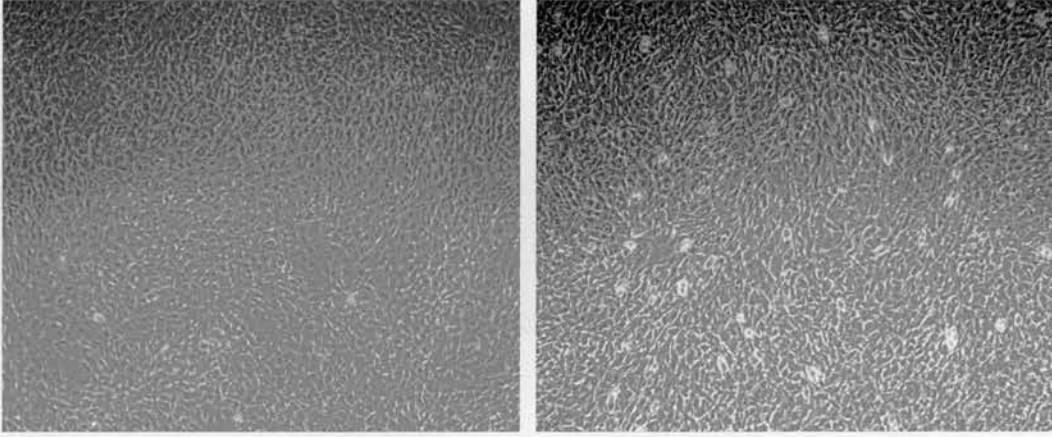
(a) Protein extracts from Wnt1-HA, Wnt8b-HA and Wnt10a-HA stably transfected HEK 293 cells were incubated at 37°C with Endo H for 1, 4 or 24 hours. Endo H removed all N-linked carbohydrates and revealed the size of the unglycosylated protein which was 36kDa for Wnt1, approximately 34kDa for Wnt8b and approximately 38kDa for Wnt10a. (b) Complete removal of all N-linked carbohydrates was detected after just 1 hour of Endo H treatment.

6.2.2.1 Functional assay 1: C57 mammary epithelial cells

As described in section 6.1, C57MG cells are an epithelial cell line derived from normal mouse mammary tissue (Vaidya *et al.*, 1978), which grow in a monolayer with a regular, cuboidal appearance at confluence (Figure 6.4a). Subsequent elimination of serum from the cell culture medium suppresses the background of spontaneously semi-transformed colonies sometimes observed when untransfected C57MG cells are grown in the presence of serum (Figure 6.4b). Additionally, the morphological changes induced by *Wnt1* are more readily observed in serum free medium (Mason *et al.*, 1992). Transfection efficiency of C57MG cells using the FuGeneTM6 transfection reagent was examined using an EGFP (enhanced green fluorescent protein) expression plasmid, which produces a tagged EGFP that localises to the mitochondria of cells. This experiment indicated that transfection efficiency was low as only 4-5 clones of EGFP positive cells could be detected per T75 tissue culture flask (Figure 6.5a). The PGK *Wnt1*-HA, *Wnt8b*-HA and *Wnt10a*-HA expression plasmids were then transfected into C57MG cells and the culture medium changed after 24 hours to select for stable transfections. Stable clones were then pooled and once the cells were 90% confluent the medium was replaced with a serum free medium. *Wnt1*-HA was again used as a positive control as its effects in C57MG cells are well documented (Brown *et al.*, 1986; Jue *et al.*, 1992; Mason *et al.*, 1992). Additionally, Shimizu *et al.* (1997) have reported that the placement of the HA epitope tag at the C-terminus does not interfere with *Wnt1* function in C57MG cells. As expected, *Wnt1* expression induced a morphological change from flat cuboidal cells to elongated, densely packed, highly refractile cells (semi-transformed phenotype) (Figure 6.5b). However, when these stably transfected *Wnt1* expressing clones were pooled and the medium changed to serum free medium not all cells displayed a semi-transformed phenotype (Figure 6.5c).

Wnt8b expression also induced a morphological change identical to that of *Wnt1* (Figure 6.6a). The stably transfected *Wnt8b* clones were pooled, grown to 90% confluence and the medium replaced with serum free medium. However, as for

(a)



(b)

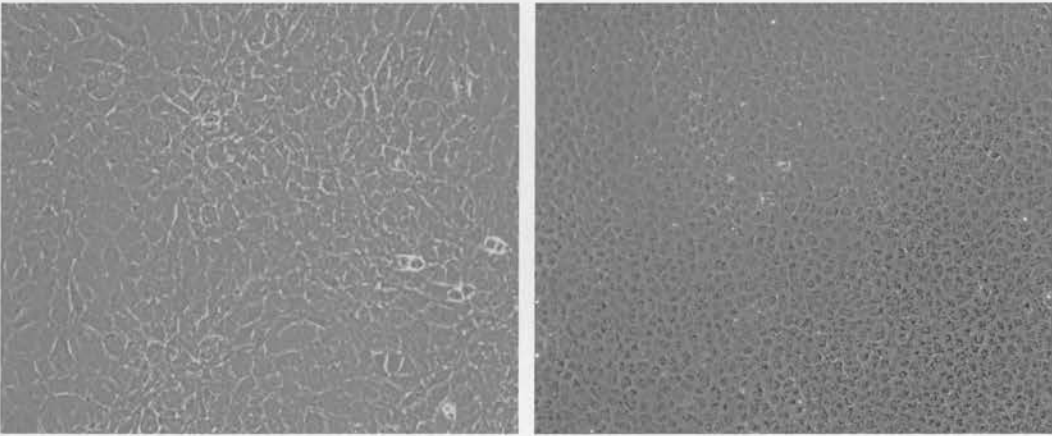


Figure 6.4 Control untransfected C57 mammary epithelial cells

(a) C57MG cells at confluence showing a regular, cuboidal appearance. **(b)** C57MG cells grown in serum free conditions so as to suppress spontaneous semi-transformation and thus facilitate the observation of any morphological changes induced by *Wnt* genes.

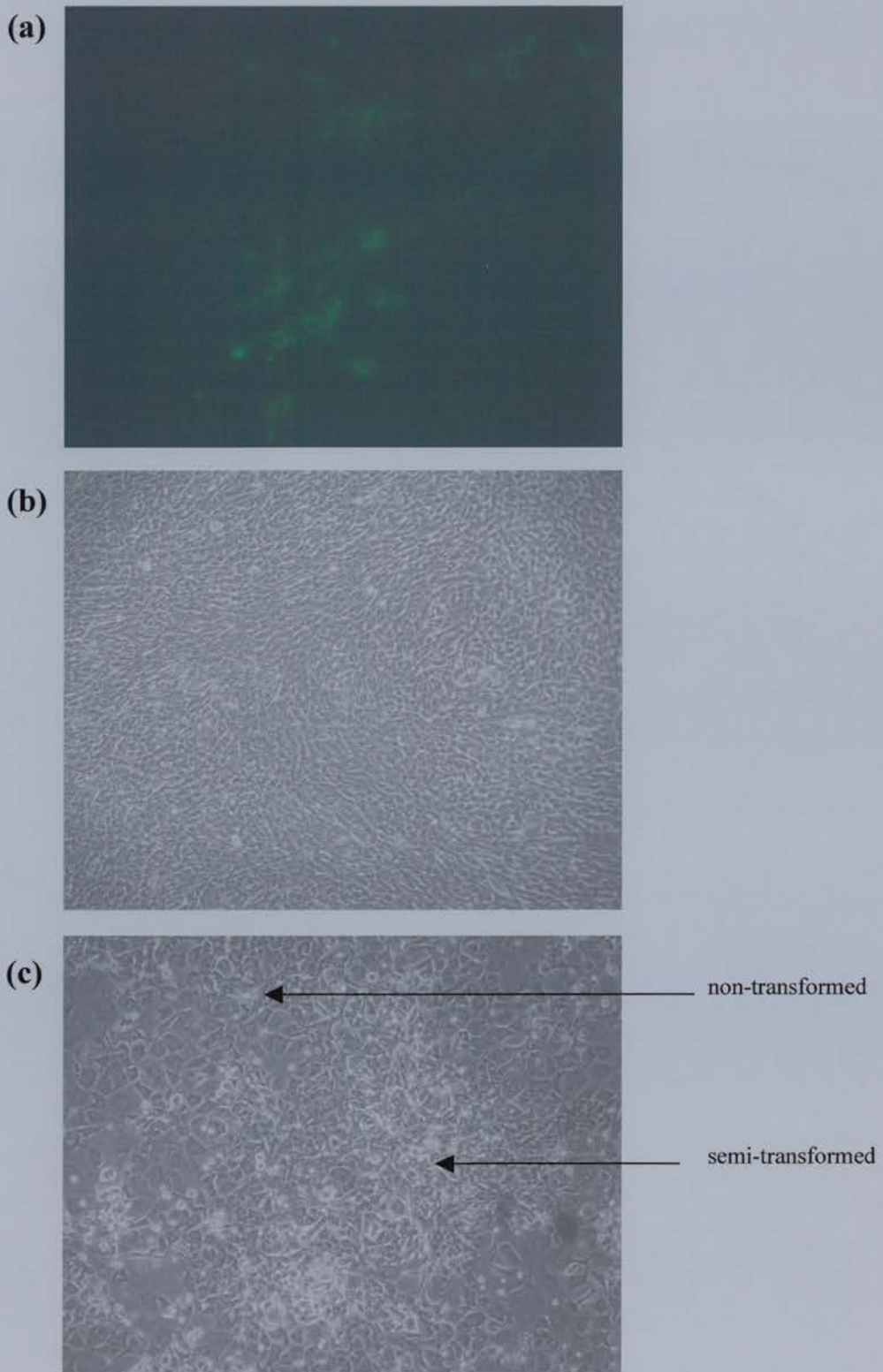


Figure 6.5 Control transfections of C57 mammary epithelial cells

(a) Control EGFP transfection showing a pool of EGFP positive cells. (b) A stably transfected *Wnt1* expressing clone showing a semi-transformed phenotype (i.e. morphological change from flat cuboidal cells to elongated, densely packed, highly refractile cells). (c) Pooled stably transfected *Wnt1* expressing clones in serum free medium showing areas of semi-transformed and non-transformed cells.

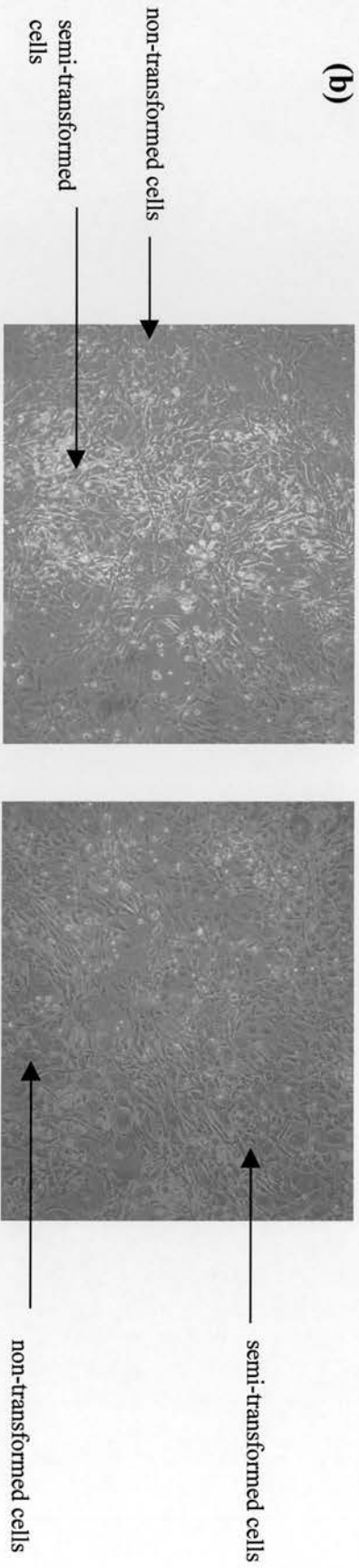
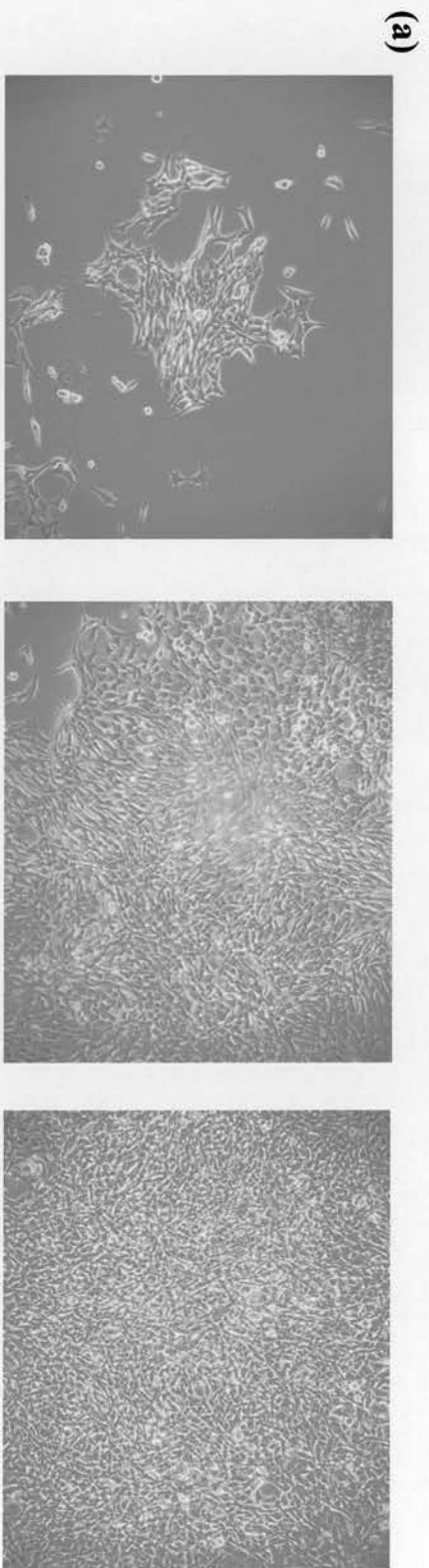


Figure 6.6 *Wnt8b* transfected C57 mammary epithelial cells
 (a) Stably transfected *Wnt8b* expressing clones showing morphological change from flat cuboidal cells to elongated, densely packed, highly refractile cells. (b) Pooled stably transfected *Wnt8b* expressing clones in serum free medium showing areas of semi-transformed and non-transformed cells.

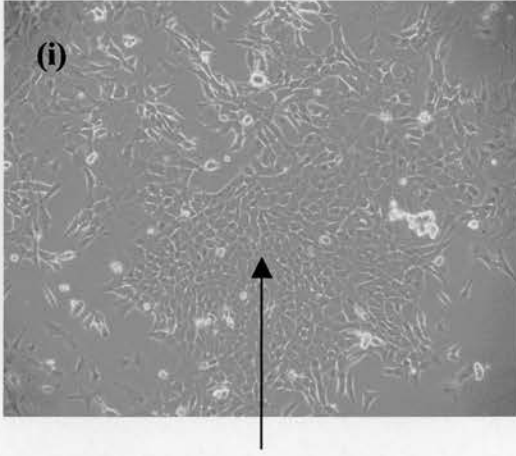
Wnt1, this resulted in some loss of the semi-transformed phenotype, with many cells appearing indistinguishable from control cells (Figure 6.6b).

The results for *Wnt10a* were less clear as its expression resulted in some stable clones with a non-transformed phenotype and others where morphological alteration had been induced (Figure 6.7a). However, upon pooling of all stably transfected clones and a switch to serum free medium, all cells appeared flat and cuboidal and indistinguishable from control cells (Figure 6.7b).

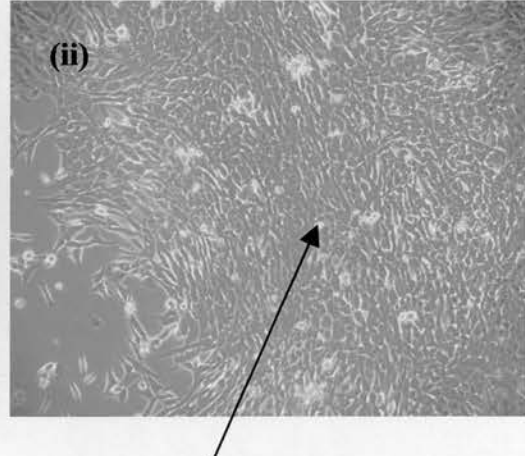
6.2.2.2 Functional assay 2: *Xenopus* embryos

The second assay of *Wnt* gene function involved the overexpression of *Wnt1*, *Wnt8b*, and *Wnt10a* in *Xenopus* embryos through mRNA injection. Ectopic expression of the *Wnt1* class in *Xenopus* embryos causes anterior duplication of the embryonic axis, whilst the *Wnt5a* class perturbs gastrulation but does not result in axial duplication (McMahon and Moon, 1989; Moon *et al.*, 1993b). The HA tagged Wnts (1, 8b and 10a) were directionally cloned into the *Xenopus* expression vectors pSP64TBX or pSP64TXB (Appendix E). The *Xenopus Wnt* gene, *XWnt5a*, was used as a negative control as its overexpression in *Xenopus* embryos (ventral injection) does not cause axis duplication (Moon *et al.*, 1993b). The *Xenopus XWnt8* gene, which causes axis duplication, was used as a positive control (Christian *et al.*, 1991). Following linearisation, mRNA was generated through in vitro transcription from the Sp6 promoter. This mRNA was quantified by gel electrophoresis (Figure 6.8) and 10ng/μl was injected ventrally into two-cell stage *Xenopus* embryos. *Xenopus* injections were performed by Dr. Stefan Hoppler, University of Dundee. Embryos were then cultured, at 18°C for 24 – 48 hours, and their development monitored. The effects of ectopic expression of *Wnt1*, *Wnt8b* and *Wnt10a* are shown in Figure 6.9. *XWnt8* expression resulted in the complete dorsalisation of 98% of injected *Xenopus* embryos. The *XWnt5a* negative control resulted in axis duplication in 39.5% of *Xenopus* embryos. Ectopic *Wnt1* expression caused axis duplication in only 1.8% of

(a)



non-transformed cells



semi-transformed cells

(b)

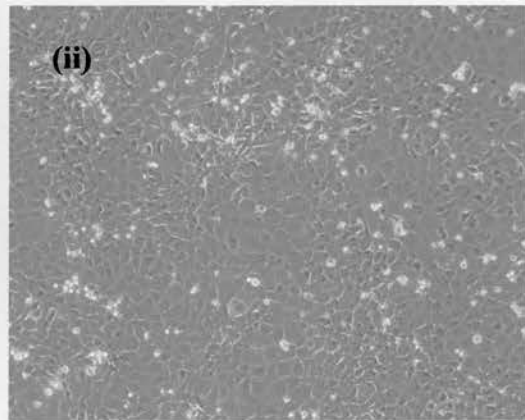
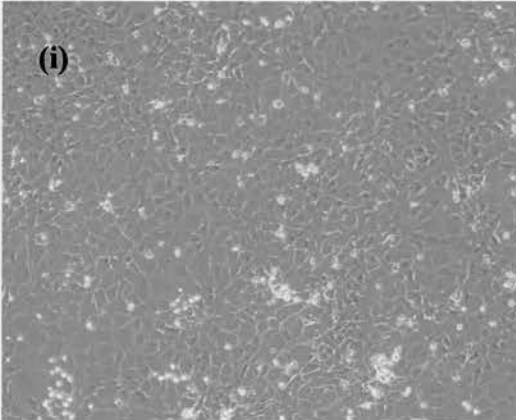


Figure 6.7 *Wnt10a* transfected C57 mammary epithelial cells

(a)(i) Stably transfected *Wnt10a* expressing clones showing a non-transformed phenotype identical to untransfected cells. **(ii)** Stably transfected *Wnt10a* expressing clones showing morphological change from flat cuboidal cells to elongated, densely packed, highly refractile cells. **(b)** Pooled stably transfected *Wnt10a* expressing clones in serum free medium displaying a non-transformed phenotype.

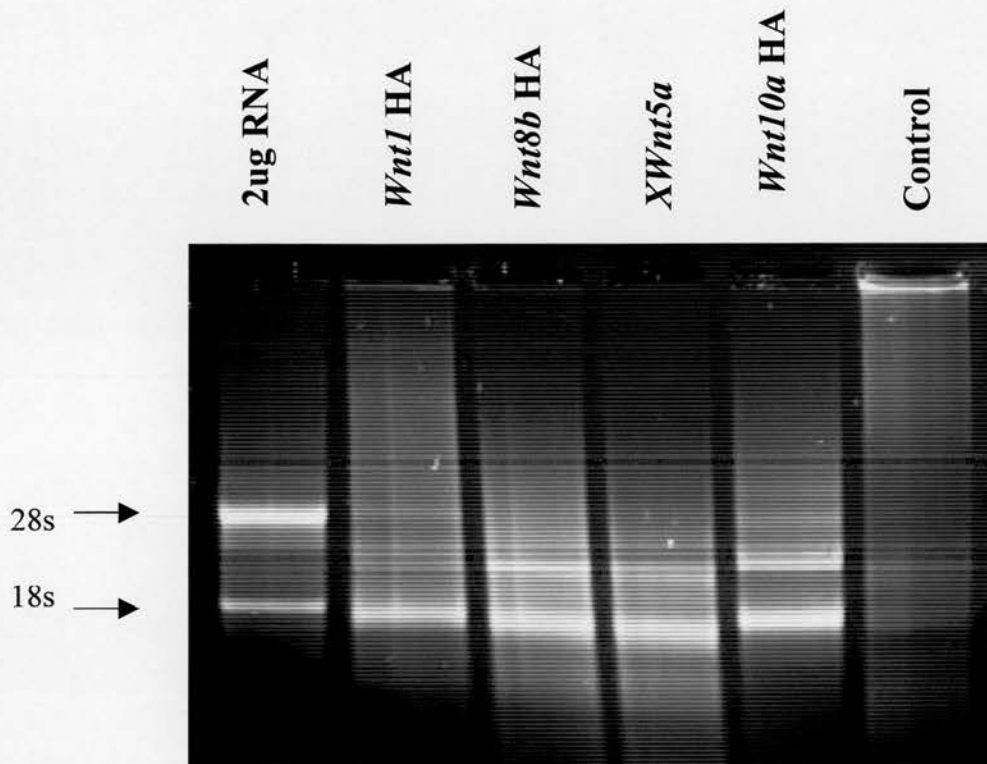


Figure 6.8 *Wnt* mRNA for *Xenopus* injection

Wnt1, *Wnt8b*, *Wnt10a* and *XWnt5a* mRNA generated by in vitro transcription using the Ambion mMESSAGE MACHINE™ transcription kit. A control template that was supplied in this kit was in vitro transcribed in parallel so as to ensure reactions were at optimum efficiency. mRNA (2µl) was subjected to denaturing agarose gel electrophoresis prior to *Xenopus* injection to analyse the quality and quantity of mRNA synthesised. Quantification was estimated by comparing the intensity of the *Wnt* mRNAs to an aliquot of RNA of known concentration (2µg/µl). *Wnt1* was estimated to be the same concentration as the known sample (i.e. 2 µg/µl). *Wnt8b* appeared to be approximately twice this concentration (4 µg/µl). *XWnt5a* and *Wnt10a* were estimated to be just less than twice the concentration of the known sample (3.5 µg/µl).

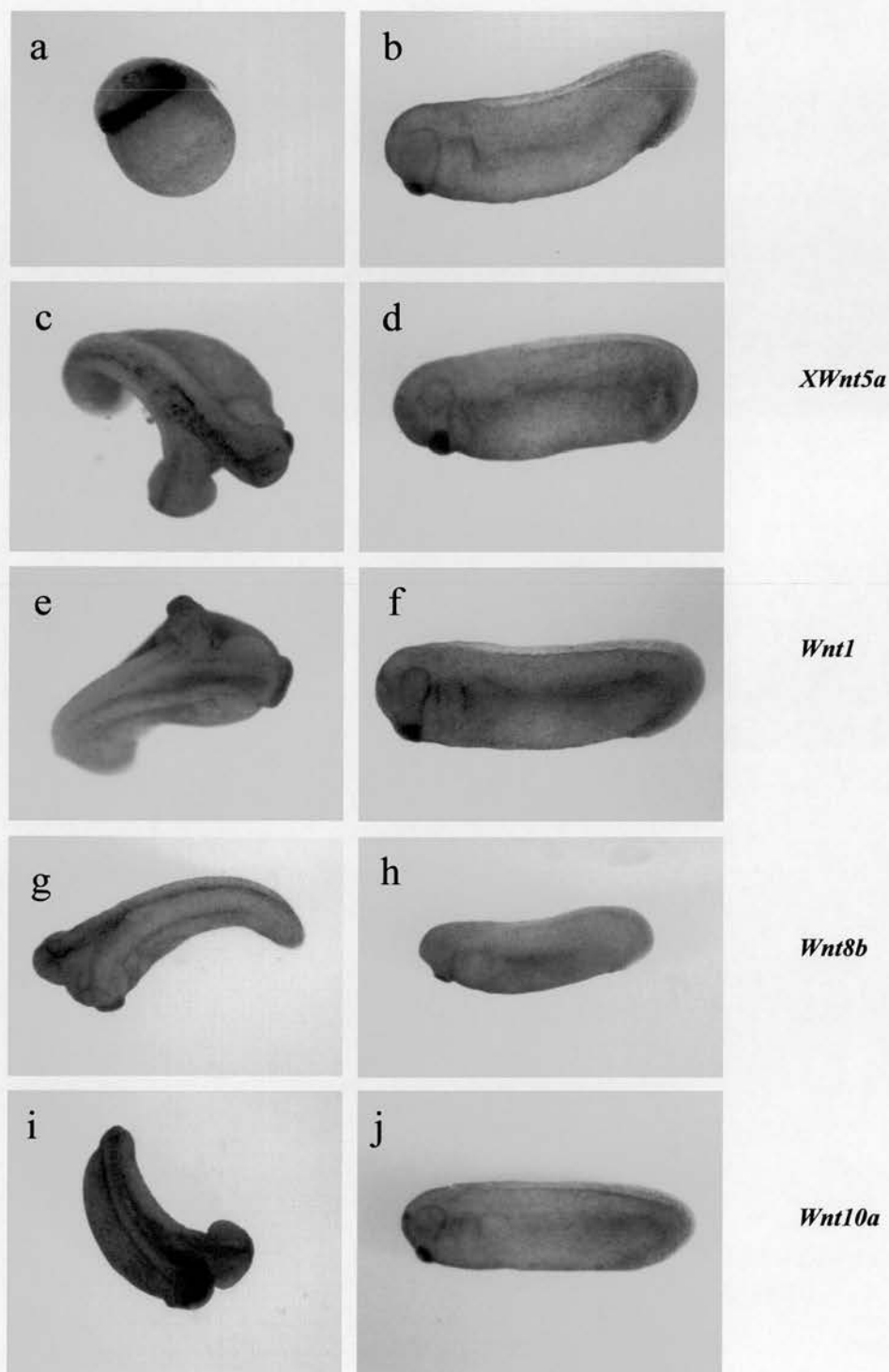


Figure 6.9 Effects of ectopic expression of *Wnt* genes (1, 8b, and 10a) on normal *Xenopus* development (a) Ectopic expression of *Xwnt8* causes complete dorsalisation of *Xenopus* embryos. Axis duplication was observed following injection with (c) *XWnt5a*, (e) *Wnt1*, (g) *Wnt8b* and (i) *Wnt10a*. (b) Uninjected *Xenopus* embryo showing normal development. *Xenopus* embryos showing no effect of ectopic expression of (d) *XWnt5a*, (f) *Wnt1*, (h) *Wnt8b* and (j) *Wnt10a*.

injected *Xenopus* embryos, while 31% of embryos showed axis duplication following *Wnt8b* injection. *Wnt10a* expression resulted in axis duplication in 1.6% of injected *Xenopus* embryos (Figure 6.10). Although this data is surprising, there was insufficient time available to repeat the experiments. Thus meaningful interpretation of this data is therefore difficult and is discussed in section 6.3.2.2.

6.3 Discussion

6.3.1 Biochemical analysis of *Wnt8b* and *Wnt10a* proteins

A biochemical analysis of two *Wnt* genes (*Wnt8b* and *Wnt10a*) identified from mouse mammary gland cDNA was carried out. Proteins extracted from *Wnt1*-HA, *Wnt8b*-HA and *Wnt10a*-HA, stably transfected HEK 293 cells were subjected to western analysis, which confirmed that these cells were expressing Wnt protein. The glycosylation status of *Wnt8b* and *Wnt10a* proteins was investigated with the use of a glycosidase (Endo H) because the amino acid sequence of these proteins predicts several potential N-linked glycosylation sites.

The deduced *Wnt8b* protein sequence contains two potential N-linked glycosylation sites, at positions N102 and N258, and was predicted to produce up to three different protein species of approximately 36kDa (predicted using a peptide molecular weight calculator). Western analysis identified three *Wnt8b* protein species at 37kDa, 40kDa and 42kDa suggesting that both glycosylation sites were used. These proteins were larger than predicted and this could be due to the secondary structure of the *Wnt8b* protein. Glycosidase treatment did not reduce *Wnt8b* protein to a single unglycosylated form. Specifically, it appears that the 42kDa band was reduced to 40kDa and the 37kDa band was reduced to 32kDa.

Wnt10a protein sequence indicates two potential N-linked glycosylation sites at positions N106 and N36, which predict three different *Wnt10a* protein species of

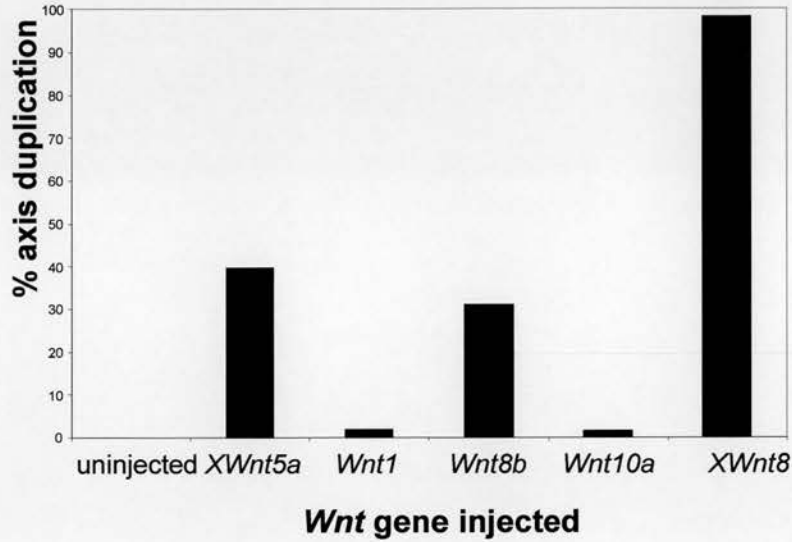


Figure 6.10 *Xenopus* axis duplication assay

For each *Wnt* gene to be tested between 50 and 60 two-cell stage *Xenopus* embryos were ventrally injected with 100pg of *Wnt* RNA. *XWnt8* resulted in the complete dorsalisation of 98% of injected *Xenopus* embryos. *Xwnt5a* resulted in axis duplication in 39.5% of *Xenopus* embryos injected. *Wnt1* caused axis duplication in only 1.8% of injected *Xenopus* embryos, while 31% of embryos showed axis duplication following *Wnt8b* injection. *Wnt10a* expression resulted in axis duplication in 1.6% of injected *Xenopus* embryos. Axis duplication was not observed in uninjected embryos.

approximately 42kDa. However, only one Wnt10a protein species was identified by western analysis, which resolved at approximately 40kDa. Subsequent Endo H treatment reduced this protein species to a single unglycosylated form that resolved at approximately 38kDa. This result suggests that Wnt10a is normally glycosylated at only one of its two potential N-linked glycosylation sites. Additionally, the Wnt10a protein was expressed at much lower levels in HEK 293 cells than either the Wnt1 or Wnt8b proteins. Shimizu *et al.*, (1997) report similar findings for the Wnt4 and Wnt5b proteins. Western analysis indicated that Wnt4 and Wnt5b were expressed at much lower levels in C57MG cells than Wnt1. To overcome this problem and improve the expression of these proteins, the Wnt1 5' untranslated region (UTR) was substituted for the 5'UTR of Wnt4 and Wnt5b. Subsequent western analysis of transiently transfected C57MG cells showed that the levels of these proteins had increased to levels comparable to that of other Wnt proteins (Shimizu *et al.*, (1997). Thus, 5' UTR switch could be used to overcome the problem of low expression levels of Wnt10a in future experiments.

Wnt1-HA was used as a positive control as its protein species are well documented. Wnt1 has four potential N-linked glycosylation sites (N29, N316, N346 and N359) producing five different protein species of 36, 38, 40, 42 and 44 kDa (Brown *et al.*, 1987; Papkoff *et al.*, 1987). In this analysis only two of these protein species were observed (38kDa and 40kDa). This can be explained by the fact that experiments identifying all five Wnt1 protein species involved *in vivo* labelling, whereas western analysis identifies only the mature protein species. This suggests that the 38kDa and 40kDa proteins represent the mature Wnt1 protein species produced in HEK 293 cells. One explanation why these two proteins represent the predominant forms produced in HEK 293 cells is that the potential glycosylation site at position N29 may not be available for glycosylation. Wnt1 protein contains an N-terminal signal sequence (necessary for the entry of nascent Wnt1 protein into the ER) cleavage of which is predicted to occur after either alanine 27 or alanine 28. However, presumptive cleavage at position 28 inhibits glycosylation at N29 suggesting that the choice of cleavage site determines whether this glycosylation occurs (Mason *et al.*, 1992). Additionally, Mason *et al.*, (1992) identified through mutational analysis that

normally all, or almost all, of the Wnt1 protein chains are glycosylated at positions N316 and N359. However, only occasional glycosylation at N346 was reported (Mason *et al.*, 1992; Papkoff *et al.*, 1987) and this may be due to the presence of cysteine residues on either side of N346, which if involved in disulphide bond may impede access of glycosylation machinery (Mason *et al.*, 1992). The two protein species identified by western analysis at 38kDa and 40kDa most likely represent Wnt1 proteins glycosylated at one or both of positions N316 and N359. Subsequent glycosidase treatment (Endo H) removed the N-linked carbohydrates and converted Wnt1 to its unglycosylated form, which resolved at the expected size of 36kDa (Brown *et al.*, 1987).

6.3.2 Functional analysis of *Wnt8b* and *Wnt10a*

6.3.2.1 Morphological transformation of C57MG cells

Morphological transformation of C57MG cells has been used to assay the biological activity of different *Wnt* gene family members. This assay groups *Wnt* genes into one of three functional classes, highly transforming (*Wnt1/3/3a/7a/8*), transforming (*Wnt2/5b/7b*) and non-transforming (*Wnt4/5a/11*) depending on their ability to induce morphological transformation and altered growth characteristics of the C57 mammary epithelial cell line (Wong *et al.*, 1994). Morphological transformation, as defined by experiments with Wnt1, is characterised by three observations; (1) a morphological change in shape from flat cuboidal cells to elongated, densely packed, highly refractile cells, (2) loss of contact inhibition, and (3) decreased serum dependency (Brown *et al.*, 1986; Jue *et al.*, 1992). However, this transformation is considered partial because cells are unable to form tumours in syngeneic host animals (semi-transformation) (Brown *et al.*, 1986). In this analysis, although the *Wnt1* positive control induced morphological transformation of C57 mammary epithelial cells, when these stably transfected *Wnt1* expressing clones were pooled and the medium changed to serum free medium not all cells displayed the semi-transformed phenotype. One possible explanation for this phenotype is that some

cells were no longer expressing *Wnt1*. The results for *Wnt8b* were similar, specifically initial transfection of C57MG cells resulted in *Wnt8b* expressing clones displaying a morphologically transformed phenotype with cells changing in shape from flat, cuboidal cells to elongated highly refractile cells that had lost contact inhibition. Pooling of *Wnt8b* stably transfected clones, followed by serum deprivation resulted in some loss of semi-transformation with patches of cells appearing indistinguishable from control cells. Thus it appears some cells may have lost *Wnt8b* expression. These observations suggest that *Wnt8b* belongs to the *Wnt1* class of highly transforming *Wnt* genes, although ideally the entire culture should display the morphologically transformed phenotype. C57MG cells stably transfected with *Wnt10a* mostly appeared identical to control cells with only a few stable clones displaying a morphologically transformed phenotype. Upon pooling of all *Wnt10a* stably transfected clones and a switch to serum free medium, all cells appeared flat and cuboidal and indistinguishable from control cells. The results for *Wnt10a* suggest that it belongs to the *Wnt5a* class of non-transforming *Wnt* genes, as stably transfected clones grown in serum free conditions were flat and cuboidal. The appearance of some semi-transformed cells following *Wnt10a* transfection is most likely due to spontaneous semi-transformation, which was suppressed when C57MG cells were switched to serum free medium. However, it is noteworthy that western analysis indicated that *Wnt10a* expression levels were much lower than either *Wnt1* or *Wnt8b* (section 6.2.1), and this may account for the lack of effect in the C57 semi-transformation assay.

C57 mammary epithelial cells expressing *Wnt* proteins display compromised growth patterns, with cells growing and dividing more slowly (personal communication (Dr. J.O. Mason)). One hypothesis for the observation that stably transfected *Wnt1* and *Wnt8b* clones when pooled lost some of their semi-transformed phenotype is that any untransfected cells or cells that have spontaneously lost *Wnt* expression have a selective growth advantage over *Wnt* expressing cells and thus dominate the culture. To overcome this problem in future experiments, stably transfected clones should not be pooled as this may increase the chance of contamination by either untransfected cells or cells that have spontaneously lost *Wnt* expression. A further recommendation

is that the transfections should be performed in smaller (e.g. 10cm tissue culture dishes) rather than the large T75 tissue culture flasks that were used in this experiment. However, shortage of time prevented further analysis, thus these observations remain preliminary.

6.3.2.2 Axis duplication in *Xenopus* embryos

Overexpression of *Wnts* in *Xenopus* embryos through mRNA injection has been used to assay *Wnt* gene function (Moon *et al.*, 1993a). Two distinct phenotypes are observed. Injection of mRNAs encoding *Xenopus Wnt8* (*XWnt8*) (Christian *et al.*, 1991), *XWnt3a* (Wolda *et al.*, 1993), *Drosophila wg* (Chakrabarti *et al.*, 1992) or mouse *Wnt1* (McMahon and Moon, 1989) leads to dorsal axis duplication in *Xenopus* embryos due to the induction of an ectopic Spemann organiser (Sokol *et al.*, 1991). In contrast, overexpression of *XWnt5a* affects morphogenetic movements without producing a duplication of the axis (Moon *et al.*, 1993b). These observations divide *Wnt* genes into one of two functional classes, the *Wnt1* class (*Wnt1/3/3a/8*), which causes duplication of the embryonic axis, and the *Wnt5a* class (*Wnt4/5a* and *Wnt6*), which does not (McMahon and Moon, 1989; Moon *et al.*, 1993b). In this study ventral injection of the *XWnt8* mRNA (positive control) resulted in the complete dorsalisation of 98% of injected *Xenopus* embryos. In contrast ectopic *Wnt1* expression caused axis duplication in only 1.8% of injected *Xenopus* embryos. This unexpected result probably represents the overestimation of the quantity of *Wnt1* RNA injected. It has been observed that RNA doses of less than 1pg do not have any effect on *Xenopus* embryos (Sokol *et al.*, 1991). Additionally, the negative control, *XWnt5a*, induced axis duplication in 39.5% of *Xenopus* embryos injected. It has been observed that non-duplicating *Wnts* will cause axis duplication in RNA doses of ~500pg (compared with 30pg for a duplicating *Wnt*)(Dr. Stefan Hoppler, personal communication) thus it is feasible that this result represents an underestimation of the quantity of mRNA injected. *Wnt8b* expression induced axis duplication in 31% of injected *Xenopus* embryos, while *Wnt10a* expression resulted in axis duplication in 1.6% of injected *Xenopus* embryos. These preliminary observations suggest that

Wnt8b belongs to the *Wnt1* class of *Wnt* genes and *Wnt10a* belongs to the *Wnt5a* class of *Wnt* genes, and correlates with the results of the C57MG cell transformation assay. These data fit a model in which *Wnt8b* and *Wnt10a* proteins have intrinsically different functions and different signalling pathways.

7 Final Discussion

7.1 Summary

The background work to this thesis involved the generation of a transgenic mouse with conditional inactivation of the *Apc* gene in the mammary gland. To specifically inactivate *Apc* in the mouse mammary gland, mice harbouring a floxed allele of *Apc* (*Apc*^{580S/580S}) were crossed to transgenic mice expressing a transgene that drives expression of cre recombinase specifically in the mammary gland (BLG-cre), and the progeny, BLG-cre floxed *Apc* mice (cre⁺ *Apc*^{580S/580S}), underwent specific inactivation of mammary *Apc* (Gallagher *et al.*, 2002). Preliminary phenotypic data highlighted a critical role of *Apc* in both the growth and development of the mammary gland whereby virgins displayed delayed ductal growth and areas of metaplasia which increased during lactation (Gallagher *et al.*, 2002). Using the BLG-cre floxed *Apc* mice (cre⁺ *Apc*^{580S/580S}) this thesis further explored the role of wild type *Apc* in the mouse mammary gland.

Further characterisation of the cre⁺ *Apc*^{580S/580S} mice involving proliferation analysis and immunohistochemistry of candidate downstream genes confirmed that conditional inactivation of *Apc* from the mouse mammary gland resulted in dysregulated *Wnt* signalling and increased proliferation within the metaplastic lesions. Several groups have observed mammary hyperplasia and adenocarcinoma as a consequence of dysregulated *Wnt* signalling in the mouse mammary gland (Tsukamoto *et al.*, 1988; Edwards *et al.*, 1992; Wang *et al.*, 1994; Imbert *et al.*, 2001; Michaelson and Leder, 2001). Additionally, mammary tumours induced by mutations in genes of the canonical *Wnt* pathway exhibit characteristic features, the most characteristic of which is squamous differentiation. The authors speculate that this may be related to the dysregulation of β -catenin (Rosner *et al.*, 2002; Miyoshi *et al.*, 2002). In this thesis, conditional inactivation of *Apc* from the mouse mammary secretory epithelium did result in the formation of multiple extensive metaplastic nodules, within which β -catenin was dysregulated (section 3.2)(Gallagher *et al.*,

2002). However neoplasia was not a phenotype of the $cre^+ Apc^{580S/580S}$ mice. The author speculates that the levels of β -catenin dysregulation may be a critical determinant in mammary gland tumorigenesis, and that in this instance deficiency of *Apc* alone was insufficient to result in complete deregulation of β -catenin in the mouse mammary secretory epithelium.

In an effort to understand the relationship between *Apc* deficiency and mouse mammary gland metaplasia, DDRT-PCR was incorporated into this analysis as a means of investigating the effect of *Apc* deletion on expression levels of downstream genes. Several genes were identified as being differentially expressed as a consequence of *Apc* deletion, including *casein*, *$\alpha 1$ type IV collagen*, *Gm2a* and three *novel* genes. In addition, due to the spatial and temporal expression of some of these (*$\alpha 1$ type IV collagen*, *novel 1* and *novel 2*) it was speculated that their functions might be related to metaplastic nodule formation. Despite these efforts, the relationship between mammary gland metaplasia and *Apc* deficiency remains unclear. These observations highlight the complexity of *Apc* function in mouse mammary gland secretory epithelium.

7.2 Technical limitations of differential display

Although several widely used techniques exist for the identification and subsequent isolation of differentially expressed genes, DDRT-PCR was the method chosen in this thesis. DDRT-PCR has several advantages over other techniques (section 4.1.1). However, a criticism of this technique include reports of significantly high false positive rates, where expression studies using isolated clones have failed to replicate the differential expression patterns seen on the original display gel (Li *et al.*, 1994; Sun *et al.*, 1994). There exist two methods of overcoming the isolation of false positives (mSSCP and cold Southern blotting) and these were incorporated into this study to decrease the incidence of false positives. Despite this, differential display had several technical limitations. Firstly, the main drawback of the protocol is that the analysis of large populations of mRNA with differential display requires about

240 different primer combinations per sample to achieve 95% coverage of the genome (Liang and Pardee, 1997). Thus, due to constraints of time and resources this thesis analysed only a quarter of the mammary gland transcriptome. Secondly, differential display is only capable of determining the 3' region of the gene so full-length cDNA needs to be isolated by probing a cDNA library or by doing rapid amplification of cDNA ends (5'RACE), thus making differential display very laborious. Finally, despite including several steps to decrease the chances of isolating false positives, they still remain a significant drawback to this technique.

7.3 Future Work

This thesis aimed to gain insight into the relationship between mammary gland metaplasia and *Apc* deficiency using a method of differential analysis to identify transcriptional changes in response to loss of *Apc* in the mouse mammary gland. DDRT-PCR was the method chosen although as described above this has several technical limitations. As a parallel analysis our collaborators have initiated a study employing cDNA microarray technology, a method in its infancy at the time of commencing this study. Microarrays are microscopic-slide-sized glass plates dotted with several thousand genes that can be analysed in one hybridisation experiment. The major advantage of DNA microarrays is that they are capable of profiling gene expression patterns of tens of thousands of genes in a single experiment. However it is not a good method to look for novel genes as it is limited by what has been put on the slide. In contrast, using DDRT-PCR and microarrays in parallel provides a powerful analysis of gene expression. A study has been initiated using Affymetrix GeneChip™ technology (oligonucleotide array) to identify transcriptional changes in response to loss of *Apc* in the mouse mammary gland. The RNA isolated and used for DDRT-PCR in this thesis has been provided for this collaborative effort. It remains to be seen if this array technique identifies any of the genes isolated in this thesis. Additionally, it is possible that the microarray experiment will provide information that may help understand the relationship between mammary gland metaplasia and *Apc* deficiency.

Another experiment that could be used to examine the function of wild type *Apc* in the mouse mammary gland involves primary mouse mammary epithelial cell culture. Primary cultures of mammary epithelial cells from mice harbouring floxed alleles of *Apc* (*Apc*^{580S/580S}) could be used to examine the *in vitro* effects of *Apc* inactivation using an adenovirus cre recombinase. RNA isolated from cultures of primary mouse mammary epithelial cells before and after cre recombinase adenovirus treatment could be used in DDRT-PCR or microarray experiments to examine transcriptional changes in response to loss of *Apc* in mouse mammary epithelial cells. This experiment would prove useful for the identification of direct targets of *Apc* in mouse mammary epithelial cells. In addition to the analysis of transcriptional changes in primary epithelial cultures following *Apc* deletion, one could also assess the effects of *Apc* deficiency by functional assay. For example, one could examine ductal branching in the mouse mammary gland by exploiting the property of mammary epithelial cells to organize into duct-like structures when grown embedded within or on top of collagen gels (Daniel *et al.*, 1984; Ormerod and Rudland, 1988). This may provide insight into the observed marked delay in normal ductal development in *Apc* deleted mouse mammary glands. In addition, when mouse mammary epithelial cells are cultured on Engelbreth-Holm-Swarm (EHS) matrix (a reconstituted basement membrane derived from the Engelbreth-Holm-Swarm tumour) they aggregate and develop three-dimensional structures that resemble secretory alveoli *in vivo*. These alveolar-like structures secrete milk proteins into the lumen thus reproducing the dual role of mammary epithelia to secrete and sequester milk proteins (Barcellos-Hoff, *et al.*, 1989). Thus the role of *Apc* in alveolar formation its function in mouse mammary gland secretory epithelium could be examined.

These experiments and those carried out in this thesis would provide an in-depth analysis of the role of *Apc* in the mouse mammary gland and should lead to the identification of downstream targets of *Apc*. This information might help understand the relationship between *Apc* mutation and human breast cancer.

8 References

- Aberle, H., Schwartz, H., and Kemler, R. (1996). Cadherin-catenin complex: protein interactions and their implications for cadherin function. *J. Cell Biochem.* **61**, 514-523.
- Aberle, H., Bauer, A., Stappert, J., Kispert, A., and Kemler, R. (1997). beta-catenin is a target for the ubiquitin-proteasome pathway. *EMBO J.* **16**, 3797-3804.
- Adler, P. N. and Lee, H. (2001). Frizzled signaling and cell-cell interactions in planar polarity. *Curr. Opin. Cell Biol.* **13**, 635-640.
- Adler, P. N. and Taylor, J. (2001). Asymmetric cell division: plane but not simple. *Curr. Biol.* **11**, R233-R236.
- Agah, R., Frenkel, P. A., French, B. A., Michael, L. H., Overbeek, P. A., and Schneider, M. D. (1997). Gene recombination in postmitotic cells. Targeted expression of Cre recombinase provokes cardiac-restricted, site-specific rearrangement in adult ventricular muscle in vivo. *J. Clin. Invest* **100**, 169-179.
- Ahmed, Y., Hayashi, S., Levine, A., and Wieschaus, E. (1998). Regulation of armadillo by a Drosophila APC inhibits neuronal apoptosis during retinal development. *Cell* **93**, 1171-1182.
- Ahmed, Y., Nouri, A., and Wieschaus, E. (2002). Drosophila Apc1 and Apc2 regulate Wingless transduction throughout development. *Development* **129**, 1751-1762.
- Alexander, C. M., Reichsman, F., Hinkes, M. T., Lincecum, J., Becker, K. A., Cumberledge, S., and Bernfield, M. (2000). Syndecan-1 is required for Wnt-1-induced mammary tumorigenesis in mice. *Nat. Genet.* **25**, 329-332.
- Alexander, C. M., Selvarajan, S., Mudgett, J., and Werb, Z. (2001). Stromelysin-1 regulates adipogenesis during mammary gland involution. *J. Cell Biol.* **152**, 693-703.
- Alle, K. M., Henshall, S. M., Field, A. S., and Sutherland, R. L. (1998). Cyclin D1 protein is overexpressed in hyperplasia and intraductal carcinoma of the breast. *Clin. Cancer Res.* **4**, 847-854.
- Amit, S., Hatzubai, A., Birman, Y., Andersen, J. S., Ben Shushan, E., Mann, M., Ben Neria, Y., and Alkalay, I. (2002). Axin-mediated CKI phosphorylation of beta-catenin at Ser 45: a molecular switch for the Wnt pathway. *Genes Dev.* **16**, 1066-1076.
- Askham, J.M., Moncur, P., Markham, A.F., Morrison, E.E. (2000). Regulation and function of the interaction between the APC tumour suppressorprotein and EB1. *Oncogene.* **19**, 1950-1958.
- Axelrod, J. D., Miller, J. R., Shulman, J. M., Moon, R. T., and Perrimon, N. (1998). Differential recruitment of Dishevelled provides signaling specificity in the planar cell polarity and Wingless signaling pathways. *Genes Dev.* **12**, 2610-2622.
- Bafico, A., Liu, G., Yaniv, A., Gazit, A., and Aaronson, S. A. (2001). Novel mechanism of Wnt signalling inhibition mediated by Dickkopf-1 interaction with LRP6/Arrow. *Nat. Cell Biol.* **3**, 683-686.

- Barcellos-Hoff, M. H., Aggeler, J., Ram, T. G., and Bissell, M. J.** (1989). Functional differentiation and alveolar morphogenesis of primary mammary cultures on reconstituted basement membrane. *Development* **105**, 223-235.
- Bardos, J., Sulekova, Z., and Ballhausen, W. G.** (1997). Novel exon connections of the brain-specific (BS) exon of the adenomatous polyposis coli gene. *Int.J.Cancer* **73**, 137-142.
- Barlow, C., Schroeder, M., Lekstrom-Himes, J., Kylefjord, H., Deng, C. X., Wynshaw-Boris, A., Spiegelman, B. M., and Xanthopoulos, K. G.** (1997). Targeted expression of Cre recombinase to adipose tissue of transgenic mice directs adipose-specific excision of loxP-flanked gene segments. *Nucleic Acids Res.* **25**, 2543-2545.
- Bauer, D., Warthoe, P., Rohde, M., and Strauss, M.** (1994). Detection and differential display of expressed genes by DDRT-PCR. *PCR Methods Appl.* **4**, S97-108.
- Baylin, S. B., Herman, J. G., Graff, J. R., Vertino, P. M., and Issa, J. P.** (1998). Alterations in DNA methylation: a fundamental aspect of neoplasia. *Adv.Cancer Res.* **72**, 141-196.
- Beccari, T., Balducci, C., Aisa, M. C., Fazia, M. A., Servillo, G., and Orlacchio, A.** (2001). Promoter characterization and expression of the gene coding for the human GM2 activator protein. *Biosci.Rep.* **21**, 55-62.
- Behrens, J., von Kries, J. P., Kuhl, M., Bruhn, L., Wedlich, D., Grosschedl, R., and Birchmeier, W.** (1996). Functional interaction of beta-catenin with the transcription factor LEF-1. *Nature* **382**, 638-642.
- Behrens, J., Jerchow, B. A., Wurtele, M., Grimm, J., Asbrand, C., Wirtz, R., Kuhl, M., Wedlich, D., and Birchmeier, W.** (1998). Functional interaction of an axin homolog, conductin, with beta-catenin, APC, and GSK3beta. *Science* **280**, 596-599.
- Bellachioma, G., Stirling, J. L., Orlacchio, A., and Beccari, T.** (1993). Cloning and sequence analysis of a cDNA clone coding for the mouse GM2 activator protein. *Biochem.J.* **294** (Pt 1), 227-230.
- Ben Ze'ev, A. and Geiger, B.** (1998). Differential molecular interactions of beta-catenin and plakoglobin in adhesion, signaling and cancer. *Curr.Opin.Cell Biol.* **10**, 629-639.
- Bhanot, P., Brink, M., Samos, C. H., Hsieh, J. C., Wang, Y., Macke, J. P., Andrew, D., Nathans, J., and Nusse, R.** (1996). A new member of the frizzled family from Drosophila functions as a Wingless receptor. *Nature* **382**, 225-230.
- Bhanot, P., Fish, M., Jemison, J. A., Nusse, R., Nathans, J., and Cadigan, K. M.** (1999). Frizzled and Dfrizzled-2 function as redundant receptors for Wingless during Drosophila embryonic development. *Development* **126**, 4175-4186.
- Bienz, M.** (1999). APC: the plot thickens. *Curr.Opin.Genet.Dev.* **9**, 595-603.
- Bienz, M.** (2002). The subcellular destinations of APC proteins. *Nat.Rev.Mol.Cell Biol.* **3**, 328-338.
- Boudreau, N., Myers, C., and Bissell, M. J.** (1995). From Laminin to lamin: regulation of tissue-specific gene expression by the ECM. *Trends in Cell Biology* **5**, 1-4.
- Bradley, R. S. and Brown, A. M.** (1990). The proto-oncogene int-1 encodes a secreted protein associated with the extracellular matrix. *EMBO J.* **9**, 1569-1575.

- Brannon, M., Gomperts, M., Sumoy, L., Moon, R. T., and Kimelman, D.** (1997). A beta-catenin/XTcf-3 complex binds to the siamois promoter to regulate dorsal axis specification in *Xenopus*. *Genes Dev.* **11**, 2359-2370.
- Brisken, C., Park, S., Vass, T., Lydon, J. P., O'Malley, B. W., and Weinberg, R. A.** (1998). A paracrine role for the epithelial progesterone receptor in mammary gland development. *Proc.Natl.Acad.Sci.U.S.A* **95**, 5076-5081.
- Brisken, C., Kaur, S., Chavarria, T. E., Binart, N., Sutherland, R. L., Weinberg, R. A., Kelly, P. A., and Ormandy, C. J.** (1999). Prolactin controls mammary gland development via direct and indirect mechanisms. *Dev.Biol.* **210**, 96-106.
- Brisken, C., Heineman, A., Chavarria, T., Elenbaas, B., Tan, J., Dey, S. K., McMahon, J. A., McMahon, A. P., and Weinberg, R. A.** (2000). Essential function of Wnt-4 in mammary gland development downstream of progesterone signaling. *Genes Dev.* **14**, 650-654.
- Brown, A. M., Wildin, R. S., Prendergast, T. J., and Varmus, H. E.** (1986). A retrovirus vector expressing the putative mammary oncogene int-1 causes partial transformation of a mammary epithelial cell line. *Cell* **46**, 1001-1009.
- Brown, A. M., Papkoff, J., Fung, Y. K., Shackelford, G. M., and Varmus, H. E.** (1987). Identification of protein products encoded by the proto-oncogene int-1. *Mol.Cell Biol.* **7**, 3971-3977.
- Bryant, P. J., Watson, K. L., Justice, R. W., and Woods, D. F.** (1993). Tumor suppressor genes encoding proteins required for cell interactions and signal transduction in *Drosophila*. *Dev.Suppl* 239-249.
- Buchholz, F., Refaeli, Y., Trumpp, A., and Bishop, J. M.** (2000). Inducible chromosomal translocation of AML1 and ETO genes through Cre/loxP-mediated recombination in the mouse. *EMBO Rep.* **1**, 133-139.
- Buhler, T. A., Dale, T. C., Kieback, C., Humphreys, R. C., and Rosen, J. M.** (1993). Localization and quantification of Wnt-2 gene expression in mouse mammary development. *Dev.Biol.* **155**, 87-96.
- Bui, T. D., Rankin, J., Smith, K., Huguet, E. L., Ruben, S., Strachan, T., Harris, A. L., and Lindsay, S.** (1997). A novel human Wnt gene, WNT10B, maps to 12q13 and is expressed in human breast carcinomas. *Oncogene* **14**, 1249-1253.
- Cabrera, C. V., Alonso, M. C., Johnston, P., Phillips, R. G., and Lawrence, P. A.** (1987). Phenocopies induced with antisense RNA identify the wingless gene. *Cell* **50**, 659-663.
- Cadigan, K. M. and Nusse, R.** (1997). Wnt signaling: a common theme in animal development. *Genes Dev.* **11**, 3286-3305.
- Callahan, R. and Smith, G. H.** (2000). MMTV-induced mammary tumorigenesis: gene discovery, progression to malignancy and cellular pathways. *Oncogene* **19**, 992-1001.
- Callard, D., Lescure, B., and Mazzolini, L.** (1994). A method for the elimination of false positives generated by the mRNA differential display technique. *Biotechniques* **16**, 1096-3.
- Chakrabarti, A., Matthews, G., Colman, A., and Dale, L.** (1992). Secretory and inductive properties of *Drosophila* wingless protein in *Xenopus* oocytes and embryos. *Development* **115**, 355-369.

- Chapman, R. S., Lourenco, P. C., Tonner, E., Flint, D. J., Selbert, S., Takeda, K., Akira, S., Clarke, A. R., and Watson, C. J.** (1999). Suppression of epithelial apoptosis and delayed mammary gland involution in mice with a conditional knockout of Stat3. *Genes Dev.* **13**, 2604-2616.
- Chen, C. M. and Struhl, G.** (1999). Wingless transduction by the Frizzled and Frizzled2 proteins of *Drosophila*. *Development* **126**, 5441-5452.
- Chomczynski, P. and Sacchi, N.** (1987). Single-step method of RNA isolation by acid guanidinium thiocyanate-phenol-chloroform extraction. *Anal. Biochem.* **162**, 156-159.
- Christian, J. L., McMahon, J. A., McMahon, A. P., and Moon, R. T.** (1991). Xwnt-8, a *Xenopus* Wnt-1/int-1-related gene responsive to mesoderm-inducing growth factors, may play a role in ventral mesodermal patterning during embryogenesis. *Development* **111**, 1045-1055.
- Coleman, S., Silberstein, G. B., and Daniel, C. W.** (1988). Ductal morphogenesis in the mouse mammary gland: evidence supporting a role for epidermal growth factor. *Dev. Biol.* **127**, 304-315.
- Collins, E. C., Pannell, R., Simpson, E. M., Forster, A., and Rabbitts, T. H.** (2000). Inter-chromosomal recombination of Mll and Af9 genes mediated by cre-loxP in mouse development. *EMBO Rep.* **1**, 127-132.
- Cumberledge, S. and Reichsman, F.** (1997). Glycosaminoglycans and WNTs: just a spoonful of sugar helps the signal go down. *Trends Genet.* **13**, 421-423.
- Dale, T. C., Weber-Hall, S. J., Smith, K., Huguet, E. L., Jayatilake, H., Gusterson, B. A., Shuttleworth, G., O'Hare, M., and Harris, A. L.** (1996). Compartment switching of WNT-2 expression in human breast tumors. *Cancer Res.* **56**, 4320-4323.
- Daniel, C. W., Berger, J. J., Strickland, P., and Garcia, R.** (1984). Similar growth pattern of mouse mammary epithelium cultivated in collagen matrix in vivo and in vitro. *Dev. Biol.* **104**, 57-64.
- Dhoot, G. K., Gustafsson, M. K., Ai, X., Sun, W., Standiford, D. M., and Emerson, C. P., Jr.** (2001). Regulation of Wnt signaling and embryo patterning by an extracellular sulfatase. *Science* **293**, 1663-1666.
- Dickson, C., Smith, R., Brookes, S., and Peters, G.** (1984). Tumorigenesis by mouse mammary tumor virus: proviral activation of a cellular gene in the common integration region int-2. *Cell* **37**, 529-536.
- Dikovskaya, D., Zumbunn, J., Penman, G. A., and Nathke, I. S.** (2001). The adenomatous polyposis coli protein: in the limelight out at the edge. *Trends Cell Biol.* **11**, 378-384.
- Doppler, W., Hock, W., Hofer, P., Groner, B., and Ball, R. K.** (1990). Prolactin and glucocorticoid hormones control transcription of the beta-casein gene by kinetically distinct mechanisms. *Mol. Endocrinol.* **4**, 912-919.
- Du, S. J., Purcell, S. M., Christian, J. L., McGrew, L. L., and Moon, R. T.** (1995). Identification of distinct classes and functional domains of Wnts through expression of wild-type and chimeric proteins in *Xenopus* embryos. *Mol. Cell Biol.* **15**, 2625-2634.
- Edwards, P. A., Hiby, S. E., Papkoff, J., and Bradbury, J. M.** (1992). Hyperplasia of mouse mammary epithelium induced by expression of the Wnt-1 (int-1) oncogene in reconstituted mammary gland. *Oncogene* **7**, 2041-2051.

- Esteller, M., Sparks, A., Toyota, M., Sanchez-Cespedes, M., Capella, G., Peinado, M. A., Gonzalez, S., Tarafa, G., Sidransky, D., Meltzer, S. J., Baylin, S. B., and Herman, J. G.** (2000). Analysis of adenomatous polyposis coli promoter hypermethylation in human cancer. *Cancer Res.* **60**, 4366-4371.
- Fagotto, F., Jho, E., Zeng, L., Kurth, T., Joos, T., Kaufmann, C., and Costantini, F.** (1999). Domains of axin involved in protein-protein interactions, Wnt pathway inhibition, and intracellular localization. *J. Cell Biol.* **145**, 741-756.
- Fan, M. J., Gruning, W., Walz, G., and Sokol, S. Y.** (1998). Wnt signaling and transcriptional control of Siamois in *Xenopus* embryos. *Proc. Natl. Acad. Sci. U.S.A* **95**, 5626-5631.
- Farini, E. and Whitelaw, C. B.** (1995). Ectopic expression of beta-lactoglobulin transgenes. *Mol. Gen. Genet.* **246**, 734-738.
- Fata, J. E., Leco, K. J., Moorehead, R. A., Martin, D. C., and Khokha, R.** (1999). Timp-1 is important for epithelial proliferation and branching morphogenesis during mouse mammary development. *Dev. Biol.* **211**, 238-254.
- Feil, R., Brocard, J., Mascrez, B., LeMeur, M., Metzger, D., and Chambon, P.** (1996). Ligand-activated site-specific recombination in mice. *Proc. Natl. Acad. Sci. U.S.A* **93**, 10887-10890.
- Fodde, R., Edelmann, W., Yang, K., van Leeuwen, C., Carlson, C., Renault, B., Breukel, C., Alt, E., Lipkin, M., Khan, P. M., and .** (1994). A targeted chain-termination mutation in the mouse *Apc* gene results in multiple intestinal tumors. *Proc. Natl. Acad. Sci. U.S.A* **91**, 8969-8973.
- Fodde, R., Kuipers, J., Rosenberg, C., Smits, R., Kielman, M., Gaspar, C., van Es, J. H., Breukel, C., Wiegant, J., Giles, R. H., and Clevers, H.** (2001). Mutations in the APC tumour suppressor gene cause chromosomal instability. *Nat. Cell Biol.* **3**, 433-438.
- Furuuchi, K., Tada, M., Yamada, H., Kataoka, A., Furuuchi, N., Hamada, J., Takahashi, M., Todo, S., and Moriuchi, T.** (2000). Somatic mutations of the APC gene in primary breast cancers. *Am. J. Pathol.* **156**, 1997-2005.
- Galea, M. A., Eleftheriou, A., and Henderson, B. R.** (2001). ARM domain-dependent nuclear import of adenomatous polyposis coli protein is stimulated by the B56 alpha subunit of protein phosphatase 2A. *J. Biol. Chem.* **276**, 45833-45839.
- Gallagher, R. C., Hay, T., Meniel, V., Naughton, C., Anderson, T. J., Shibata, H., Ito, M., Clevers, H., Noda, T., Sansom, O. J., Mason, J. O., and Clarke, A. R.** (2002). Inactivation of *Apc* perturbs mammary development, but only directly results in acanthoma in the context of Tcf-1 deficiency. *Oncogene* **21**, 6446-6457.
- Gavin, B. J. and McMahon, A. P.** (1992). Differential regulation of the Wnt gene family during pregnancy and lactation suggests a role in postnatal development of the mammary gland. *Mol. Cell Biol.* **12**, 2418-2423.
- Groden, J., Thliveris, A., Samowitz, W., Carlson, M., Gelbert, L., Albertsen, H., Joslyn, G., Stevens, J., Spirio, L., Robertson, M., Sargeant, L., Krapcho, K., Wolff, E., Burt, R., Hughes, J., Warrington, J., McPherson, J., Wasmuth, J., Le Paslier, D., Abderrahim, H., Cohen, D., Leppert, M., and White, R.** (1991). Identification and characterization of the familial adenomatous polyposis coli gene. *Cell* **66**, 589-600.
- Groden, J., Joslyn, G., Samowitz, W., Jones, D., Bhattacharyya, N., Spirio, L., Thliveris, A., Robertson, M., Egan, S., Meuth, M., and White, R.** (1995). Response of colon cancer cell

- lines to the introduction of APC, a colon-specific tumour suppressor gene. *Cancer Res.* **55**, 1531-1539.
- Gu, H., Marth, J. D., Orban, P. C., Mossmann, H., and Rajewsky, K.** (1994). Deletion of a DNA polymerase beta gene segment in T cells using cell type-specific gene targeting. *Science* **265**, 103-106.
- Guger, K. A. and Gumbiner, B. M.** (2000). A mode of regulation of beta-catenin signaling activity in *Xenopus* embryos independent of its levels. *Dev.Biol.* **223**, 441-448.
- Gumbiner, B. M.** (1995). Signal transduction of beta-catenin. *Curr.Opin.Cell Biol.* **7**, 634-640.
- Guru, S. C., Agarwal, S. K., Manickam, P., Olufemi, S. E., Crabtree, J. S., Weisemann, J. M., Kester, M. B., Kim, Y. S., Wang, Y., Emmert-Buck, M. R., Liotta, L. A., Spiegel, A. M., Boguski, M. S., Roe, B. A., Collins, F. S., Marx, S. J., Burns, L., and Chandrasekharappa, S. C.** (1997). A transcript map for the 2.8-Mb region containing the multiple endocrine neoplasia type 1 locus. *Genome Res.* **7**, 725-735.
- Gustafsson, E., Brakebusch, C., Hietanen, K., and Fassler, R.** (2001). Tie-1-directed expression of Cre recombinase in endothelial cells of embryoid bodies and transgenic mice. *J.Cell Sci.* **114**, 671-676.
- Ha, H. Y., Moon, H. B., Nam, M. S., Lee, J. W., Ryoo, Z. Y., Lee, T. H., Lee, K. K., So, B. J., Sato, H., Seiki, M., and Yu, D. Y.** (2001). Overexpression of membrane-type matrix metalloproteinase-1 gene induces mammary gland abnormalities and adenocarcinoma in transgenic mice. *Cancer Res.* **61**, 984-990.
- Hadsell, D. L., Greenberg, N. M., Fligger, J. M., Baumrucker, C. R., and Rosen, J. M.** (1996). Targeted expression of des(1-3) human insulin-like growth factor I in transgenic mice influences mammary gland development and IGF-binding protein expression. *Endocrinology* **137**, 321-330.
- Haggitt, R. C. and Reid, B. J.** (1986). Hereditary gastrointestinal polyposis syndromes. *Am.J.Surg.Pathol.* **10**, 871-887.
- Hamada, F., Murata, Y., Nishida, A., Fujita, F., Tomoyasu, Y., Nakamura, M., Toyoshima, K., Tabata, T., Ueno, N., and Akiyama, T.** (1999). Identification and characterization of E-APC, a novel *Drosophila* homologue of the tumour suppressor APC. *Genes Cells* **4**, 465-474.
- Hamada, F. and Bienz, M.** (2002). A *Drosophila* APC tumour suppressor homologue functions in cellular adhesion. *Nat.Cell Biol.* **4**, 208-213.
- Hamilton, S. R., Liu, B., Parsons, R. E., Papadopoulos, N., Jen, J., Powell, S. M., Krush, A. J., Berk, T., Cohen, Z., Tetu, B., and .** (1995). The molecular basis of Turcot's syndrome. *N.Engl.J.Med.* **332**, 839-847.
- Han, M.** (1997). Gut reaction to Wnt signaling in worms. *Cell* **90**, 581-584.
- Harada, N., Tamai, Y., Ishikawa, T., Sauer, B., Takaku, K., Oshima, M., and Taketo, M. M.** (1999). Intestinal polyposis in mice with a dominant stable mutation of the beta-catenin gene. *EMBO J.* **18**, 5931-5942.
- Hart, M. J., de los, S. R., Albert, I. N., Rubinfeld, B., and Polakis, P.** (1998). Downregulation of beta-catenin by human Axin and its association with the APC tumor suppressor, beta-catenin and GSK3 beta. *Curr.Biol.* **8**, 573-581.

- Hayashi, K.** (1991). PCR-SSCP: a simple and sensitive method for detection of mutations in the genomic DNA. *PCR Methods Appl.* **1**, 34-38.
- Hayashi, S., Rubinfeld, B., Souza, B., Polakis, P., Wieschaus, E., and Levine, A. J.** (1997). A Drosophila homolog of the tumor suppressor gene adenomatous polyposis coli down-regulates beta-catenin but its zygotic expression is not essential for the regulation of Armadillo. *Proc.Natl.Acad.Sci.U.S.A* **94**, 242-247.
- Hayashi, S. and McMahon, A. P.** (2002). Efficient recombination in diverse tissues by a tamoxifen-inducible form of Cre: a tool for temporally regulated gene activation/inactivation in the mouse. *Dev.Biol.* **244**, 305-318.
- He, T. C., Sparks, A. B., Rago, C., Hermeking, H., Zawel, L., da Costa, L. T., Morin, P. J., Vogelstein, B., and Kinzler, K. W.** (1998). Identification of c-MYC as a target of the APC pathway. *Science* **281**, 1509-1512.
- He, X., Saint-Jeannet, J. P., Wang, Y., Nathans, J., Dawid, I., and Varmus, H.** (1997). A member of the Frizzled protein family mediating axis induction by Wnt- 5A. *Science* **275**, 1652-1654.
- Henderson, B. R.** (2000). Nuclear-cytoplasmic shuttling of APC regulates beta-catenin subcellular localization and turnover. *Nat.Cell Biol.* **2**, 653-660.
- Hennighausen, L. and Robinson, G. W.** (1998). Think globally, act locally: the making of a mouse mammary gland. *Genes Dev.* **12**, 449-455.
- Hennighausen, L. and Robinson, G. W.** (2001). Signaling pathways in mammary gland development. *Dev.Cell* **1**, 467-475.
- Hennighausen, L. G. and Sippel, A. E.** (1982). Characterization and cloning of the mRNAs specific for the lactating mouse mammary gland. *Eur.J.Biochem.* **125**, 131-141.
- Hiltunen, M. O., Alhonen, L., Koistinaho, J., Myohanen, S., Paakkonen, M., Marin, S., Kosma, V. M., and Janne, J.** (1997). Hypermethylation of the APC (adenomatous polyposis coli) gene promoter region in human colorectal carcinoma. *Int.J.Cancer* **70**, 644-648.
- Hinck, L., Nathke, I.S., Papkoff, J., and Nelson, W.J.** (1994). Dynamics of cadherin/catenin complex formation; novel protein interactions and pathways of complex assembly. *J. Cell Biol.* **125**, 1327-40
- Hirschl, D., Bayer, P., and Muller, O.** (1996). Secondary structure of an armadillo single repeat from the APC protein. *FEBS Lett.* **383**, 31-36.
- Ho, K. Y., Kalle, W. H., Lo, T. H., Lam, W. Y., and Tang, C. M.** (1999). Reduced expression of APC and DCC gene protein in breast cancer. *Histopathology* **35**, 249-256.
- Hoier, E. F., Mohler, W. A., Kim, S. K., and Hajnal, A.** (2000). The Caenorhabditis elegans APC-related gene apr-1 is required for epithelial cell migration and Hox gene expression. *Genes Dev.* **14**, 874-886.
- Hollyday, M., McMahon, J. A., and McMahon, A. P.** (1995). Wnt expression patterns in chick embryo nervous system. *Mech.Dev.* **52**, 9-25.
- Horii, A., Nakatsuru, S., Icgii, S., Nagase, H., and Nakamura, Y.** (1993) Multiple forms of the APC gene transcripts and their alternative splicing in the region 5' to exon 1 of the APC gene. *Human Mol. Genet.* **2**, 283-287.

- Horseman, N. D.** (1999). Prolactin and mammary gland development. *J.Mammary.Gland.Biol.Neoplasia*. **4**, 79-88.
- Hsieh, J. C., Kodjabachian, L., Rebbert, M. L., Rattner, A., Smallwood, P. M., Samos, C. H., Nusse, R., Dawid, I. B., and Nathans, J.** (1999). A new secreted protein that binds to Wnt proteins and inhibits their activities. *Nature* **398**, 431-436.
- Hsu, S. C., Galceran, J., and Grosschedl, R.** (1998). Modulation of transcriptional regulation by LEF-1 in response to Wnt-1 signaling and association with beta-catenin. *Mol.Cell Biol.* **18**, 4807-4818.
- Hsu, W., Zeng, L., and Costantini, F.** (1999). Identification of a domain of Axin that binds to the serine/threonine protein phosphatase 2A and a self-binding domain. *J.Biol.Chem.* **274**, 3439-3445.
- Huang, H., Mahler-Araujo, B. M., Sankila, A., Chimelli, L., Yonekawa, Y., Kleihues, P., and Ohgaki, H.** (2000). APC mutations in sporadic medulloblastomas. *Am.J.Pathol.* **156**, 433-437.
- Huber, A. H., Nelson, W. J., and Weis, W. I.** (1997). Three-dimensional structure of the armadillo repeat region of beta- catenin. *Cell* **90**, 871-882.
- Huguet, E. L., McMahon, J. A., McMahon, A. P., Bicknell, R., and Harris, A. L.** (1994). Differential expression of human Wnt genes 2, 3, 4, and 7B in human breast cell lines and normal and disease states of human breast tissue. *Cancer Res.* **54**, 2615-2621.
- Hulsken, J., Birchmeier, W., and Behrens, J.** (1994). E-cadherin and APC compete for the interaction with beta-catenin and the cytoskeleton. *J.Cell Biol.* **127**, 2061-2069.
- Huttenhofer, A., Kiefmann, M., Meier-Ewert, S., O'Brien, J., Lehrach, H., Bachellerie, J. P., and Brosius, J.** (2001). RNomics: an experimental approach that identifies 201 candidates for novel, small, non-messenger RNAs in mouse. *EMBO J.* **20**, 2943-2953.
- Ihle, J. N.** (1996). STATs: signal transducers and activators of transcription. *Cell* **84**, 331-334.
- Ikeda, S., Kishida, S., Yamamoto, H., Murai, H., Koyama, S., and Kikuchi, A.** (1998). Axin, a negative regulator of the Wnt signaling pathway, forms a complex with GSK-3beta and beta-catenin and promotes GSK-3beta- dependent phosphorylation of beta-catenin. *EMBO J.* **17**, 1371-1384.
- Ilyas, M. and Tomlinson, I. P.** (1997). The interactions of APC, E-cadherin and beta-catenin in tumour development and progression. *J.Pathol.* **182**, 128-137.
- Imbert, A., Eelkema, R., Jordan, S., Feiner, H., and Cowin, P.** (2001). Delta N89 beta-catenin induces precocious development, differentiation, and neoplasia in mammary gland. *J.Cell Biol.* **153**, 555-568.
- Itoh, H., Hirata, K., and Ohsato, K.** (1993). Turcot's syndrome and familial adenomatous polyposis associated with brain tumor: review of related literature. *Int.J.Colorectal Dis.* **8**, 87-94.
- Jimbo, T., Kawasaki, Y., Koyama, R., Sato, R., Takada, S., Haraguchi, K., and Akiyama, T.** (2002). Identification of a link between the tumour suppressor APC and the kinesin superfamily. *Nature Cell Biology* **4**, 323-327.
- Jin, Z., Tamura, G., Tsuchiya, T., Sakata, K., Kashiwaba, M., Osakabe, M., and Motoyama, T.** (2001). Adenomatous polyposis coli (APC) gene promoter hypermethylation in primary breast cancers. *Br.J.Cancer* **85**, 69-73.

- Joslyn, G., Carlson, M., Thliveris, A., Albertsen, H., Gelbert, L., Samowitz, W., Groden, J., Stevens, J., Spirio, L., Robertson, M., and . (1991). Identification of deletion mutations and three new genes at the familial polyposis locus. *Cell* **66**, 601-613.
- Joslyn, G., Richardson, D. S., White, R., and Alber, T. (1993). Dimer formation by an N-terminal coiled coil in the APC protein. *Proc.Natl.Acad.Sci.U.S.A* **90**, 11109-11113.
- Kaplan, K. B., Burds, A. A., Swedlow, J. R., Bekir, S. S., Sorger, P. K., and Nathke, I. S. (2001). A role for the Adenomatous Polyposis Coli protein in chromosome segregation. *Nat.Cell Biol.* **3**, 429-432.
- Kashiwaba, M., Tamura, G., and Ishida, M. (1994). Aberrations of the APC gene in primary breast carcinoma. *J.Cancer Res.Clin.Oncol.* **120**, 727-731.
- Kawasaki, Y., Senda, T., Ishidate, T., Koyama, R., Morishita, T., Iwayama, Y., Higuchi, O., Akiyama, T. (2000). Asef, a link between the tumour suppressor APC and G-protein signaling. *Science* **289**, 1194-1197
- Keely, P. J., Wu, J. E., and Santoro, S. A. (1995). The spatial and temporal expression of the alpha 2 beta 1 integrin and its ligands, collagen I, collagen IV, and laminin, suggest important roles in mouse mammary morphogenesis. *Differentiation* **59**, 1-13.
- Kintner, C. (1992). Regulation of embryonic cell adhesion by the cadherin cytoplasmic domain. *Cell* **69**, 225-236.
- Kinzler, K. W., Nilbert, M. C., Su, L. K., Vogelstein, B., Bryan, T. M., Levy, D. B., Smith, K. J., Preisinger, A. C., Hedge, P., McKechnie, D., and . (1991). Identification of FAP locus genes from chromosome 5q21. *Science* **253**, 661-665.
- Kinzler, K. W. and Vogelstein, B. (1996). Lessons from hereditary colorectal cancer. *Cell* **87**, 159-170.
- Kishida, S., Yamamoto, H., Hino, S., Ikeda, S., Kishida, M., and Kikuchi, A. (1999). DIX domains of Dvl and axin are necessary for protein interactions and their ability to regulate beta-catenin stability. *Mol.Cell Biol.* **19**, 4414-4422.
- Klima, H., Tanaka, A., Schnabel, D., Nakano, T., Schroder, M., Suzuki, K., and Sandhoff, K. (1991). Characterization of full-length cDNAs and the gene coding for the human GM2 activator protein. *FEBS Lett.* **289**, 260-264.
- Klinowska, T. C., Soriano, J. V., Edwards, G. M., Oliver, J. M., Valentijn, A. J., Montesano, R., and Streuli, C. H. (1999). Laminin and beta1 integrins are crucial for normal mammary gland development in the mouse. *Dev.Biol.* **215**, 13-32.
- Korach, K. S., Couse, J. F., Curtis, S. W., Washburn, T. F., Lindzey, J., Kimbro, K. S., Eddy, E. M., Migliaccio, S., Snedeker, S. M., Lubahn, D. B., Schomberg, D. W., and Smith, E. P. (1996). Estrogen receptor gene disruption: molecular characterization and experimental and clinical phenotypes. *Recent Prog.Horm.Res.* **51**, 159-186.
- Kordon, E. C. and Smith, G. H. (1998). An entire functional mammary gland may comprise the progeny from a single cell. *Development* **125**, 1921-1930.
- Kuhl, M., Sheldahl, L. C., Park, M., Miller, J. R., and Moon, R. T. (2000). The Wnt/Ca2+ pathway: a new vertebrate Wnt signaling pathway takes shape. *Trends Genet.* **16**, 279-283.

- Kuhl, M., Sheldahl, L. C., Malbon, C. C., and Moon, R. T.** (2000). Ca²⁺/calmodulin-dependent protein kinase II is stimulated by Wnt and Frizzled homologs and promotes ventral cell fates in *Xenopus*. *J.Biol.Chem.* **275**, 12701-12711.
- Kuhn, R., Schwenk, F., Aguet, M., and Rajewsky, K.** (1995). Inducible gene targeting in mice. *Science* **269**, 1427-1429.
- Laird, P. W., Jackson-Grusby, L., Fazeli, A., Dickinson, S. L., Jung, W. E., Li, E., Weinberg, R. A., and Jaenisch, R.** (1995). Suppression of intestinal neoplasia by DNA hypomethylation. *Cell* **81**, 197-205.
- Laken, S. J., Petersen, G. M., Gruber, S. B., Oddoux, C., Ostrer, H., Giardiello, F. M., Hamilton, S. R., Hampel, H., Markowitz, A., Klimstra, D., Jhanwar, S., Winawer, S., Offit, K., Luce, M. C., Kinzler, K. W., and Vogelstein, B.** (1997). Familial colorectal cancer in Ashkenazim due to a hypermutable tract in APC. *Nat.Genet.* **17**, 79-83.
- Lako, M., Lindsay, S., Bullen, P., Wilson, D. I., Robson, S. C., and Strachan, T.** (1998). A novel mammalian wnt gene, WNT8B, shows brain-restricted expression in early development, with sharply delimited expression boundaries in the developing forebrain. *Hum.Mol.Genet.* **7**, 813-822.
- Lamlum, H., Ilyas, M., Rowan, A., Clark, S., Johnson, V., Bell, J., Frayling, I., Efstathiou, J., Pack, K., Payne, S., Roylance, R., Gorman, P., Sheer, D., Neale, K., Phillips, R., Talbot, I., Bodmer, W., and Tomlinson, I.** (1999). The type of somatic mutation at APC in familial adenomatous polyposis is determined by the site of the germline mutation: a new facet to Knudson's 'two-hit' hypothesis. *Nat.Med.* **5**, 1071-1075.
- Lane, T. F. and Leder, P.** (1997). Wnt-10b directs hypermorphic development and transformation in mammary glands of male and female mice. *Oncogene* **15**, 2133-2144.
- Larabell, C. A., Torres, M., Rowning, B. A., Yost, C., Miller, J. R., Wu, M., Kimelman, D., and Moon, R. T.** (1997). Establishment of the dorso-ventral axis in *Xenopus* embryos is presaged by early asymmetries in beta-catenin that are modulated by the Wnt signaling pathway. *J.Cell Biol.* **136**, 1123-1136.
- Larsson, C., Skogseid, B., Oberg, K., Nakamura, Y., and Nordenskjold, M.** (1988). Multiple endocrine neoplasia type 1 gene maps to chromosome 11 and is lost in insulinoma. *Nature* **332**, 85-87.
- Laurent, M. N., Blitz, I. L., Hashimoto, C., Rothbacher, U., and Cho, K. W.** (1997). The *Xenopus* homeobox gene *twin* mediates Wnt induction of gooseoid in establishment of Spemann's organizer. *Development* **124**, 4905-4916.
- Lee, F. S., Lane, T. F., Kuo, A., Shackelford, G. M., and Leder, P.** (1995). Insertional mutagenesis identifies a member of the Wnt gene family as a candidate oncogene in the mammary epithelium of int-2/Fgf-3 transgenic mice. *Proc.Natl.Acad.Sci.U.S.A* **92**, 2268-2272.
- Lejeune, S., Huguet, E. L., Hamby, A., Poulson, R., and Harris, A. L.** (1995). Wnt5a cloning, expression, and up-regulation in human primary breast cancers. *Clin.Cancer Res.* **1**, 215-222.
- Levy, D. B., Smith, K. J., Beazer-Barclay, Y., Hamilton, S. R., Vogelstein, B., and Kinzler, K. W.** (1994). Inactivation of both APC alleles in human and mouse tumors. *Cancer Res.* **54**, 5953-5958.
- Li, F., Barnathan, E. S., and Kariko, K.** (1994). Rapid method for screening and cloning cDNAs generated in differential mRNA display: application of northern blot for affinity capturing of cDNAs. *Nucleic Acids Res.* **22**, 1764-1765.

- Li, L., Yuan, H., Weaver, C. D., Mao, J., Farr, G. H., III, Sussman, D. J., Jonkers, J., Kimelman, D., and Wu, D. (1999). Axin and Frat1 interact with dvl and GSK, bridging Dvl to GSK in Wnt- mediated regulation of LEF-1. *EMBO J.* **18**, 4233-4240.
- Li, Y., Hively, W. P., and Varmus, H. E. (2000). Use of MMTV-Wnt-1 transgenic mice for studying the genetic basis of breast cancer. *Oncogene* **19**, 1002-1009.
- Liang, P. and Pardee, A. B. (1992). Differential display of eukaryotic messenger RNA by means of the polymerase chain reaction. *Science* **257**, 967-971.
- Liang, P. and Pardee, A. B. (1997). Differential display. A general protocol. *Methods Mol.Biol.* **85**, 3-11.
- Lin, S. Y., Xia, W., Wang, J. C., Kwong, K. Y., Spohn, B., Wen, Y., Pestell, R. G., and Hung, M. C. (2000). Beta-catenin, a novel prognostic marker for breast cancer: its roles in cyclin D1 expression and cancer progression. *Proc.Natl.Acad.Sci.U.S.A* **97**, 4262-4266.
- Lin, X. and Perrimon, N. (1999). Dally cooperates with Drosophila Frizzled 2 to transduce Wingless signalling. *Nature* **400**, 281-284.
- Liotta, L. A., Rao, C. N., and Barsky, S. H. (1983). Tumor invasion and the extracellular matrix. *Lab Invest* **49**, 636-649.
- Liu, C., Li, Y., Semenov, M., Han, C., Baeg, G. H., Tan, Y., Zhang, Z., Lin, X., and He, X. (2002). Control of beta-catenin phosphorylation/degradation by a dual-kinase mechanism. *Cell* **108**, 837-847.
- Liu, X., Robinson, G. W., Wagner, K. U., Garrett, L., Wynshaw-Boris, A., and Hennighausen, L. (1997). Stat5a is mandatory for adult mammary gland development and lactogenesis. *Genes Dev.* **11**, 179-186.
- Lochter, A. and Bissell, M. J. (1995). Involvement of extracellular matrix constituents in breast cancer. *Semin.Cancer Biol.* **6**, 165-173.
- Lund, L. R., Bjorn, S. F., Sternlicht, M. D., Nielsen, B. S., Solberg, H., Usher, P. A., Osterby, R., Christensen, I. J., Stephens, R. W., Bugge, T. H., Dano, K., and Werb, Z. (2000). Lactational competence and involution of the mouse mammary gland require plasminogen. *Development* **127**, 4481-4492.
- Luongo, C., Gould, K., Su, L., Kinzler, K., Vogelstein, B., Dietrich, W., Lander, E., and Moser, A. R. (1993). Mapping of multiple intestinal neoplasia (Min) to proximal chromosome 18 of the mouse. *Genomics.* **15**, 3-8.
- Luongo, C., Moser, A. R., Gledhill, S., and Dove, W. F. (1994). Loss of Apc⁺ in intestinal adenomas from Min mice. *Cancer Res.* **54**, 5947-5952.
- MacArthur, C. A., Shankar, D. B., and Shackleford, G. M. (1995). Fgf-8, activated by proviral insertion, cooperates with the Wnt-1 transgene in murine mammary tumorigenesis. *J.Virol.* **69**, 2501-2507.
- Mahmoud, N. N., Boolbol, S. K., Bilinski, R. T., Martucci, C., Chadburn, A., and Bertagnolli, M. M. (1997). Apc gene mutation is associated with a dominant-negative effect upon intestinal cell migration. *Cancer Res.* **57**, 5045-5050.
- Mahmoud, N. N., Bilinski, R. T., Churchill, M. R., Edelmann, W., Kucherlapati, R., and Bertagnolli, M. M. (1999). Genotype-phenotype correlation in murine Apc mutation: differences in enterocyte migration and response to sulindac. *Cancer Res.* **59**, 353-359.

- Mahuran, D. J.** (1998). The GM2 activator protein, its roles as a co-factor in GM2 hydrolysis and as a general glycolipid transport protein. *Biochim.Biophys.Acta* **1393**, 1-18.
- Mahuran, D. J.** (1999). Biochemical consequences of mutations causing the GM2 gangliosidosis. *Biochim.Biophys.Acta* **1455**, 105-138.
- Mao, B., Wu, W., Li, Y., Hoppe, D., Stannek, P., Glinka, A., and Niehrs, C.** (2001). LDL-receptor-related protein 6 is a receptor for Dickkopf proteins. *Nature* **411**, 321-325.
- Mason, J. O., Kitajewski, J., and Varmus, H. E.** (1992). Mutational analysis of mouse Wnt-1 identifies two temperature-sensitive alleles and attributes of Wnt-1 protein essential for transformation of a mammary cell line. *Mol.Biol.Cell* **3**, 521-533.
- Mathieu-Daude, F., Welsh, J., Vogt, T., and McClelland, M.** (1996). DNA rehybridization during PCR: the 'Cot effect' and its consequences. *Nucleic Acids Res.* **24**, 2080-2086.
- Matsumine, A., Ogai, A., Senda, T., Okumura, N., Satoh, K., Baeg, G. H., Kawahara, T., Kobayashi, S., Okada, M., Toyoshima, K., and Akiyama, T.** (1996). Binding of APC to the human homolog of the Drosophila discs large tumor suppressor protein. *Science* **272**, 1020-1023.
- Mayer, U., Mann, K., Timpl, R., and Murphy, G.** (1993). Sites of nidogen cleavage by proteases involved in tissue homeostasis and remodelling. *Eur.J.Biochem.* **217**, 877-884.
- McCartney, B. M., Dierick, H. A., Kirkpatrick, C., Moline, M. M., Baas, A., Peifer, M., and Bejsovec, A.** (1999). Drosophila APC2 is a cytoskeletally-associated protein that regulates wingless signaling in the embryonic epidermis. *J.Cell Biol.* **146**, 1303-1318.
- McKendry, R., Hsu, S. C., Harland, R. M., and Grosschedl, R.** (1997). LEF-1/TCF proteins mediate wnt-inducible transcription from the Xenopus nodal-related 3 promoter. *Dev.Biol.* **192**, 420-431.
- McMahon, A. P. and Moon, R. T.** (1989). Ectopic expression of the proto-oncogene int-1 in Xenopus embryos leads to duplication of the embryonic axis. *Cell* **58**, 1075-1084.
- McMahon, A. P. and Moon, R. T.** (1989). int-1--a proto-oncogene involved in cell signalling. *Development* **107 Suppl**, 161-167.
- Medeiros, A. C., Nagai, M. A., Neto, M. M., and Brentani, R. R.** (1994). Loss of heterozygosity affecting the APC and MCC genetic loci in patients with primary breast carcinomas. *Cancer Epidemiol.Biomarkers Prev.* **3**, 331-333.
- Michaelson, J. S. and Leder, P.** (2001). beta-catenin is a downstream effector of Wnt-mediated tumorigenesis in the mammary gland. *Oncogene* **20**, 5093-5099.
- Midgley, C. A., White, S., Howitt, R., Save, V., Dunlop, M. G., Hall, P. A., Lane, D. P., Wyllie, A. H., and Bubb, V. J.** (1997). APC expression in normal human tissues. *J.Pathol.* **181**, 426-433.
- Miele, G., MacRae, L., McBride, D., Manson, J., and Clinton, M.** (1998). Elimination of false positives generated through PCR re-amplification of differential display cDNA. *Biotechniques* **25**, 138-144.
- Miele, G., Slee, R., Manson, J., and Clinton, M.** (1999). A rapid protocol for the authentication of isolated differential display RT-PCR CDNAs. *Prep.Biochem.Biotechnol.* **29**, 245-255.

- Miller, J. R., Hocking, A. M., Brown, J. D., and Moon, R. T. (1999). Mechanism and function of signal transduction by the Wnt/beta-catenin and Wnt/Ca²⁺ pathways. *Oncogene* **18**, 7860-7872.
- Mimori-Kiyosue, Y., Shiina, N., and Tsukita, S. (2000). Adenomatous polyposis coli (APC) protein moves along microtubules and concentrates at their growing ends in epithelial cells. *J. Cell Biol.* **148**, 505-518.
- Miyaki, M., Konishi, M., Kikuchi-Yanoshita, R., Enomoto, M., Tanaka, K., Takahashi, H., Muraoka, M., Mori, T., Konishi, F., and Iwama, T. (1993). Coexistence of somatic and germ-line mutations of APC gene in desmoid tumors from patients with familial adenomatous polyposis. *Cancer Res.* **53**, 5079-5082.
- Miyoshi, K., Shillingford, J. M., Le Provost, F., Gounari, F., Bronson, R., von Boehmer, H., Taketo, M. M., Cardiff, R. D., Hennighausen, L., and Khazaie, K. (2002). Activation of beta -catenin signaling in differentiated mammary secretory cells induces transdifferentiation into epidermis and squamous metaplasias. *Proc.Natl.Acad.Sci.U.S.A* **99**, 219-224.
- Miyoshi, Y., Nagase, H., Ando, H., Horii, A., Ichii, S., Nakatsuru, S., Aoki, T., Miki, Y., Mori, T., and Nakamura, Y. (1992). Somatic mutations of the APC gene in colorectal tumors: mutation cluster region in the APC gene. *Hum.Mol.Genet.* **1**, 229-233.
- Molenaar, M., van de, W. M., Oosterwegel, M., Peterson-Maduro, J., Godsave, S., Korinek, V., Roose, J., Destree, O., and Clevers, H. (1996). XTcf-3 transcription factor mediates beta-catenin-induced axis formation in *Xenopus* embryos. *Cell* **86**, 391-399.
- Monkley, S. J., Delaney, S. J., Pennisi, D. J., Christiansen, J. H., and Wainwright, B. J. (1996). Targeted disruption of the Wnt2 gene results in placentation defects. *Development* **122**, 3343-3353.
- Moon, R. T., Campbell, R. M., Christian, J. L., McGrew, L. L., Shih, J., and Fraser, S. (1993). Xwnt-5A: a maternal Wnt that affects morphogenetic movements after overexpression in embryos of *Xenopus laevis*. *Development* **119**, 97-111.
- Moon, R. T., Christian, J. L., Campbell, R. M., McGrew, L. L., DeMarais, A. A., Torres, M., Lai, C. J., Olson, D. J., and Kelly, G. M. (1993). Dissecting Wnt signalling pathways and Wnt-sensitive developmental processes through transient misexpression analyses in embryos of *Xenopus laevis*. *Dev.Suppl* 85-94.
- Moon, R. T., Brown, J. D., Yang-Snyder, J. A., and Miller, J. R. (1997). Structurally related receptors and antagonists compete for secreted Wnt ligands. *Cell* **88**, 725-728.
- Moser, A. R., Pitot, H. C., and Dove, W. F. (1990). A dominant mutation that predisposes to multiple intestinal neoplasia in the mouse. *Science* **247**, 322-324.
- Moser, A. R., Mattes, E. M., Dove, W. F., Lindstrom, M. J., Haag, J. D., and Gould, M. N. (1993). ApcMin, a mutation in the murine Apc gene, predisposes to mammary carcinomas and focal alveolar hyperplasias. *Proc.Natl.Acad.Sci.U.S.A* **90**, 8977-8981.
- Moser, A. R., Shoemaker, A. R., Connelly, C. S., Clipson, L., Gould, K. A., Luongo, C., Dove, W. F., Siggers, P. H., and Gardner, R. L. (1995). Homozygosity for the Min allele of Apc results in disruption of mouse development prior to gastrulation. *Dev.Dyn.* **203**, 422-433.
- Moss, S. F., Liu, T. C., Petrotos, A., Hsu, T. M., Gold, L. I., and Holt, P. R. (1996). Inward growth of colonic adenomatous polyps. *Gastroenterology* **111**, 1425-1432.

- Munemitsu, S., Souza, B., Muller, O., Albert, I., Rubinfeld, B., and Polakis, P.** (1994). The APC gene product associates with microtubules in vivo and promotes their assembly in vitro. *Cancer Res.* **54**, 3676-3681.
- Munemitsu, S., Albert, I., Souza, B., Rubinfeld, B., and Polakis, P.** (1995). Regulation of intracellular beta-catenin levels by the adenomatous polyposis coli (APC) tumor-suppressor protein. *Proc.Natl.Acad.Sci.U.S.A* **92**, 3046-3050.
- Munemitsu, S., Albert, I., Rubinfeld, B., and Polakis, P.** (1996). Deletion of an amino-terminal sequence beta-catenin in vivo and promotes hyperphosphorylation of the adenomatous polyposis coli tumor suppressor protein. *Mol.Cell Biol.* **16**, 4088-4094.
- Muthukumar, G., Blumberg, B., and Kurkinen, M.** (1989). The complete primary structure for the alpha 1-chain of mouse collagen IV. Differential evolution of collagen IV domains. *J.Biol.Chem.* **264**, 6310-6317.
- Nagarajan, S., Chen, H. C., Li, S. C., Li, Y. T., and Lockyer, J. M.** (1992). Evidence for two cDNA clones encoding human GM2-activator protein. *Biochem.J.* **282 (Pt 3)**, 807-813.
- Nakagawa, H., Murata, Y., Koyama, K., Fujiyama, A., Miyoshi, Y., Monden, M., Akiyama, T., and Nakamura, Y.** (1998). Identification of a brain-specific APC homologue, APCL, and its interaction with beta-catenin. *Cancer Res.* **58**, 5176-5181.
- Nakagawa, H., Koyama, K., Murata, Y., Morito, M., Akiyama, T., and Nakamura, Y.** (2000). EB3, a novel member of the EB1 family preferentially expressed in the central nervous system, binds to a CNS-specific APC homologue. *Oncogene* **19**, 210-216.
- Nakamura, T., Hamada, F., Ishidate, T., Anai, K., Kawahara, K., Toyoshima, K., and Akiyama, T.** (1998). Axin, an inhibitor of the Wnt signalling pathway, interacts with beta-catenin, GSK-3beta and APC and reduces the beta-catenin level. *Genes Cells* **3**, 395-403.
- Nathke, I. S., Adams, C. L., Polakis, P., Sellin, J. H., and Nelson, W. J.** (1996). The adenomatous polyposis coli tumor suppressor protein localizes to plasma membrane sites involved in active cell migration. *J.Cell Biol.* **134**, 165-179.
- Nathke, I. S.** (1999). The adenomatous polyposis coli protein. *Mol.Pathol.* **52**, 169-173.
- Nelson, R. D., Stricklett, P., Gustafson, C., Stevens, A., Ausiello, D., Brown, D., and Kohan, D. E.** (1998). Expression of an AQP2 Cre recombinase transgene in kidney and male reproductive system of transgenic mice. *Am.J.Physiol* **275**, C216-C226.
- Neuenschwander, S., Schwartz, A., Wood, T. L., Roberts, C. T., Jr., Henninghausen, L., and LeRoith, D.** (1996). Involution of the lactating mammary gland is inhibited by the IGF system in a transgenic mouse model. *J.Clin.Invest* **97**, 2225-2232.
- Neufeld, K. L. and White, R. L.** (1997). Nuclear and cytoplasmic localizations of the adenomatous polyposis coli protein. *Proc.Natl.Acad.Sci.U.S.A* **94**, 3034-3039.
- Neufeld, K. L., Nix, D. A., Bogerd, H., Kang, Y., Beckerle, M. C., Cullen, B. R., and White, R. L.** (2000). Adenomatous polyposis coli protein contains two nuclear export signals and shuttles between the nucleus and cytoplasm. *Proc.Natl.Acad.Sci.U.S.A* **97**, 12085-12090.
- Neufeld, K. L., Zhang, F., Cullen, B. R., and White, R. L.** (2000). APC-mediated downregulation of beta-catenin activity involves nuclear sequestration and nuclear export. *EMBO Rep.* **1**, 519-523.

- Nugent, K. P., Phillips, R. K., Hodgson, S. V., Cottrell, S., Smith-Ravin, J., Pack, K., and Bodmer, W. F.** (1994). Phenotypic expression in familial adenomatous polyposis: partial prediction by mutation analysis. *Gut* **35**, 1622-1623.
- Nusse, R. and Varmus, H. E.** (1982). Many tumors induced by the mouse mammary tumor virus contain a provirus integrated in the same region of the host genome. *Cell* **31**, 99-109.
- Nusse, R.** (2001). Developmental biology. Making head or tail of Dickkopf. *Nature* **411**, 255-256.
- Nusslein-Volhard, C. and Roth, S.** (1989). Axis determination in insect embryos. *Ciba Found.Symp.* **144**, 37-55.
- Nusslein-Volhard, C.** (1991). Determination of the embryonic axes of Drosophila. *Dev.Suppl* **1**, 1-10.
- O'Connor.** (1998). Survival factors and apoptosis. In *Advances in biochemical engineering/biotechnology.* (ed. T.H. Scheper), **62**, 138-162. Springer-Verlag, Berlin, Germany.
- Olson, D. J. and Papkoff, J.** (1994). Regulated expression of Wnt family members during proliferation of C57mg mammary cells. *Cell Growth Differ.* **5**, 197-206.
- Ormerod, E. J. and Rudland, P. S.** (1988). Mammary gland morphogenesis in vitro: extracellular requirements for the formation of tubules in collagen gels by a cloned rat mammary epithelial cell line. *In Vitro Cell Dev.Biol.* **24**, 17-27.
- Oshima, H., Oshima, M., Kobayashi, M., Tsutsumi, M., and Taketo, M. M.** (1997). Morphological and molecular processes of polyp formation in Apc(delta716) knockout mice. *Cancer Res.* **57**, 1644-1649.
- Oshima, M., Sugiyama, H., Kitagawa, K., and Taketo, M.** (1993). APC gene messenger RNA: novel isoforms that lack exon 7. *Cancer Res.* **53**, 5589-5591.
- Oshima, M., Oshima, H., Kitagawa, K., Kobayashi, M., Itakura, C., and Taketo, M.** (1995). Loss of Apc heterozygosity and abnormal tissue building in nascent intestinal polyps in mice carrying a truncated Apc gene. *Proc.Natl.Acad.Sci.U.S.A* **92**, 4482-4486.
- Ozawa, M., Terada, H., and Pedraza, C.** (1995). The fourth armadillo repeat of plakoglobin (gamma-catenin) is required for its high affinity binding to the cytoplasmic domains of E-cadherin and desmosomal cadherin Dsg2, and the tumor suppressor APC protein. *J.Biochem.(Tokyo)* **118**, 1077-1082.
- Papkoff, J., Brown, A. M., and Varmus, H. E.** (1987). The int-1 proto-oncogene products are glycoproteins that appear to enter the secretory pathway. *Mol.Cell Biol.* **7**, 3978-3984.
- Parkhurst, S. M.** (1998). Groucho: making its Marx as a transcriptional co-repressor. *Trends Genet.* **14**, 130-132.
- Peters, G., Brookes, S., Smith, R., Placzek, M., and Dickson, C.** (1989). The mouse homolog of the hst/k-FGF gene is adjacent to int-2 and is activated by proviral insertion in some virally induced mammary tumors. *Proc.Natl.Acad.Sci.U.S.A* **86**, 5678-5682.
- Peters, J. M., McKay, R. M., McKay, J. P., and Graff, J. M.** (1999). Casein kinase I transduces Wnt signals. *Nature* **401**, 345-350.
- Piccolo, S., Agius, E., Leyns, L., Bhattacharyya, S., Grunz, H., Bouwmeester, T., and De Robertis, E. M.** (1999). The head inducer Cerberus is a multifunctional antagonist of Nodal, BMP and Wnt signals. *Nature* **397**, 707-710.

- Pinson, K. I., Brennan, J., Monkley, S., Avery, B. J., and Skarnes, W. C. (2000). An LDL-receptor-related protein mediates Wnt signalling in mice. *Nature* **407**, 535-538.
- Pittius, C. W., Sankaran, L., Topper, Y. J., and Hennighausen, L. (1988). Comparison of the regulation of the whey acidic protein gene with that of a hybrid gene containing the whey acidic protein gene promoter in transgenic mice. *Mol.Endocrinol.* **2**, 1027-1032.
- Pollack, A.L., Barth, A. I., Altschuler, Y., Nelson, W. J., Mostov, K. E. (1997). Dynamics of beta-catenin interactions with APC protein regulate epithelial tubulogenesis. *J. Cell Biol.* **137**, 1651-62.
- Polakis, P. (1995). Mutations in the APC gene and their implications for protein structure and function. *Curr.Opin.Genet.Dev.* **5**, 66-71.
- Polakis, P. (1997). The adenomatous polyposis coli (APC) tumor suppressor. *Biochim.Biophys.Acta* **1332**, F127-F147.
- Polakis, P. (2000). Wnt signaling and cancer. *Genes Dev.* **14**, 1837-1851.
- Pollard, J. W. and Hennighausen, L. (1994). Colony stimulating factor 1 is required for mammary gland development during pregnancy. *Proc.Natl.Acad.Sci.U.S.A* **91**, 9312-9316.
- Powell, S. M., Zilz, N., Beazer-Barclay, Y., Bryan, T. M., Hamilton, S. R., Thibodeau, S. N., Vogelstein, B., and Kinzler, K. W. (1992). APC mutations occur early during colorectal tumorigenesis. *Nature* **359**, 235-237.
- Prendergast, G. (1999). Mechanisms of apoptosis by c-Myc. *Oncogene* **18**, 2967-2987
- Pyles, R. B., Santoro, I. M., Groden, J., and Parysek, L. M. (1998). Novel protein isoforms of the APC tumor suppressor in neural tissue. *Oncogene* **16**, 77-82.
- Ray, M. K., Fagan, S. P., Moldovan, S., DeMayo, F. J., and Brunnicardi, F. C. (1998). A mouse model for beta cell-specific ablation of target gene(s) using the Cre-loxP system. *Biochem.Biophys.Res.Comm.* **253**, 65-69.
- Redston, M., Nathanson, K. L., Yuan, Z. Q., Neuhausen, S. L., Satagopan, J., Wong, N., Yang, D., Nafa, D., Abrahamson, J., Ozcelik, H., Antin-Ozerkis, D., Andrulis, I., Daly, M., Pinsky, L., Schrag, D., Gallinger, S., Kaback, M., King, M. C., Woodage, T., Brody, L. C., Godwin, A., Warner, E., Weber, B., Foulkes, W., and Offit, K. (1998). The APC11307K allele and breast cancer risk. *Nat.Genet.* **20**, 13-14.
- Regan, C. P., Manabe, I., and Owens, G. K. (2000). Development of a smooth muscle-targeted cre recombinase mouse reveals novel insights regarding smooth muscle myosin heavy chain promoter regulation. *Circ.Res.* **87**, 363-369.
- Reichsman, F., Smith, L., and Cumberledge, S. (1996). Glycosaminoglycans can modulate extracellular localization of the wingless protein and promote signal transduction. *J.Cell Biol.* **135**, 819-827.
- Richardson, M., Redmond, D., Watson, C. J., and Mason, J. O. (1999). Mouse Wnt8B is expressed in the developing forebrain and maps to chromosome 19. *Mamm.Genome* **10**, 923-925.
- Riese, J., Yu, X., Munnerlyn, A., Eresh, S., Hsu, S. C., Grosschedl, R., and Bienz, M. (1997). LEF-1, a nuclear factor coordinating signaling inputs from wingless and decapentaplegic. *Cell* **88**, 777-787.

- Rigat, B., Wang, W., Leung, A., and Mahuran, D. J.** (1997). Two mechanisms for the recapture of extracellular GM2 activator protein: evidence for a major secretory form of the protein. *Biochemistry* **36**, 8325-8331.
- Rijsewijk, F., van Deemter, L., Wagenaar, E., Sonnenberg, A., and Nusse, R.** (1987). Transfection of the int-1 mammary oncogene in cuboidal RAC mammary cell line results in morphological transformation and tumorigenicity. *EMBO J.* **6**, 127-131.
- Ringold, G. M.** (1979). Glucocorticoid regulation of mouse mammary tumor virus gene expression. *Biochim.Biophys.Acta* **560**, 487-508.
- Ringold, G. M., Shank, P. R., Varmus, H. E., Ring, J., and Yamamoto, K. R.** (1979). Integration and transcription of mouse mammary tumor virus DNA in rat hepatoma cells. *Proc.Natl.Acad.Sci.U.S.A* **76**, 665-669.
- Robinson, G. W., McKnight, R. A., Smith, G. H., and Hennighausen, L.** (1995). Mammary epithelial cells undergo secretory differentiation in cycling virgins but require pregnancy for the establishment of terminal differentiation. *Development* **121**, 2079-2090.
- Robinson, G. W. and Hennighausen, L.** (1997). Inhibins and activins regulate mammary epithelial cell differentiation through mesenchymal-epithelial interactions. *Development* **124**, 2701-2708.
- Roelink, H., Wagenaar, E., Lopes, d. S., and Nusse, R.** (1990). Wnt-3, a gene activated by proviral insertion in mouse mammary tumors, is homologous to int-1/Wnt-1 and is normally expressed in mouse embryos and adult brain. *Proc.Natl.Acad.Sci.U.S.A* **87**, 4519-4523.
- Roose, J., Huls, G., van Beest, M., Moerer, P., van der, H. K., Goldschmeding, R., Logtenberg, T., and Clevers, H.** (1999). Synergy between tumor suppressor APC and the beta-catenin-Tcf4 target Tcf1. *Science* **285**, 1923-1926.
- Rosin-Arbesfeld, R., Townsley, F., and Bienz, M.** (2000). The APC tumour suppressor has a nuclear export function. *Nature* **406**, 1009-1012.
- Rosner, A., Miyoshi, K., Landesman-Bollag, E., Xu, X., Seldin, D. C., Moser, A. R., MacLeod, C. L., Shyamala, G., Gillgrass, A. E., and Cardiff, R. D.** (2002). Pathway pathology: histological differences between ErbB/Ras and Wnt pathway transgenic mammary tumors. *Am.J.Pathol.* **161**, 1087-1097.
- Rubinfeld, B., Souza, B., Albert, I., Munemitsu, S., and Polakis, P.** (1995). The APC protein and E-cadherin form similar but independent complexes with alpha-catenin, beta-catenin, and plakoglobin. *J.Biol.Chem.* **270**, 5549-5555.
- Rubinfeld, B., Tice, D. A., and Polakis, P.** (2001). Axin-dependent phosphorylation of the adenomatous polyposis coli protein mediated by casein kinase Iepsilon. *J.Biol.Chem.* **276**, 39037-39045.
- Sakanaka, C., Leong, P., Xu, L., Harrison, S. D., and Williams, L. T.** (1999). Casein kinase Iepsilon in the wnt pathway: regulation of beta-catenin function. *Proc.Natl.Acad.Sci.U.S.A* **96**, 12548-12552.
- Sakurai, Y., Sullivan, M., and Yamada, Y.** (1986). Alpha 1 type IV collagen gene evolved differently from fibrillar collagen genes. *J.Biol.Chem.* **261**, 6654-6657.
- Salomon, D. S., Liotta, L. A., and Kidwell, W. R.** (1981). Differential response to growth factor by rat mammary epithelium plated on different collagen substrata in serum-free medium. *Proc.Natl.Acad.Sci.U.S.A* **78**, 382-386.

- Sanger, F., Nicklen, S., and Coulson, A. R. (1977). DNA sequencing with chain-terminating inhibitors. *Proc.Natl.Acad.Sci.U.S.A* **74**, 5463-5467.
- Santoro, I. M. and Groden, J. (1997). Alternative splicing of the APC gene and its association with terminal differentiation. *Cancer Res.* **57**, 488-494.
- Sasisekharan, R., Shriver, Z., Venkataraman, G., and Narayanasami, U. (2002). Roles of heparan-sulphate glycosaminoglycans in cancer. *Nat.Rev.Cancer* **2**, 521-528.
- Satokata, I., Ma, L., Ohshima, H., Bei, M., Woo, I., Nishizawa, K., Maeda, T., Takano, Y., Uchiyama, M., Heaney, S., Peters, H., Tang, Z., Maxson, R., and Maas, R. (2000). Msx2 deficiency in mice causes pleiotropic defects in bone growth and ectodermal organ formation. *Nat.Genet.* **24**, 391-395.
- Sauer, B. and Henderson, N. (1988). Site-specific DNA recombination in mammalian cells by the Cre recombinase of bacteriophage P1. *Proc.Natl.Acad.Sci.U.S.A* **85**, 5166-5170.
- Schlosshauer, P. W., Brown, S. A., Eisinger, K., Yan, Q., Guglielminetti, E. R., Parsons, R., Ellenson, L. H., and Kitajewski, J. (2000). APC truncation and increased beta-catenin levels in a human breast cancer cell line. *Carcinogenesis* **21**, 1453-1456.
- Seeling, J. M., Miller, J. R., Gil, R., Moon, R. T., White, R., and Virshup, D. M. (1999). Regulation of beta-catenin signaling by the B56 subunit of protein phosphatase 2A. *Science* **283**, 2089-2091.
- Selbert, S., Bentley, D. J., Melton, D. W., Rannie, D., Lourenco, P., Watson, C. J., and Clarke, A. R. (1998). Efficient BLG-Cre mediated gene deletion in the mammary gland. *Transgenic Res.* **7**, 387-396.
- Semenov, M. V., Tamai, K., Brott, B. K., Kuhl, M., Sokol, S., and He, X. (2001). Head inducer Dickkopf-1 is a ligand for Wnt coreceptor LRP6. *Curr.Biol.* **11**, 951-961.
- Sheldahl, L. C., Park, M., Malbon, C. C., and Moon, R. T. (1999). Protein kinase C is differentially stimulated by Wnt and Frizzled homologs in a G-protein-dependent manner. *Curr.Biol.* **9**, 695-698.
- Shibata, H., Toyama, K., Shioya, H., Ito, M., Hirota, M., Hasegawa, S., Matsumoto, H., Takano, H., Akiyama, T., Toyoshima, K., Kanamaru, R., Kanegae, Y., Saito, I., Nakamura, Y., Shiba, K., and Noda, T. (1997). Rapid colorectal adenoma formation initiated by conditional targeting of the Apc gene. *Science* **278**, 120-123.
- Shih, I. M., Zhou, W., Goodman, S. N., Lengauer, C., Kinzler, K. W., and Vogelstein, B. (2001). Evidence that genetic instability occurs at an early stage of colorectal tumorigenesis. *Cancer Res.* **61**, 818-822.
- Shimizu, H., Julius, M. A., Giarre, M., Zheng, Z., Brown, A. M., and Kitajewski, J. (1997). Transformation by Wnt family proteins correlates with regulation of beta-catenin. *Cell Growth Differ.* **8**, 1349-1358.
- Shoemaker, A. R., Luongo, C., Moser, A. R., Marton, L. J., and Dove, W. F. (1997). Somatic mutational mechanisms involved in intestinal tumor formation in Min mice. *Cancer Res.* **57**, 1999-2006.
- Silberstein, G. B. (2001). Postnatal mammary gland morphogenesis. *Microsc.Res.Tech.* **52**, 155-162.

- Smalley, M. J., Sara, E., Paterson, H., Naylor, S., Cook, D., Jayatilake, H., Fryer, L. G., Hutchinson, L., Fry, M. J., and Dale, T. C. (1999). Interaction of axin and Dvl-2 proteins regulates Dvl-2-stimulated TCF-dependent transcription. *EMBO J.* **18**, 2823-2835.
- Smith, K. J., Levy, D. B., Maupin, P., Pollard, T. D., Vogelstein, B., and Kinzler, K. W. (1994). Wild-type but not mutant APC associates with the microtubule cytoskeleton. *Cancer Res.* **54**, 3672-3675.
- Smits, R., Kielman, M. F., Breukel, C., Zurcher, C., Neufeld, K., Jagmohan-Changur, S., Hofland, N., van Dijk, J., White, R., Edelmann, W., Kucherlapati, R., Khan, P. M., and Fodde, R. (1999). Apc1638T: a mouse model delineating critical domains of the adenomatous polyposis coli protein involved in tumorigenesis and development. *Genes Dev.* **13**, 1309-1321.
- Sokol, S., Christian, J. L., Moon, R. T., and Melton, D. A. (1991). Injected Wnt RNA induces a complete body axis in *Xenopus* embryos. *Cell* **67**, 741-752.
- Soriano, P. (1999). Generalized lacZ expression with the ROSA26 Cre reporter strain. *Nat. Genet.* **21**, 70-71.
- Sorlie, T., Bukholm, I., and Borresen-Dale, A. L. (1998). Truncating somatic mutation in exon 15 of the APC gene is a rare event in human breast carcinomas. Mutations in brief no. 179. Online. *Hum. Mutat.* **12**, 215.
- St Onge, L., Furth, P. A., and Gruss, P. (1996). Temporal control of the Cre recombinase in transgenic mice by a tetracycline responsive promoter. *Nucleic Acids Res.* **24**, 3875-3877.
- Stark, K., Vainio, S., Vassileva, G., and McMahon, A. P. (1994). Epithelial transformation of metanephric mesenchyme in the developing kidney regulated by Wnt-4. *Nature* **372**, 679-683.
- Stein, J. and Liang, P. (2002). Differential display technology: a general guide. *Cell Mol. Life Sci.* **59**, 1235-1240.
- Sternlicht, M.D., and Werb, Z. (1999). ECM proteinases. In *Guidebook to the Extracellular matrix and adhesion proteins*. (ed. T. Kreis and R. Vale), pages 503-562. Oxford University Press, New York.
- Sternlicht, M. D., Lochter, A., Sympon, C. J., Huey, B., Rougier, J. P., Gray, J. W., Pinkel, D., Bissell, M. J., and Werb, Z. (1999). The stromal proteinase MMP3/stromelysin-1 promotes mammary carcinogenesis. *Cell* **98**, 137-146.
- Streuli, C. H. and Edwards, G. M. (1998). Control of normal mammary epithelial phenotype by integrins. *J. Mammary Gland. Biol. Neoplasia.* **3**, 151-163.
- Su, L. K., Kinzler, K. W., Vogelstein, B., Preisinger, A. C., Moser, A. R., Luongo, C., Gould, K. A., and Dove, W. F. (1992). Multiple intestinal neoplasia caused by a mutation in the murine homolog of the APC gene. *Science* **256**, 668-670.
- Su, L. K., Johnson, K. A., Smith, K. J., Hill, D. E., Vogelstein, B., and Kinzler, K. W. (1993). Association between wild type and mutant APC gene products. *Cancer Res.* **53**, 2728-2731.
- Su, L. K., Vogelstein, B., and Kinzler, K. W. (1993). Association of the APC tumor suppressor protein with catenins. *Science* **262**, 1734-1737.

- Sulekova, Z., Reina-Sanchez, J., and Ballhausen, W. G. (1995). Multiple APC messenger RNA isoforms encoding exon 15 short open reading frames are expressed in the context of a novel exon 10A-derived sequence. *Int.J.Cancer* **63**, 435-441.
- Sun, Y., Hegamyer, G., and Colburn, N. H. (1994). Molecular cloning of five messenger RNAs differentially expressed in preneoplastic or neoplastic JB6 mouse epidermal cells: one is homologous to human tissue inhibitor of metalloproteinases-3. *Cancer Res.* **54**, 1139-1144.
- Sutherland, R. L. and Musgrove, E. A. (2002). Cyclin D1 and mammary carcinoma: new insights from transgenic mouse models. *Breast Cancer Res.* **4**, 14-17.
- Tada, M. and Smith, J. C. (2000). Xwnt11 is a target of Xenopus Brachyury: regulation of gastrulation movements via Dishevelled, but not through the canonical Wnt pathway. *Development* **127**, 2227-2238.
- Tamai, K., Semenov, M., Kato, Y., Spokony, R., Liu, C., Katsuyama, Y., Hess, F., Saint-Jeannet, J. P., and He, X. (2000). LDL-receptor-related proteins in Wnt signal transduction. *Nature* **407**, 530-535.
- Tarutani, M., Itami, S., Okabe, M., Ikawa, M., Tezuka, T., Yoshikawa, K., Kinoshita, T., and Takeda, J. (1997). Tissue-specific knockout of the mouse Pig-a gene reveals important roles for GPI-anchored proteins in skin development. *Proc.Natl.Acad.Sci.U.S.A* **94**, 7400-7405.
- Tekmal, R. R. and Keshava, N. (1997). Role of MMTV integration locus cellular genes in breast cancer. *Front Biosci.* **2**, d519-d526.
- Tetsu, O. and McCormick, F. (1999). Beta-catenin regulates expression of cyclin D1 in colon carcinoma cells. *Nature* **398**, 422-426.
- Thliveris, A., Samowitz, W., Matsunami, N., Groden, J., and White, R. (1994). Demonstration of promoter activity and alternative splicing in the region 5' to exon 1 of the APC gene. *Cancer Res.* **54**, 2991-2995.
- Thompson, A. M., Morris, R. G., Wallace, M., Wyllie, A. H., Steel, C. M., and Carter, D. C. (1993). Allele loss from 5q21 (APC/MCC) and 18q21 (DCC) and DCC mRNA expression in breast cancer. *Br.J.Cancer* **68**, 64-68.
- Tonner, E., Barber, M. C., Travers, M. T., Logan, A., and Flint, D. J. (1997). Hormonal control of insulin-like growth factor-binding protein-5 production in the involuting mammary gland of the rat. *Endocrinology* **138**, 5101-5107.
- Townsley, F. M. and Bienz, M. (2000). Actin-dependent membrane association of a Drosophila epithelial APC protein and its effect on junctional Armadillo. *Curr.Biol.* **10**, 1339-1348.
- Travers, M. T., Barber, M. C., Tonner, E., Quarrie, L., Wilde, C. J., and Flint, D. J. (1996). The role of prolactin and growth hormone in the regulation of casein gene expression and mammary cell survival: relationships to milk synthesis and secretion. *Endocrinology* **137**, 1530-1539.
- Tsukamoto, A. S., Grosschedl, R., Guzman, R. C., Parslow, T., and Varmus, H. E. (1988). Expression of the int-1 gene in transgenic mice is associated with mammary gland hyperplasia and adenocarcinomas in male and female mice. *Cell* **55**, 619-625.
- Vaidya, A. B., Lasfargues, E. Y., Sheffield, J. B., and Coutinho, W. G. (1978). Murine mammary tumor virus (MuMTV) infection of an epithelial cell line established from C57BL/6 mouse mammary glands. *Virology* **90**, 12-22.

- Vainio, S., Heikkila, M., Kispert, A., Chin, N., and McMahon, A. P. (1999). Female development in mammals is regulated by Wnt-4 signalling. *Nature* **397**, 405-409.
- van de, W. M., Cavallo, R., Dooijes, D., van Beest, M., van Es, J., Loureiro, J., Ypma, A., Hursh, D., Jones, T., Bejsovec, A., Peifer, M., Mortin, M., and Clevers, H. (1997). Armadillo coactivates transcription driven by the product of the *Drosophila* segment polarity gene dTCF. *Cell* **88**, 789-799.
- van Es, J. H., Kirkpatrick, C., van de, W. M., Molenaar, M., Miles, A., Kuipers, J., Destree, O., Peifer, M., and Clevers, H. (1999). Identification of APC2, a homologue of the adenomatous polyposis coli tumour suppressor. *Curr.Biol.* **9**, 105-108.
- van Es, J. H., Giles, R. H., and Clevers, H. C. (2001). The many faces of the tumor suppressor gene APC. *Exp.Cell Res.* **264**, 126-134.
- van Genderen, C., Okamura, R. M., Farinas, I., Quo, R. G., Parslow, T. G., Bruhn, L., and Grosschedl, R. (1994). Development of several organs that require inductive epithelial-mesenchymal interactions is impaired in LEF-1-deficient mice. *Genes Dev.* **8**, 2691-2703.
- Venkitaraman, A. R. (2002). Cancer susceptibility and the functions of BRCA1 and BRCA2. *Cell* **108**, 171-182.
- Vinson, C. R., Conover, S., and Adler, P. N. (1989). A *Drosophila* tissue polarity locus encodes a protein containing seven potential transmembrane domains. *Nature* **338**, 263-264.
- Virmani, A. K., Rathi, A., Sathyanarayana, U. G., Padar, A., Huang, C. X., Cunnigham, H. T., Farinas, A. J., Milchgrub, S., Euhus, D. M., Gilcrease, M., Herman, J., Minna, J. D., and Gazdar, A. F. (2001). Aberrant methylation of the adenomatous polyposis coli (APC) gene promoter 1A in breast and lung carcinomas. *Clin.Cancer Res.* **7**, 1998-2004.
- Vleminckx, K., Wong, E., Guger, K., Rubinfeld, B., Polakis, P., and Gumbiner, B. M. (1997). Adenomatous polyposis coli tumor suppressor protein has signaling activity in *Xenopus laevis* embryos resulting in the induction of an ectopic dorsoanterior axis. *J.Cell Biol.* **136**, 411-420.
- Vleminckx, K., Kemler, R., and Hecht, A. (1999). The C-terminal transactivation domain of beta-catenin is necessary and sufficient for signaling by the LEF-1/beta-catenin complex in *Xenopus laevis*. *Mech.Dev.* **81**, 65-74.
- Vogel, W. F., Aszodi, A., Alves, F., and Pawson, T. (2001). Discoidin domain receptor 1 tyrosine kinase has an essential role in mammary gland development. *Mol.Cell Biol.* **21**, 2906-2917.
- Wagner, K. U., McAllister, K., Ward, T., Davis, B., Wiseman, R., and Hennighausen, L. (2001). Spatial and temporal expression of the Cre gene under the control of the MMTV-LTR in different lines of transgenic mice. *Transgenic Res.* **10**, 545-553.
- Wallingford, J. B., Rowning, B. A., Vogeli, K. M., Rothbacher, U., Fraser, S. E., and Harland, R. M. (2000). Dishevelled controls cell polarity during *Xenopus* gastrulation. *Nature* **405**, 81-85.
- Wallingford, J. B. and Harland, R. M. (2001). *Xenopus* Dishevelled signaling regulates both neural and mesodermal convergent extension: parallel forces elongating the body axis. *Development* **128**, 2581-2592.
- Walton, K. D., Wagner, K. U., Rucker, E. B., III, Shillingford, J. M., Miyoshi, K., and Hennighausen, L. (2001). Conditional deletion of the bcl-x gene from mouse mammary

- epithelium results in accelerated apoptosis during involution but does not compromise cell function during lactation. *Mech.Dev.* **109**, 281-293.
- Waltzer, L. and Bienz, M.** (1998). Drosophila CBP represses the transcription factor TCF to antagonize Wingless signalling. *Nature* **395**, 521-525.
- Wang, J. and Shackleford, G. M.** (1996). Murine Wnt10a and Wnt10b: cloning and expression in developing limbs, face and skin of embryos and in adults. *Oncogene* **13**, 1537-1544.
- Wang, T. C., Cardiff, R. D., Zukerberg, L., Lees, E., Arnold, A., and Schmidt, E. V.** (1994). Mammary hyperplasia and carcinoma in MMTV-cyclin D1 transgenic mice. *Nature* **369**, 669-671.
- Weber-Hall, S. J., Phippard, D. J., Niemeyer, C. C., and Dale, T. C.** (1994). Developmental and hormonal regulation of Wnt gene expression in the mouse mammary gland. *Differentiation* **57**, 205-214.
- Wehrli, M., Dougan, S. T., Caldwell, K., O'Keefe, L., Schwartz, S., Vaizel-Ohayon, D., Schejter, E., Tomlinson, A., and DiNardo, S.** (2000). arrow encodes an LDL-receptor-related protein essential for Wingless signalling. *Nature* **407**, 527-530.
- Weinstat-Saslow, D., Merino, M. J., Manrow, R. E., Lawrence, J. A., Bluth, R. F., Wittenbel, K. D., Simpson, J. F., Page, D. L., and Steeg, P. S.** (1995). Overexpression of cyclin D mRNA distinguishes invasive and in situ breast carcinomas from non-malignant lesions. *Nat.Med.* **1**, 1257-1260.
- Werb, Z.** (1997). ECM and cell surface proteolysis: regulating cellular ecology. *Cell* **91**, 439-442.
- Whitelaw, C. B., Harris, S., McClenaghan, M., Simons, J. P., and Clark, A. J.** (1992). Position-independent expression of the ovine beta-lactoglobulin gene in transgenic mice. *Biochem.J.* **286** (Pt 1), 31-39.
- Willert, K., Brink, M., Wodarz, A., Varmus, H., and Nusse, R.** (1997). Casein kinase 2 associates with and phosphorylates dishevelled. *EMBO J.* **16**, 3089-3096.
- Wiseman, B. S. and Werb, Z.** (2002). Stromal effects on mammary gland development and breast cancer. *Science* **296**, 1046-1049.
- Wodarz, A. and Nusse, R.** (1998). Mechanisms of Wnt signaling in development. *Annu.Rev.Cell Dev.Biol.* **14**, 59-88.
- Wolda, S. L., Moody, C. J., and Moon, R. T.** (1993). Overlapping expression of Xwnt-3A and Xwnt-1 in neural tissue of *Xenopus laevis* embryos. *Dev.Biol.* **155**, 46-57.
- Wong, G. T., Gavin, B. J., and McMahon, A. P.** (1994). Differential transformation of mammary epithelial cells by Wnt genes. *Mol.Cell Biol.* **14**, 6278-6286.
- Wong, M. H., Hermiston, M. L., Syder, A. J., and Gordon, J. I.** (1996). Forced expression of the tumor suppressor adenomatosis polyposis coli protein induces disordered cell migration in the intestinal epithelium. *Proc.Natl.Acad.Sci.U.S.A* **93**, 9588-9593.
- Wysolmerski, J. J., Philbrick, W. M., Dunbar, M. E., Lanske, B., Kronenberg, H., and Broadus, A. E.** (1998). Rescue of the parathyroid hormone-related protein knockout mouse demonstrates that parathyroid hormone-related protein is essential for mammary gland development. *Development* **125**, 1285-1294.

- Yamanaka, S., Johnson, O. N., Lyu, M. S., Kozak, C. A., and Proia, R. L.** (1994). The mouse gene encoding the GM2 activator protein (Gm2a): cDNA sequence, expression, and chromosome mapping. *Genomics* **24**, 601-604.
- Yanagawa, S., Matsuda, Y., Lee, J. S., Matsubayashi, H., Sese, S., Kadowaki, T., and Ishimoto, A.** (2002). Casein kinase I phosphorylates the Armadillo protein and induces its degradation in *Drosophila*. *EMBO J.* **21**, 1733-1742.
- Young, W. S., III, Shepard, E., Amico, J., Hennighausen, L., Wagner, K. U., LaMarca, M. E., McKinney, C., and Ginns, E. I.** (1996). Deficiency in mouse oxytocin prevents milk ejection, but not fertility or parturition. *J.Neuroendocrinol.* **8**, 847-853.
- Yu, X., Waltzer, L., and Bienz, M.** (1999). A new *Drosophila* APC homologue associated with adhesive zones of epithelial cells. *Nat.Cell Biol.* **1**, 144-151.
- Zeng, L., Fagotto, F., Zhang, T., Hsu, W., Vasicek, T. J., Perry, W. L., III, Lee, J. J., Tilghman, S. M., Gumbiner, B. M., and Costantini, F.** (1997). The mouse Fused locus encodes Axin, an inhibitor of the Wnt signaling pathway that regulates embryonic axis formation. *Cell* **90**, 181-192.
- Zhang, F., White, R. L., and Neufeld, K. L.** (2000). Phosphorylation near nuclear localization signal regulates nuclear import of adenomatous polyposis coli protein. *Proc.Natl.Acad.Sci.U.S.A* **97**, 12577-12582.
- Zhang, Y., Riesterer, C., Ayrall, A. M., Sablitzky, F., Littlewood, T. D., and Reth, M.** (1996). Inducible site-directed recombination in mouse embryonic stem cells. *Nucleic Acids Res.* **24**, 543-548.
- Zhu, Y., Romero, M. I., Ghosh, P., Ye, Z., Charnay, P., Rushing, E. J., Marth, J. D., and Parada, L. F.** (2001). Ablation of NF1 function in neurons induces abnormal development of cerebral cortex and reactive gliosis in the brain. *Genes Dev.* **15**, 859-876.
- Zumbrunn, J., Kinoshita, K., Hyman, A. A., and Nathke, I. S.** (2001). Binding of the adenomatous polyposis coli protein to microtubules increases microtubule stability and is regulated by GSK3 beta phosphorylation. *Curr.Biol.* **11**, 44-49.

Appendix A

Solutions and Reagents

Ampicillin (Amp)

0.5g Ampicillin (Sigma A-9518)
dH₂O to 100ml, filter-sterilise and store at -20°C (100µg/ml working concentration)

10% Ammonium persulphate

1g Ammonium persulphate
dH₂O to 10ml (store at 4°C)

BCA Reagent A

250ml of reagent containing sodium carbonate, sodium bicarbonate, bicinchoninic acid and sodium tartrate in 0.1M sodium hydroxide

BCA Reagent B

25ml solution containing 4% cupric sulphate

Buffer QBT (Equilibration buffer)

750mM NaCl
50mM MOPS (pH 7.0)
15% isopropanol
0.15% Triton® X-100.

Buffer QC (wash buffer)

1.0M NaCl
50mM MOPS (pH 7.0)
15% isopropanol.

Buffer QF (Elution buffer)

1.25M NaCl
50mM Tris (pH 8.5)
15% isopropanol

Church Hybridisation Buffer

5g BSA (Bovine Serum Albumin)
Dissolve in 75 ml of water, then add
250ml 1M Na₂HPO₄ (pH 7.2)
175ml 20% SDS
1ml 0.5M EDTA

Church Wash

40ml 1M Na₂HPO₄ (pH 7.2)
50ml 20% SDS
2ml 0.5M EDTA

DNase-free RNase A

200mg RNase A (Sigma R-5500)
3.3µl 3M NaOAc, pH 4.5
dH₂O to 10ml
boil for 10minutes (aliquot and store at -20°C)

0.5 M EDTA, pH 8.0 (disodium ethylenediamine tetraacetate)

186.1g Na₂EDTA
Dissolve in approx. 400ml dH₂O, adjust pH to 8.0 with 10 N NaOH, and adjust to 1 litre final volume with water.

100 mM EDTA

20ml 0.5 M EDTA
80ml dH₂O

5mg/ml ethidium bromide (EtBr)

500mg EtBr (Sigma H-3375)
dH₂O to 100ml

Filter lift-denaturing solution

1.5M NaCl
0.5M NaOH

Filter lift-neutralising solution

1.5M NaCl
1mM EDTA
0.5M Tris-HCL (pH=7.2)

Haematoxylin Counterstain**Solution A**

1g haematoxylin
40ml ethanol
360ml water

Solution B

0.2g sodium iodate
48g aluminium potassium sulphate
48g choral hydrate
600ml water

Solution B heated gently, added to solution A and left at room temperature for 48 hours. 1ml glacial acetic acid added.

Lambda broth

10g tryptone
2.5g NaCl
dH₂O to 1 litre of water, aliquot into 250ml bottles and autoclave.

Lambda plates

10g tryptone
2.5g NaCl
10g agar

dH₂O to 1 litre of water, autoclave to sterilize, and pour into sterile petri dishes (approx. 45ml/plate). Plates warmed to 37°C before use.

Lambda top agar

10g tryptone
2.5g NaCl
7g agar

dH₂O to 1 litre, aliquot into 250ml bottles and autoclave to sterilize, cool to 47°C before use.

LB Medium

10g Bacto-Tryptone
5g Bacto-yeast extract
10g NaCl

dH₂O to 950ml, adjust pH to 7.0 with 5M NaOH, and adjust volume to 1L with distilled water, aliquot into 250ml bottles and autoclave to sterilize.

LB plates

10g Bacto-Tryptone
10g NaCl
15g Bacto-agar

dH₂O to 1 litre, autoclave to sterilize, cool to 55°C, add antibiotic if desired, and pour into sterile petri dishes (approx. 20ml/plate).

Lysis/Solution P2

200mM NaOH
1% SDS

Stored at room temperature

Loading Buffer 6X**1 M MOPS**

20.93g MOPS (3-(β -morpholino)propanesulphonic acid) (Sigma M-1254)
Dissolved in 80ml dH₂O, adjust pH to 7.5 with 1 N NaOH, and bring volume to 100ml.

10X MOPS buffer

0.2M MOPS (Sigma M-1254)
0.5M sodium acetate
0.01M EDTA

dH₂O to 950ml, adjust pH to 7.0 with 1 N NaOH, and adjust volume to 1L with distilled water. Store in a bottle covered with aluminium foil to protect from light.

mSSCP Loading Buffer

80% deionised formamide
0.01% bromophenol blue
0.01% xylene cyanol
1mM EDTA
10mM NaOH

Stored at -20°C

Neutralisation/Solution P3

3M potassium acetate, pH 5.5

Stored at room temperature

NZY broth

5g NaCl
2g MgSO₄.7H₂O
5g Bacto-yeast extract
10g NZ amine (casein hydrolysate)
dH₂O to 950ml, adjust pH to 7.5 with 1 N NaOH, and adjust volume to 1L with distilled water. Autoclave to sterilize.

NZY agar

5g NaCl
2g MgSO₄.7H₂O
5g Bacto-yeast extract
10g NZ amine (casein hydrolysate)
15g agar
dH₂O to 950ml, adjust pH to 7.5 with 1 N NaOH, and adjust volume to 1L with distilled water. Autoclave to sterilize and pour into sterile petri dishes (approx. 45ml/plate).

NZY top agar

0.7% (w/v) agarose

1 litre NZY broth

autoclave to sterilise and cooled to 47°C before use.

PCR 10x reaction buffer

100mM Tris-HCL (pH 8.3)

15mM MgCl₂

500mM KCL

Phenol/chloroform (TE-saturated)

Mix equal amounts of phenol and chloroform, equilibrate the mixture by extracting several times with 0.1M Tris HCL (pH 7.6). Store the equilibrated mixture under an equal volume of 0.1M Tris HCL (pH 7.6) at 4°C.

Phenol/chloroform/isoamyl alcohol (25:25:1)

100ml TE-saturated phenol
100ml chloroform
4ml isoamyl alcohol

Phosphate –Buffered Saline (PBS)

8g NaCl
0.2g KCL
1.44g Na₂HPO₄
0.24g KH₂PO₄

dH₂O to 800ml, adjust pH to 7.4 with 1N HCL and adjust volume to 1L with distilled water.

Resuspension/Solution P1

50mM Tris-HCl (pH 8.0)
10mM EDTA
100µg/ml RNase A
Stored at 4°C after addition of RNase A.

RIPA Buffer

50mM NaCl
1% NP-40
12mM deoxycholate
3mM SDS
50mM Tris-HCl (pH 7.5)

RNA Sample Buffer

50% deionised formamide
18% formaldehyde
10% MOPS.
Stored at -20° C

10% SDS (sodium dodecyl sulfate)

10g SDS (Fisher S529-3)
dH₂O to 100ml

Sequenase® enzyme dilution buffer

10mM Tris-HCl (pH 7.5)
5mM DTT
0.1mM EDTA
0.5mg/ml Acetylated BSA

Sequencing Gel Solution

250g Urea
75ml 40% acrylamide solution
50ml 10Xtbe
175ml dH₂O.

For each 60ml of the above solution was mixed with 60µl of TEMED and 60µl of fresh 25% ammonium persulphate (in dH₂O) and immediately poured.

Sequencing Stop Solution

95% v/v formamide
20mM EDTA
0.5g/l bromophenol blue
0.5g/l xylene cyanol FF

Sequencing Termination Mixes

one each of:

80 μ M dATP + 8 μ M ddATP
80 μ M dCTP + 8 μ M ddCTP
80 μ M dGTP + 8 μ M ddGTP
80 μ M dTTP + 8 μ M ddTTP

SM buffer

5.8g NaCl
2g Magnesium sulphate
50ml 1M Tris-Cl pH 7.5
5ml gelatin
dH₂O to 1L and autoclave

SOC Media

2% w/v Bacto- tryptone
0.5% w/v Bacto-yeast extract
0.05% NaCl

Autoclave and add the following filter sterilised reagents. 1% (v/v) 1M MgCl₂, 1% (v/v) 1M MgSO₄ and 0.1% (v/v) 2M glucose solution.

3M NaOAc, pH 4.5

408.24g NaOAc-3H₂O

Dissolve in approx. 800ml dH₂O, adjust pH to 4.5 with glacial acetic acid and bring to a final volume of 1 L with dH₂O.

10N NaOH (sodium hydroxide)

40g NaOH dissolved
dH₂O to 100ml

1N NaOH

10ml 10 N NaOH
dH₂O to 100ml

Southern denaturing solution

0.4M NaOH
0.6M NaCl

Southern neutralisation solution

1.5M NaCl
0.5M Tris-HCL (pH=7.5)

SSC (20X) (standard saline-citrate)

88.3g sodium citrate
175.3g NaCl

Dissolved in approximately 900ml water, adjust pH to 7.0 with 1N HCL and bring final volume to 1L.

1X SSC

5ml 20X SSC
95ml dH₂O

10 X TBE

109g Tris base
55g boric acid
9.3g EDTA
dH₂O to 1L

TE buffer

10ml 1 M Tris-HCl (pH 7.6)
2ml 0.5 M EDTA
dH₂O to 1L

TENT buffer

20mM Tris HCL (pH 8.5)
2mM EDTA
150mM NaCl
1% Triton

TEMED (N,N,N',N'-Tetramethylethylenediamine)

Promega

Store protected from light at 15°C.

Tissue Lysis Buffer

100mM Tris HCL (pH 8.5)
5mM EDTA
200mM NaCl
0.2% SDS

Proteinase K added to final concentration of 100µg /ml prior to use.

Transfer Buffer

1.45g Tris buffer
7.2g Glycine
200ml methanol
dH₂O to 1L

Tris-Buffered Saline (TBS)

8g NaCl

0.2g KCL

3g Tris base

dH₂O to 800ml, adjust pH to 7.4 with 1N HCL and bring final volume to 1L.**TBS-T**

100ml 10x TBS

1ml 20% (v/v) Triton

dH₂O to 1L**1M Tris-HCl, pH 7.6, 8.0, 8.5, 9.0, 9.5**

121.1g Tris base

dH₂O to 800mlAdjust pH with concentrated HCl and then add dH₂O to 1 L.**T4 DNA polymerase reaction buffer**

50mM NaCl

10mM Tris-HCl

10mM MgCl₂

1mM DTT

pH 7.9 at 25°C

Type III loading buffer

0.25% bromophenol blue

0.25% xylene cyanol

30% glycerol

2XTY medium

16g Bacto- tryptone

10g Bacto-yeast extract

5g NaCl

dH₂O to 1L

Appendix B

Mouse breeding pairs

Control ($cre^+ Apc^{+/580S}$)			<i>Apc</i> deleted ($cre^+ Apc^{580S/580S}$)		
Male		Female	Male		Female
401I	414 $cre^+ Apc^{580S/580S}$	434, 438 $cre^+ Apc^{+/580S}$	400I	416 $cre^+ Apc^{580S/580S}$	425, 426 $cre^+ Apc^{+/580S}$
402I	415 $cre^+ Apc^{580S/580S}$	435, 436 $cre^+ Apc^{+/580S}$	399I	399 $cre^+ Apc^{580S/580S}$	432, 436 $cre^+ Apc^{+/580S}$
403I	427 $cre^+ Apc^{580S/580S}$	437 $cre^+ Apc^{+/580S}$	398I	228 $cre^+ Apc^{+/580S}$	430 $cre^+ Apc^{580S/580S}$

Mammary gland collection data

Control (Cre+APC ^{+/580s} mice)								
Female	Mid-gestation		Day 0		Day 2 lactation		Day 4 lactation	
<i>Cre+APC^{580s/580s}</i> x <i>Cre+APC^{+/580s}</i>	144	Pair no: 3981	109	Pair no: 4021	11	Pair no: 4011	55	Pair no: 3981
		D.O.B: 12/04/00		D.O.B: 7/03/00		D.O.B: 16/01/00		D.O.B: 8/02/00
		Mate@ 14/06/00		Mate@ 9/05/00		Mate@ 19/03/00		Mate@ 11/04/00
		Plug: 15/06/00		Plug: 10/05/00		Plug: 21/03/00		Plug: 28/04/00
		Take: 28/06/00		Take: 29/05/00		Take: 11/04/00		Take: 21/05/00
	145	Pair no: 3981	110	Pair no: 4021	36	Pair no: 4011	2	Pair no: 4021
		D.O.B: 12/04/00		D.O.B: 7/03/00		D.O.B: 31/01/00		D.O.B: 16/01/00
		Mate@ 14/06/00		Mate@ 9/05/00		Mate@ 3/04/00		Mate@ 19/03/00
		Plug: 17/06/00		Plug: 11/05/00		Plug: 9/04/00		Plug: 21/03/00
		Take: 30/06/00		Take: 30/05/00		Take: 30/04/00		Take: 15/04/00
	147	Pair no: 3981	111	Pair no: 4021	43	Pair no: 4021	3	Pair no: 4021
		D.O.B: 12/04/00		D.O.B: 7/03/00		D.O.B: 9/02/00		D.O.B: 16/01/00
		Mate@ 14/06/00		Mate@ 9/05/00		Mate@ 12/04/00		Mate@ 19/03/00
		Plug: 17/06/00		Plug: 13/05/00		Plug: 13/04/00		Plug: 21/03/00
		Take: 30/06/00		Take: 30/05/00		Take: 5/05/00		Take: 12/04/00
	148	Pair no: 3981	63	Pair no: 4021	61	Pair no: 4021	7	Pair no: 4021
		D.O.B: 12/04/00		D.O.B: 16/02/00		D.O.B: 16/02/00		D.O.B: 16/01/00
		Mate@ 14/06/00		Mate@ 19/04/00		Mate@ 19/04/00		Mate@ 19/03/00
		Plug: 17/06/00		Plug: 20/04/00		Plug: 3/05/00		Plug: 23/03/00
		Take: 30/06/00		Take: 12/05/00		Take: 24/05/00		Take: 15/04/00
118	Pair no: 4021	138	Pair no: 4031	134	Pair no: 4011	42	Pair no: 4021	
	D.O.B: 15/03/00		D.O.B: 14/04/00		D.O.B: 14/04/00		D.O.B: 9/02/00	
	Mate@ 17/05/00		Mate@ 16/06/00		Mate@ 16/06/00		Mate@ 12/04/00	
	Plug: 16/06/00		Plug: 18/06/00		Plug: 17/06/00		Plug: 10/05/00	
	Take: 29/06/00		Take: 7/07/00		Take: 8/07/00		Take: 2/06/00	

Experimental (Cre+APC ^{580s/580s})								
Female	Mid-gestation		Day 0		Day 2 lactation		Day 4 lactation	
<i>Cre+APC^{580s/580s}</i> x <i>Cre+APC^{580s/580s}</i>	19	Pair no: 400I	21	Pair no: 400I	150	Pair no: 400I	23	Pair no: 400I
		D.O.B: 24/01/00		D.O.B: 24/01/00		D.O.B: 12/04/00		D.O.B: 24/01/00
		Mate@ 27/03/00		Mate@ 27/03/00		Mate@ 14/06/00		Mate@ 27/03/00
		Plug: 30/03/00		Plug: 28/03/00		Plug: 5/07/00		Plug: 2/04/00
		Take: 12/04/00		Take: 17/03/00		Take: 27/07/00		Take: 25/04/00
	24	Pair no: 400I	52	Pair no: 400I	14	Pair no: 399I	31	Pair no: 399I
		D.O.B: 24/01/00		D.O.B: 11/02/00		D.O.B: 20/01/00		D.O.B: 30/01/00
		Mate@ 27/03/00		Mate@ 14/04/00		Mate@ 23/03/00		Mate@ 2/04/00
		Plug: 30/03/00		Plug: 16/04/00		Plug: 31/01/00		Plug: 3/04/00
		Take: 12/04/00		Take: 5/05/00		Take: 22/04/00		Take: 26/04/00
	71	Pair no: 399I	159	Pair no: 399I	73	Pair no: 399I	75	Pair no: 399I
		D.O.B: 19/02/00		D.O.B: 15/04/00		D.O.B: 19/02/00		D.O.B: 19/02/00
Mate@ 12/04/00		Mate@ 17/06/00		Mate@ 22/04/00		Mate@ 22/04/00		
Plug: 27/04/00		Plug: 4/07/00		Plug: 28/04/00		Plug: 27/04/00		
Take: 10/05/00		Take: 23/07/00		Take: 19/05/00		Take: 20/05/00		
<i>Cre+APC^{580s/580s}</i> x <i>Cre+APC^{+/580s}</i>	5	Pair no: 402I	112	Pair no: 402I	37	Pair no: 401I	56	Pair no: 398I
		D.O.B: 16/01/00		D.O.B: 7/03/00		D.O.B: 9/02/00		D.O.B: 8/02/00
		Mate@ 19/03/00		Mate@ 9/05/00		Mate@ 12/04/00		Mate@ 11/04/00
		Plug: 24/03/00		Plug: 10/05/00		Plug: 15/04/00		Plug: 14/04/00
		Take: 6/04/00		Take: 29/05/00		Take: 6/05/00		Take: 7/05/00
	44	Pair no: 402I	129	Pair no: 401I	8	Pair no: 403I	35	Pair no: 401I
		D.O.B: 9/02/00		D.O.B: 14/04/00		D.O.B: 16/01/00		D.O.B: 31/01/00
		Mate@ 12/04/00		Mate@ 16/06/00		Mate@ 19/03/00		Mate@ 3/04/00
		Plug: 13/04/00		Plug: 22/06/00		Plug: 21/03/00		Plug: 4/04/00
		Take: 26/04/00		Take: 8/07/00		Take: 11/04/00		Take: 26/04/00

Appendix C

DDRT-PCR Oligonucleotides

DDRT-PCR Anchored oligonucleotides

d(T)₁₂AA: 5' - d(TTTTTTTTTTTTAA) - 3'
d(T)₁₂GA: 5' - d(TTTTTTTTTTTTGA) - 3'
d(T)₁₂CA: 5' - d(TTTTTTTTTTTTCA) - 3'
d(T)₁₂AG: 5' - d(TTTTTTTTTTTTAG) - 3'
d(T)₁₂GG: 5' - d(TTTTTTTTTTTTGG) - 3'
d(T)₁₂CG: 5' - d(TTTTTTTTTTTTCG) - 3'
d(T)₁₂AC: 5' - d(TTTTTTTTTTTTAC) - 3'
d(T)₁₂GC: 5' - d(TTTTTTTTTTTTGC) - 3'
d(T)₁₂CC: 5' - d(TTTTTTTTTTTTCC) - 3'
d(T)₁₂AT: 5' - d(TTTTTTTTTTTTAT) - 3'
d(T)₁₂GT: 5' - d(TTTTTTTTTTTTGT) - 3'
d(T)₁₂CT: 5' - d(TTTTTTTTTTTTCT) - 3'

DDRT-PCR Arbitrary oligonucleotides

R1: 5' -d (GGAACTCCGT) -3'	R15: 5' -d (GATCTGACTG) -3'
R2: 5' -d (GGCAAGTCAC) -3'	R16: 5' -d (GATCTAAGGC) -3'
R3: 5' -d (CCTCCGTAAG) -3'	R17: 5' -d (GATCTAACCG) -3'
R4: 5' -d (AGGACCGCTA) -3'	R18: 5' -d (GGAACCAATC) -3'
R5: 5' -d (CGGACCCCGG) -3'	R19: 5' -d (CTTCTACCC) -3'
R6: 5' -d (TAACTAACTC) -3'	R20: 5' -d (AGCCAGCGAA) -3'
R7: 5' -d (TACAACGAGG) -3'	Sox: 5' -d (GCGACCCATG) -3'
R8: 5' -d (TGGATTGGTC) -3'	TK2: 5' -d (CTTGATTGCC) -3'
R9: 5' -d (TGGTAAAGGG) -3'	Max2: 5' -d (CACAGTTTGC) -3'
R10: 5' -d (TCGGTCATAG) -3'	Max3: 5' -d (CCACAGAGTA) -3'
R11: 5' -d (TACCTAAGCG) -3'	Amh1: 5' -d (ACAGAGCACA) -3'
R12: 5' -d (CTGCTTGATG) -3'	Amh2: 5' -d (ACGTATCCAG) -3'
R13: 5' -d (GATCTGACAC) -3'	P3: 5' -d (GCCGTTGGAT) -3'
R14: 5' -d (GATCGCATTG) -3'	

Reamplification Extended oligonucleotides (EcoR1 sites):

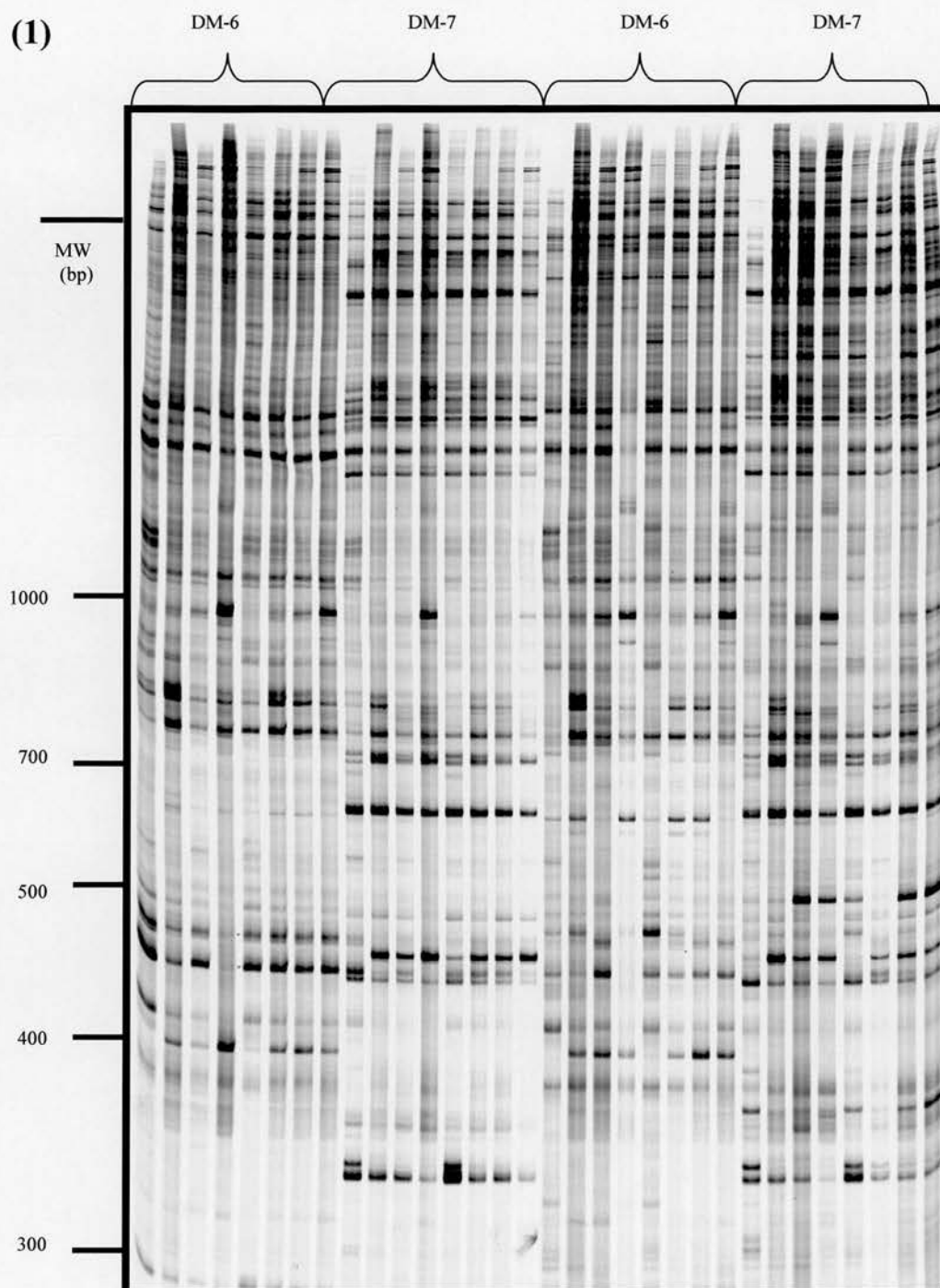
d(T)₁₂ext: 5' - d (GGGTCAGAATTCTTTTTTTTTTTT) - 3'
P3ext: 5' - d (GTCAGAATTCGCCGTTCCAT) - 3'
P4ext: 5' - d (GTCAGAATTCAGGACCGCTA) - 3'
R17ext: 5' - d (GTCAGAATTCGATCTAACCG) - 3'
R18ext: 5' - d (GTCAGAATTCGGAACCAATC) - 3'

Appendix D

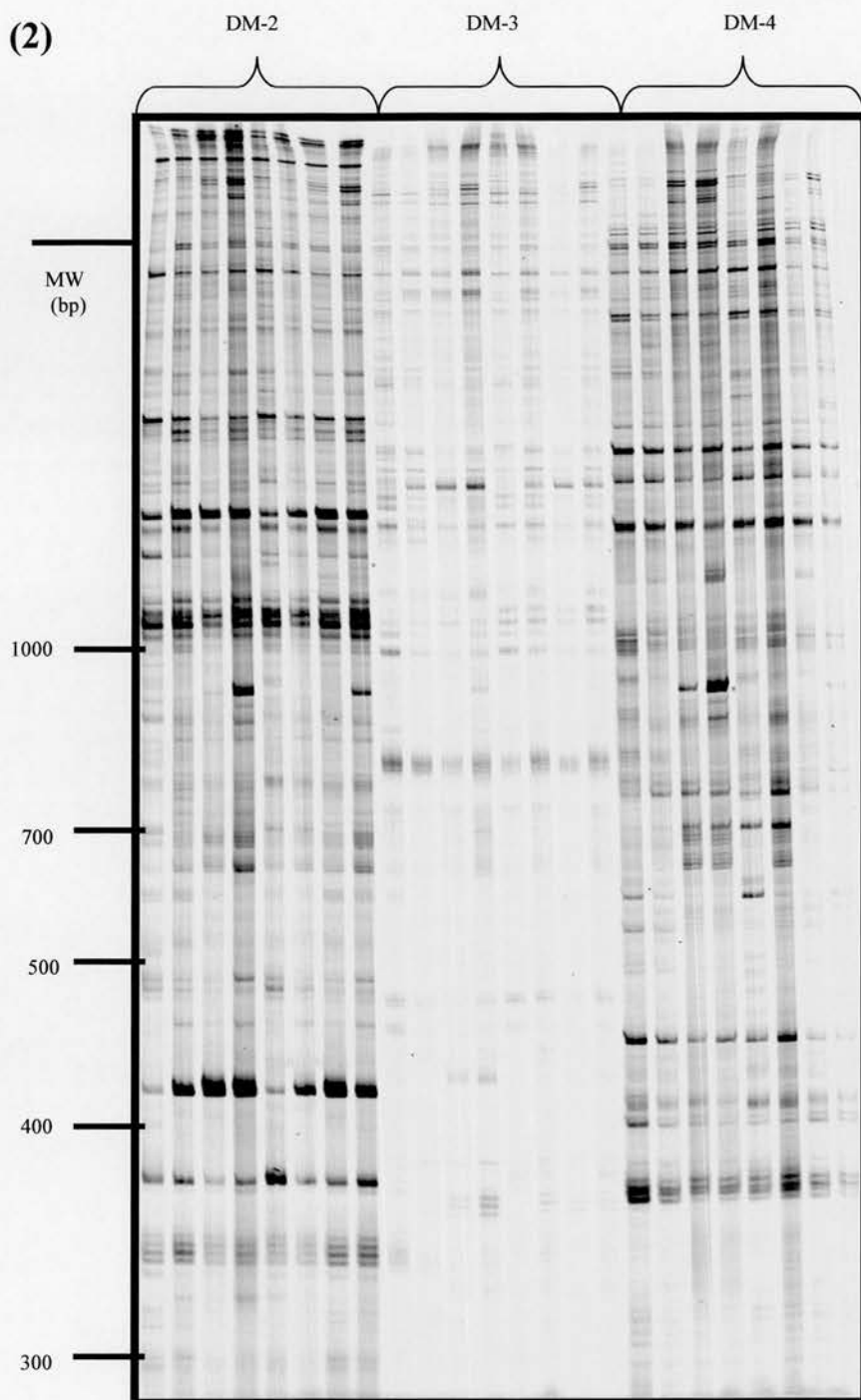
DDRT-PCR Autoradiographs

Autoradiograph no.	Primer combinations
DDRT-PCR gel 1:	d(T) ₁₂ MC and DM-6, DM-7
DDRT-PCR gel 2	d(T) ₁₂ MC and DM-2, DM-3, DM-4
DDRT-PCR gel 3	d(T) ₁₂ MC and DM-1, DM-5, DM-8, DM-9
DDRT-PCR gel 4	d(T) ₁₂ MC and DM-8, DM-10, DM-11, DM-12
DDRT-PCR gel 5	d(T) ₁₂ MC and DM-13, DM-14, DM-15, DM-16
DDRT-PCR gel 6	d(T) ₁₂ MC and DM-17, DM-18, DM-19, DM-20
DDRT-PCR gel 7	d(T) ₁₂ MC and A4, A5, A7, A8
DDRT-PCR gel 8	d(T) ₁₂ MC and R2, R4, R5, R6
DDRT-PCR gel 9	d(T) ₁₂ MC and SOX, MAX 1, MAX 2, DM-5
DDRT-PCR gel 10	d(T) ₁₂ MC and AMH1, AMH2, MAX 3, R20
DDRT-PCR gel 11	d(T) ₁₂ MC and DM-5, DM-6, DM-9, DM-15
DDRT-PCR gel 12	d(T) ₁₂ MC and DM-10, A5, A7, A9
DDRT-PCR gel 13	d(T) ₁₂ MC and DM-5, DM-20, R4, MAX 3
DDRT-PCR gel 14	d(T) ₁₂ MC and DM-20, R4, MAX 3, DM-5
DDRT-PCR gel 15	d(T) ₁₂ MC and DM-1, DM-7, DM-13, DM-14
DDRT-PCR gel 16	d(T) ₁₂ MC and A7, A8, DM-9, DM-11
DDRT-PCR gel 17	d(T) ₁₂ MC and DM-6, DM-7

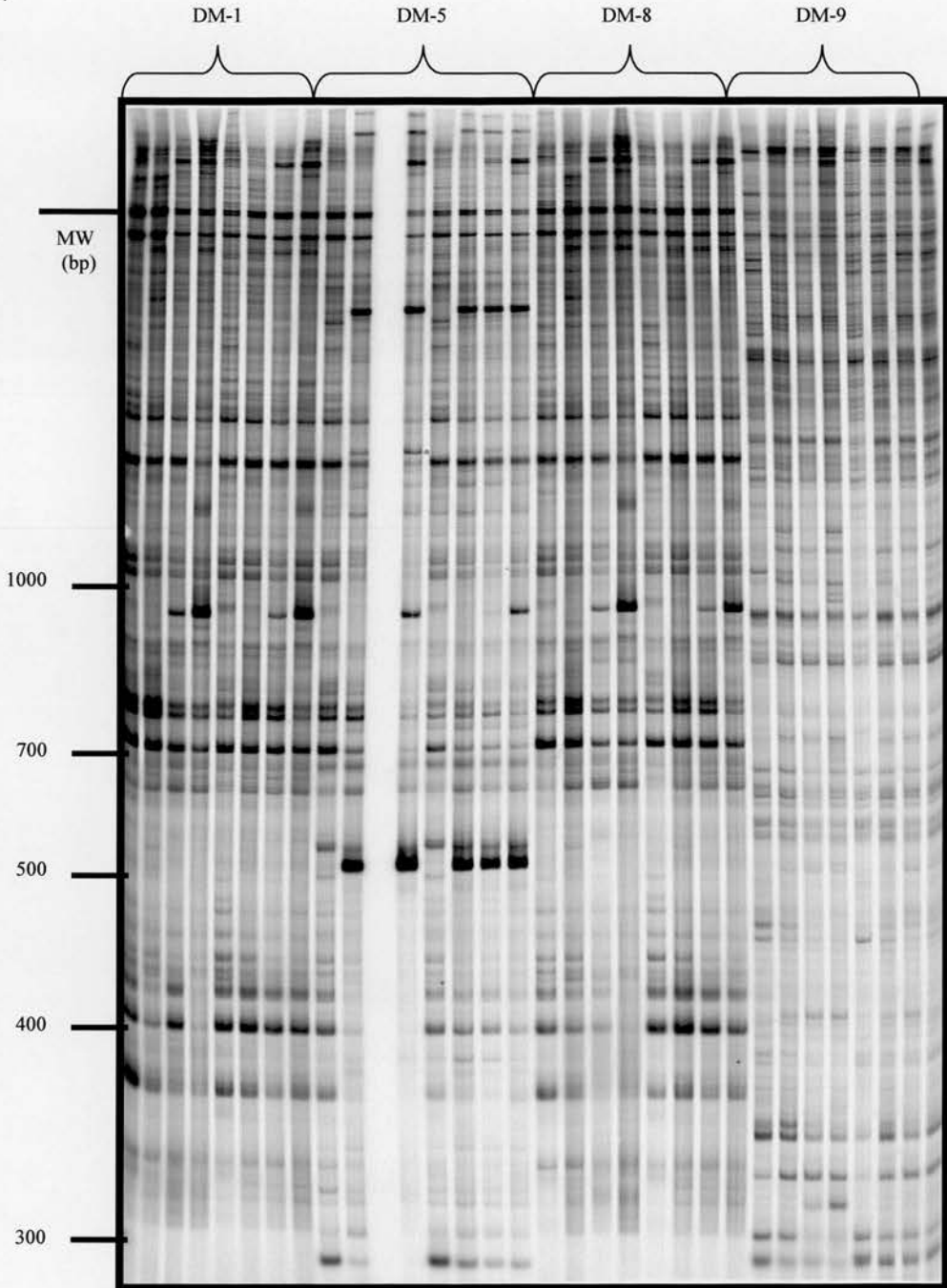
(1)



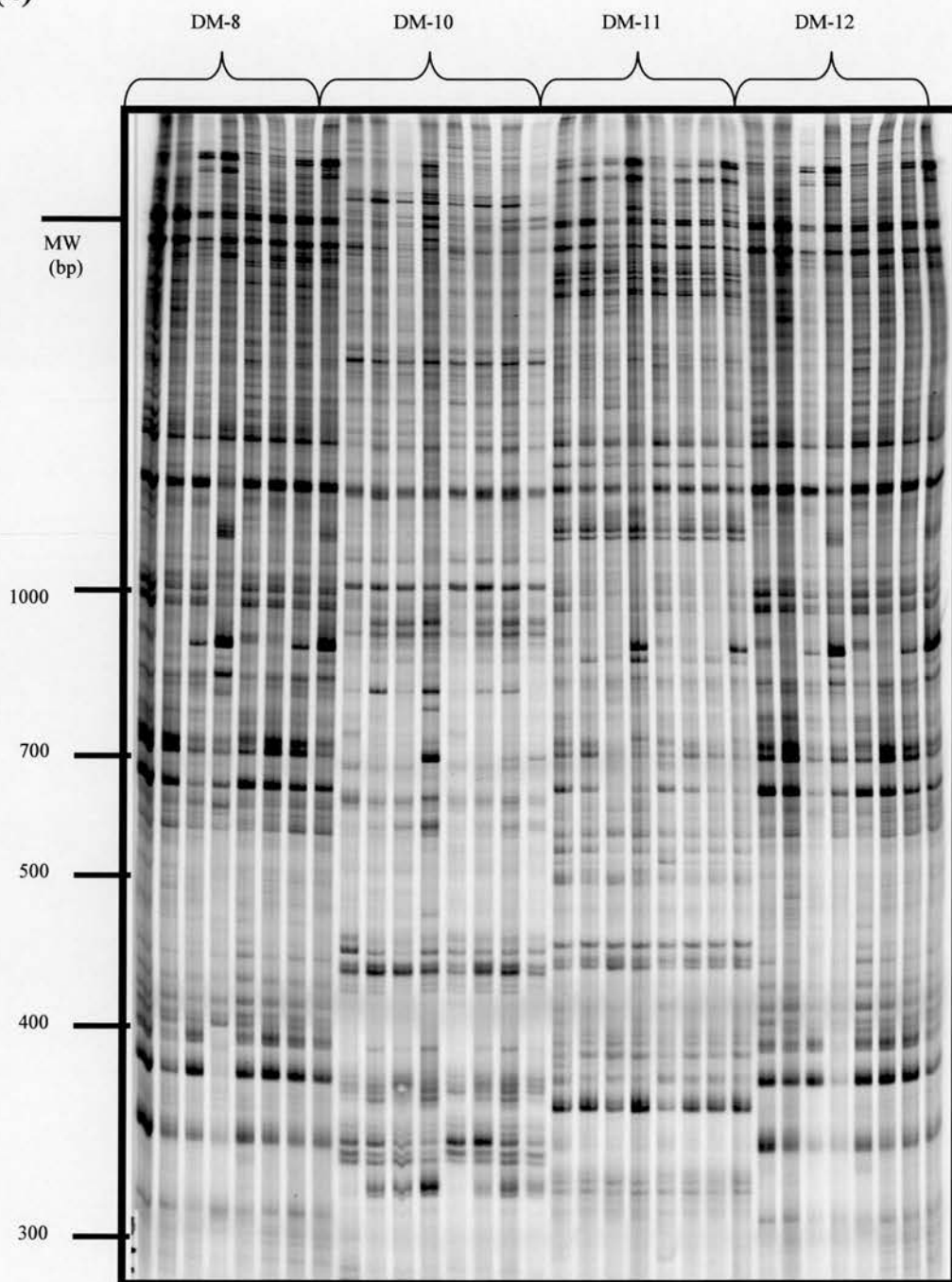
(2)

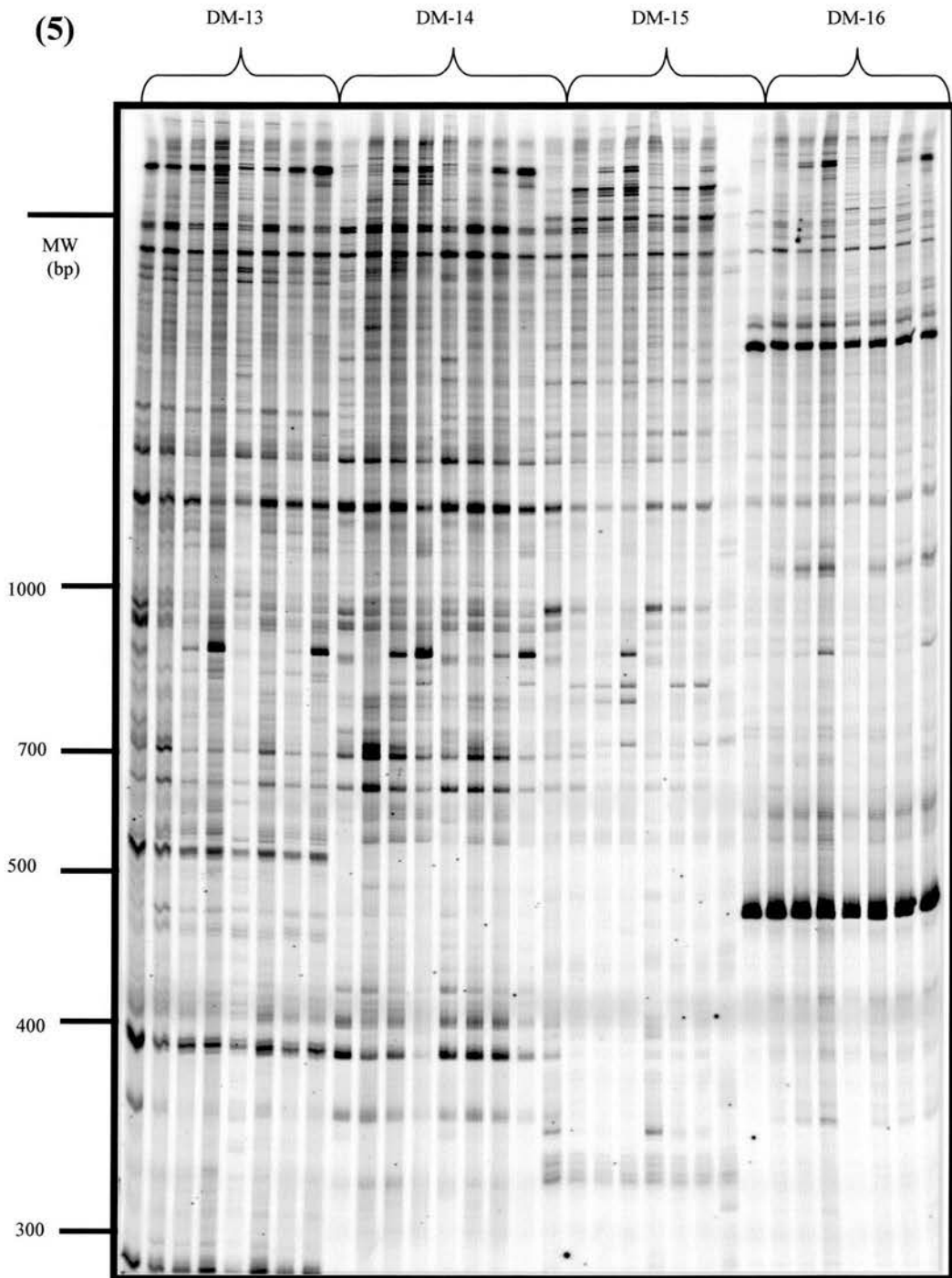


(3)

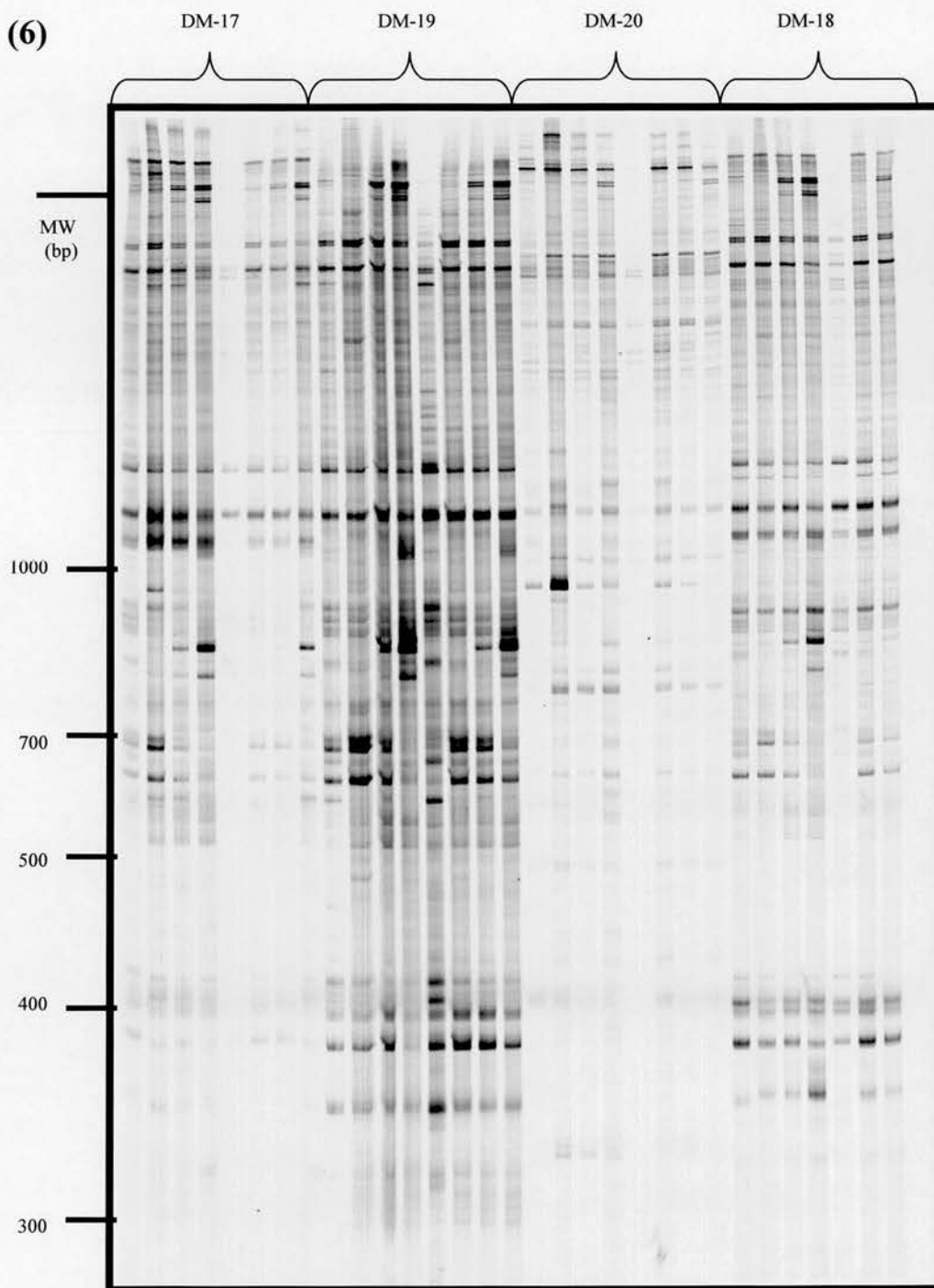


(4)

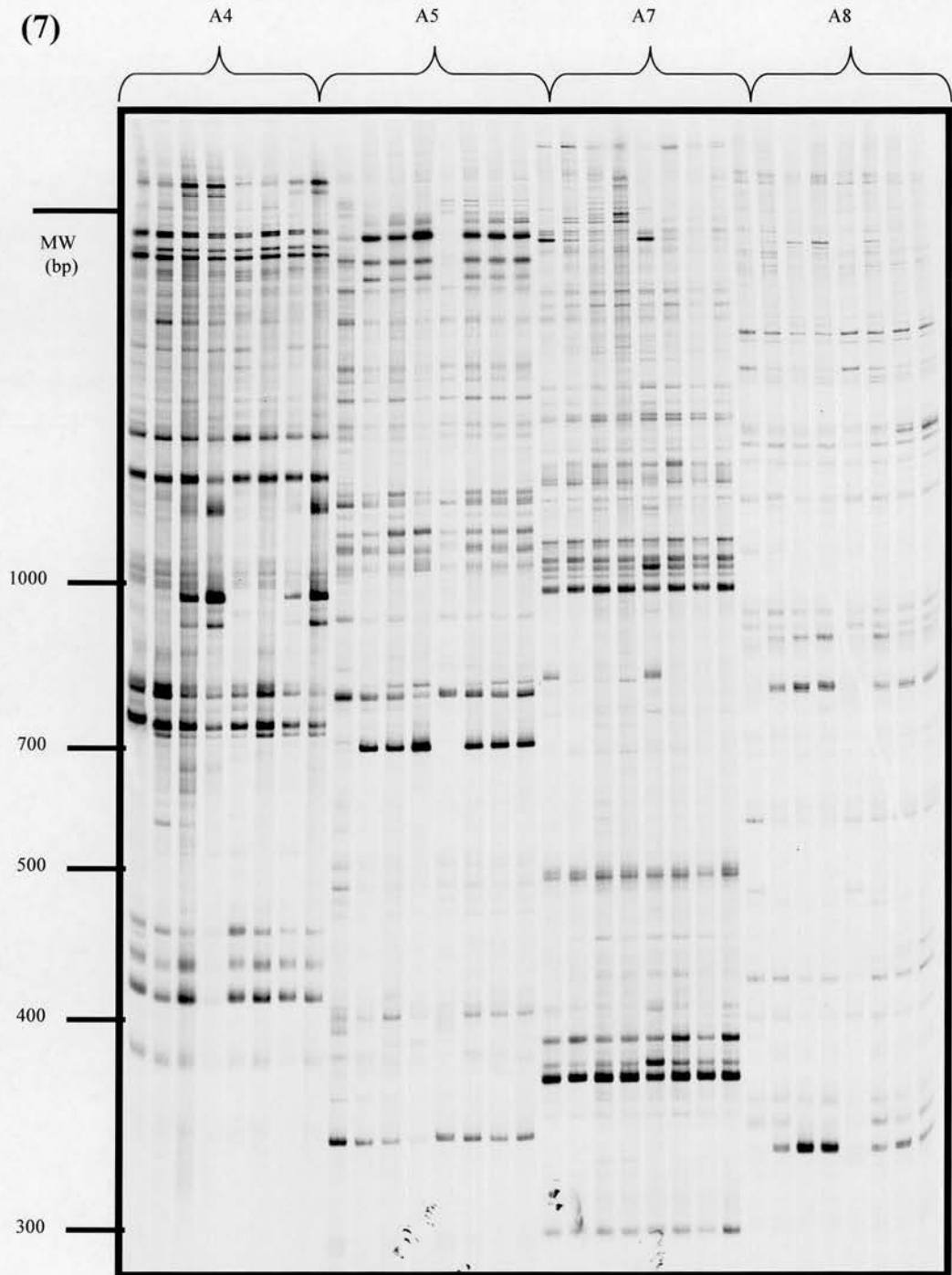




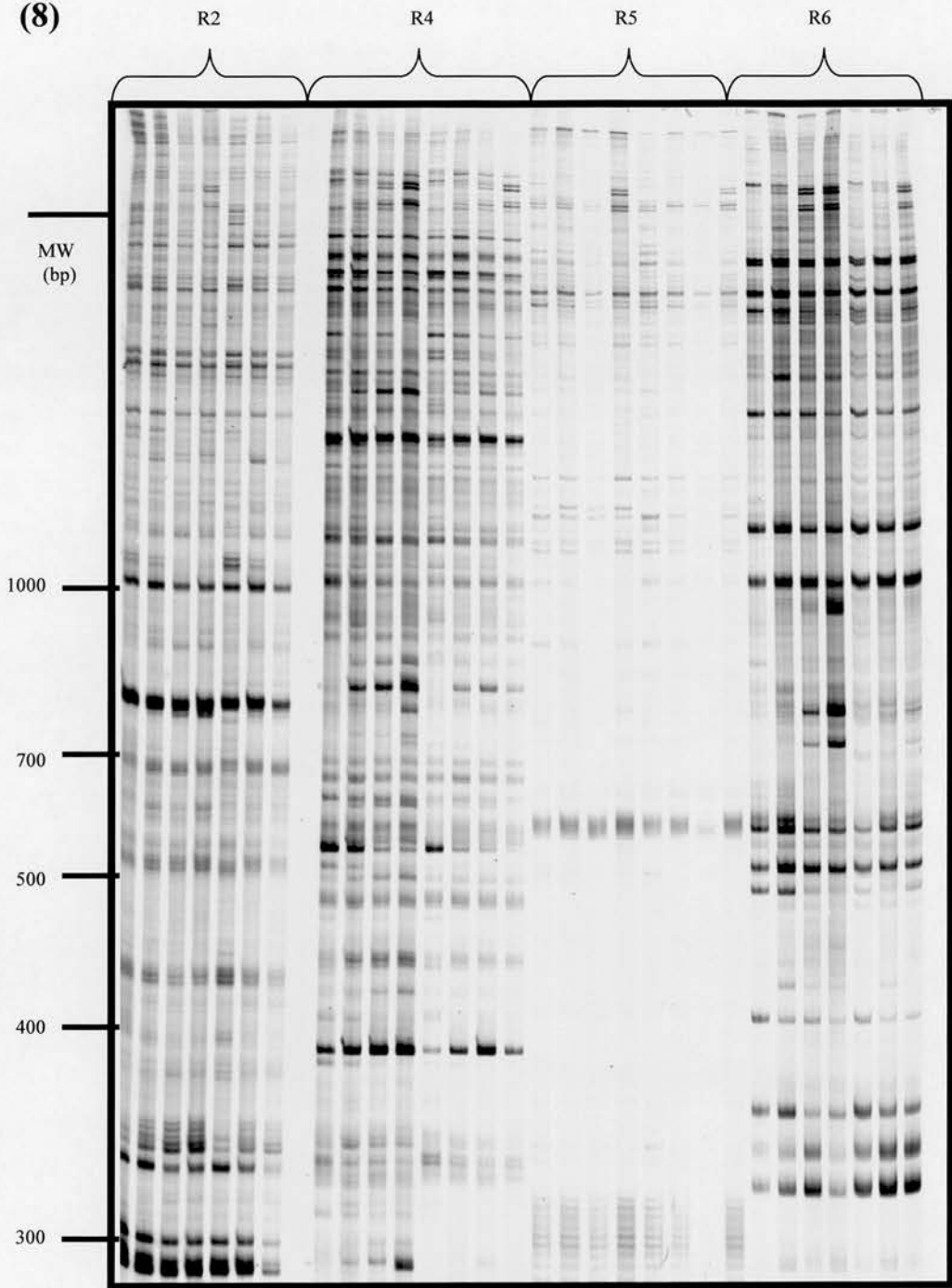
(6)



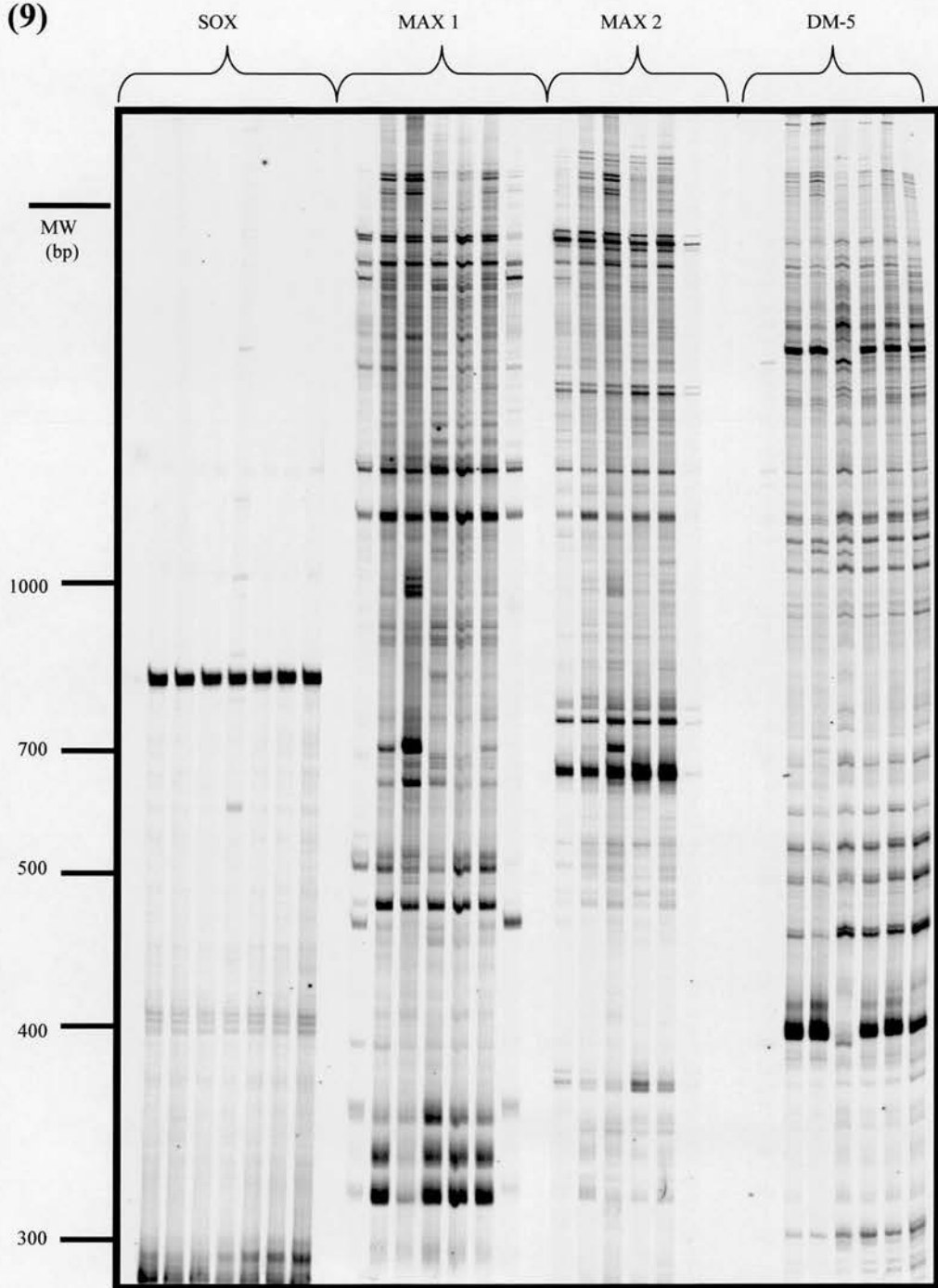
(7)



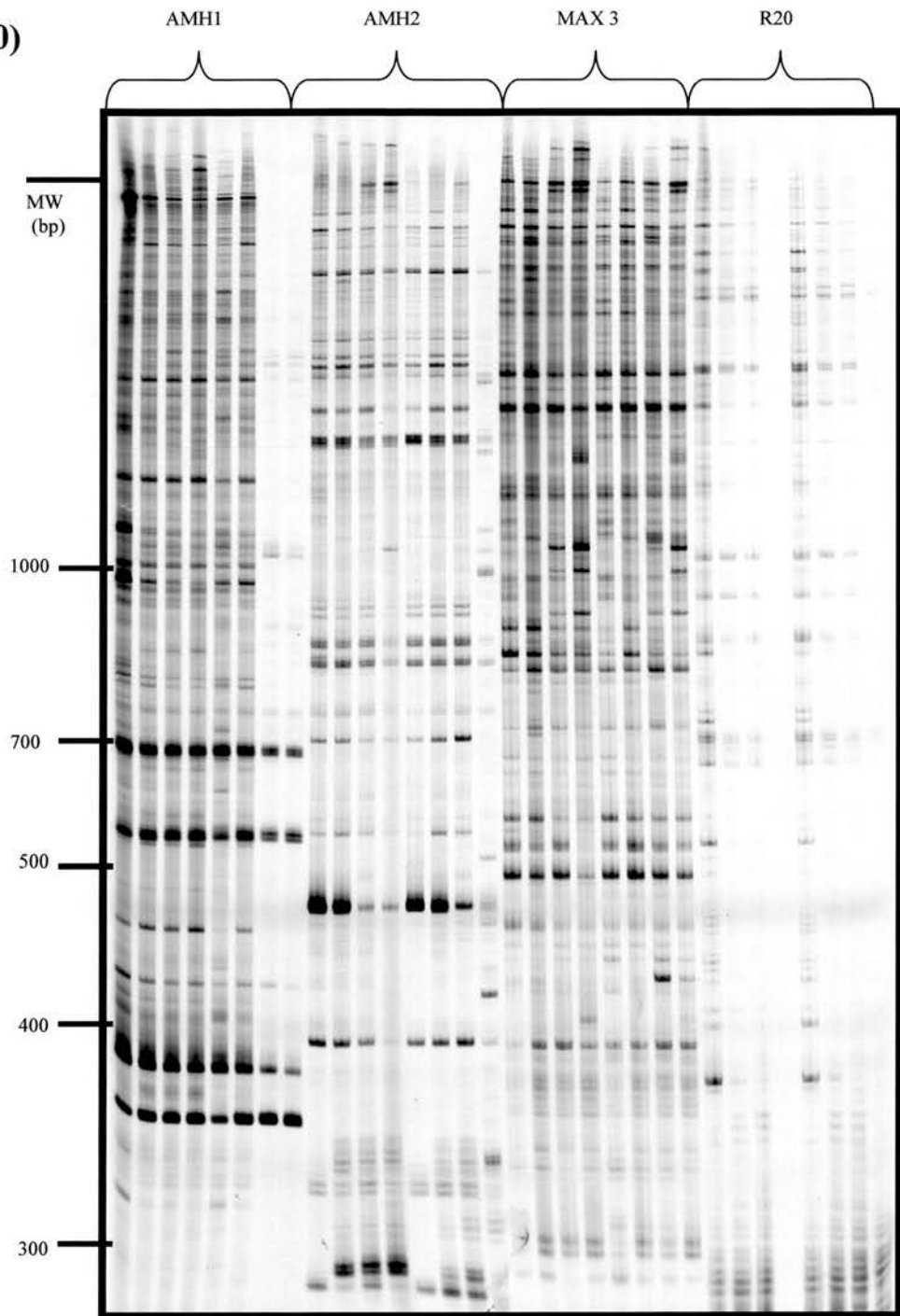
(8)



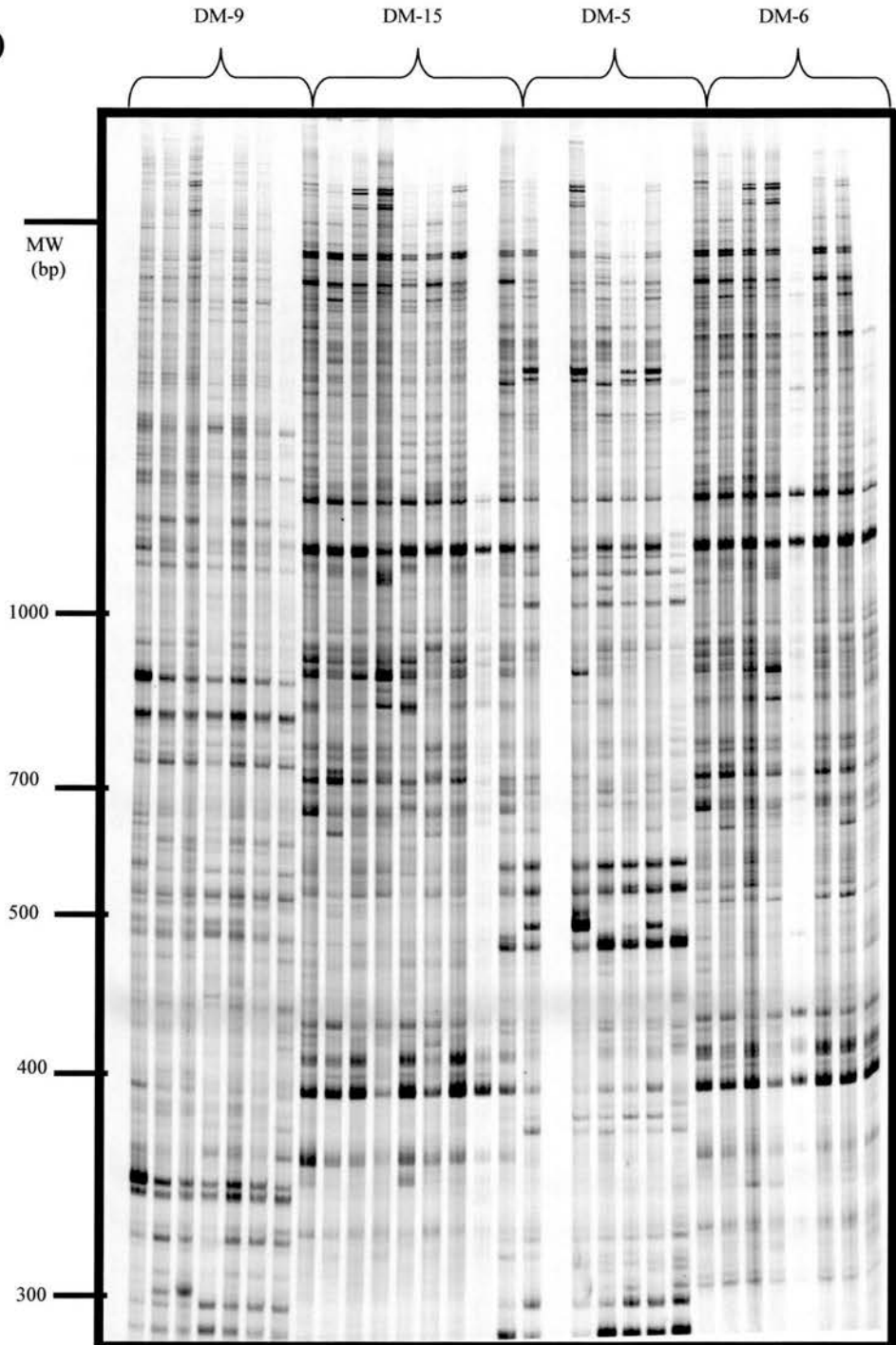
(9)



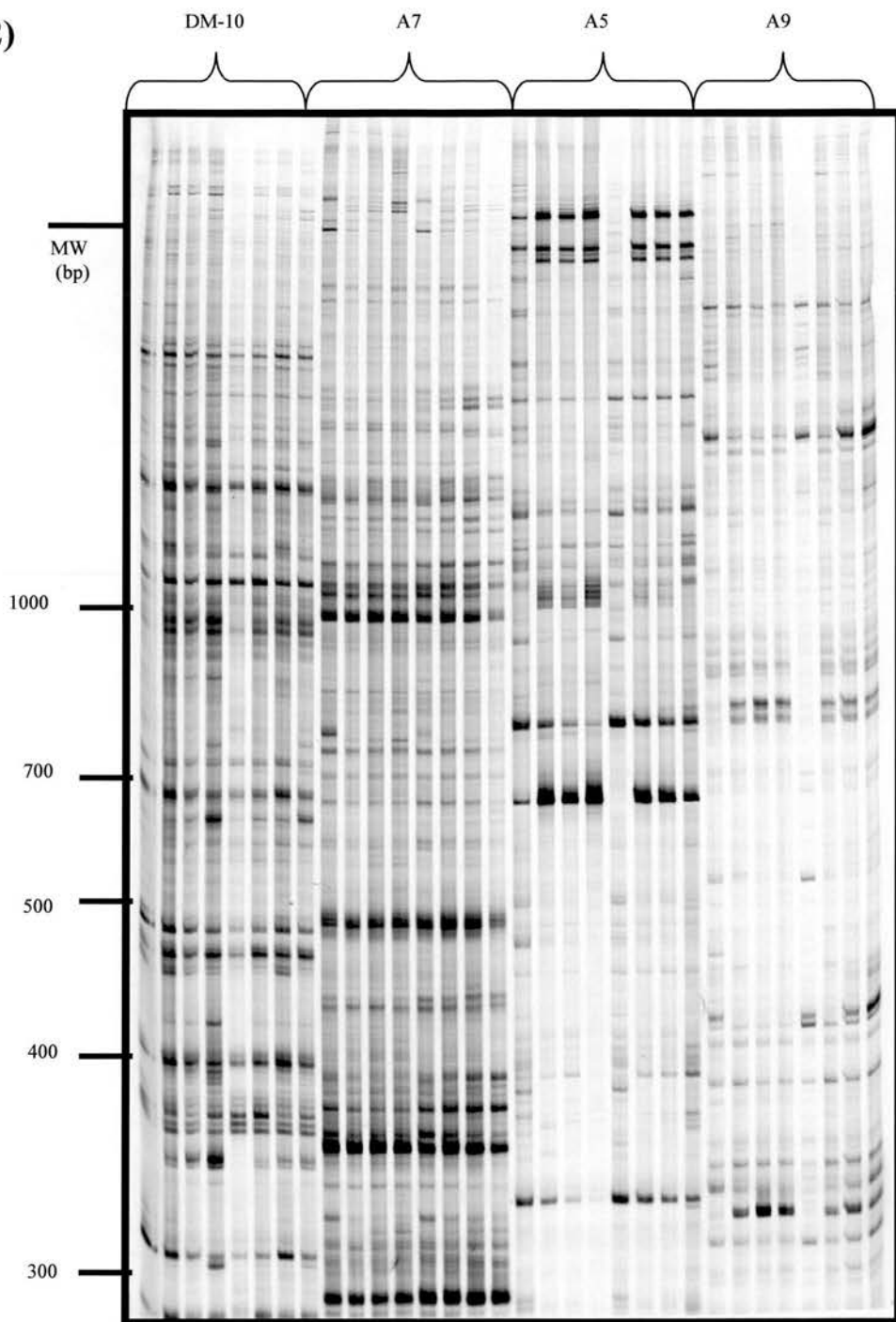
(10)



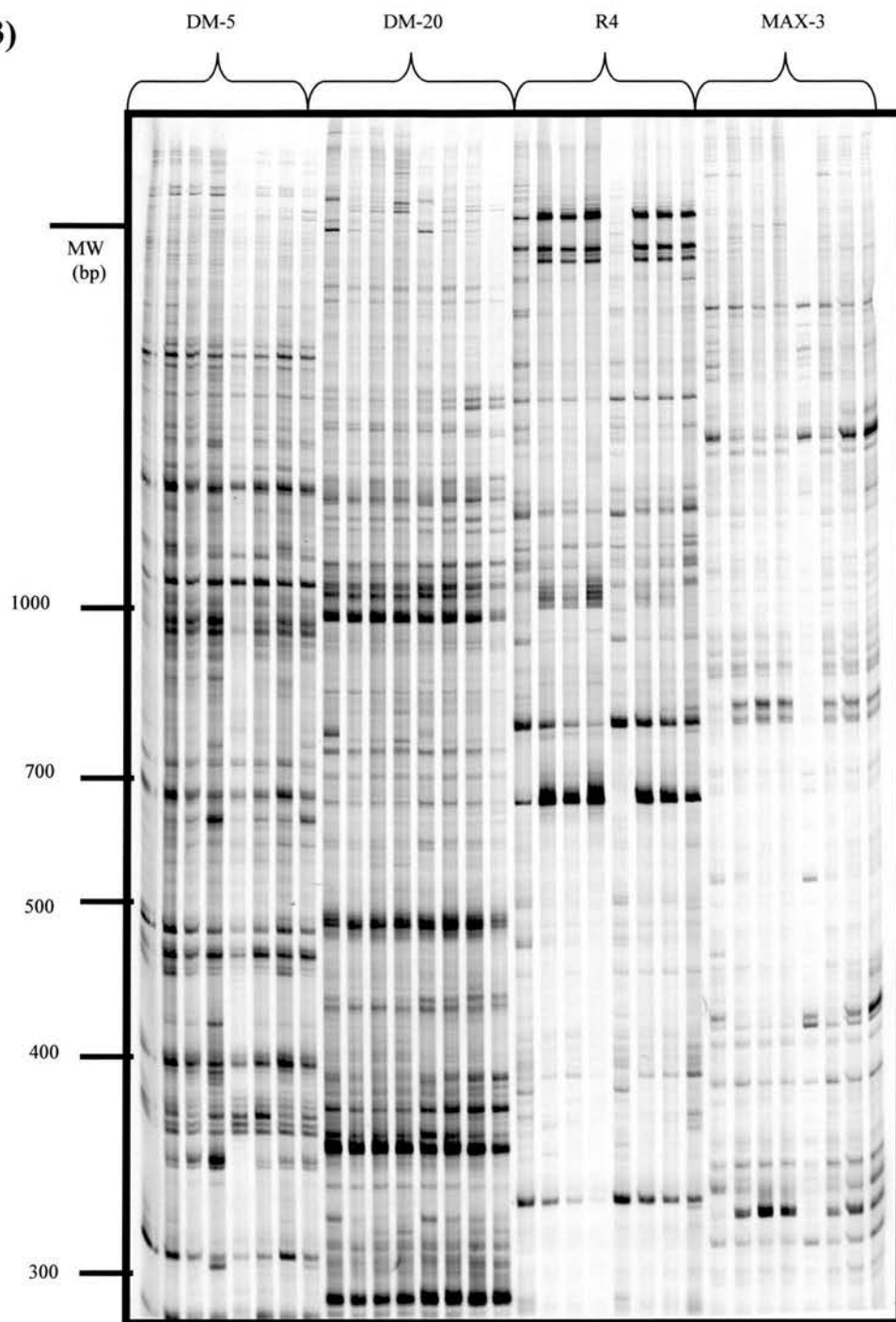
(11)



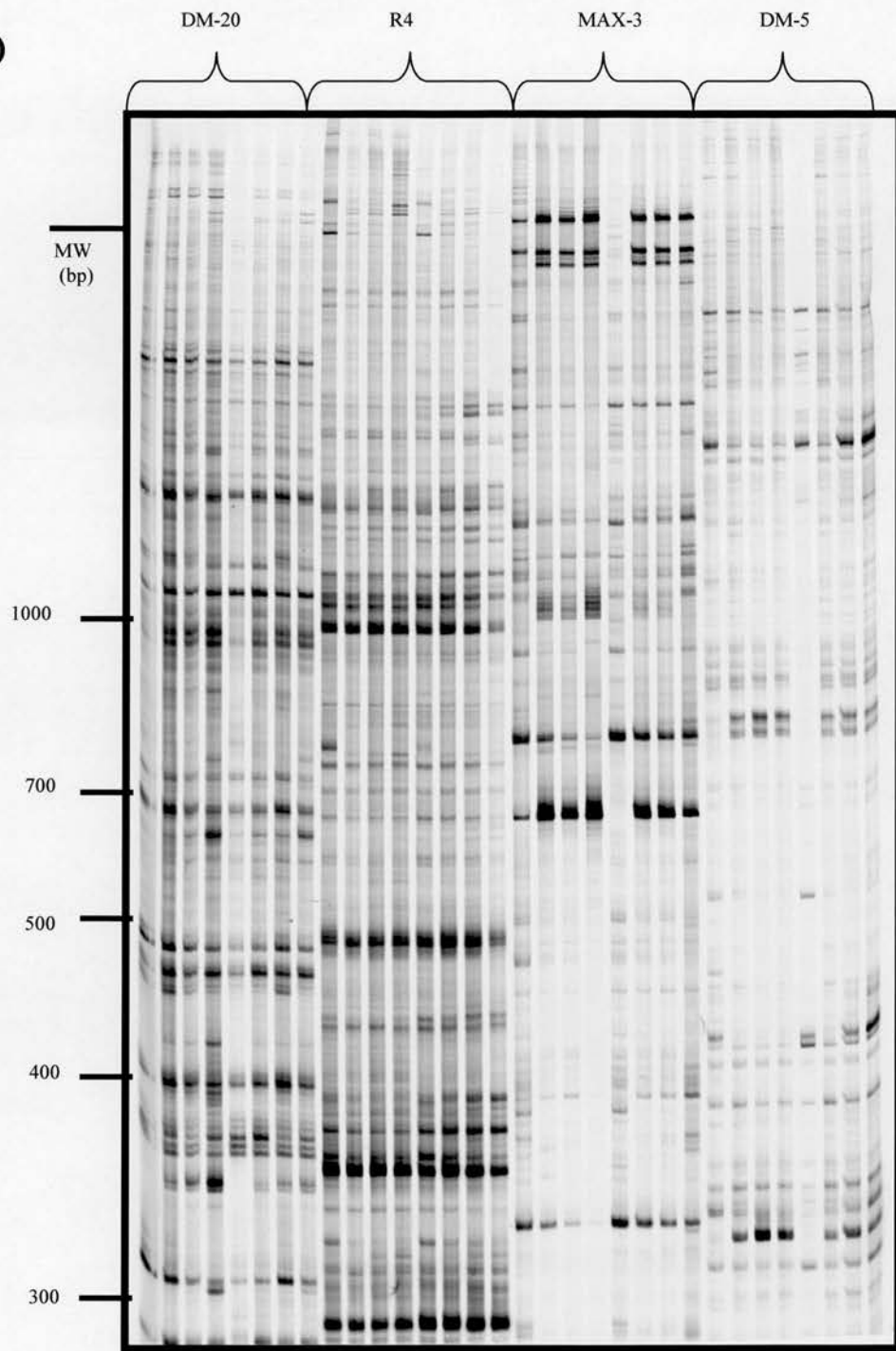
(12)



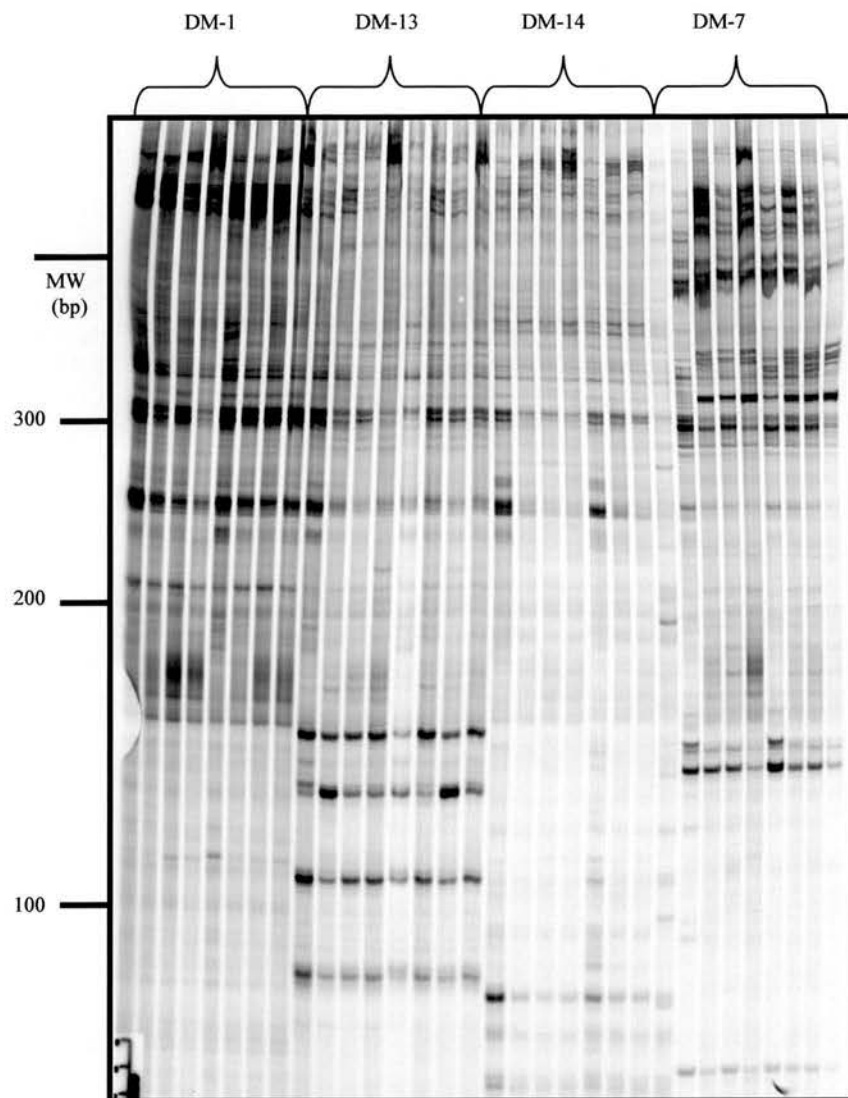
(13)



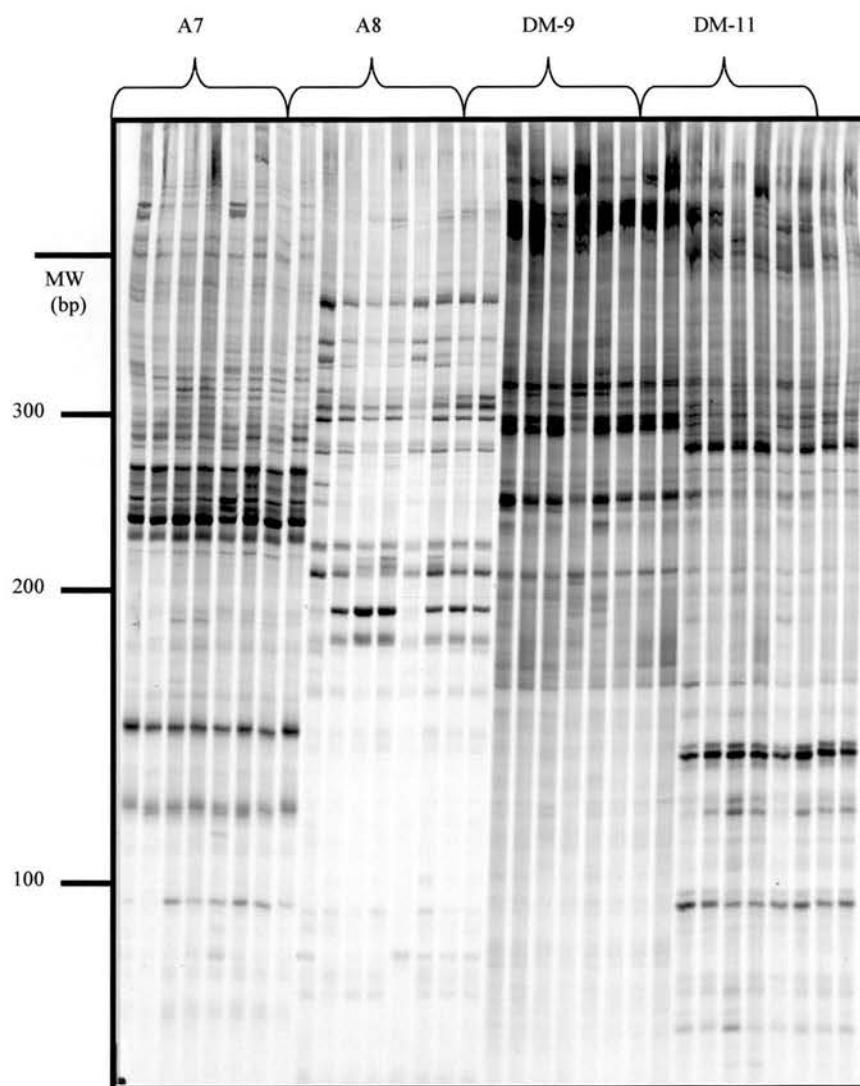
(14)



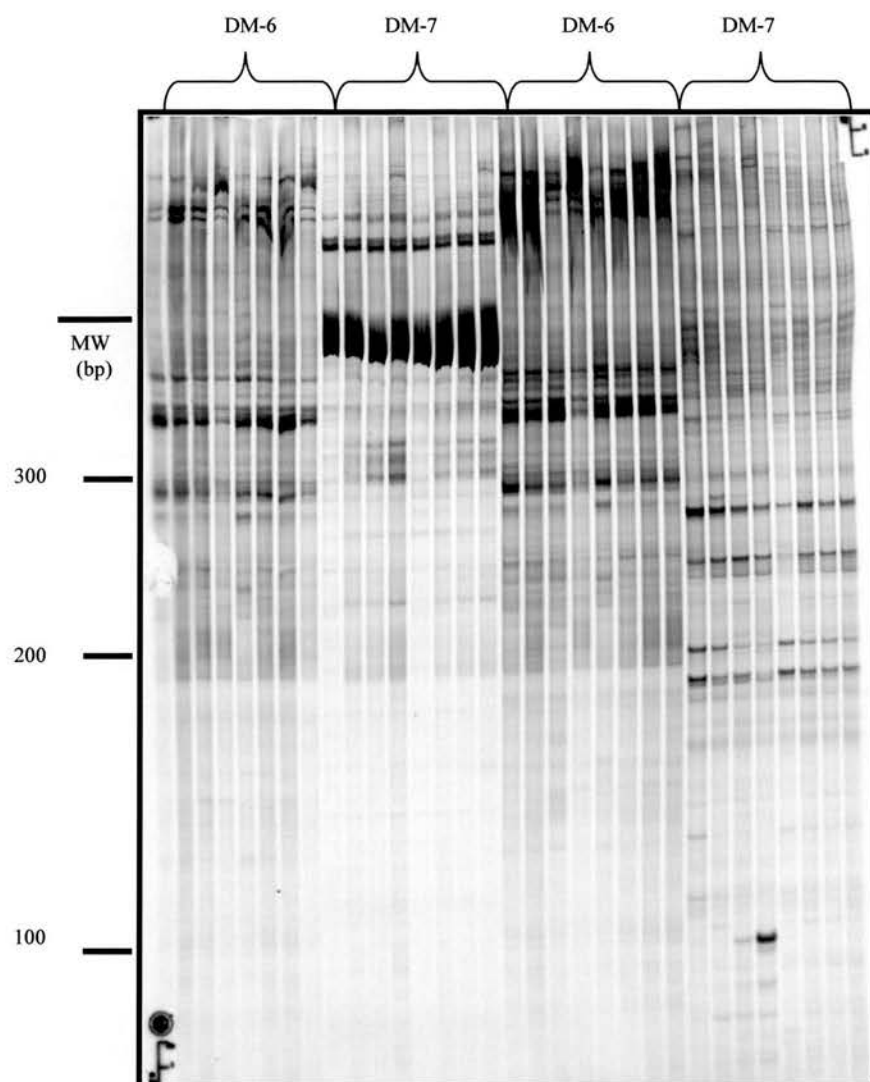
(15)



(16)



(17)



Appendix E

(a) Ha oligonucleotide epitope tag

(57bp)

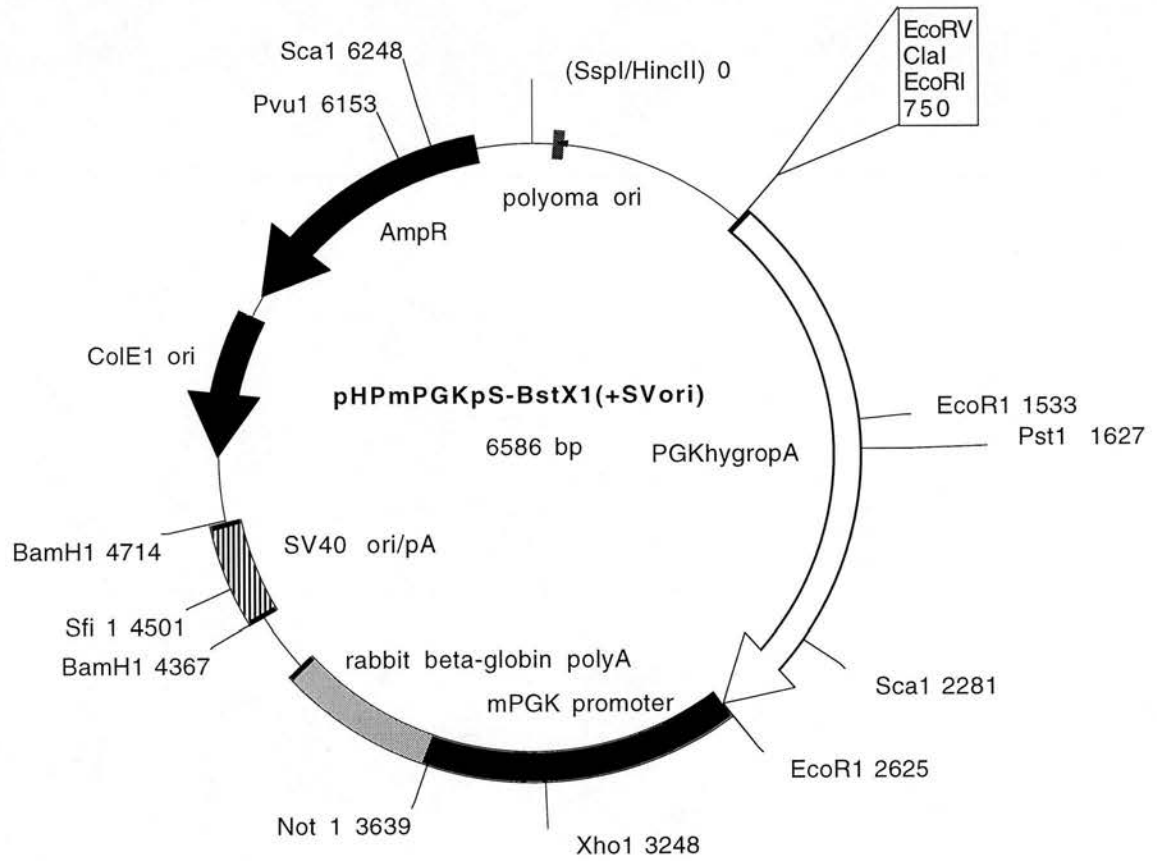
3' - TCG, TAC, CGT, ATG, GGG, ATG, CTA, CAG, GGT, CTG, ATA, CGC,
TCA, AAT, CCC, GGG, CCT, GGA, ATT - 5'

(18aa)

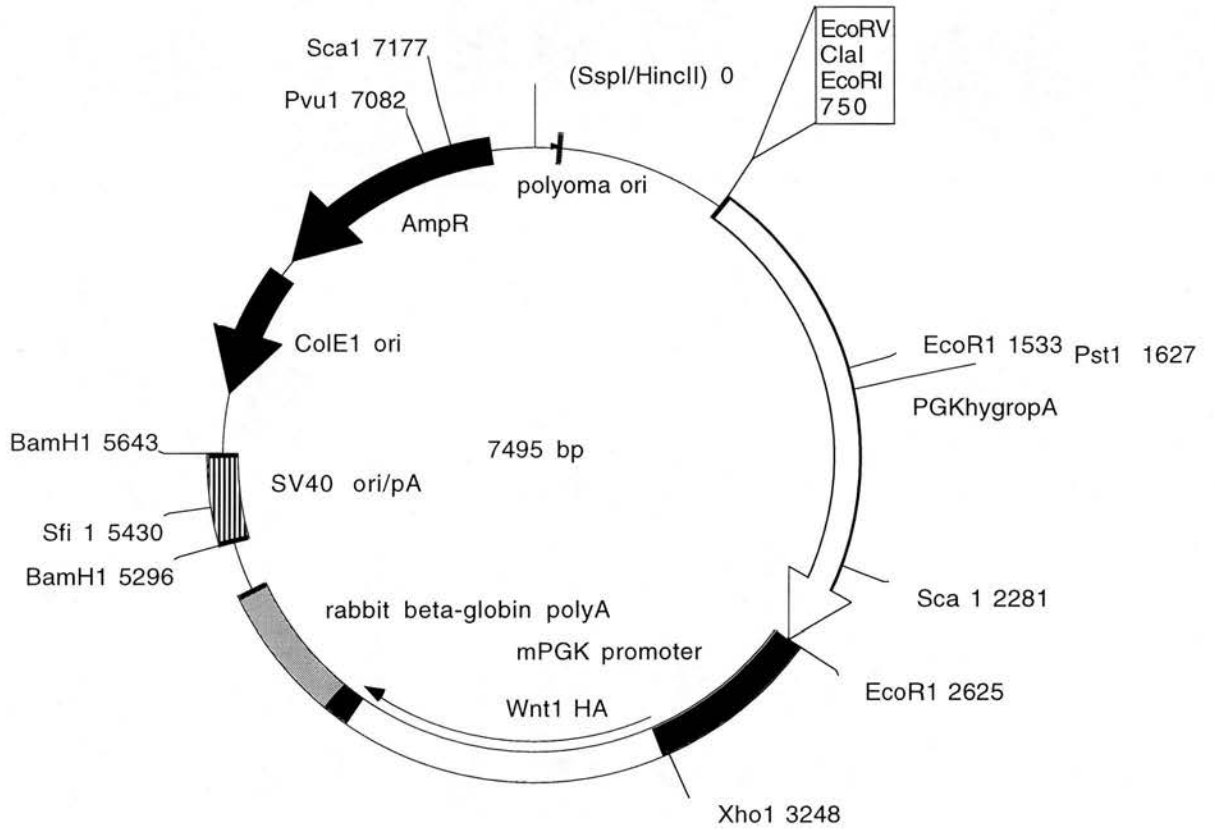
SMAYPYDVPDYASLGPGP stop

(b) Phagemid Cloning Vectors

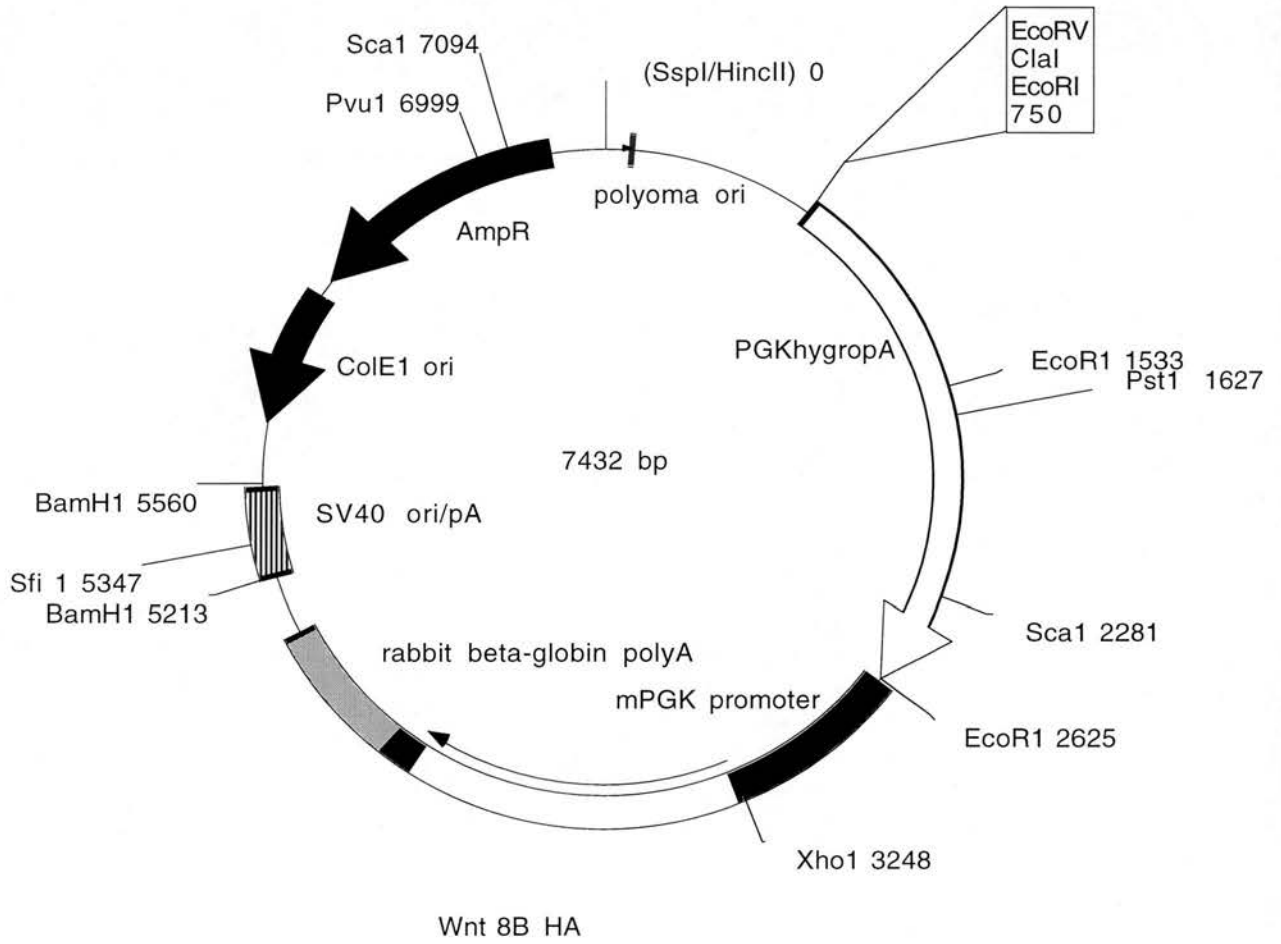
PGK Vector (pHPmPGKpS-BstX1(+ SVori))



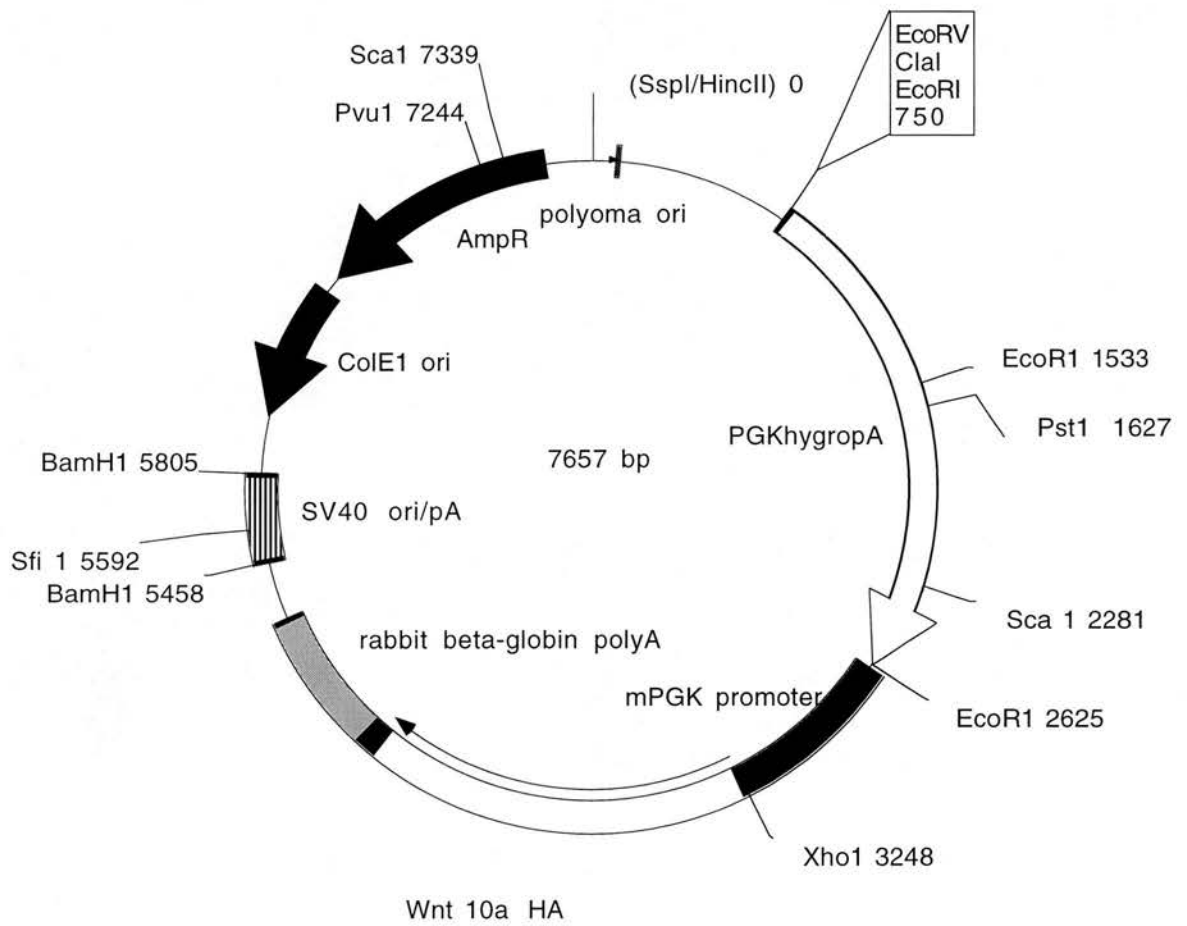
Wnt1 HA PGK

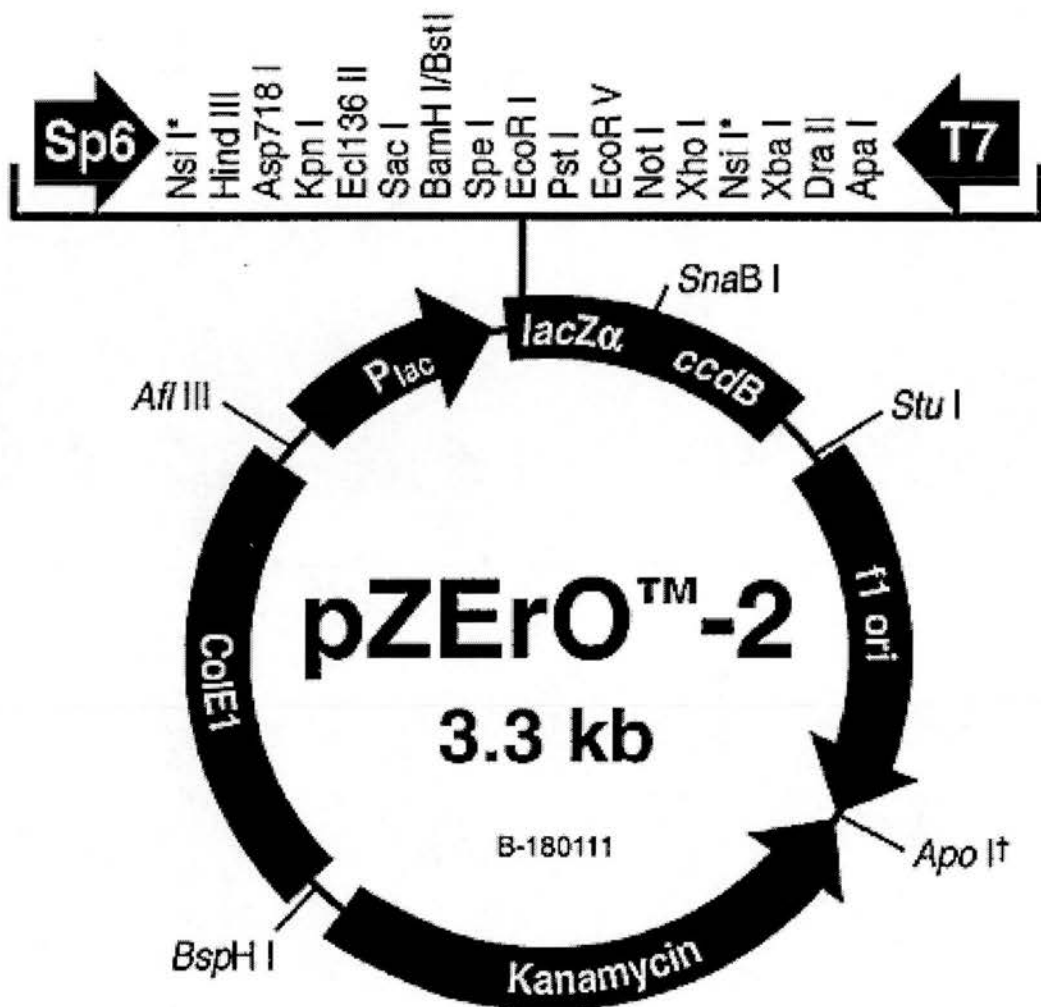


Wnt8b HA PGK



Wnt10 HA PGK

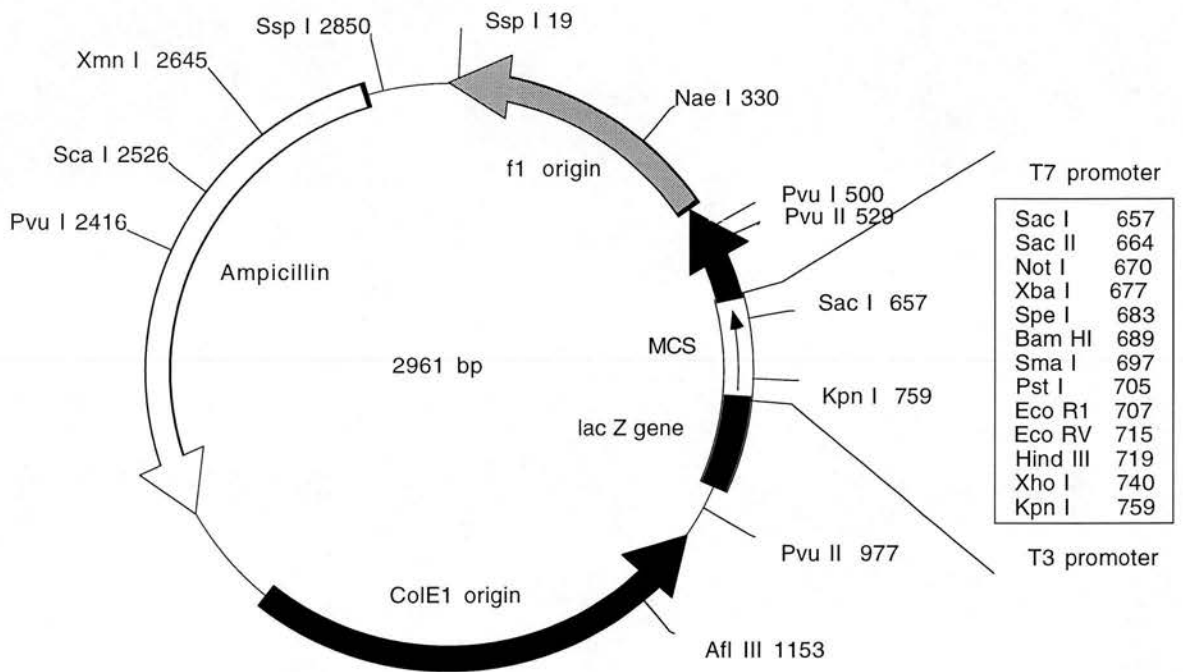




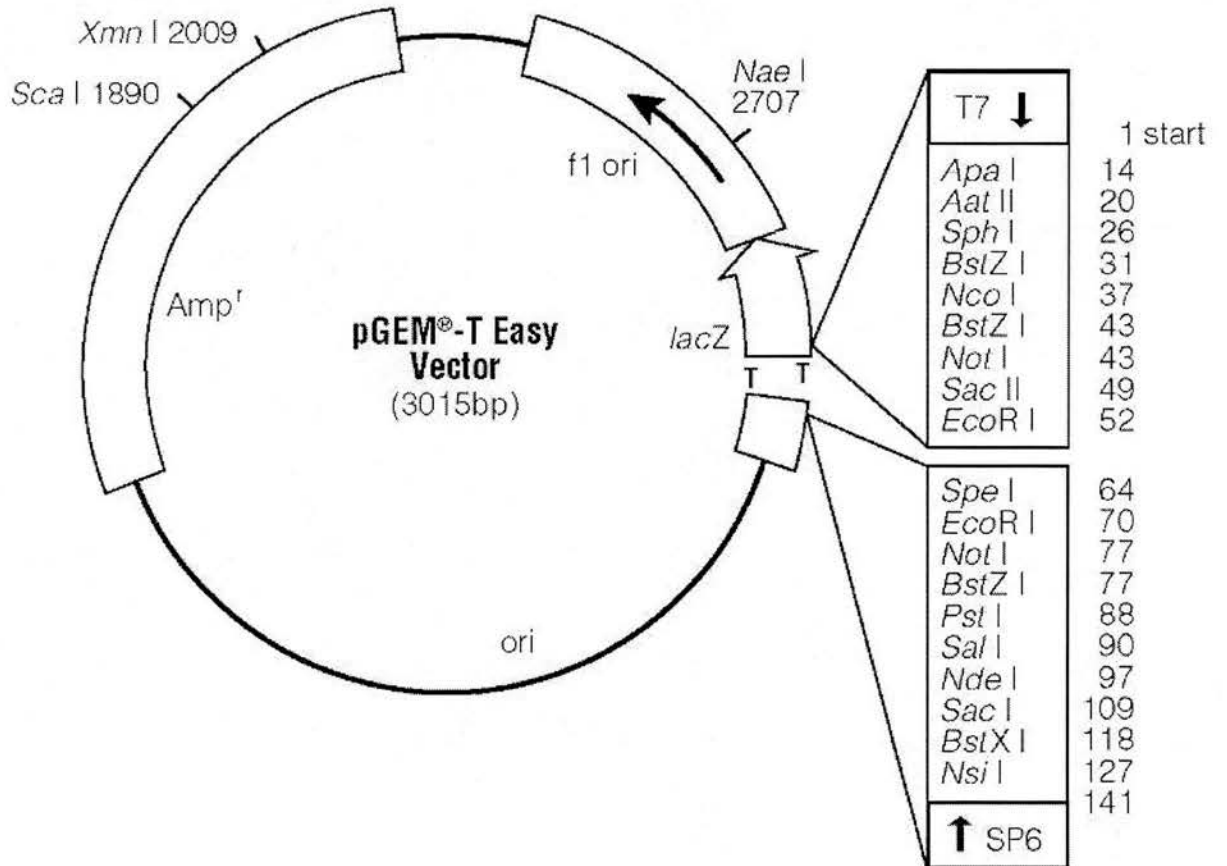
* The two *Nsi* I sites in the MCS are the only sites in the vector.

† There are two tandem *Apo* I sites at this location. *Apo* I also recognizes the *EcoR* I site.

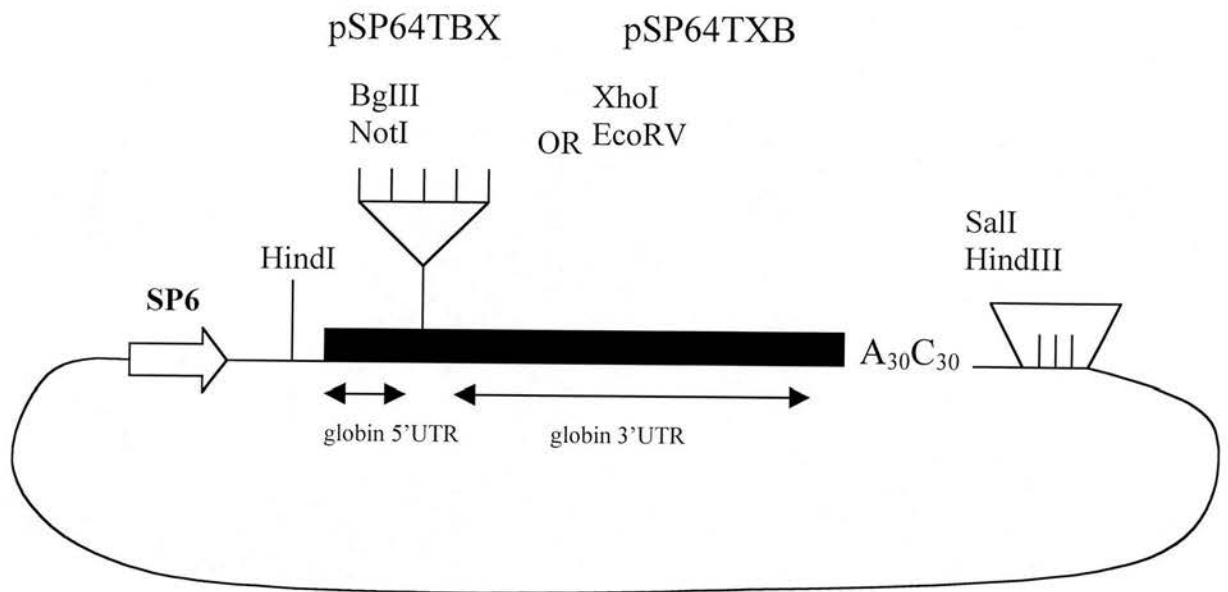
pBluescript II KS +



pGEM[®]-T Easy Vector



Xenopus vector Psp64TBX or Psp64TXB



Inactivation of *Apc* perturbs mammary development, but only directly results in acanthoma in the context of *Tcf-1* deficiency

Ronald CJ Gallagher^{2,3,6}, Trevor Hay¹, Valerie Meniel¹, Catherine Naughton², Thomas J Anderson³, Hiroyuki Shibata⁴, Masaki Ito⁴, Hans Clevers⁵, Tetsuo Noda⁴, Owen J Sansom¹, John O Mason² and Alan R Clarke^{*1}

¹Department of Biological Sciences, Cardiff University, Cardiff CF10 3US, UK; ²Department of Biomedical Sciences, University of Edinburgh, Medical School, Teviot Place, Edinburgh EH8 9AG, UK; ³Department of Pathology, University of Edinburgh, Medical School, Teviot Place, Edinburgh EH8 9AG, UK; ⁴Department of Cell Biology, Cancer Institute, Toshima-ku, Tokyo 170, Japan; ⁵Department of Immunology and Centre for Biomedical Genetic University Medical Center, Utrecht, The Netherlands

Apc (adenomatous polyposis coli) encodes a tumour suppressor gene that is mutated in the majority of colorectal cancers. Recent evidence has also implicated *Apc* mutations in the aetiology of breast tumours. *Apc* is a component of the canonical Wnt signal transduction pathway, of which one target is *Tcf-1*. In the mouse, mutations of both *Apc* and *Tcf-1* have been implicated in mammary tumorigenesis. We have conditionally inactivated *Apc* in both the presence and absence of *Tcf-1* to examine the function of these genes in both normal and neoplastic development. Mice harbouring mammary-specific mutations in *Apc* show markedly delayed development of the mammary ductal network. During lactation, the mice develop multiple metaplastic growths which, surprisingly, do not spontaneously progress to neoplasia up to a year following their induction. However, additional deficiency of *Tcf-1* completely blocks normal mammary development and results in acanthoma.

Oncogene (2002) 21, 6446–6457. doi:10.1038/sj.onc.1205892

Keywords: *Apc*; *Tcf-1*; mammary; acanthoma; cre

Introduction

The tumour suppressor gene *adenomatous polyposis coli* (*Apc*) was first identified in the dominantly inherited disorder familial adenomatous polyposis (FAP) (Grodin *et al.*, 1991). This is characterized by the development of multiple colorectal adenomas some of which progress to carcinoma. It is now clear that *Apc* is mutated in the vast majority of colorectal cancers, both spontaneous and inherited (Fearnhead *et al.*, 2001). *Apc* encodes a very large protein of 2843 amino

acids. Our understanding of the mechanisms by which loss of *Apc* function leads to colon cancer is far from complete. However, it is clear that one of the functions of *Apc* lies in its regulation of the Wnt signalling pathway. Wnts are secretory glycoproteins that have important roles in the development of many tissues (Cadigan and Nusse, 1997). Activation of the canonical Wnt signalling pathway leads to the stabilisation of β -catenin, a multifunctional protein normally found in adherens junctions. *Apc* forms part of a complex which normally targets cytoplasmic β -catenin for degradation by the proteasome (Fearnhead *et al.*, 2001; Polakis, 2000). In response to Wnt signals, stabilized cytoplasmic β -catenin translocates to the nucleus where it interacts with members of the LEF/TCF family of transcription factors (Roose and Clevers, 1999). Many *Apc* mutations associated with neoplasia give rise to a form of the protein unable to target β -catenin for ubiquitination and degradation, resulting in accumulation of nuclear β -catenin. It is now commonly accepted that the key tumour suppressor function of *Apc* lies in its ability to destabilize free β -catenin (Smits *et al.*, 1999; Bienz and Clevers, 2000). A number of genes activated by this pathway have been identified, including cyclin D1 (Tetsu and McCormick, 1999; Shtutman *et al.*, 1999), *c-myc* (He *et al.*, 1998), *PPAR δ* (He *et al.*, 1999) and *Tcf-1* (Roose *et al.*, 1999). Cyclin D1 has recently been shown to be central to ras and neu mediated mammary oncogenesis, although this despondency apparently does not extend to pathways driven by *c-myc* or *Wnt1* (Yu *et al.*, 2001). TCF functions often depend on partner proteins and on simultaneous signalling by other pathways. Thus, TCF is believed to play a key role in integrating multiple positional inputs (Bienz and Clevers, 2000). The activation of *Tcf-1* by β -catenin/*Tcf-4* acts within a feedback repressor pathway, whereby *Tcf-1* isoforms lacking a β -catenin interaction domain bind to DNA target sequences but fail to mediate gene activation. Negative regulation by *Tcf-1* may also involve Groucho-related transcriptional repressors, as *Tcf-1* has been shown to interact with Groucho proteins in *Xenopus* (Roose *et al.*, 1998, 1999).

*Correspondence: AR Clarke; E-mail: ClarkeAR@cf.ac.uk

⁶Current address: SNBTS Cell Therapy Group, John Hughes Bennett Lab, Western General Hospital, Crewe Road, Edinburgh EH4 2XU
 Received 12 April 2002; revised 17 July 2002; accepted 18 July 2002

Overexpression of *Wnt1*, *Wnt3* and *Wnt10B* genes in the mammary epithelium promotes tumorigenesis (Nusse and Varmus, 1982; Tsukamoto *et al.*, 1988; Lane and Leder, 1997); and stabilization of cytoplasmic β -catenin is critical for Wnt-mediated oncogenicity (Shimizu *et al.*, 1997). It has recently been shown by two groups that mice overexpressing a mutant, stabilized form of β -catenin in the mammary gland also develop tumours (Imbert *et al.*, 2001; Michaelson and Leder, 2001), although other workers have reported that conditional mutation of β -catenin can lead to metaplasia, rather than neoplasia (Miyoshi *et al.*, 2002).

Mice deficient in *Tcf-1* are viable and capable of lactation, but acanthomas are reported to develop in the females, with an earliest onset of 4 months and with a peak incidence of 25% at 12 months of age (Roose *et al.*, 1999). Synergy has already been demonstrated between mutations in *Tcf-1* and *Apc* through accelerated tumorigenesis on the *Apc*^{Min} heterozygous background (Roose *et al.*, 1999).

Although *Wnt1* overexpression leads to tumour development, *Wnt1* itself is not normally expressed in the mammary gland, suggesting that ectopically expressed Wnt mediates its effect through receptors for other Wnts that are normally expressed there. A number of Wnts are expressed in dynamic patterns in the mammary gland and some of these have been shown to affect its normal development (Bradbury *et al.*, 1995; Briskin *et al.*, 2000).

In the last few years, strong evidence of a link between *Apc* mutation and human breast cancer has begun to accumulate. First, loss of heterozygosity at 5q21 (the chromosomal location of human *Apc*) has been observed in sporadic tumours of the breast (Kashiwaba *et al.*, 1994; Thompson *et al.*, 1993). Second, lost or reduced *Apc* protein expression has been demonstrated in human breast cancers (Ho *et al.*, 1999; Schlosshauer *et al.*, 2000). Third, the *Apc* I1307K polymorphism has been shown to increase the risk of breast cancer in association with *BRCA* founder mutations (Woodage *et al.*, 1998). Fourth, a recent study has demonstrated the presence of somatic *Apc* mutations in 18% of primary breast cancers of a range of histological types (Furuuchi *et al.*, 2000). Interestingly, the mutations reported by Furuuchi *et al.* (2000) are scattered throughout the *Apc* coding region and not confined to the mutation cluster region (MCR) defined by *Apc* mutations found in colon tumours. Finally, it has now been shown that the *Apc* promoter is frequently hypermethylated in breast cancers (Jin *et al.*, 2001). Of note, this study was performed over a range of histological classes of primary breast cancer, with no clear association reported between histological type and methylation status.

Mice homozygous for inactivating mutations in *Apc* (such as *Apc*^{Min}) die at an early embryonic stage (Moser *et al.*, 1995). Heterozygous mice are viable, but prone to the development of intestinal adenomas and mammary carcinomas (Moser *et al.*, 1993). Homozygous lethality therefore precludes the direct analysis

of the developmental role of *Apc* in adult organ systems. In order to analyse the role of *Apc* both in the development of the mammary gland and in mammary tumorigenesis, we have used a *cre-loxP* based strategy (Gu *et al.*, 1994) to conditionally inactivate *Apc*. We have also investigated the interaction between *Apc* and *Tcf-1* deficiency by subsequently crossing onto a *Tcf-1* null background. Here we report that deficiency of *Apc* perturbs development and leads to metaplasia, and that combined deficiency of *Apc* and *Tcf-1* blocks normal mammary gland development and results directly in acanthoma formation.

Results

Mammary gland specific inactivation of Apc

Mice homozygous for a *loxP*-flanked ('floxed') exon 14 *Apc* have previously been shown to develop normally. These were designated *Apc*^{580s/580s}, where 's' denotes silent mutation. *Cre*-mediated excision of the floxed exon 14 leads to a frameshift mutation at codon 580, in the region of the armadillo repeats. These mice developed adenomas within 4 weeks when *cre* recombinase was introduced to the colorectal region via infection with an adenovirus encoding the recombinase (Shibata *et al.*, 1997). To examine the role played by *Apc* in mammary gland development we used a transgenic approach where the *cre* gene is under the control of the ovine β -lactoglobulin enhancer (BLG-*cre*). This transgene has previously been shown to induce very efficient excision of floxed DNA molecules in mice (Selbert *et al.*, 1998; Chapman *et al.*, 1999).

We generated mice homozygous for the floxed *Apc* allele (*Apc*^{580s/580s}) and carrying the BLG-*cre* transgene. All mice so far generated have developed normally with litter sizes being similar between *cre*⁺ *Apc*^{580s/580s}, *cre*⁺ *Apc*^{580s/+} and *cre*⁻ *Apc*^{580s/580s} females. Numbers of male and female offspring have shown no bias towards either sex from control *versus* experimental strains. However, it was noted that offspring from the *cre*⁺ *Apc*^{580s/580s} mothers did not thrive.

As a sensitive measure of *cre* recombinase activity in the epithelium of virgin glands, we crossed our BLG-*cre* transgenic animals to the *cre* ROSA reporter strain (Soriano, 1999). Virgin mammary glands were removed from double transgenics and stained for β -galactosidase activity (Figure 1). Wholmount and histological analysis of these glands showed widespread and highly efficient recombination throughout the epithelium of the virgin gland. By day 10 of lactation the level of recombination as scored by the reporter strain rose to nearly 100% of epithelial cells (Figure 1). This analysis reflects the efficiency of *cre* mediated recombination at a single *lox* flanked allele.

Despite the very high levels of recombination indicated by the reporter strain and previous high levels of recombination obtained at other loci using this strain (Chapman *et al.*, 1999; Selbert *et al.*, 1998), densitometric analysis of Southern blots showed only

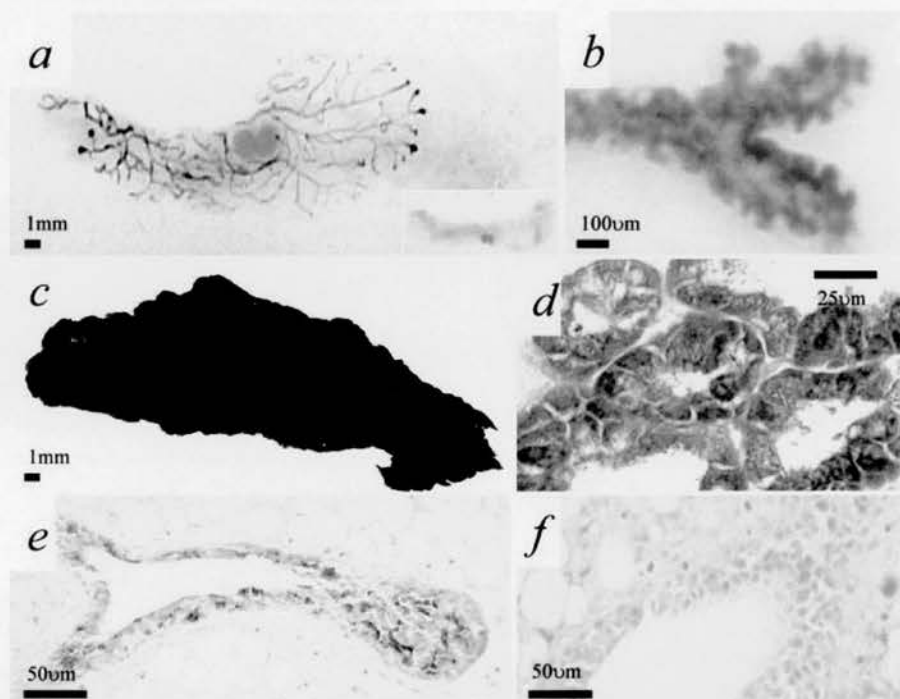


Figure 1 The pattern of Cre-mediated recombination as scored using the flox-STOP Rosa 26 reporter strain, where LacZ positivity indicates cre mediated recombination: (a) 8 week old virgin gland transgenic for the BLG-cre transgene and for the reporter construct ($\times 4$ magnification). Inset shows an age matched control virgin (BLG-cre negative, reporter construct positive, $\times 1$ magnification) within which no LacZ staining was evident at either high or low power; (b) medium power ($\times 30$ magnification) of detail in (a) showing a mosaic pattern of recombination within duct termini; (c) Cre mediated recombination at full lactation, low power photograph of an entire BLG-cre positive, reporter construct positive gland. No LacZ staining was observed in control glands. (d) High power ($\times 400$) of a $5 \mu\text{m}$ section showing recombination in alveoli derived from (c); (e) High power ($\times 400$) of a $5 \mu\text{m}$ section showing recombination in a duct derived from (a); (f) High power ($\times 200$) of a $5 \mu\text{m}$ section showing no recombination in a duct derived from control mice

approximately 30% of entire mammary gland DNA from cre^+ , *Apc*^{580s/580s} had undergone cre mediated recombination at day 10 of lactation (unpublished data). This reduced level of recombination may reflect relatively inefficient recombination at the *Apc* allele, the requirement for two recombination events within each cell or the effect of inclusion of non-epithelial cells (Southern analysis was performed on entire mammary glands, inclusive of lymph nodes). If, indeed, the low level of recombination directly reflects low efficiency recombination, this would predict a high incidence of heterozygous *Apc* mutant cells within the gland, and rather small numbers of homozygous mutant cells. We favour a second possibility, namely that of efficient recombination at the *Apc* allele, but subsequent strong selection against the recombined cells during mammary gland development, possibly mediated by apoptotic deletion of the recombined cells. We are currently investigating this possibility within our model.

Apc is required in virgin mammary gland

To investigate any potential role for *Apc* in the virgin gland, we examined wholemount mammary gland preparations from virgin animals. The extent of ductal growth of mammary glands from cre^+ *Apc*^{580s/580s}

mice was markedly delayed when compared with littermate control genotypes (Figure 2), consistent with a role for *Apc* in the normal growth of the gland. Although delayed in development, mutant glands appeared otherwise normal, showing neither the increased branching observed in MMTV-*Wnt1* transgenic mice (Tsukamoto *et al.*, 1988; Imbert *et al.*, 2001) or the precocious lobulo-alveolar development seen in MMTV- $\Delta\text{N}89\beta$ -catenin mice (Imbert *et al.*, 2001).

Loss of *Apc* leads to mammary gland metaplasia

We next analysed the consequence of *Apc* disruption during lactation. Histological examination of day 10 lactating mammary glands from cre^+ *Apc*^{580s/580s} mice revealed extensive metaplastic nodules throughout each mammary gland examined. This phenotype was 100% penetrant, being observed in all glands in all mice examined. The nodules consist of tightly bound balls of epithelial cells emanating from ducts, which transdifferentiate into squamous cells (Figure 3f). Small areas of similar appearance were found in virgin mammary sections (Figure 3b). Immunohistochemistry was performed to confirm that these areas arose following loss of *Apc* function using a c-

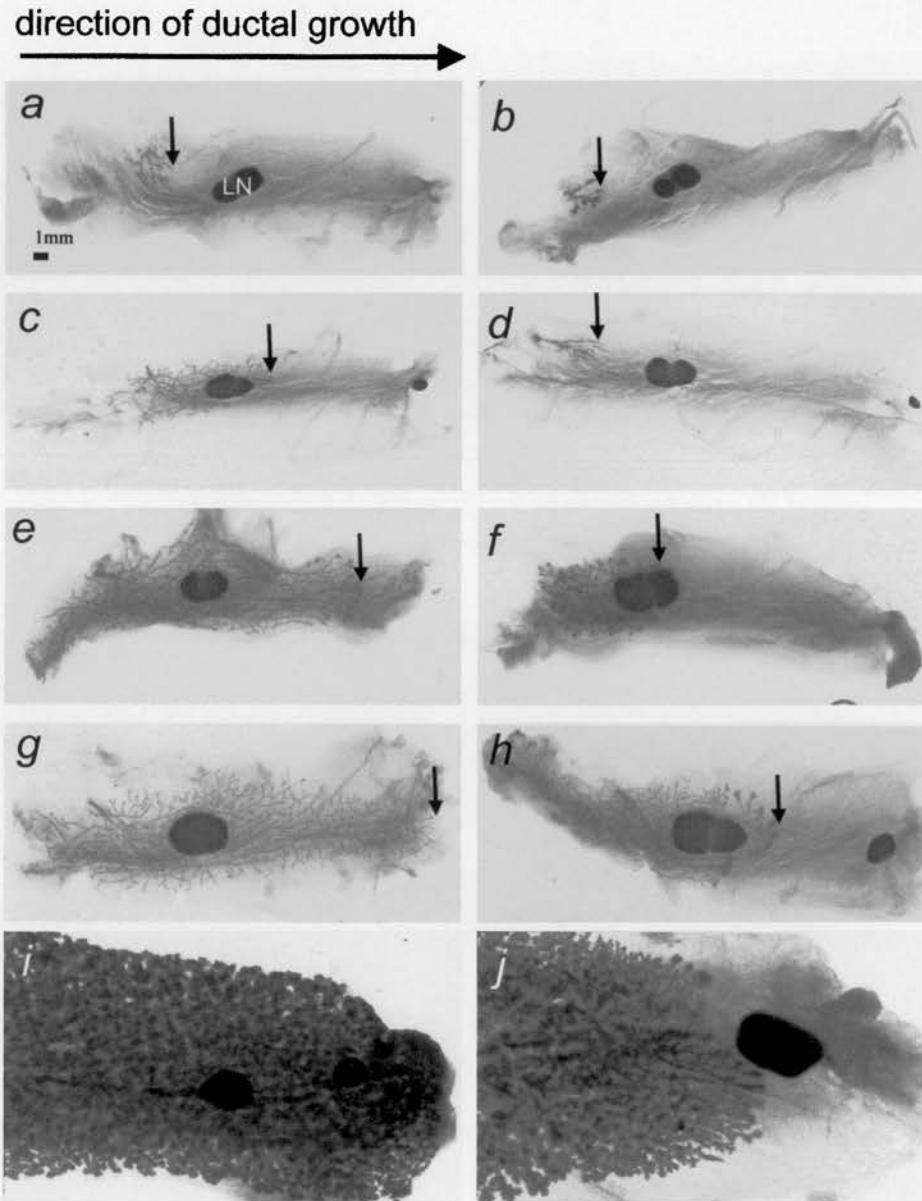


Figure 2 Growth of the mammary ductal network is delayed in $cre^+ Apc^{580s/580s}$ animals. A minimum of three mice were analysed for each genotype at each time point and representative photographs taken. Wholemount mammary preparations from $cre^+ Apc^{580s/+}$ animals (a,c,e,g,i) and $cre^+ Apc^{580s/580s}$ littermates (b,d,f,h,j). Growth of the ductal network initiates at the nipple end of the mammary fat pad (left) and progresses past the lymph node (LN) to completely fill the pad. The tip of the growing ductal network is marked by an arrow. Virgin glands shown are 4 weeks (a,b), 6 weeks (c,d), 8 weeks (e,f) and 12 weeks (g,h). (i) shows a 70 day control mammary at parturition and (j) shows a 70 day experimental mammary at parturition. Note that at this time point, despite the mammary having developed lobular alveolar structures, ductal growth has failed to reach the end of the fat pad. Analyses of older $cre^+ Apc^{580s/580s}$ mice show that ductal growth does eventually succeed in reaching the end of the fat pad

terminal *Apc* antibody. This analysis confirmed loss of *Apc* specifically within the tightly bound balls of epithelial cells (see Figure 6g,h) Ductal structures in mutant mammary glands appeared disorganized and papillary growth occurs into ducts (Figure 3g). Figure 3h shows a section of normal ductal epithelium with a secretory lobule apparently developing from it that shows prominent squamous

metaplasia. We observed keratohyaline granules, the hallmark of keratinizing squamous differentiation (Figure 4a), although more often we noted an eosinophilic material deriving from non-keratinizing squamous differentiation (Figures 3f and 4c). This material was frequently seen to form areas which contained no nuclei, but which were characterized by open spaces (Figure 4c).

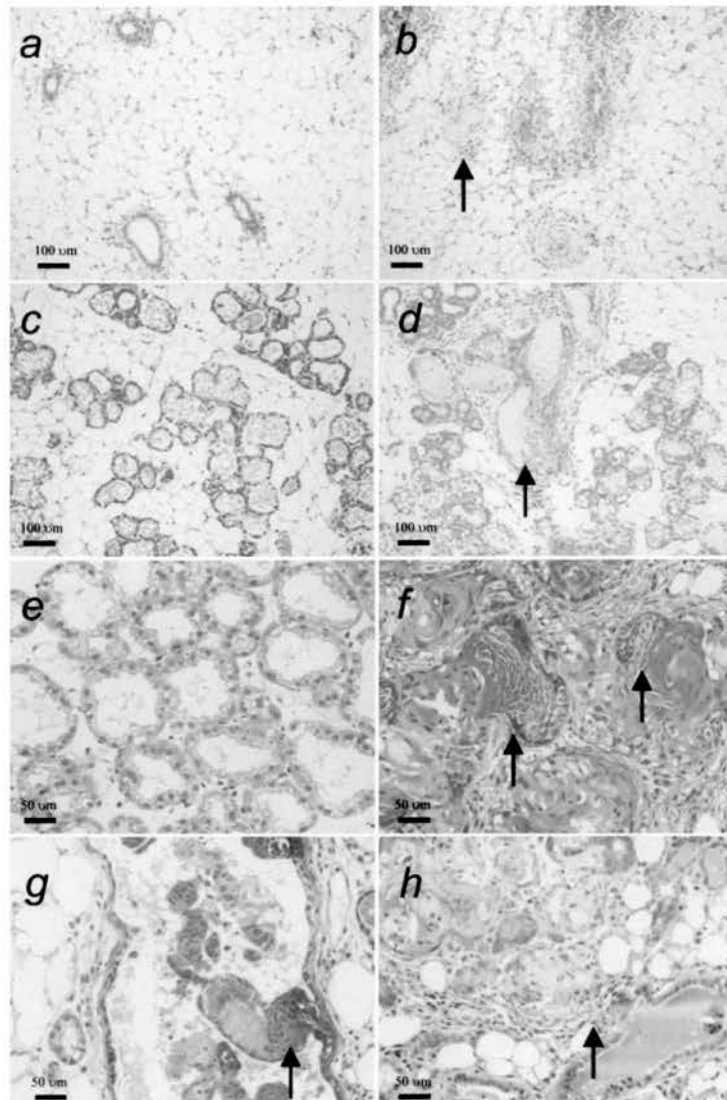


Figure 3 Mammary glands of $cre^+ Apc^{580s/580s}$ animals contain metaplastic lesions. At each time point a minimum of three animals were scored of each genotype and representative photographs taken. Haematoxylin and eosin stained sections of mammary glands from $cre^+ Apc^{580s/+}$ (**a,c,e**) and $cre^+ Apc^{580s/580s}$ (**b,d,f,g,h**) animals, examples of metaplastic areas are indicated by arrows: (**a,b**), 8 week old virgin glands; (**c,d**) mammary glands at parturition; (**e,f**), mammary glands at day 10 of lactation; (**g**), a section from a mutant mammary gland at day 10 of lactation showing metaplastic areas extending into the lumen of the duct; (**h**), shows what would presumably have been a secretory lobule developing away from a duct

The number of metaplastic nodules increased during lactation, with least evidence of the phenotype at parturition (Figure 3d). By day 10 of lactation, multiple foci were apparent (Figure 3f). To investigate if the mammary metaplasias would revert to normal tissue, we examined glands that had undergone postlactational involution. We found that the area of metaplasia remain after involution and increased in number and extent after two lactation cycles (Figure 5), but that no progression to neoplasia occurred. Mice have been allowed to pass through up to four complete lactation cycles, however, we have not observed progression to neoplasia up to 1 year following the initial lactation cycle ($n=10$).

Characterization of the metaplastic lesions

In order to investigate whether the metaplastic areas were composed of cycling cells, we assessed which cells were in S phase by the use of BrdU labelling. In contrast to the acinar epithelial cells, the parabasal cells in the metaplastic units were frequently found to be cycling (Figure 6b). Histological analysis revealed frequent apoptosis within areas associated with the maturing squamous cells, but not in the mature squamous epithelium (Figure 4b). TUNEL analysis confirmed the presence of apoptosis, but also showed the mature squamous cells to be weakly TUNEL positive (Figure 4d). This latter observation may reflect a process of anucleation within these cells, which

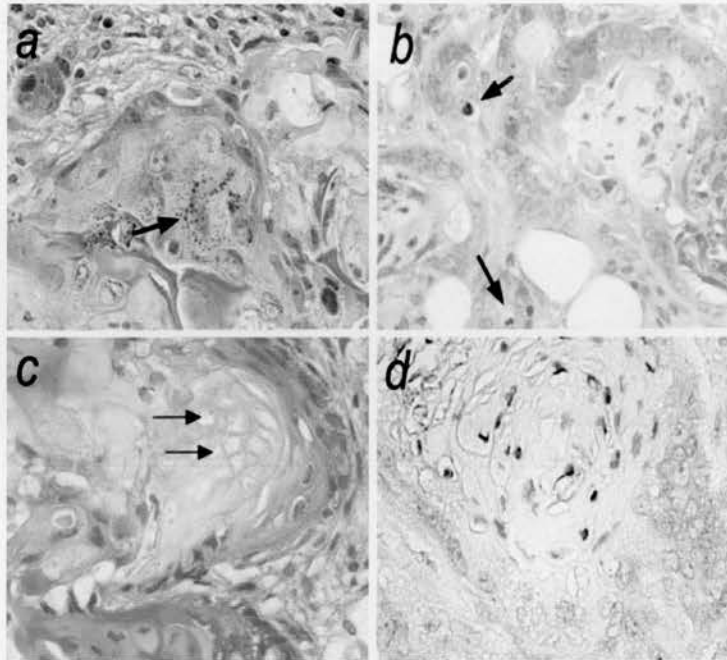


Figure 4 Histological analysis of metaplastic lesions: (a) Keratohyaline granules in squamous cells associated with metaplasia (arrowed); (b) apoptosis (examples indicated by arrows); (c) eosinophilic area, apparently the result of extensive cell death – example ghosts of nuclei are marked by the arrows; (d) TUNEL analysis, identifying weakly TUNEL positive cells within an area of squamous cells

ultimately results in the formation of ‘ghost’ nuclei and open spaces.

To examine whether β -catenin is dysregulated in these metaplasias, we used immunohistochemistry to examine the localization of β -catenin in mammary tissue. The balls of metaplastic squamous epithelium stain strongly for β -catenin throughout the cell cytoplasm and nucleus (Figure 6d), whereas normal mammary acinar epithelium stains only at the cell membrane where β -catenin is found in adherens junctions (Figure 6c). Little or no expression of β -catenin was observed in the mature squamous epithelium (Figure 6b,d). We analysed expression of cyclin D1 and *c-myc*, two of the putative target genes activated by the β -catenin-TCF/LEF pathway. We found increased levels of cyclin D1 could be detected in the balls of epithelial cells (Figure 6f), but could not show upregulation of *c-myc* by immunohistochemistry (data not shown).

*Synergy between the *Apc*^{580s} mutation and *Tcf-1* deficiency*

Tcf-1 deficient mice have previously been reported to develop acanthoma, with earliest onset of 7 months and with approximately 15% penetrance by 12 months (Roose *et al.*, 1999). This phenotype is accelerated on the *Apc*^{Min} background, resulting in acanthoma development as early as 2 months of age (Roose *et al.*, 1999). To address the extent of synergy between *Apc* and *Tcf-1* in our model, we crossed the

floxed *Apc* allele onto a *Tcf-1* null background. Female mice which were BLG-cre positive and homozygous for both the floxed *Apc* allele and the null *Tcf-1* allele were examined at between 3.5 weeks and 8 weeks of age (Figure 7). At all ages no normal mammary epithelium was observed, with each gland in every mouse analysed ($n=6$) being replaced by adenoacanthoma. No tumours have been observed in age matched *Tcf-1* +/+, Cre⁺ *Apc*^{580s/580s} littermates derived from this cross. These results therefore show that absence of both genes absolutely blocks the normal programme of mammary development and directly results in acanthoma. The very rapid onset of neoplasia in the absence of both genes is particularly remarkable given the level of recombination reported by the lacZ reporter strain. This phenotype presumably reflects very rapid outgrowth from cells marked by early recombination.

Discussion

*A role for *Apc* in virgin mammary gland*

We have conditionally inactivated *Apc* in mammary epithelium and found that functional *Apc* is required for the normal growth of virgin mammary glands. Mutant glands grow more slowly than controls (Figure 2) but do ultimately reach the end of the fat pad. In driving cre expression from the promoter of a milk protein gene, we anticipated that the effects of cre-mediated *Apc* deletion would be found primarily

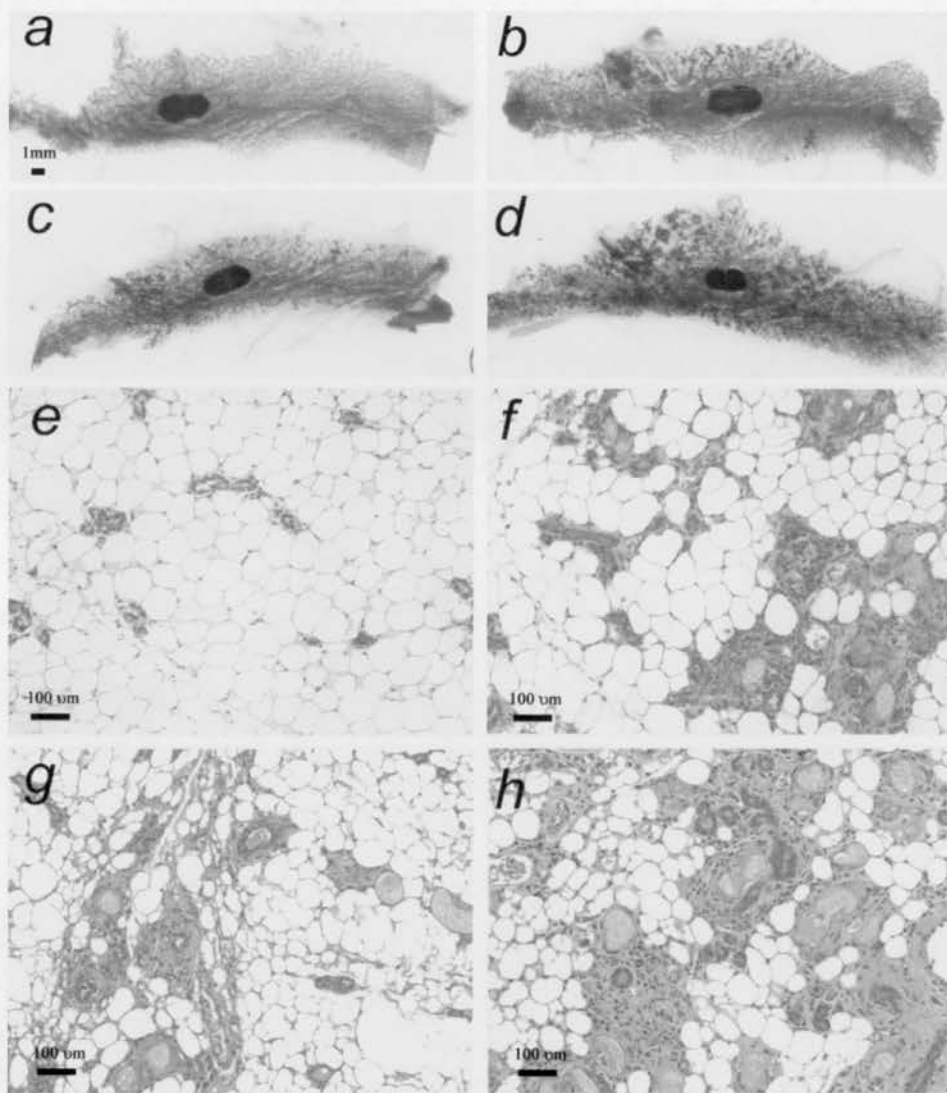


Figure 5 Metaplastic lesions remain in mutant glands during and following involution, and accumulate with subsequent pregnancies. The upper panels (a–d) show wholemounts of mammary glands during and following postlactational involution: (a) control animal at day 14 of involution; (b) $cre^+ Apc^{580s/580s}$ animal at day 14 of involution; (c) 150 day old $cre^+ Apc^{580s/580s}$ animal after one pregnancy; (d) 150 day old $cre^+ Apc^{580s/580s}$ animal after two pregnancies. The lower panels (e–h) show haematoxylin and eosin stained sections of mammary glands from the same animals shown in (a–d)

in the lactating mammary gland. Crossing the BLG-cre mice to a reporter strain demonstrated the presence of substantial cre activity in virgin glands (Figure 1). Thus, the discovery of a phenotype in virgin gland is not wholly unexpected. Growth retardation is perhaps a surprising consequence of loss of *Apc*, as this is more commonly associated with increased cell proliferation (and indeed we demonstrate here increased proliferation in the absence of *Apc* – see Figure 6). One potential explanation of this apparent paradox comes from the observation that *Apc* binds cytoskeletal components – both the actin cytoskeleton and microtubules (Fearnhead *et al.*, 2001). Thus, disruption of the cytoskeleton in the absence of *Apc* could lead to a decreased ability of the tip of the growing duct to invade or grow through the

fat pad. Consistent with this, Imbert *et al.* (2001) report a mild retardation in ductal extension in mice overexpressing $\Delta N89\beta$ -catenin, a mutant stabilized form of β -catenin lacking the N-terminal 89 amino acids – N-terminal deleted β -catenin has been suggested to interfere with *Apc*'s ability to bundle microtubules at the tips of cell extensions (Nathke *et al.*, 1996; Pollack *et al.*, 1997).

Several Wnt genes are expressed in the postnatal mammary gland, and these are thought to be involved in its morphogenesis. For example, *Wnt4* acts downstream of the progesterone receptor to induce side-branching in the mammary epithelial ductal network during early pregnancy (Briskin *et al.*, 2000). Overexpression of certain Wnt genes or stabilized mutant β -catenin affects morphogenesis of

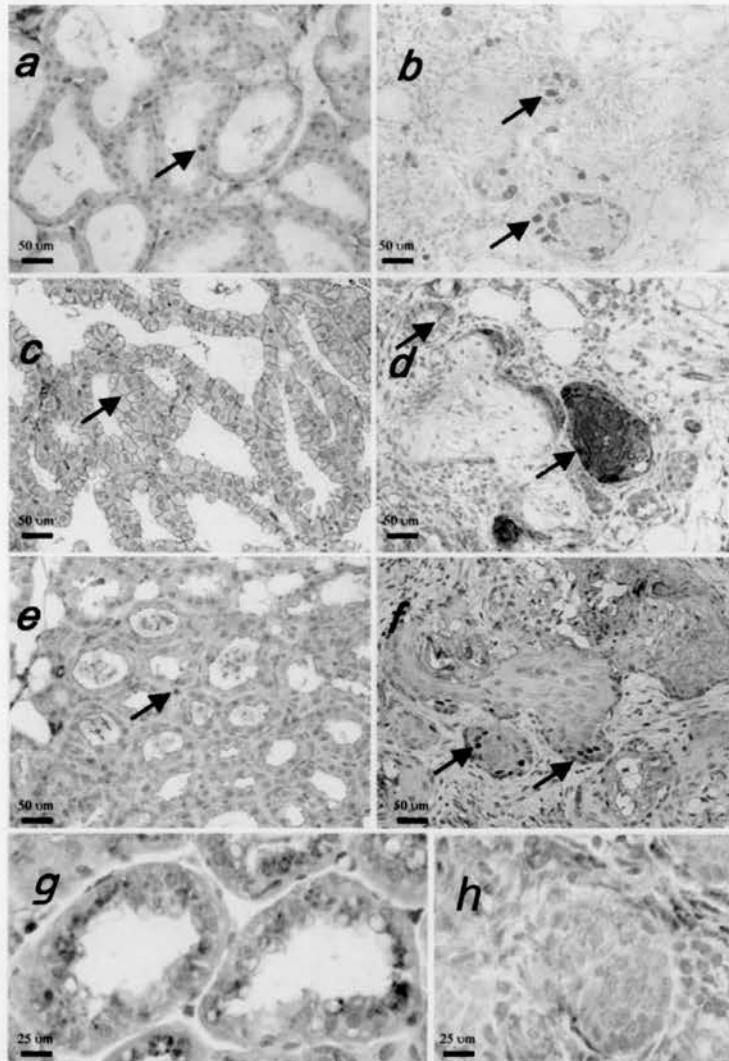


Figure 6 Cell proliferation and expression of β -catenin and cyclin D1 and *Apc* are disrupted in metaplastic areas of mutant glands. The left hand panels (a,c,e) show sections from $cre^+ Apc^{580s/+}$ control tissue. The right hand panels (b,d,f) show sections from $cre^+ Apc^{580s/580s}$ mutant tissue. (a,b) BrdU labelling. Note the increased number of BrdU labelled cells (arrows) in the acinar epithelial cells of the mutant gland. (c,d) β -catenin immunohistochemistry on day 10 lactation mammary tissue. In control tissue (c) β -catenin is detected in the adherens junctions (example arrowed) but not in the nuclei. In mutant glands (d) β -catenin is found in the adherens junctions of normal epithelium (arrow, top left), but also in the nuclei of basal cells and within metaplastic cells within epithelial balls (arrow, bottom right). (e,f) Cyclin D1 immunohistochemistry on day 10 lactation tissue. Arrows indicate cyclin D1 positive cells. Again, these are increased in the mutant and localized to the parabasal regions. (g,h) Immunohistochemical analysis of *Apc* expression in (g) wild type glands, showing expression of *Apc* within the alveoli: note this staining appears predominantly cytoplasmic, although it is concentrated towards the apical surface; (h) Failure to stain for *Apc* within the tightly bound balls of epithelial cells characteristic of the metaplasias

the mammary ductal network. Mice overexpressing *Wnt1* or *Wnt10B* in the mammary gland exhibit ductal hyperbranching and increased lobuloalveolar development (Tsukamoto *et al.*, 1988; Lane and Leder, 1997), whereas mammary expression of $\Delta N89\beta$ -catenin leads to inappropriate lobuloalveolar development in virgin glands (Imbert *et al.*, 2001). In our mice, loss of *Apc* leads to reduced ductal growth, but there are no comparable morphological effects to those described above (Figure 2). Possible explanations for these apparent discrepancies are discussed below.

Metaplasia as a consequence of loss of Apc

$Cre^+ Apc^{580s/580s}$ animals develop numerous small areas of metaplasia in the ductal epithelium (Figure 3b). Pregnancy in these mice results in multiple metaplastic foci, none of which has so far progressed to neoplasia. Although we do not observe tumorigenesis, many of the histological features we report here resemble those observed in adenosquamous carcinomas, as defined by the Annapolis meeting (Cardiff *et al.*, 2000), however the multiple intraduct squamous papillomas reported here are novel. These results show

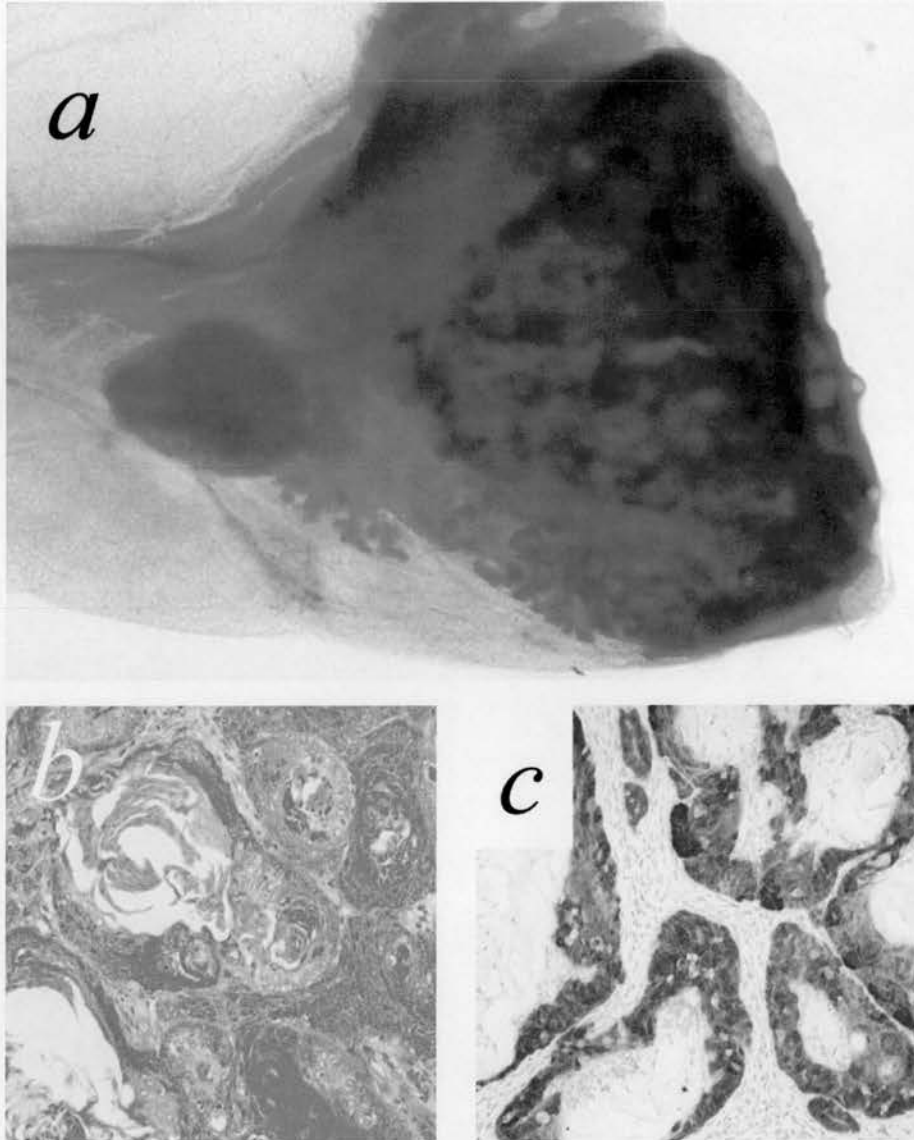


Figure 7 The effects of conditional mutation of *Apc* in a *Tcf-1* deficient background: (a) Wholemount of example gland showing acanthoma. No glands were found with normal architecture; (b) Representative acanthoma histology (haematoxylin and eosin stained, $\times 200$); (c) the pattern of β -catenin expression in the acanthomas

that *Apc* controls the structural development and differentiation state of the gland, processes at least partly mediated through β -catenin and cyclin D1. We also show that additional loss of *Tcf-1* transforms this phenotype by directly promoting acanthoma development, which strongly argues that *Tcf-1* and *Apc* act in consort to maintain the normal differentiation programme.

Apc mutation is associated with mammary tumorigenesis in both human (Woodage *et al.*, 1998; Furuuchi *et al.*, 2000) and mouse (Moser *et al.*, 1993), most likely as a consequence of increased β -catenin stability. Hyperplasia and malignant transformation has previously been reported in mouse mammary epithelium when *Wnt1*, *Wnt10B* or

truncated forms of β -catenin (both $\Delta N89$ and $\Delta N90$ mutants) are overexpressed (Tsukamoto *et al.*, 1988; Edwards *et al.*, 1992; Imbert *et al.*, 2001; Michaelson and Leder, 2001), again most likely as a result of increased β -catenin levels. This contrasts with the apparent failure to observe malignancy in the absence of *Apc* in our model (at least at high frequency considering the high number of *Apc* deficient cells present within the postlactational gland). There are subtle differences in the experimental paradigms that make direct comparisons difficult; however, in the single absence of *Apc*, although this leads to β -catenin stabilization (and accompanying high levels of cyclin D1) within areas of metaplasia, no tumours are seen.

Thus, in both the virgin gland and during pregnancy and lactation, the effects of inactivating *Apc* appear to differ from the effects of ectopic Wnt signalling or overexpression of stabilized β -catenin. There are several possible explanations for these apparent differences. First, the transgenes may be expressed in different cell types. The adult mammary gland contains a population of stem cells that are able to give rise to complete, functional mammary glands (Kordon and Smith, 1998) and it has been suggested that MMTV-induced mammary tumours arise from infection of these stem cells (Callahan and Smith, 2000). Thus, one possibility was that the BLG promoter was failing to drive deletion of the *Apc* gene within those stem cells that can give rise to tumours. Clearly, our results from the *Tcf-1* intercross show that this is not the case, as the BLG promoter is clearly driving loss of *Apc* in cells which can be the founders of tumours.

Second, levels of β -catenin may be critical. Different levels of β -catenin might determine whether mammary ductal development proceeds normally, or whether hyperbranching or precocious lobuloalveolar development occurs instead. Further, there may be a threshold level of β -catenin above which tumorigenesis is triggered. This explanation fits well with the reported failure to observe tumorigenesis following cre mediated mutation of β -catenin (Miyoshi et al., 2002), as this model does not rely on over expression of mutant β -catenin. In our model, one might argue that single deficiency of either *Apc* or *Tcf-1* is insufficient to result in complete deregulation of β -catenin levels, but that this occurs in the absence of both genes. Alternatively, transcriptional activity may be regulated by the ratio of β -catenin to *Tcf-1*. Both of these explanations imply that β -catenin levels are a critical determinant of activity. In contrast to this view, Imbert et al. (2001) have argued that β -catenin levels are not relevant, as both high and low-expressing lines of their MMTV- $\Delta N\beta$ -catenin transgenic mice display the same phenotype, with low expressors showing a longer latency. However, given that expression of endogenous β -catenin is downregulated in these animals, and that even the low expressing line produces around threefold more β -catenin from the transgene than the endogenous locus, it is difficult to draw clear conclusions about β -catenin levels from these experiments.

Third, mutant forms of β -catenin may have different properties to wild type β -catenin. As described above, MMTV- $\Delta N\beta$ -catenin transgenic mice develop mammary adenocarcinomas (Imbert et al., 2001; Michaelson and Leder, 2001) β -catenin has a cluster of putative phosphorylation sites for GSK3 β in its amino terminal region. Phosphorylation at these sites results in targeting of the protein for proteasomal degradation. Deletion of the amino-terminal 89 amino acids of β -catenin results in the loss of these sites, thereby generating a stable mutant protein. However, deletion of either the 89 or 90 N-terminal amino acids may affect more than β -catenin stability. Guger and Gumbiner (2000) have shown that amino acid alterations at the amino terminus of β -catenin affect

signalling independent of any effect on β -catenin levels. Furthermore, β -catenin is thought to be required for the formation of a stable complex between the nemo-like kinase (NLK) and TCF/LEF (Ishitani et al., 1999). The effects of both $\Delta N90$ β -catenin $\Delta N89$ β -catenin overexpression could be due to disruption of such an interaction. This hypothesis fits well with our observed synergy between the *Tcf-1* and *Apc* mutations.

Fourth, it is well recognized that susceptibility to mammary hyperplasias and carcinomas in *Apc*^{min/+} mice is influenced by genetic background (Moser et al., 2001). However, our animals are on a mixed genetic background, and therefore our failure to observe neoplasia is unlikely to be a reflection of a single resistant background. Furthermore, the dramatic increase in spontaneous tumorigenesis in the additional absence of *Tcf-1* demonstrates that the background we are using is permissive for tumorigenesis.

Finally, the nature of the mutation at the *Apc* allele may determine final phenotype. There are phenotypic differences among the different *Apc* alleles described to date. Cre-mediated deletion of *Apc*^{580s} in colonic epithelium leads to the efficient formation of adenocarcinomas (Shibata et al., 1997). However, we find no (or very low penetrance) tumorigenesis when the same mutation is specifically targeted to the mammary gland, although mutation of *Apc* in the context of *Tcf-1* deficiency does directly lead to neoplasia. Thus mammary and colonic epithelia appear to respond differently following *Apc* mutation. Perhaps the mammary epithelium requires higher levels of β -catenin for malignant transformation, or perhaps some *Apc*-independent method of β -catenin regulation (such as by feedback repression by *Tcf-1*) is found in the mammary gland. Mutations in different parts of the *Apc* protein can give rise to different phenotypes, however, in this case the same allele (*Apc*^{580s}) appears to have different effects in different tissues.

We observe increased expression of cyclin D1, a putative target of β -catenin in mutant glands. Studies of human breast cancer have reported that β -catenin mediates upregulation of cyclin D1 (Lin et al., 2000), and that cyclin D1 expression is associated with metastasis (Buckholm et al., 2000). Further, mice expressing cyclin D1 under the control of the MMTV LTR develop mammary adenocarcinomas (Wang et al., 1994) and cyclin D1 deficiency has been shown to block *ras* and *neu* mediated (but critically not Wnt mediated) mammary tumorigenesis. The implication from these studies is that elevated levels of cyclin D1 can be potent in driving neoplasia. In our model high levels of both β -catenin and cyclin D1 were observed, but these were clearly associated with metaplasia and not neoplasia. It will be of great interest to study the phenotype of the *Apc* and *Tcf-1* mutants in the additional absence of cyclin D1.

In conclusion, we propose a model whereby loss of *Apc* within mammary epithelial cells leads to dysregulated growth, as a consequence of which cells adopt a transdifferentiation programme to non-cycling squamous epithelial cells. Dysregulation of β -catenin

characterizes these areas of metaplasia. In the presence of functional *Tcf-1*, this process either fails to lead to neoplasia or does so at very low efficiency. In contrast, combined loss of *Tcf-1* and *Apc* dramatically blocks normal mammary development and results in the direct formation of acanthoma. As we know that deficiency of *Apc* (from studies of the *Apc^{Min}* mouse) can predispose to acanthoma these results therefore strongly implicate loss of *Tcf-1* as a secondary event in this process. Investigation of the mechanism underlying these findings should yield valuable insights into the normal functions of *Apc* and *Tcf-1* in the mammary gland, and also into their role in suppressing neoplasia within this tissue.

Materials and methods

Genotyping of mice

Detection of *Apc* and *Tcf-1* alleles was carried out by PCR as previously described (Shibata *et al.*, 1997; Roose *et al.*, 1999). The BLG-cre transgene was detected using the PCR also previously described (Selbert *et al.*, 1998). Mice were maintained on an outbred genetic background segregating for C57Bl/6, Ola129 and C3H genomes and therefore where direct comparisons were performed these were made between littermates.

Mammary gland wholemount

This procedure was carried out as described on the mammary gland website: <http://mammary.nih.gov>.

Tissue sections and immunohistochemistry

Five μm sections were cut from paraffin embedded tissue retrieved at necropsy. For control tissue, lung, liver, pancreas, salivary gland, spleen and kidney were taken. Control tissues were stained with haematoxylin and eosin and examined, no dysregulated growth or histological abnormalities were found. Immunohistochemistry was carried out using the DAKO EnVision plus system (cat. no. K4006) following the

manufacturer's instructions. Animals were injected with BrdU (70 $\mu\text{g/g}$ in sterile saline, i.p.) 2 h before sacrifice. Detection of BrdU incorporation was by antibody (Roche). *Apc* was detected using a c-terminus antibody (Midgeley *et al.*, 1997) at a dilution of 1/100. Antigen retrieval was by microwaving in 10 mM citrate pH 6 for 2 \times 3 min. β -catenin was detected using a mouse monoclonal antibody supplied by Transduction Laboratories (cat. no. C19220), used at 1/50 dilution. Antigen retrieval was by microwaving in 10 mM citrate buffer, pH 6.0 for 3 \times 5 min. Cyclin D1 was detected using the mouse monoclonal DCS-6 (Nova Castra) at a dilution of 1/100. High pH Target Retrieval Solution (Dako, cat. no. S3308) was used for antigen retrieval, following the manufacturer's instructions. TUNEL staining was carried out using the ApopTag Peroxidase *in situ* apoptosis detection kit (Intergen) following manufacturer's instructions.

lacZ staining

The protocol was adapted from that described by Brisken *et al.* (1998). Mammary glands were removed, spread in a histocassette and fixed for 2 h in ice-cold 4% paraformaldehyde in PBS. Glands were then rinsed in (2 mM MgCl_2 , 0.1% sodium deoxycholate, 0.2% NP40 in PBS) at room temperature for 3 \times 30 min and stained overnight at 37°C without agitation in the dark in X-gal staining buffer (1 mg/ml X-gal, 5 mM K-ferricyanide, 5 mM K-ferrocyanide in rinse buffer). Glands were rinsed gently in PBS for 30 min at room temperature, dehydrated through 70, 95 and 100% ethanol (30 min each), cleared in BABB (2:1 ratio of benzyl alcohol:benzyl benzoate) and mounted in DPX medium prior to photography. For sections, this material was then embedded in paraffin and sectioned as normal. Sections were counterstained with 1% eosin, dehydrated through 70, 95 and 100% ethanol, cleared briefly in xylene and mounted in DPX mounting medium.

Acknowledgements

This work was supported by the Royal Society, the BBSRC and the Association for International Cancer Research (AICR). We are grateful to Inke Nathke for the gift of the anti-APC antibody.

References

- Bienz M and Clevers H. (2000). *Cell*, **103**, 311–320.
- Bradbury J, Edwards P, Niemeyer C and Dale T. (1995). *Dev. Biol.*, **170**, 553–563.
- Brisken C, Park S, Vass T, Lydon JP, O'Malley BW and Weinberg RA. (1998). *Proc. Natl. Acad. Sci. USA*, **95**, 5076–5081.
- Brisken C, Heineman A, Chavvaria T, Elenbaas B, Tan J, Dey S, McMahon J, McMahon A and Weinberg R. (2000). *Genes Dev.*, **14**, 650–654.
- Buckholm I, Nesland J and Borresen-Dale A-L. (2000). *J. Pathol.*, **190**, 15–19.
- Cadigan K and Nusse R. (1997). *Genes Dev.*, **11**, 3286–3305.
- Cardiff R, Anver M, Gusterson B, Hennighausen L, Jensen R, Merino M, Rehm S, Russo J, Tavassoli F, Wakefield L, Ward J and Green E. (2000). *Oncogene*, **19**, 968–988.
- Callahan R and Smith GH. (2000). *Oncogene*, **19**, 992–1001.
- Chapman R, Laurencio P, Tonner E, Flint D, Selbert S, Takeda K, Akira S, Clarke AR and Watson CJ. (1999). *Genes Dev.*, **13**, 2604–2616.
- Edwards PAW, Hiby S, Papkoff J and Bradbury JM. (1992). *Oncogene*, **7**, 2041–2051.
- Fearnhead NS, Britton MP and Bodmer WF. (2001). *Hum. Molec. Genetics*, **10**, 721–733.
- Furuuchi K, Tada M, Yamada H, Kataoka A, Furuuchi N, Hamada J, Takahashi M, Todo S and Moriuchi T. (2000). *Am. J. Pathol.*, **156**, 1997–2005.
- Groden J, Thliveris A, Samowitz W, Carlson M, Gelbert L, Albertson H, Joslyn G, Stevens J, Spirio L and Robertson M. (1991). *Cell*, **66**, 589–600.
- Guger KA and Gumbiner BM. (2000). *Dev. Biol.*, **223**, 441–448.
- Gu H, Marth J, Orban P, Mossman H and Rajewsky K. (1994). *Science*, **265**, 103–106.
- He T-C, Sparks A, Rago C, Hermeking H, Zawel L, da Costa L, Morin P, Vogelstein B and Kinzler KW. (1998). *Science*, **281**, 1509–1512.
- He T-C, Chan TA, Vogelstein B and Kinzler KW. (1999). *Cell*, **99**, 335–345.

- Ho K, Kalle W, Lo THS, Lam W and Tang C. (1999). *Histopathology*, **35**, 249–256.
- Imbert A, Eelkema R, Jordan S, Feiner H and Cowin P. (2001). *J. Cell Biol.*, **153**, 555–568.
- Ishitani T, Ninomiya-Tsuji J, Nagai S, Nishita M, Meneghini M, Barker N, Waterman M, Bowerman B, Clevers H, Shibuya H and Matsumoto K. (1999). *Nature*, **399**, 798–802.
- Jin Z, Tamura G, Tsuchiya T, Sakata K, Kashiwaba M, Osakabe M and Motoyama T. (2001). *Br. J. Cancer*, **85**, 69–73.
- Kashiwaba M, Tamura G and Ishida M. (1994). *J. Cancer Res. Clin. Oncol.*, **120**, 727–731.
- Kordon EC and Smith GH. (1998). *Development*, **125**, 1921–1930.
- Lane TF and Leder P. (1997). *Oncogene*, **15**, 2133–2144.
- Lin S-Y, Xia W, Wang J, Kwong K, Spohn B, Wen Y, Pestell R and Hung M-C. (2000). *Proc. Natl. Acad. Sci. USA*, **97**, 4262–4266.
- Michaelson JS and Leder P. (2001). *Oncogene*, **20**, 5093–5099.
- Midgley CA, White S, Howitt R, Save V, Dunlop MG, Hall PA, Lane DP, Wyllie AH and Bubb VJ. (1997). *J. Pathol.*, **181**, 426–433.
- Miyoshi K, Shillingford JM, Le Provost F, Gounari F, Bronson R, von Boehmer H, Taketo MM, Cardiff RD, Hennighausen L and Khazaie K. (2002). *Proc. Natl. Acad. Sci. USA*, **99**, 219–224.
- Moser AR, Mattes EM, Dove WF, Lindstrom MJ, Haag JD and Gould MN. (1993). *Proc. Natl. Acad. Sci. USA*, **90**, 8977–8981.
- Moser AR, Shoemaker AR, Connelly CS, Clipson L, Gould KA, Luongo C, Dove WF, Siggers PH and Gardner RL. (1995). *Dev. Dyn.*, **203**, 422–433.
- Moser R, Hegg F and Cardiff RD. (2001). *Cancer Res.*, **61**, 3480–3485.
- Nathke I, Adams C, Polakis P, Sellin J and Nelson WJ. (1996). *J. Cell Biol.*, **134**, 165–179.
- Nusse R and Varmus HE. (1982). *Cell*, **31**, 99–109.
- Polakis P. (2000). *Genes Dev.*, **14**, 1837–1851.
- Pollack AL, Barth AI, Altschuler Y, Nelson WJ and Mostov KE. (1997). *J. Cell Biol.*, **137**, 1651–1662.
- Roose J, Molenaar M, Peterson J, Hurenkamp J, Brantjes H, Moerer P, van de Wetering M, Destree O and Clevers H. (1998). *Nature*, **395**, 608–612.
- Roose J and Clevers H. (1999). *Biochim. Biophys. Acta*, **87456**, M23–M37.
- Roose J, Huls G, van Beest M, Moerer P, van der Horn K, Goldschmeding R, Logtenberg T and Clevers H. (1999). *Science*, **285**, 1923–1926.
- Schlosshauer P, Brown S, Eisenger K, Yan Q, Guglielminetti E, Parsons R, Ellenson L and Kitajewski J. (2000). *Carcinogenesis*, **21**, 1453–1456.
- Selbert S, Bentley D, Melton D, Rannie D, Laurenco P, Watson C and Clarke AR. (1998). *Transgenic Res.*, **7**, 387–396.
- Shibata H, Toyama K, Shioya H, Ito M, Hirota M, Hasegawa S, Matsumoto H, Takano H, Akiyama T, Toyoshima K, Kanamaru R, Kanegae Y, Sarb I, Nakamura Y, Shiba K and Noda T. (1997). *Science*, **278**, 120–123.
- Shimizu H, Julius M, Giarre M, Zheng Z, Brown A and Kitajewski J. (1997). *Cell Growth Differ.*, **8**, 1349–1358.
- Shtutman M, Zhurinsky J, Simcha I, Albanese C, D'Amico M, Pestell R and Ben-Ze'ev B. (1999). *Proc. Natl. Acad. Sci. USA*, **96**, 5522–5527.
- Soriano P. (1999). *Nat. Genet.*, **21**, 70–71.
- Smits R, Kielman M, Breukel C, Zurcher C, Neufeld K, Jagmohan-Changur S, Hoffland N, van Dijk J, White R, Edelmann W, Kucherlapati R, Khan PM and Fodde R. (1999). *Genes Dev.*, **13**, 1309–1321.
- Tetsu O and McCormick F. (1999). *Nature*, **398**, 422–426.
- Thompson A, Morris R, Wallace M, Wyllie A, Steel C and Carter D. (1993). *Br. J. Cancer*, **68**, 64–68.
- Tsukamoto A, Grosschedl R, Guzman R, Parslow T and Varmus H. (1988). *Cell*, **55**, 619–625.
- Wang TC, Cardiff RD, Zukerberg L, Lees E, Arnold A and Schmidt EV. (1994). *Nature*, **369**, 669–671.
- Woodage T, King S, Wacholder S, Hartge P, Struewing J, McAdams M, Laken S, Tucker M and Brody L. (1998). *Nature Genet.*, **20**, 62–65.
- Yu Q, Geng Y and Sicinski P. (2001). *Nature*, **411**, 1017–1021.